Volumetric properties of Arabinogalactan-proteins from Acacia Gum

Verónica Mejia Tamayo

THÈSE POUR OBTENIR LE GRADE DE DOCTEUR DE L'UNIVERSITÉ DE MONTPELLIER

En Biochimie et Physicochimie alimentaire

École doctorale GAIA
Agroressourses, Procédés, Aliments, Produits

Unité de recherche
Ingénierie des Agropolymères et des Technologies Emergentes

Propriétés volumétriques des Arabinogalactane-protéines d'exsudats de gommes d'Acacia

Présentée par Verónica MEJIA TAMAYO
Le 28 novembre 2018

Sous la direction de Christian SANCHEZ
et Michaël NIGEN

Devant le jury composé de

Mr Ali ASSIFAOUI, Maître de conférences, Université de Bourgogne	Rapporteur
Mr Stéphane PEZENNEC, Chargé de recherche, INRA	Rapporteur
Mme Adeline BOIRE, Chargée de Recherche, INRA	Examinateur
Mme Christine EBEL, Directrice de Recherche, CNRS	Examinateur
Mme Marie-Hélène MOREL, Directrice de Recherche, INRA	Examinateur
Mr Christian SANCHEZ, Professeur, Université de Montpellier	Directeur de thèse

UNIVERSITÉ DE MONTPELLIER

Volumetric Properties of Arabinogalactan-Proteins from Acacia gums

Verónica MEJIA TAMAYO

Ph.D. Thesis

Supervisors: Christian SANCHEZ and Michaël NIGEN

November, 2018

To my late grandfather ‘Papi Hector’

Who always believed in me

Thanks for everything!

"Nothing in life is to be feared, it is only to be understood.

Now is the time to understand more, so that we may fear less."

— Marie Curie

Table of contents

List of Abbreviations of gums and other biomolecules

AG	Arabinogalactan fraction	HIC-F2	Fraction 2 obtained by HIC
AGP	Arabinogalactan protein	HIC-F3	Fraction 2 obtained by HIC
Ara	Arabinose	IEC-F1	Fraction 1 obtained by IEC
Gal	Galactose	IEC-F2	Fraction 2 obtained by IEC
GP	Glycoprotein fraction	Rha	Rhamnose
HIC-F1	Fraction 1 obtained by HIC		

List of Abbreviations of Methods and Techniques

AUC	Analytical ultracentrifugation	IEC	Ionic exchange chromatography
AUC-EV	Analytical ultracentrifugation-Sedimentation equilibrium	PPC	Pressure perturbation calorimetric
AUC-SV	Analytical ultracentrifugation-Sedimentation velocity	MALS	Multi angle light scattering
DAM	Dummy atom model	NMR	Nuclear magnetic resonance
DTG	Derivative thermo-gravimetric	SANS	Small neutron scattering
DOSY-NRM	Diffusion ordered nuclear magnetic spectroscopy	SAXS	Small angle x-ray scattering
DSC	Differential scanning calorimetry	SLS	Static light scattering
DLS	Dynamic light scattering	SEC	Size exclusion chromatography
HIC	Hydrophobic interaction chromatography	TEM	Transmission electron microscopy
HPSEC	High performance size exclusion chromatography	TGA	Thermogravimetric analysis

List of Abbreviations used in Equations

A	Pre-exponential factor	d_f	Fractal dimension
B	Constant of proportionality	dn/dc	Refractive index increment
a_η, a_G, a_S, a_D	KMHS coefficients	D_T	Translation diffusion coefficient
B_M	Coefficient of proportionality	E°	Partial specific expansibility
C	Concentration	E_a	Flow activation energy
C_a	Concentration in which half of available sites of the capillary glass wall are occupied	$g^{(1)}$	Intensity of the signal (photon count)
C_s	Concentration of solute	k_B	Boltzman constant
k	Constant describing the adsorption degree on capillary wall glass	R_G	Gyration radius

K_η, K_G, K_S, K_D	KMHS prefactors	$R\eta$	Hydrodynamic radius (from intrinsic viscosity)
k_s	Gralen parameter	R_H	Hydrodynamic radius (from diffusion coefficient)
k_H	Huggins constant	S_o	Sedimentation coefficient
K_M	Intrinsic partial molar compressibility of solute	S	Sedimentation velocity
KMHS	Kuhn-Mark-Houwink-Sakurada	T	Temperature
k_s°	Partial specific adiabatic compressibility	T_1	First transition temperature
K_s°	Partial molar adiabatic compressibility	T_2	Second transition temperature
K_{sh}°	Partial molar adiabatic compressibility of water in hydration shell	T_{on}	Onset temperature
K_{so}°	Partial molar adiabatic compressibility of water in bulk state	T_{off}	Offset temperature
K_r	Partial molar adiabatic compressibility due to relaxation	u	Sound velocity
K_S	Adiabatic compressibility	V	Volume
K_T	Isothermal compressibility	V_I	Interaction molar volume
K_s°	Partial molar adiabatic compressibility	V_M	Intrinsic partial molar volume of solute
m_i	Amount of the component i, in mass units	V_T	Partial molar thermal volume
M_n	Number-averaged molar mass	v_s°	Partial specific volume
M_w	Weight-averaged molar mass	V_s°	Partial molar volume of solute at infinite dilution
M_w/M_n	Polydispersity index	v_H	Hydrodynamic volume
n	Amount of moles	V_h°	Partial molar volume of water in hydration shell
N_A	Avogadro's number	V_o°	Partial molar volume of water in bulk state
n_h	Hydration number	V_v	Number average hydrodynamically effective volume
P	Pressure	V_{void}	Partial molar specific volume of voids
Q	Heat	V_{vdW}	Van der walls volume partial molar volume
r	Radial distance of the boundary	V_{sw}	Swollen volume
R	Ideal gas constant		

List of Greek symbols

$[\eta]$	Intrinsic viscosity	η_o	Dynamic viscosity of the solvent
α	Thermal expansion coefficient	η_{rel}	Relative viscosity
β_M	Coefficient of adiabatic compressibility of the biopolymer interior	η_{sp}	Specific viscosity
β_s	Adiabatic compressibility coefficient	K_T	Isothermal compressibility
β_s°	Partial specific adiabatic compressibility coefficient	ν	Viscosity increment
β_{so}	Adiabatic compressibility coefficient of the solvent	ρ	Density of dispersion
β_T	Isothermal compressibility coefficient	ρ_0	Density of solvent
β_{T0}	Coefficient of isothermal compressibility of solvent	ρ_M	Molecular packing density
Γ	Decay constant	Φ	Apparent specific volume
Δ	Layer of constant thickness around the surface of the molecule (thermal volume)	τ	Decay time
η	Dynamic viscosity	ω	Angular velocity

Chapter I: General Introduction

1. Background Information

1.1. Acacia gum

Acacia Gum (A. gum, E414), also known as Gum Arabic is defined by the FAO/WHO Joint Expert Committee for Food Additives (JECFA) as "a dried exudate obtained from the stems and branches of *Acacia senegal* (L) Willdenow or *Acacia seyal* (Fam. Leguminosae)" [1-3].

A. gum exudates (Figure I.1) are produced as a response to an environmental stress (e.g. extreme weather conditions or animal injuries). Its main function is to protect the tree from insects and fungi invasion, to seal wounds and prevent dehydration [2,4,5]. A. gum is produced in the African region known as the sub-saharian belt, constituted by the regions of Sudan, Nigeria, Chad and Senegal [5-7], but also in the regions beyond Pakistan and India [2,8]. Sudan is the mayor producer with a market share of about 70% - 80% [6]. In addition, A. gum is important for the economy of the rural populations of the sub-saharian area because it provides an income in the dry-season [9].

Figure I. 1. Nodules of A. *senegal* gum before the purification process

A. gum use can be traced up to the Stone Age where it was used as a food ingredient and adhesive for tool manufacturing [2,10,11] and later in foods, in pigments and adhesive in the ancient Egypt [2,6,12]. Medicinal use of A. gum can be traced to Cleopatra's time as a contraceptive and as a topic remedy to cure superficial irritation [2,13]. A. gum was

introduced in Europe via Arabian ports and was called Arabic gum due to its origin [6]. In the middle ages, A. gum was used mainly in pigments for manuscripts and paintings [2]. In the modern times, A. gum has found a wide range of industrial applications due to its interesting properties such as good emulsification and stabilization properties, low water-absorption, high water-solubility and capacity to form molecular assemblies [2,6]. One of the most interesting application nowadays is in the nutritional industry due to its potential health benefits (prebiotic, soluble fiber, stimulation of the growth and activity of the beneficial bacteria in the colon) [5]. More traditional applications of A. gums are found in the confectionery (chewing gum, candies), sodas and non-alcoholic beverages, wine and beer brewing and bakery industries [5,6]. In addition, in the non-food industry, A. gum is used in the pharmaceutical (e.g. syrups, coatings and encapsulation of bioactive compounds), cosmetic (e.g. creams, lotions, soaps), fragrance and painting industries [5,6].

1.2. Composition and chemical structure of Acacia gums

A. gum exudates contain structurally complex biopolymers and minor associated components such as minerals, traces of lipids and flavonoids, and enzymes [2,14]. A. gum biopolymers are highly glycosylated hydroxyproline-rich arabinogalactan-peptide and arabinogalactan-proteins (AGPs) that belong to the glycoprotein superfamily [15-17]. AGPs are the most structurally complex hydroxyproline-rich protein and are implicated to function in plant growth, development, signaling, and plant–pathogen interactions [18,19]. They are found in plasma membranes, cell walls, and plant exudates [20]. AGPs are defined by three criteria: the presence of type II arabino-3,6-galactan chains, a hydroxyproline-rich protein backbone, and the ability of most AGPs to bind to a class of synthetic phenylazo dyes, the β-glycosyl Yariv reagents [21]. AGP protein backbones are typically rich in hydroxyproline alternating with alanine, threonine and serine, whereas their carbohydrate moieties are mostly composed of galactose and arabinose with varying amounts of rhamnose, fucose, and glucuronic acid [22].

In Acacia gums, various populations of hyperbranched slightly acidic amphiphilic AGPs coexist [14], presenting slightly different sugar, amino acid and mineral composition, sugar to amino acid molar ratio, charge density, molar mass, size, shape and anisotropy [4,7,23-28]. They are composed of D-galactose (Gal), L-arabinose (Ara), L-rhamnose (Rha), D-glucuronic acid and 4-O-methylglucuronic acid [2,29], being Gal and Ara the main sugars present [2,4,7,24,30-32]. In addition, it contains about 1-3% of proteins, 0.2-0.4% nitrogen and around 12-16% of moisture [2]. The protein moiety of A. gums is mainly composed of hydroxyproline

and serine, but important quantities of proline and aspartic acid have been also reported. The chemical structure of AGPs is formed of a backbone of 1-3 linked β–D-galactopyranosyl units with side chains formed of two or five units joint to the main chain by 1,6 linkages. Both chains have units of α-L-arabinofuranosyl, α-L-rhamnopyranosyl, β-D-glucuronopyranosyl and 4-O-methyl-β-D-glucoronopyranosyl, being the last two end units [2,4,6,33-35].

The capacity of A. gums to form assemblies or aggregates with itself or other compounds (e. g. proteins) has been studied by size exclusion chromatography (SEC), static light scattering (SLS), small angle x-ray scattering (SAXS), small angle neutron scattering (SANS), microscopy and cryo-TEM [2,26,27,36-41]. The self-assembly properties of A. gums has been explained due to a natural mechanism which depends on the characteristics of the tree itself and its ageing process [2,38].

A. gum has a natural variability, which depends on its variety, origin, age of the tree, climatic conditions, soil composition, place of the tree from where the gum is collected and post-harvest practices (e.g. purification, maturation and storage processes) [2,6,7,38,42,43]. A summary of the main structural properties of A. gums and HIC-fractions from A. *senegal* found in literature are presented in Table I.1. The structural properties of A. gums and HIC-fractions have been mainly studied using size exclusion chromatography (SEC) and the results found in literature differ depending on the type of salt used ($LiNO_3$, NaCl or $NaNO_3$) and concentration used in the analysis (0.05–1 M). The two main varieties of A. gum, Acacia *senegal* (A. *senegal*) and Acacia *seyal* (A. *seyal*), differ mainly by their sugar, protein content, amino acid profile and branching degree. A. *senegal* has a higher protein content (around 3% and 1%, respectively) and branching degree (around 80% and 60% respectively) than A. *seyal* [7,32]. A. *seyal* has higher Arabinose and 4-O-Me-Glucuronic Acid content than A. *senegal* [7,32]. In addition, a more compact structure of A. *seyal* in comparison to A. *senegal* has been suggested [32]. Regarding the structural properties, values of weight-average molar mass (M_w) in the range of 2–7 $x10^5$ and 7-10 $x10^5$ $g.mol^{-1}$, polydispersity index (M_w/M_n) in the range 1.2-2.7 and 1.5-2.5, intrinsic viscosity ($[\eta]$) in the range of 8–40 and 9-18 $mL.g^{-1}$, and hydrodynamic radius (R_H) in the range 10–15 nm and 17 nm have been reported for A. *senegal* and A. *seyal*, respectively [4,7,24,31,32,38,44-48].

Table I.1. Summary of the structural properties of A. *senegal*, A. *seyal* and HIC fractions from A. *senegal* (...)

Gum or fraction	M_w (g.mol^{-1})	M_w/M_n	R_H (nm)	R_g (nm)	[η] (mL.g^{-1})	Salt used	Concentration (M)	Reference
A. gums								
A. *seyal*	8.2 x10^5	1.5		17.1	16.5 [a]	LiNO3	0.10	[32]
	7.7 x10^5	2.2			6.0 [a]	$LiNO_3$	0.10	[44]
	7.2 x10^5	2.0			13.0 [a]	NaCl	1.00	[31]
	1.9 x10^6	2.5		29.5	14.6 [a]	NaCl	0.50	[49]
	1.6 x10^6	2.4		24.0		NaCl	0.50	[48]
	1.2 x10^6	1.9			14.8 [a]	NaCl	0.50	[47]
	1.1 x10^6	1.7	17.3	24.0 [b]		$NaNO_3$	0.10	[45]
A. *senegal*	6.8 x10^5	2.0		30.8	22.8 [a]	$LiNO_3$	0.10	[32]
	3.1 x10^5	1.3	10.7	11.8	17.3 [a]	$NaNO_3$	0.05	[4]
	4.9 – 6.5 x10^5	1.8 – 2.7 [a]				NaCl	0.50	[42]
	5.4 x10^5	2.0 [a]				$LiNO_3$	0.10	[50]
	4.0-5.3 x10^5	1.8 – 2.1			8.0 [a]	$LiNO_3$	0.10	[44]
	4.6 x10^5		14.1 [d]			NaCl	0.50	[24]
	2.0 – 7.9 x10^5	1.3 – 1.8 [b]			10.4 - 19.8 [b]	NaCl	1.00	[38]
	5.3 x10^5	2.3			23 [a]	$NaNO_3$	0.05	[39]
	1.4 x10^5 – 1.4 x10^6				16.0 - 40.0 [a]	NaCl	1.00	[51]
					16.5 [b]	NaCl	0.35	[52]
	6.2 x10^5				18.2 [a]	NaCl	0.20	[53]
	5.7 - 7.5 x10^5				17.7 [a]	NaCl	1.00	[31]
					15.5 [b]	NaCl	1.00	[54]
	9.0 x10^5				16.4 [b]			[43]
	5.9 x10^5	2.1		25.0 [b]		NaCl	0.50	[49]

(a) Size Exclusion Chromatography (SEC). (b) Viscometry.

Table I.1. Summary of the structural properties of A. *senegal*, A. *seyal* and HIC fractions of A. *senegal* (continuation)

Gum or fraction	M_w (g.mol^{-1})	M_w/M_n	R_H (nm)	R_g (nm)	[η] (mL.g^{-1})	Salt	Concentration (M)	Reference
A. *senegal* (continuation)	4.2 x10^5	1.9			16.3 [a]	NaCl	0.50	[47]
	6.2 x10^5		14.5	16.5 [b]		$NaNO_3$	0.10	[45]
	8.6 – 9.6 x10^5	1.3-1.6	12.5-15.5		25.1-27.9 [a]	NaCl	0.1-0.3	[55]
	4.0 - 7.7 x10^5		11.9 [a]		19.8 [b]	Water	--	[56]
AGP fractions								
HIC-F1	2.9 x10^5	1.3	10.7	11.3	16.2 [a]	$NaNO_3$	0.05	[4]
	3.8 x10^5		9.2 [c]			NaCl	0.50	[24]
	2.9 x10^5	1.3			16.2	$NaNO_3$	0.05	[26]
	2.7 x10^5	1.2			18.0	$NaNO_3$	0.05	[39]
	2.8 x10^5	1.3		8				[27]
HIC-F2	1.9 x10^6	1.3	34.4	30.0	70.7 [a]	$NaNO_3$	0.05	[4,40]
	1.5 x10^6 [b]		22.8 [c]			NaCl	0.50	[24]
	2.0 x10^6		27.5	45.0 [a]		NaCl	0.20	[25]
	2.3 x10^6	1.3 [a]				$NaNO_3$	0.05	[39]
	1.8 x10^6	1.3		33.0 [a]	73.5			[27]
HIC-F3	2.7 x10^5; 7.8 x10^5; 3.0 x10^5	1.1; 1.0; 1.0	16.1; 26.8	41.3; 25.3; 19.5	102.6; 64.4; 29.8 [a]	$NaNO_3$	0.05	[4,27]
	2.5 x10^5 [a]					NaCl	0.20	[24]
	1.8 x10^5	1.3	27.5	33.0	73.5 [a]	$NaNO_3$	0.05	[27]

(a) Size Exclusion Chromatography (SEC). (b) Viscometry. (c) Obtained from the translational diffusion coefficient (D_T).

1.3. Structure of AGPs obtained using Hydrophobic Interaction Chromatography (HIC) fractionation of A. *senegal*

As already indicated, A. gum can be seen as a continuum of macromolecules differing in sugar, protein and mineral composition, charge density, molar mass, size, shape and anisotropy [4,7,23-25,28,32,40,41]. Using, as others before, hydrophobic interaction chromatography, A. gum, and more specifically A. *senegal*, can be separated into three main fractions, Arabinogalactan (AG) or F1, Arabinogalactan-protein complex (AGP) or F2, and Glycoproteins (GP) or F3 [4,7,24]. These fractions were formerly named based on their protein content. However, studies have shown that all these fractions react to Yariv's reactant and have carbohydrate chains of arabinogalactan type II. Therefore, all macromolecular fractions can be strictly considered as AGP's [2,17]. In order to elude confusions, these fractions will be named in the following, based on their elution order, as HIC-F1, HIC-F2 and HIC-F3, then in theory from the most polar AGP (HIC-F1) to the less one (HIC-F3).

1.3.1 Structure of the HIC-F1 fraction

According to this separation methodology, A. gum is formed mainly by the HIC-F1 fraction. It represents around 85-90% of the total gum, has a low protein content (around 1%), a low molar mass (M_w) around $3x10^5$ $g.mol^{-1}$ and a hydrodynamic radius, R_H, of about 9 nm [2,4,24-26,38]. In addition, an intrinsic viscosity in the range from 16 - 18 $mL.g^{-1}$ has been reported [4,24,26,39]. This fraction is characterized by a higher amount of arabinose (Ara) as compared to the other fractions. Due to its content in uronic acids, it has been described as a weak polyelectrolyte [4]. Furthermore, it has been suggested that the high carbohydrate moiety of this fraction is responsible for the water sorption capacity of the gum [57]. Its hyperbranched and compact structure is typically at the origin of the low viscosity of A. gum dispersions [26].

Using small angle neutron scattering (SANS) and *ab initio* calculations, Sanchez et al (2008) proposed an original model for the structure of HIC-F1 fraction. A highly organized open disk structure with an inner-branched structure composed of sugars with a diameter of 20 nm and less than 2 nm of thickness was suggested (Figure I-2) [2,4,26]. In addition, semiaxes of 9.6x9.6x0.7 nm were obtained for the ellipsoid using a dummy atom model (DAM) [26].

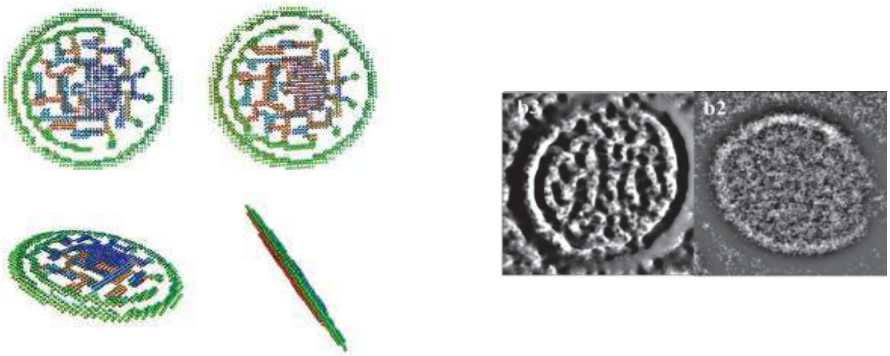

Figure I.2. Thin oblate ellipsoid model proposed for the HIC-F1 fraction. Images were obtained using the DAM method (left) and transition electron micrographs (TEM) after FFT filtering (right). The dimensions of the ellipsoid semiaxes: 9.6 x 9.6 x 0.7 nm. Adapted from: Sanchez et al. (2008) [26].

1.3.2. Structure of the HIC-F2 fraction

The HIC-F2 fraction represents around 9-15% of the total gum. It has a protein content of around 9-12% and a high molar mass (M_w), in the range of 1-3 x10^6 g.mol^{-1}. Regarding its hydrodynamic properties, intrinsic viscosity ([η]) around 70 mL.g^{-1} and R_H in the range of 23–35 nm, respectively, were reported [2,4,24,33,38,40,46,47,58-60]. It has a highly branched and compact structure with carbohydrate blocks that could have a thin oblate morphology [25]. This feature is a hypothesis that has not been confirmed experimentally. In addition, the protein moiety contains molecular secondary structures of the type polyproline II, β-sheets, β-turns and disordered structures, but apparently it does not contain α-helices [4]. The high M_w of HIC-F2 and the relatively high protein content play an important role in the good emulsification, stabilization and unusual observed thixotropic behavior of A. gums dispersions, mainly due to its surface properties [61] and capacity to form aggregates [2,62]. However, it denatures upon heating losing its emulsification properties and reducing its viscosity [33]. Presence of aggregates has been reported in this fraction [40,41], suggesting weak intermolecular attractive forces between protein moieties or carbohydrate residues [25,40].

Three models have been proposed to explain the structure of HIC-F2: the 'wattle blossom', the 'hairy rope' and the 'self-similarity' models. The 'wattle blossom' model was initially proposed by Fincher et al (1983) [63] and was used to describe the structure of plant AGPs (Figure I.3). It suggests that the HIC-F2 fraction is formed by large carbohydrates units with

a M_w of $2x10^5$ $g.mol^{-1}$ which are covalently bonded to a common polypeptide chain [34,63]. Later studies, shown the presence of smaller carbohydrate blocks of 4.5x $x10^4$ $g.mol^{-1}$ linked to serine and hydroxyproline [25]. In addition, two folded polypeptide chains with molar masses corresponding to 250 and 45 amino acids residues were reported [25].

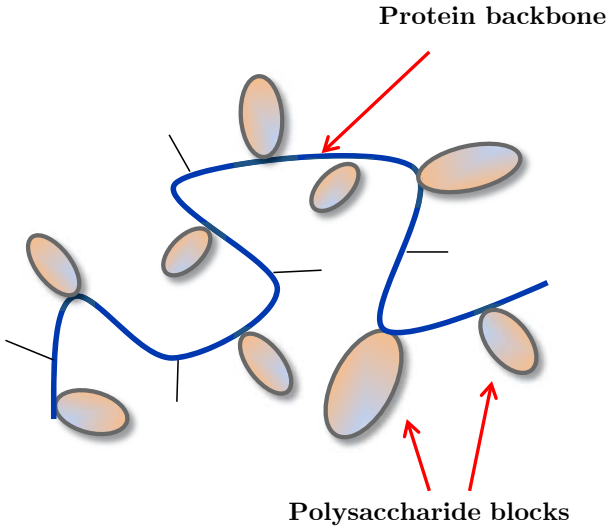

Figure I.3. 'Wattle blossom' model proposed for the HIC-F2 fraction. Adapted from: Mahendran et al. (2008) [25].

The 'twisted-hairy rope' model was proposed by Qi et al. (1991)[64]. Using TEM micrographs, a rod like structure for the HIC-F2 fraction was suggested (Figure I.4). The proposed structure includes a semi-flexible polypeptide backbone of 150 nm formed of about 400 amino acids with small carbohydrate blocks attached via hydroxyproline along the chain. The carbohydrate blocks are formed of around 30 sugars residues with M_w around $6x10^3$ $g.mol^{-1.}$ The sidechains are constituted of 12 galactose residues with short side-branches of glucuronic acid, rhamnose and arabinose [64].

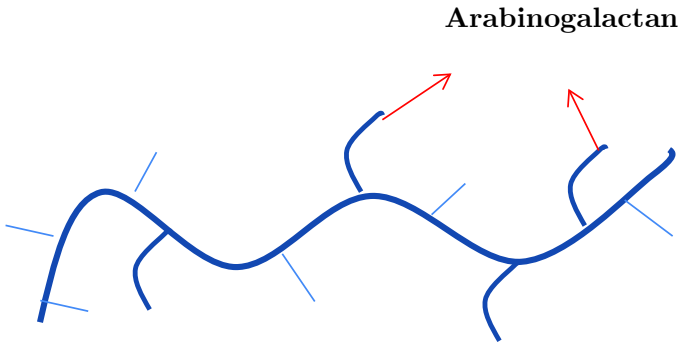

Figure I.4. 'Twisted hairy rope' model proposed for the HIC-F2 fraction. Adapted from Qi et al. (1991) [64].

The self-similarity model was proposed by Renard et al. in 2014 (Figure I.5) [27,41]. In this study, the HIC-F1 and HIC-F2 fractions were subjected to an enzymatic degradation using different enzymes. The results showed that the HIC-F1 fraction was not affected. On the other hand, HIC-F2 showed a decrease on its M_w but without strong effect of its conformation, suggesting that this fraction is composed of smaller units forming a self-similar structure. Regardless of the enzyme used, the units showed a similar triaxial ellipsoid conformation (Figure I.5), with different M_w and dimensions. In addition, it was suggested that the branches are composed of two blocks, the first one being a short chain composed of 45 amino acids with M_w of $4x10^4$ $g.mol^{-1}$, the second chain being a five-fold repetition of the first, with 250 amino acids and M_w of $2x10^5$ $g.mol^{-1}$ [27].

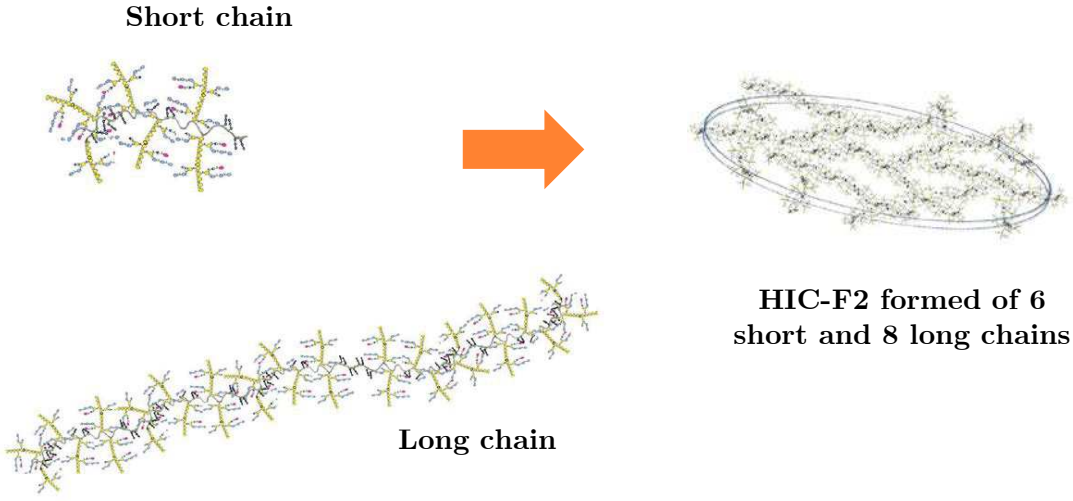

Figure I.5. Self-similarity model proposed for the HIC-F2 fraction. The dimensions of the ellipsoid semiaxes: 58 x 86 x 1.2 nm. Adapted from Renard et al. (2014)[27].

1.3.3. Structure of the HIC-F3 fraction

The HIC-F3 fraction is the minor component of A. gum and comprises around 1-2% of the total gum. This fraction is rich in proteins (25-50%) [28,34] and it is formed of at least three different macromolecular populations. It has a weight-molar mass, M_w, ranging between $2x10^5$ and $3x10^6$ $g.mol^{-1}$ and hydrodynamic radius in the range of 15-30 nm [2,4,24,28]. In addition, it has a lower content of hydroxyproline and serine than HIC-F1 and HIC-F2 [2,4].

The structure of HIC-F3 was analyzed using SAXS and TEM (Figure I.6). Micrographs revealed a mixture of a great number of monomers with ring-like shapes and long branches, and supramolecular assemblies. Performing microscopic imaging with HIC-F3, and with all gums and fractions, is a highly difficult because of the surface effects of AGPs that adsorb easily onto the use microscopy grids and form a macromolecular layer. SAXS highlighted the triaxial ellipsoidal morphology of AGPs and thin objects with 7-9 nm diameters were thus identified. The most remarkable feature of all these micrographs was the presence of ring-like objects. These ring-like objects were also observed with HIC-F2. Finally, the molecular structure of the protein moiety was composed by β-sheets, β-turns, polyproline II and α-helices. We then noted a difference in the averaged distribution of secondary structures between HIC-F2 and HIC-F3 [28].

The increased amount of protein and hydrophobic amino acids (glycine, valine, leucine and phenylalanine) contributes to a great extent to the self-assembly properties of HIC-F3 [2,4]. In addition, this fraction does not rehydrate easily, due to a low water affinity which contributes to its increased non polar characteristic [2,41].

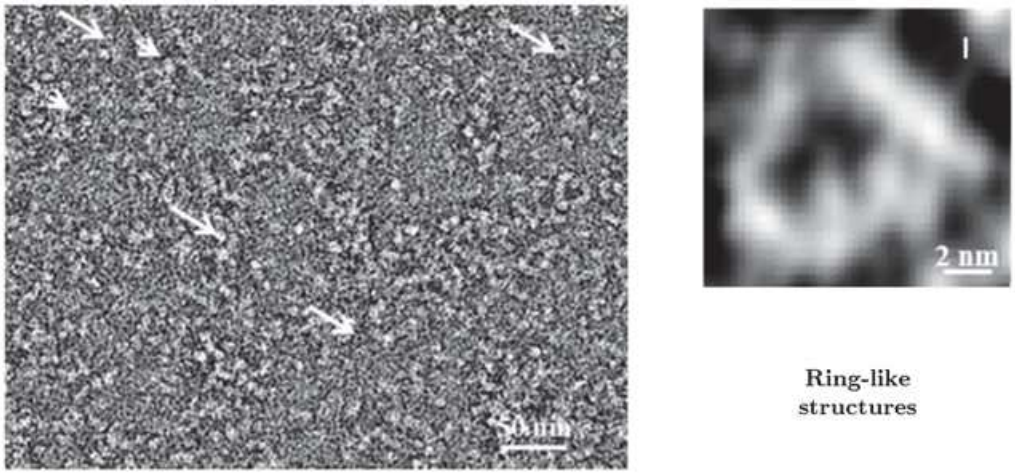

Figure I.6. TEM micrographs of the structure of the HIC-F3 fraction. The dimensions of the ellipsoid semiaxes: 26.9 x 8.2 x 0.8 nm. Adapted from Renard et al. (2014)[28].

1.4. Hydration properties of biopolymers

1.4.1 Generalities

Water is present in all living organisms, then it strongly impacts all biological functions as well as physicochemical properties and structure of biomolecules [65-69]. In addition, the extent of hydration directly influences the hydrodynamic properties (e. g. friction coefficient and intrinsic viscosity) of macromolecules [70]. For instance, the hydration effect on the crosslinking of collagen has been found to play a role on the biomechanical properties of the cornea [69]. Other important biopolymer properties influenced by the hydration are, for instance, molecular flexibility, conformational changes, adsorption, assembly ability, transport properties, viscoelasticity, and catalytic activity of enzymes [69,71,72].

Water is able to interact with charged and polar groups of biomolecules, mainly by forming hydrogen bonds. Other type of interactions includes electrostatic and hydrophobic effects [66,72]. Non polar groups do not interact directly with water molecules but perturb the water structure, especially its compressibility. Each water molecule is able to form up to four hydrogen bonds with neighboring water molecules. Then, a dynamic water matrix is formed by constant breaking and formation of new hydrogen bonds. This process is extremely rapid and occurs in a time range of about 1-5 ps [72]. Once a solute molecule is introduced in water, its dynamics is perturbed [72-74]. A schema of the hydration of a solute molecule in water is presented in Figure I.7.

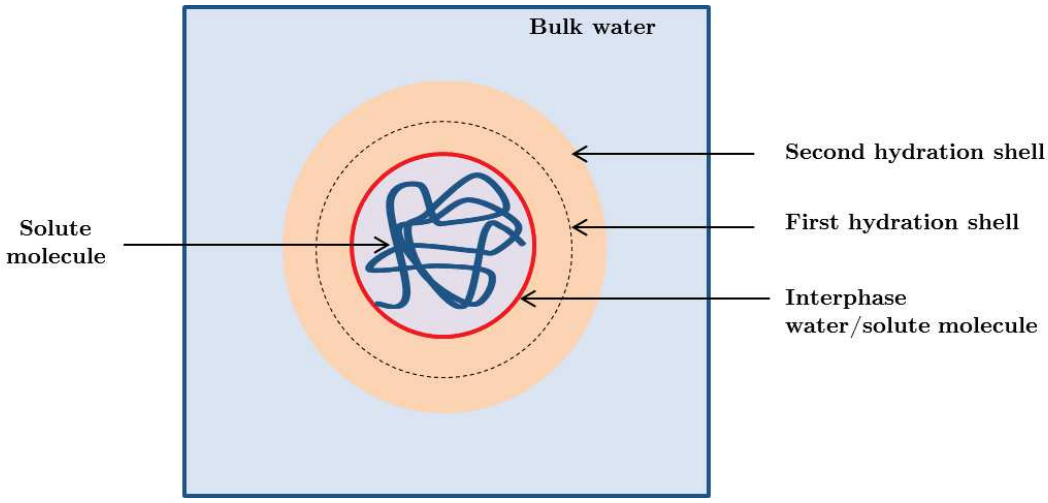

Figure I.7. Schematic representation of the hydration shell of a solute molecule dispersed in bulk water

The water that does not interact with the molecule itself is known as bulk water. This water is used to assess the changes in the hydration properties induced by the solute molecule and corresponds to the majority of water found in an aqueous dispersion or in living cells. For instance, studies performed in E. coli cells using nuclear magnetic resonance (NMR) found that around 80% of cell water corresponded to bulk water [72]. The hydration shell or 'interfacial water' is defined as a layer or layers of water which surround the solute molecule and interacts with it. It includes all water molecules which its physicochemical properties have been perturbed by the presence of the solute molecule [72,75]. Studies on proteins have found that the main differences between interfacial and bulk water are higher density, slower dynamics, a weaker structured hydrogen bond network and different viscosity at the protein surface [73,75]. The thickness of the hydration shell depends on the nature of the solute. For instance, hydrophilic molecules tend to attract water meanwhile hydrophobic molecules will repel it. In addition, a dependence of hydration with the molecular surface in contact with water has been found [63]. Furthermore, the heterogeneity of the solute plays a role on its hydration properties [70,72,76]. Studies performed in proteins showed evidence that water molecules are not evenly distributed along the solute surface, but rather attached via hydrogen bonds to specific locations [70,76]. Therefore, for the same molecule, the hydration shell can change with the solute conformation. Typically, the thickness of the hydration shell is determined by calculating the number of water molecules affected by the presence of the solute. This parameter is known as hydration number, n_h, it can be calculated using

molecular dynamics, simulations or using the solvent accessible surface [77]. Another way to access this kind of information is using volumetric properties (static and dynamic), which will be further discussed.

1.4.2. Classification of hydration water

In a general way, water in biopolymer systems can be categorized into two or three types depending on the definition used. For instance, hydration obtained via densitometry, ultrasound measurements and viscometry can be categorized like bound water if its properties such as partial specific volume (v_s°) and partial adiabatic compressibility (β_s°) are lower than that of bulk water [78]. However, it depends on the distance of the water molecule from the solute surface, then on the strength of water-molecule interactions. For instance, water molecules present in the first hydration layer have a slower orientational/translational dynamic than bulk water. Therefore, they are strongly bound to the molecule (strongly bound water). Water molecules present in the second hydrating layer do not have direct contact with the solute molecule, thus they do not form hydrogen bonds with the molecule, but their properties are still perturbed by the solute presence (weakly bound water) [78]. In this two state-water system, the physical properties of weakly bound water are close to those of bulk water [77]. Therefore, only two types of water are practically considered, bound water from the first hydration shell (hydrating water) and bulk water. For instance, for the case of the glucose molecule, approximately 8-10 water molecules are considered as strongly bound water, meanwhile up to 40 water molecules can exist in the glucose matrix as weakly hydrated molecules [78,79]. As already explained, the bound water can be described using the hydration number. In the case of monosaccharides such as arabinose and galactose, which are the main sugars found in A. gums, the n_h is 13.0 and 16.2 mol H_2O/mol sugar, respectively. For globular proteins, e. g. hemoglobin and trypsin, the n_h is 1.4 and 2.5 mol H_2O/mol protein, respectively [77].

On the other hand, when hydration is estimated via calorimetric methods (e. g. DSC and TGA), water can be categorized into three types: free water, bound freezing water and bound non-freezing water [78,80]. In this case, free water behaves as bulk water and is not bound to the solute molecule. The freezing water is bound water with weak interactions with the molecule. The non-freezing water is tightly bound to the molecule [66,67,71,81] and remains

unfrozen at lower temperatures than the freezing temperature of bulk water [78,82]. Structurally, this water is an integral part of the molecule itself.

In this study we will use a two-state model, where the bound water refers to all water molecules physicochemically perturbed by the presence of the solute, and bulk water as all water molecules whose physicochemical properties have not been perturbed by the solute.

1.4.3. Acacia gums

In spite of the importance of hydration on the functional properties, information regarding the hydration properties of A. gums is scarce. The observed hydrophilic nature of AG has probably not motivated many studies on the hydration properties. Studies have been performed mostly in A. *senegal* using differential scanning calorimetry (DSC). They highlight the capacity of A. gums to retain a larger amount of non-freezing water as compared to other polysaccharides [71]. The total amount of water at saturation was about 3-4 g H_2O/g AGP with very low amount of free water [57]. Total freezing bound water was around 2.5 g H_2O/g AGP and non-freezing water was around 0.5 g H_2O/g AGP bound water [2,71,83]. Obviously, the water retaining capacity is enhanced by the presence of ionic groups which are able to fix water molecules in their matrix [71,84]. In addition, the DSC curves showed that non-freezing water is first bounded to the hydrophilic groups in the carbohydrate moiety. Therefore, this moiety is likely to be responsible for the good sorption capacity of A. gums [85]. However, a possible effect of the protein content on water restraining capacity of A. gums was suggested [66]. In a subsequent study, a hydration of 0.9 g water/g for Ca gum and 1.1 g water/g for Na gum was measured using a membrane equilibrium method [86]. A minimal value of 0.6-0.7 g water/g of gum was found by a cryoscopic method.

1.5. Volumetric Properties

1.5.1. Generalities

In general, solubility and interfacial properties of biopolymers, the two most important functional properties of A. gums, are determined both by intrinsic properties of macromolecules (composition, accessibility and spatial division of charged, polar and nonpolar atomic groups, chain density, molar mass, conformation, flexibility) and their ability to dynamically interact with the solvent. On the other hand, volumetric properties are thermodynamic properties that have been linked to solute intrinsic molecular properties and solute-solvent interactions, more specifically solute flexibility and hydration [87]. Then,

volumetric properties of biopolymers are important determinant of their functionality. The main advantage of volumetric related experimental methods, over other methods to obtain hydration such as x-ray crystallography and nuclear magnetic spectroscopy (NMR) or dielectric spectroscopy, is that they are non-selective, allowing a complete look of the entire water molecule population perturbed by the solute [88,89]. Another advantage is that they allow the description of thermodynamic macroscopic properties, such as the partial specific volume, v_s^o, and adiabatic compressibility β_s^o, in terms of microscopic events [89]. Main efforts in the past have been focused on proteins, amino acids and nucleic acids, but also on polysaccharides and sugars. Details will be given in Chapter II. In the following, we will provide a summary of the main definitions commonly used in volumetric studies.

1.5.2. Partial specific volume

The partial specific volume, v_s^o ($cm^3.g^{-1}$), is the change in volume of the system caused by the introduction of a single solute molecule at constant pressure and temperature [90-93]. It represents the thermodynamic volume of a solute. The experimental determination of changes on the volume is a difficult task. Then, v_s^o is calculated using the apparent volume, which is defined as the difference between the total volume of the solution and the solvent alone (without solute) at the same temperature and pressure [91]. This determination is possible since at infinite dilution they have the same value [93]:

$$v_s^\circ = \frac{1}{\rho_0} \lim_{c \to 0} \frac{\rho - \rho_0}{C} \quad \text{(I.1)}$$

where ρ_0 and ρ are the density of the solvent and dispersion ($g.cm^{-3}$) and C is the concentration of the solute ($g.cm^{-3}$). Values in the range of 0.69-0.76 $cm^3.g^{-1}$ are characteristic of proteins and amino acids [93], for neutral and modified polysaccharides classical values are around 0.60-0.62 and 0.41-0.72 $cm^3.g^{-1}$, respectively [94]. For glycoproteins v_s° around 0.58-0.68 $cm^3.g^{-1}$ have been reported. Furthermore, presence of ions (e.g. Na^+, K^+, Li^+) are known to reduce the partial specific volume [94].

1.5.3. Compressibility

The adiabatic (Ks, Pa^{-1}) and isothermal compressibility (K_T, Pa^{-1}) of isotropic solutions (e.g. aqueous solutions) offer a more in depth look to the solute-solvent interactions because they can be related to the molecular flexibility [95-97]. They are defined as the adiabatic or isothermal derivative of the volume [98,99] :

$$K_T = \beta_T V = -\left(\frac{\partial V}{\partial P}\right)_T \quad (I.2)$$

$$K_S = \beta_S V = -\left(\frac{\partial V}{\partial P}\right)_S \quad (I.3)$$

where β_T (Pa^{-1}) and β_s (Pa^{-1}) are the isothermal and adiabatic compressibility coefficients. The adiabatic compressibility is used in most studies mostly due to difficulties associated to the determination of K_T [93]. The former is determined using ultrasonic methods (e.g. sonodensimetry), meanwhile K_T is obtained using pressure perturbation calorimetric methods (PPC).

The coefficient of partial specific adiabatic compressibility, β_s, is defined as the change in the partial specific volume respect to the pressure of the system caused by the addition of a solute molecule [93]. It can be calculated using the Newton-Laplace equation: $\beta_S = \frac{1}{\rho u^2}$, where ρ is the density ($g.cm^{-3}$) and u is the sound velocity ($m.s^{-1}$) [93,95,100,101].

The partial specific adiabatic compressibility coefficient, β_s^o, can be calculated using the expression [93,100,102]:

$$\beta_S^o = -\left(\frac{1}{v_s}\right)\lim_{c\to 0}\frac{1}{C}\left[\frac{\beta_s}{\beta_o} - \frac{\rho - C}{\rho_o}\right] \quad (I.4)$$

where β_s and β_o are the adiabatic compressibility coefficients of dispersion and solvent. In a general way, characteristic β_s° of globular and fibrous proteins are in the range of $-41x10^{-11}$ to $11x10^{-11}$ Pa^{-1}, respectively [93,102]. Meanwhile, for polysaccharides (e. g. dextran and its derivatives and carrageenan) characteristic β_s° are in the range of $-70x10^{-11}$ to $-20x10^{-11}$ Pa^{-1} [103-107]. Positive values of β_s° indicate a larger interior compressibility of the molecule, then a higher flexibility [93,102]. Meanwhile, negative values of β_s° are associated to highly hydrated molecules such as polysaccharides but also small subunits such as sugars and amino acids.

1.5.4. Microscopic description of the volumetric properties

According to the scaled particle theory, the molecular interactions influencing the system are the result of the interactions of the solute molecule and the solvent [108]. Then, the main volumetric properties, partial specific volume and adiabatic compressibility, can be described using molecular contributions or 'microscopic events' [109]. In this line, v_s° can be decomposed into three main individual contributions, the cavity contribution (v_C), the interaction volume (v_I) and the ideal term (β_{T0} RT) [110-112]:

$$v_s^\circ = v_C + v_l + \beta_{TO}RT \quad (I.3)$$

The cavity contribution, v_C, refers to the volume created in the solvent to accommodate the solute molecule, which is formed due to repulsive forces on the solvent [112]. In other words, it is the volume inaccessible by the solvent [113]. This contribution includes the volume of the solute itself or molecular volume (v_M) and a layer of constant thickness between the solute molecule and the solvent molecules, formed as a consequence of mutual molecular vibrations of the solvent and the surface of the solute [111,113]. The latter is also known as thermal volume (v_T) [110,111,114]. The molecular volume ($v_M = v_{vdw} + v_{void}$) is formed by the volume of the atoms that make up the core of the molecule or Van der waals volume (v_{vdw}) and the volume of voids in the interior of the solute formed due to imperfect packing (v_{void}) [112,114]. The interaction volume, v_l, refers to the water molecules that participate on the solvation [113]. Depending on the nature of the solute, water molecules interact with the solute through electrostriction, hydrogen bond and hydrophobic hydration for charged, polar and non-polar molecules, respectively [114]. Then, this contribution is described by the relation $v_l = n_h\ (v_h^\circ + v_o^\circ)$, where n_h is the hydration number, which represents the number of water molecules perturbed by the presence of the solute, and v_h° and v_o° are the partial specific volumes of water on the hydration shell and bulk, respectively [109]. Finally, $\beta_{TO}RT$ is known as the ideal term, it represents the movement of the solute due to their translational degree of freedom [113]. It is constituted by the isothermal compressibility (β_{TO}), the ideal constant (R) and the temperature. This term account normally for 1.1 cm^3.mol, thus for molecules with high molar mass is negligible [111,112]. In summary, the partial specific volume can be written using the following expression:

$$v_s^\circ = v_M + v_T + n_h(v_h^\circ - v_o^\circ) \quad (I.3)$$

In a general way, the molecular contribution (v_M) represents about 90% of the partial specific volume. Meanwhile, the thermal volume (v_T) and interaction contribution (v_l) represents the other 10% [111]. The latter is a negative contribution, which has been explained due to the lower volume of interacting solvent molecules as compared to the bulk [77,87,99,111].

Similar expressions can be obtained for the other volumetric properties, e.g. partial specific adiabatic compressibility and partial isothermal compressibility.

$$K_s^\circ = K_M + n_h(K_h^\circ - K_o^\circ) \quad (I.4)$$

Where K_M is the partial intrinsic adiabatic compressibility and K_h° and K_o° are the partial adiabatic compressibilities of water in the hydration shell and bulk, respectively.

In conclusion, the volumetric properties can be seen as the sum of two main contributions, the molecular and hydration contributions. The sign of the partial adiabatic compressibility (K_s) or partial adiabatic compressibility coefficient (β_s°) can be seen a competition between the voids present in the molecule, which is a positive contribution, and the negative contribution of the hydration. Then a positive value of K_s or β_s° indicates the overcome of the molecular contribution over the interaction contribution.

1.6. Hydrodynamic Properties

1.6.1. Generalities

Hydrodynamic properties refer to all properties which involve the movement of macromolecules in solution. They are obtained through non-destructive and rapid methods which are their main advantages [115]. The most commonly studied hydrodynamic properties are intrinsic viscosity ($[\eta]$), translational diffusion coefficient (D_T) and the sedimentation coefficient (S_o) [115]. From these properties, important structural parameters such as molar mass, size, and conformation can be obtained [116]. In addition, other important macromolecular characteristics such as hydration and flexibility can be also approached. In the following, we will provide a summary of the main definitions. More detailed information is provided in Chapter III.

1.6.2. Intrinsic viscosity

One of the most important hydrodynamic properties of biomolecules is the viscosity (η, mPa.s), which is a measure of its resistance to flow. It is then a function of the internal friction of the molecule [117]. According to the Newton's viscosity law, η is the ratio of the applied shear stress to the shear rate. Then, if a fluid obeys this law it is called a 'Newtonian' fluid [117]. The relative and specific viscosities of a biopolymer in relation to the solvent are given by:

$$\eta_{rel} = \frac{\eta}{\eta_o} \tag{I.5}$$

$$\eta_{sp} = \eta_{rel} - 1 = \frac{\eta - \eta_o}{\eta_o} \tag{I.6}$$

Where η_{rel} and η_{sp} are the relative and specific viscosities (adimensional) and η_o is the viscosity of the solvent.

The intrinsic viscosity ($[\eta]$, $mL.g^{-1}$) is a measure of the hydrodynamic volume (V_H) physically occupied by the isolated biopolymer molecule [117]. It depends on the structure and molar mass of the polymer and the nature of the solvent. However, it is theoretically independent of the biopolymer concentration [117], then it is measured at infinite dilution [118,119]. It can be obtained from the extrapolation of the reduced viscosity ($\eta_{red}=\eta_{sp}/C$)[118] :

$$[\eta] = \lim_{C\to 0} \eta_{red} = \lim_{C\to 0} \frac{\eta - \eta_o}{\eta_o C} \quad (I.7)$$

The intrinsic viscosity can be described using two main structural contributions, the viscosity increment and the swollen hydrated volume of the molecule [120]:

$$[\eta] = \nu . V_{sw} \quad (I.8)$$

where ν is the viscosity increment (dimensionless), which is known as Einstein or Simha-Saito parameter. It depends mainly on the particle shape or anisotropy. According to the theory developed by Einstein, ν takes a value of 2.5 [115,121-123]. This value is strictly valid only for homogeneous hard spheres. In the case of anisotropic molecules, ν takes higher values [115]. Furthermore, for ellipsoidal objects it can be calculated providing that its dimensions are known [115,121-123]. The swollen specific volume refers to the hydrated volume of the molecule. It is then directly related to the hydration number (n_h) through $V_{sw} = v_s^o + (n_h/\rho_o)$, where v_s^o is the partial specific volume and ρ_o is the density of the solvent [115].

1.6.3. Translational diffusion coefficient

The translational diffusion coefficient (D_T) is used to evaluate the mean square displacement of a macromolecule from its center of mass (ΔR_{CM}) in function of the time (t) caused by the Brownian motion of the macromolecule in solution [124]:

$$\langle (\Delta R_{CM})^2 \rangle = 6 D_T t \quad (I.9)$$

D_T is commonly determined using dynamic light scattering (DLS) methods by measuring the temporal evolution of scattered light intensity in particle dispersions. It can be also obtained using diffusion ordered nuclear magnetic spectroscopy (DOSY-NMR). It depends on the

particle size, since smaller particles diffuse faster. Then, the hydrodynamic radius (R_H) can be obtained from the Stokes-Einstein relation [122,125,126]:

$$D_T = \frac{k_B T}{6\pi\eta R_H} \quad \text{(I.10)}$$

where k_B is the Boltzman's constant (1.38×10^{-23} $m^2.kg.s^{-2}.K^{-1}$), η is the dynamic viscosity of the solvent (mPa.s) and T is the absolute temperature (K).

1.6.4. Sedimentation coefficient

The sedimentation coefficient (S_o, S) is a hydrodynamic property characteristic of a macromolecule [127]. It is defined as the rate of migration of a molecule in function of an applied centrifugal force [128]. The sedimentation coefficient is commonly obtained using analytical ultracentrifugation by measuring the displacement of the sedimentation boundary (r) caused by the depletion of the biopolymer. The rate of migration and diffusion of a molecule in dilute conditions is measured by the Lamm equation [128,129]:

$$\left(\frac{\partial C}{\partial t}\right) = -\left(\frac{1}{r}\right)\frac{\partial}{\partial r}\left[r\left(C\, S_o\, \omega^2 r - D_T \frac{\partial C}{\partial r}\right)\right] \quad \text{(I.11)}$$

where C ($g.cm^{-3}$) is the concentration at the radial distance r (cm), t is the centrifugation time (s) and ω is the velocity of the rotor (rpm). The sedimentation coefficient depends of the hydrodynamic volume of the molecule, since large molecules will exhibit a faster sedimentation velocity [129-131]. Then, the hydrodynamic radius can be obtained.

Finally, using the Svedberg equation, the sedimentation and translational diffusion coefficients, the weight-averaged molar mass (M_w) of the biopolymer can be estimated [132]:

$$M_w = \frac{s_0 RT}{D_0(1-\bar{v}\rho_0)} \quad \text{(I.12)}$$

2. Aim and Scientific Approach

A. gums are widely used in food (and non-food) industry, mainly in the beverage industry as emulsifier and in confectionaries as thickening agent. These gums are studied since more than two centuries and despite these efforts, there is still a lack of information on their structure and determinants of their physicochemical properties. More specifically, the architecture of AGPs and their conformation, flexibility and hydration properties remain to be confirmed or

determined. Indeed, its intrinsic structural properties and hydration, in relation to chemical composition and solvent affinity, determine its functional properties.

The main objective of this thesis was to study the volumetric properties of AGPs in solution, at different ionic strengths and temperature, so as to provide some new insights about the relationship between the composition, structure and physicochemical properties of Acacia gums exudates. The study was performed using the two commercially available Acacia gum species, A. *senegal* and A. *seyal*, but also AGP fractions of the former obtained via hydrophobic interaction and ionic exchange chromatographies. These fractions encompass AGPs differing in their M_w, affinity for the solvent and level of aggregation.

The first specific objective was to study the volumetric hydrostatic properties of A. gums and AGP fractions, more specifically the partial specific volume (v_s°) and partial specific adiabatic compressibility (β_s°). These thermodynamic parameters were calculated from sound rate and density measurements of gums and AGP dispersions. They give an idea about the balance between unhydrated volume, hydration and flexibility of macromolecules.

The second specific objective was to study the main hydrodynamic properties, intrinsic viscosity ($[\eta]$), translational diffusion coefficient D_T and sedimentation coefficient (S_o) of A gums. Measurements were carried out using viscometry, dynamic light scattering and NMR, and analytical ultracentrifugation. The different approaches will give in particular a more precise view of AGP hydrodynamic radius, which is a useful parameter while difficult to measure on polydisperse polyelectrolyte systems. In addition, a dynamic hydration number can be estimated and compared to the static parameter extracted from volumetric measurements.

In addition to these two major objectives, we also systematically study structural parameters (M_w, M_n) and conformation of A. gums and AGP fractions through SEC-MALS experiments. Conformation was mainly studied by analysis of the power-law exponent of the M_w dependence of $[\eta]$, that is directly related to macromolecule affinity for the solvent.

3. Outline of the thesis

This manuscript is organized in six chapters, based on three research articles, one of which has already been published and the other two are in preparation.

- **Chapter I:** presents a general introduction and the main objectives of the research study.
- **Chapter II:** presents a study of the volumetric properties of Acacia gums: Acacia *senegal* and Acacia *seyal*, and the macromolecular fractions of the former separated via hydrophobic interaction chromatography (article published in Colloids and Interfaces).
- **Chapter III:** presents a study of the main hydrodynamic properties of A. gums and the macromolecular fractions of A. *senegal* separated using hydrophobic interaction and ionic exchange chromatography (article in preparation for Colloids and Interfaces).
- **Chapter IV:** presents a study of the effect of changes of the temperature of the system on the volumetric and hydrodynamic properties of A. gums and macromolecular fractions of A. *senegal* (article in preparation).
- **Chapter V:** presents the general conclusions and perspectives of the research study.

4. References

1. FAO. Gum arabic. Food and Nutrition Paper 52 1999
2. Sanchez, C.; Nigen, M.; Mejia Tamayo, V.; Doco, T.; Williams, P.; Amine, C.; Renard, D. Acacia gum: History of the future. *Food Hydrocolloids* **2018**.
3. Williams, P.A.; Philips, G.O. Gum arabic. In *Handbook of hydrocolloids*, G. O. Philips, P.A.W., Ed. Boca Raton: CRC Press: 2000; pp 155-168.
4. Renard, D.; Lavenant-Gourgeon, L.; Ralet, M.C.; Sanchez, C. Acacia *senegal* gum: Continuum of molecular species differing by their protein to sugar ratio; molecular weight and charges. *Biomacromolecules* **2006**, 2637-2649.
5. Idris, O.H.M.; Williams, P.A.; Phillips, G.O. Gum arabic's journey from tree to end user. In *Gum arabic*, Kennedy, J.; Williams, P., Eds. RSC Publishing: Cambridge, 2012.
6. Verbeken D.; Dierckx S.; K., D. Exudate gums: Occurence, production, and applications. *Applied Microbiology Biotechnology* **2003**, *63*, 10-21.
7. Islam, A.M.; Phillips, G.O.; Sljivo, A.; Snowden, M.J.; Williams, P.A. A review of recent developments on the regulatory, structural and functional aspects of gum arabic. *Food Hydrocolloids* **1997**, *11*, 493-505.

8. Cecil, C.O. Gum arabic. *Saudi Aramco World* **2005**, *56*, 36-39.
9. Wickens, G.E. Part three: The role of acacia in the rural economy. Role of Acacia species in the rural economy of dry Africa and the Near East In addition, A. gum is important for the economy of the rural populations of the sub-sahelian area (10th July), 1995
10. Wadley, L.; Hodgskiss, T.; Grant, M. Implications for complex ccognition from the hafting of tools with compound adhesives in the middle stone age, south africa. *PNAS* **2009**, *106*, 9590-9594.
11. Chevalier, A. Sur la production de la gomme arabique en afrique occidentale. *Revue de Botanique Apliquée & d'Agriculture Coloniale* **1924**, *4*, 256-263.
12. Scott, D. Ancient egyptian pigments: The examination of some coffins from the san diego musseum of man. *MRS Bulletin* **2010**, *35*, 390-396.
13. Caius, J.F.; Radha, K.S. The gum arabic of the bazaars and shops of bombay. *Journal of Bombay Natural History Science* **1942**, *41*, 261-271.
14. Nussinovitch, A. *Plant gum exudates of the world: Sources, distribution, properties and aplication*. CRC Press: Boca Raton (USA), 2010.
15. Akiyama, Y.; Eda, S.; Kato, K. Gum arabic is a kind of arabinogalactan protein. *Agric. and Biol. Chem.* **1984**, *48*, 235-237.
16. Tan, L.; Showalter, A.M.; Egelund, J.; Hernandez-Sanchez, A.; Doblin, M.S.; Bacic, A. Arabinogalactan-proteins and the research challenges for these enigmatic plant cell surface proteoglycans. *Frontiers in Plant Sci.* **2012**, *3*, 1-10.
17. Lamport, D.; Varnai, P.; Seal, C.E. Back to the future with the agp-ca^{2+} flux capacitor. *Annals of Botany* **2014**, *114*, 1069-1085.
18. Liu, C.; Mehdy, M.C. A nonclassical arabinogalactan protein gene highly expressed in vascular tissues, agp31, is transcriptionally repressed by methyl jasmonic acid in arabidopsis. *Plant Physiology* **2007**, *145*, 863-874.
19. Ellis, M.; Egelund, J.; Schultz, C.J.; Bacic, A. Arabinogalactan-proteins: Key regulators at the cell surface? *Plant Physiol* **2010**, *153*, 403-419.
20. Seifert, G.J.; Roberts, K. The biology of arabinogalactan proteins. *Annual Review of Plant Biology* **2007**, *58*, 137-161.
21. Clarke, A.; Gleeson, P.; Harrison, S.; Knox, R.B. Pollen-stigma interactions: Identification and characterization of surface components with recognition potential. *Proceedings of the National Academy of Sciences of the United States of America* **1979**, *76*, 3358-3362.
22. Qu, Y.; Egelund, J.; Gilson, P.R.; Houghton, F.; Gleeson, P.A.; Schultz, C.J.; Bacic, A. Identification of a novel group of putative arabidopsis thaliana β-(1,3)-galactosyltransferases. *Plant Molecular Biology* **2008**, *68*, 43-59.
23. Anderson, D.M.W.; Stoddart, J.F. Studies on uronic acid materials. Part xv. The use of molecular-sieve chromatography on acacia *senegal* gum (gum arabic). *Carbohydrate Research* **1966**, *2*, 104-114.
24. Randall, R.C.; Phillips, G.O.; Williams, P.A. Fractionation and characterization of gum from acacia *senegal*. *Food Hydrocolloids* **1989**, *3*, 65-75.
25. Mahendran, T.; Williams, P.; Phillips, G.; Al-Assaf, S.; Baldwin, T. New insights into the structural characteristics of the arabinogalactan-protein (agp) fraction of gum arabic. *Journal of Agricultural and Food Chemistry* **2008**, 9269-9276.
26. Sanchez, C.; Schmitt, C.; Kolodziejczyk, E.; Lapp, A.; Gaillard, C.; Renard, D. The acacia gum arabinogalactan fraction is a thin oblate ellipsoid: A new model based on small-angle neutron scattering and ab initio calculation. *Biophysical Journal* **2008**, *94*, 629-639.
27. Renard, D.; Lavenant-Gourgeon, L.; Lapp, A.; Nigen, M.; Sanchez, C. Enzymatic hydrolysis studies of arabinogalactan-protein structure from acacia gum: The self-similarity hypothesis of assembly from a common builiding block. *Carbohydrate Polymers* **2014**, *112*, 648-661.
28. Renard, D.; Lepvrier, E.; Garnier, C.; Roblin, P.; Nigen, M.; Sanchez, C. Structure of glycoproteins from acacia gum: An assembly of ring-like glycoproteins modules. *Carbohydrate Polymers* **2014**, *99*, 736-747.
29. Williams, P.A. Structural characteristics and functional properties of gum arabic. In *Gum arabic*, The Royal Society of Chemistry: 2012; pp 179-187.
30. Anderson, D.M.W.; Bridgeman, M.M.E.; Farquhar, J.G.K.; McNab, C.G.A. The chemical characterization of the test article used in toxicological studies of gum arabic (acacia senegal (l.) willd). *International Tree Crops Journal* **1983**, *2*, 245-254.
31. Flindt, C.; Alassaf, S.; Phillips, G.; Williams, P. Studies on acacia exudate gums. Part v. Structural features of acacia

seyal. *Food Hydrocolloids* **2005**, *19*, 687-701.

32. Lopez-Torrez, L.; Nigen, M.; Williams, P.; Doco, T.; Sanchez, C. Acacia *senegal* vs. Acacia *seyal* gums – part 1: Composition and structure of hyperbranched plant exudates. *Food Hydrocolloids* **2015**, *51*, 41-53.
33. Williams, P.A.; Philips, G.O.; Randall, R.C. Structure-function relantionships of gum arabic. In *Gums and stabilizers for the industry 5*, IRL Press: 1990; pp 25-36.
34. Ali, B.H.; Ziada, A.; Blunden, G. Biological effects of gum arabic: A review of some recent research. *Food and Chemical Toxicology* **2009**, *47*, 1-8.
35. Anderson, D.M.W. The amino acid composition and quantitative sugar-amino acid relationships in sequential smith-degradation products from acacia polyacantha gum. *Food Additives & Contaminants* **1986**, *3*, 123-132.
36. Wang, Q.; Burchard, W.; Cui, S.W.; Huang, X.Q.; Philips, G.O. Solution properties of conventional gum arabic and a matured gum arabic (acacia (sen) super gum). *Biomacromolecules* **2008**, *9*, 1163-1169.
37. Dror, Y.; Cohen, Y.; Yerushalmi-Rozen, R. Structure of gum arabic in aqueous solution. *J. of Polym. Sci. Pol. Phys.* **2006**, *44*, 3265-3271.
38. Idris, O.H.M.; Williams, P.A.; Phillips, G.O. Characterisation of gum from acacia *senegal* trees of different age and location using multidetection gel permation chromatography. *Food Hydrocolloids* **1998**, 379-388.
39. Sanchez, C.; Renard, D.; Robert, P.; Schmitt, C.; Lefebvre, J. Structure and rheological properties of acacia gum dispersions. *Food Hydrocolloids* **2002**, *16*, 257-267.
40. Renard, D.; Garnier, C.; Lapp, A.; Schmitt, C.; Sanchez, C. Structure of arabinogalactan-protein from acacia gum: From porous ellipsoids to supramolecular architectures. *Carbohydrate Polymers* **2012**, *90*, 322-332.
41. Renard, D.; Garnier, C.; Lapp, A.; Schmitt, C.; Sanchez, C. Corrigendum to "structure of arabinogalactan-protein from acacia gum: From porous ellipsoids to supramolecular architectures" [carbohydr. Polym. 90 (2012) 322–332]. *Carbohydrate Polymers* **2013**, *97*, 864-867.
42. Assaf, S.; Phillips, G.; Williams, P. Studies on acacia exudate gums. Part i: The molecular weight of gum exudate. *Food Hydrocolloids* **2005**, *19*, 647-660.
43. Karamalla, K.A.; Siddig, N.E.; Osman, M.E. Analytical data for acacia senegal var. Senegal gum samples collected between 1993 and 1995 from sudan. *Food Hydrocolloids* **1998**, *12*, 373-378.
44. Cozic, C.; Picton, L.; Garda, M.-R.; Marlhoux, F.; Le Cerf, D. Analysis of arabic gum: Study of degradation and water desorption processes. *Food Hydrocolloids* **2009**, *23*, 1930-1934.
45. Gashua, I.B.; Williams, P.A.; Yadav, M.P.; Baldwin, T.C. Characterisation and molecular association of nigerian and sudanese acacia gum exudates. *Food Hydrocolloids* **2015**, *51*, 405-413.
46. Al-Assaf, S.; Phillips, G.; Williams, P. Studies on acacia exudate gums: Part ii. Molecular weight comparison of the vulgares and gummiferae series of acacia gums. *Food Hydrocolloids* **2005**, *19*, 661-667.
47. Elmanan, M.; Al-Assaf, S.; Phillips, G.O.; Williams, P.A. Studies on acacia exudate gums: Part vi. Interfacial rheology of acacia *senegal* and acacia *seyal*. *Food Hydrocolloids* **2008**, *22*, 682-689.
48. Siddig, N.; Osman, M.; Alassaf, S.; Phillips, G.; Williams, P. Studies on acacia exudate gums, part iv. Distribution of molecular components in in relation to. *Food Hydrocolloids* **2005**, *19*, 679-686.
49. Hassan, E.A.; Al-Assaf, S.; Phillips, G.O.; Williams, P.A. Studies on acacia gums: Part iii molecular weight characteristics of acacia *seyal* var. Seyal and acacia *seyal* var fistula. *Food Hydrocolloids* **2005**, *19*, 669-677.
50. Picton, L.; Bataille, I.; Muller, G. Analysis of a complex polysaccharide (gum arabic) by multi-angle laser light scattering coupled on-line to size exclusion chromatography and flow field flow fractionation. *Carbohydrate Polymers* **2000**, *42*, 23-31.
51. Vandevelde, M.-C.; Fenyo, J.-C. Macromolecular distribution of acacia senegal gum (gum arabic) by size exclusio chromatography. *Carbohyd. Polym.* **1985**, *5*, 251-273.
52. Swenson, H.A.; Kaustinen, H.M.; Kaustinen, O.A.; Thompson, N.S. Structure of gum arabic and its configuration in solution. *Journal of Polymer Science Part A-2: Polymer Physics* **1968**, *6*, 1593-1606.
53. Phillips, G.O. Molecular association and function of arabinogalactan protein

complexes from tree exudates. *Structural Chemistry* **2009**, *20*, 309-315.

54. Alain, M.; McMullen, J.N. Molecular weight of acacia. *International Journal of Pharmaceutics* **1985**, *23*, 265-275.
55. Gillis, R.B.; Adams, G.G.; Alzahrani, Q.; Harding, S.E. A novel analytical ultracentrifugation based approach to the low resolution structure of gum arabic. *Biopolymers* **2016**, *105*, 618-625.
56. Massuelli, M. Hydrodynamic properties of whole arabic gum. *American Journal of Food Science and Technology* **2013**, *1*, 60-66.
57. Philips, G.O.; Takigami, S.; Takigami, M. Hydration characteristics of the gum exudate from acacia *senegal*. *Food Hydrocolloids* **1996**, *10*, 11-19.
58. Al-Assaf, S.; Phillips, G.O.; Aoki, H.; Sasaki, Y. Characterization and properties of acacia senegal (l.) willd. Var. Senegal with enhanced properties (acacia (sen) super gum™): Part 1—controlled maturation of acacia senegal var. Senegal to increase viscoelasticity, produce a hydrogel form and convert a poor into a good emulsifier. *Food Hydrocolloids* **2007**, *21*, 319-328.
59. Al-Assaf, S.; Sakata, M.; McKenna, C.; Aoki, H.; Phillips, G.O. Molecular associations in acacia gums. *Structural Chemistry* **2009**, *20*, 325-336.
60. Castellani, O.; Al-Assaf, S.; Axelos, M.; Phillips, G.O.; Anton, M. Hydrocolloids with emulsifying capacity. Part 2 – adsorption properties at the n-hexadecane–water interface. *Food Hydrocolloids* **2010**, *24*, 121-130.
61. Li, X.; Zhang, H.; Fang, Y.; Al-Assaf, S.; Phillips, G.O.; Nishinari, K. Rheological properties of gum arabic solution: The effect of arabinogalactan protein complex (agp). In *Gum arabic*, The Royal Society of Chemistry: 2012; pp 229-238.
62. Li, X.; Fang, Y.; Al-Assaf, S.; Phillips, G.O.; Nishinari, K.; Zhang, H. Rheological study of gum arabic solutions: Interpretation based on molecular self-association. *Food Hydrocolloids* **2009**, *23*, 2394-2402.
63. Fincher, G.B.; Stone, B.A.; Clarke, A.E. Arabinogalactan-proteins: Structure, biosynthesis, and function. *Annual Review of Plant Physiology* **1983**, *34*, 47-70.
64. Qi, W.; Fong, C.; Lamport, T.A. Gum arabic glycoprotein is a twisted hairy rope. A new model based on o-galactosylhydroxyproline as the polysaccharide attachment site. *Plant Physiology* **1991**, *96*, 848-855.
65. Ball, P. Water as an active constituent in cell biology. *Chemical Reviews* **2008**, *108*, 74-108.
66. Hu, X.; Kaplan, D.; Cebe, P. Dynamic protein−water relationships during β-sheet formation. *Macromolecules* **2008**, *41*, 3939-3948.
67. Huang, W.; Krishnaji, S.; Tokareva, O.R.; Kaplan, D.; Cebe, P. Influence of water on protein transitions: Thermal analysis. *Macromolecules* **2014**, *47*, 8098-8106.
68. Hatakeyama, T.; Nakamura, K.; Hatakeyama, H. Determination of bound water content in polymers by dta, dsc and tg. *Thermochimica Acta* **1988**, *123*, 153-161.
69. Kerch, G. Polymer hydration and stiffness at biointerfaces and related cellular processes. *Nanomedicine* **2018**, *14*, 13-25.
70. Bano, M.; Marek, J.; Stupak, M. Hydrodynamic parameters of hydrated macromolecules: Monte carlo calculation. *Physical Chemistry Chemical Physics* **2004**, *6*, 2358-2363.
71. Hatakeyama, T.; Uetake, T.; Inui, Y.; Hatakeyama, H. Freezing bound water restrained by gum arabic. In *Gums and stabilisers for the food industry 15*, The Royal Society of Chemistry: 2009; pp 69-76.
72. Laage, D.; Elsaesser, T.; Hynes, J.T. Water dynamics in the hydration shells of biomolecules. *Chemical Reviews* **2017**, *117*, 10694-10725.
73. Comez, L.; Lupi, L.; Morresi, A.; Paolantoni, M.; Sassi, P.; Fioretto, D. More is different: Experimental results on the effect of biomolecules on the dynamics of hydration water. *The Journal of Physical Chemistry Letters* **2013**, *4*, 1188-1192.
74. Fogarty, A.C.; Laage, D. Water dynamics in protein hydration shells: The molecular origins of the dynamical perturbation. *The Journal of Physical Chemistry B* **2014**, *118*, 7715-7729.
75. Combet, S.; Zanotti, J.M. Further evidence that interfacial water is the main 'driving force' of protein dynamics: A nuetron scattering study on perdeuterated c-phycocyanin. *Phys. Chem. Chem. Phys.* **2012**, *12*, 4927-4934.
76. Nandi, P.K.; English, N.J.; Futera, Z.; Benedetto, A. Hydrogen-bond dynamics at the bio–water interface in hydrated proteins: A molecular-dynamics study. *Physical Chemistry Chemical Physics* **2017**, *19*, 318-329.

77. Chalikian, T.V. Structural thermodynamics of hydration. *The Journal of Physical Chemistry B* **2001**, *105*, 12566-12578.
78. Shiraga, K.; Suzuki, T.; Kondo, N.; De Baerdemaeker, J.; Ogawa, Y. Quantitative characterization of hydration state and destructuring effect of monosaccharides and disaccharides on water hydrogen bond network. *Carbohydrate Research* **2015**, *406*, 46-54.
79. Lee, S.L.; Debenedetti, P.G.; Errington, J.R. A computational study of hydration, solution structure, and dynamics in dilute carbohydrate solutions. *The Journal of Chemical Physics* **2005**, *122*, 204511.
80. Hatakeyama, H.; Hatakeyama, T. Interaction between water and hydrophilic polymers. *Thermochimica Acta* **1998**, *308*, 3-22.
81. Hu, X.; Kaplan, D.; Cebe, P. Effect of water on the thermal properties of silk fibroin. *Thermochilica Acta* **2007**, *461*, 137-144.
82. Wolfe, J.; Bryant, G.; Koster, K.L. What is 'unfreezable water', how much unfreezable is it and how much is there? *CryoLetters* **2002**, *23*, 157-166.
83. Takigami, S.; Takigami, M.; Phillips, G.O. Effect of preparation method on the hydration characteristics of hylan and comparison with another highly cross-linked polysaccharide, gum arabic. *Carbohydrate Polymers* **1995**, *26*, 11-18.
84. Hatakeyama, T.; Tanaka, M.; Hatakeyama, H. Thermal properties of freezing bound water restrained by polysaccharides. *J Biomater Sci Polym Ed* **2010**, *21*, 1865-1875.
85. Phillips, G.O.; Takigami, S.; Takigami, M. Hydration characteristics of the gum exudate from *acacia senegal*. *Food Hydrocolloids* **1996**, *10*, 11-19.
86. Oakley, H.B. The hydration of gum arabic and glycogen. *Biochemical Journal* **1937**, *31*, 28-34.
87. Chalikian, T.V.; Filfil, R. How large are the volume changes accompanying protein transitions and binding? *Biophysical Chemistry* **2003**, *104*, 489-499.
88. Chalikian, T.V.; Sarvazyan, A.P.; Breslauer, K.J. Hydration and partial compressibility of biological compounds. *Biophysical Chemistry* **1994**, *51*, 89-109.
89. Chalikian, T.V.; Völker, J.; Srinivasan, A.R.; Olson, W.K.; Breslauer, K.J. The hydration of nucleic acid duplexes as assessed by a combination of volumetric and structural techniques. *Biopolymers* **1999**, *50*, 459-471.
90. Durchschlag, H. Specific volumes of biological macromolecules and some other molecules of biological interest. In *Thermodynamic data for biochemistry and biotechnology*, Hinz, H.-J., Ed. Springer: Berlin, 1986; pp 45 - 128.
91. Kupke, D.W. Density and volume change measurements. In *Physical principles and techniques of protein chemistry, part c*, Leach, S.J., Ed. Academic Press: 1973; pp 3 - 75.
92. Hoiland, H. Partial molar volumes of biochemical model compounds in aqueous solution. In *Thermodynamic data for biochemistry and biotechnology*, Hinz, H.-J., Ed. Springer-Verlag Berlin Heidelberg: 1986; pp 17 - 44.
93. Gekko, K. Volume and compressibility of proteins. In *High pressure bioscience: Basic concepts, applications and frontiers*, Akasaka, K.; Matsuki, H., Eds. Springer Netherlands: Dordrecht, 2015; pp 75-108.
94. Durchschlag, H. Determination of the partial specific volume of conjugated proteins. *Colloid & Polymer Science* **1989**, *267*, 1139 - 1150.
95. Sarvazyan, A., P. Ultrasonic velocimetry of biological compounds. *Annu. Rev. Biophys. Biophys. Chem* **1991**, *20*, 321 - 342.
96. Hoiland, H. Partial molar compressibilities of organic solutes in water. In *Thermodynamic data for biochemistry and biotechnology*, Hinz, H.-J., Ed. Springer: Berlin, 1986; pp 129 - 147.
97. Cooper, A. Thermodynamic fluctuations in protein molecules. *Proc. Natl. Acad. Sci. USA* **1976**, *79*, 2740 - 2741.
98. Chalikian, T.V.; Sarvazyan, A., P.; Breslauer, K.J. Hydration and partial compressibility of biological compounds. *Biophysical Chemistry* **1994**, *51*, 89 - 109.
99. Chalikian, T.V.; Breslauer, K.J. Thermodynamic analysis of biomolecules: A volumetric approach. *Current Opinion in Structural Biology* **1998**, *8*, 657-664.
100. Gekko, K.; Yamagami, K. Flexibility of food proteins as revealed by compressibility. *Journal Agricultural Food Chemisty* **1991**, *39*, 57 - 62.
101. Taulier, N.; Chalikian, T.V. Compressibility of protein transitions. *Biochimica et Biophysica Acta (BBA) - Protein Structure and Molecular Enzymology* **2002**, *1595*, 48-70.
102. Gekko, K.; Noguchi, H. Compressibility of globular proteins in water at 25 °c. *The Journal of Physical Chemistry* **1979**, *83*, 2706 -2714.

103. Nomura, H.; Yamaguchi, S.; Miyahara, Y. Partial compressibility of dextran. *Journal of Applied Polymer Science* **1964**, *8*, 2731-2734.
104. Nomura, H.; Onoda, M.; Miyahara, Y. Preferential solvation of dextran in water - ethanol mixtures. *Polymer Journal* **1982**, *14*, 249-253.
105. Gekko, K.; Mugishima, H.; Koga, S. Compressibility, densimetric and calorimetric studies of hydration of carrageenans in the random form. *Int. J. Biol. Macromol.* **1985**, *7*, 57 -63.
106. Gekko, K.; Noguchi, H. Physicochemical studies of oligodextran. I. Molecular weight dependence of intrinsic viscosity, partial specific compressibility and hydrated water *Biopolymers* **1971**, *10*, 1513 -1524.
107. Gekko, K.; Noguchi, H. Hydration behavior of ionic dextran derivatives. *Macromolecules* **1974**, *7*, 224 - 229.
108. Pierrotti, R. A scaled particle theory of aqueous and non aqueous solutions. *Chemical Reviews* **1976**, *76*, 717-726.
109. Chalikian, T.V.; Breslauer, K.J. On volume changes accompanying conformational transitions of biopolymers. *Biopolymers* **1996**, *39*, 619 - 626.
110. Chalikian, T.V. Volumetric properties of proteins. *Annual Review of Biophysics and Biomolecular Structure* **2003**, *32*, 207-235.
111. Chalikian, T.V.; Totrov, M.; Abagyan, R.; Breslauer, K.J. The hydration of globular proteins as derived from volume and compressibility measurements: Cross correlating thermodynamic and structural data. *Academic Press* **1996**, *260*, 588 - 603.
112. Kharakoz, D.P. Volumetric properties of proteins and their analogs in diluted water solutions. *Biophysical Chemistry* **1989**, *34*, 115-125.
113. Bánó, M.; Marek, J. How thick is the layer of thermal volume surrounding the protein? *Biophysical Chemistry* **2006**, *120*, 44-54.
114. Voloshin, V.; Medvedev, N.; Smolin, N.; Geiger, A.; Winter, R. Disentangling volumetric and hydrational properties of proteins. *Journal of Physical Chemistry B* **2015**, *115*, 1881-1890.
115. Harding, S.E. On the hydrodynamic analysis of macromolecular conformation. *Biophysical Chemistry* **1995**, *55*, 69-93.
116. Pavlov, G.M.; Perevyazko, I.Y.; Okatova, O.V.; Schubert, U.S. Conformation parameters of linear macromolecules from velocity sedimentation and other hydrodynamic methods. *Methods* **2011**, *54*, 124-135.
117. Cui, S.W. *Food carbohidrates: Chemistry, physical properties, and applications*. 1st edition ed.; CRC Press: 2005; p 411.
118. Burchard, W. Solution properties of branched macromolecules In *Branched polymers ii*, Roover, J., Ed. Springer Berlin Heidelberg: Berlin, Heidelberg, 1999; pp 113-194.
119. Simha, R. Effect of concentration on the viscosity of dilute solutions. *Journal of Research of the National Bureau of Standards* **1949**, *42*, 409-418.
120. Harding, S.E. Dilute solution viscometry of food biopolymers. In *Fuctional properties of food macromolecules*, 2nd ed.; Aspen Pub: MA, USA, 1998; pp 1-49.
121. Jamieson, A.M.; Simha, R. Newtonian viscosity of dilute, semidilute, and concentrated polymer solutions. In *Polymer physics*, 2010; pp 17-87.
122. Elias, H.G. Viscosity of dilute solutions. In *Macromolecules, volume 3: Physical structures and properties*, Wiley VCH: 2008; pp 395-425.
123. Simha, R. The influence of brownian movement on the viscosity of solutions. *The Journal of Physical Chemistry* **1940**, *44*, 25-34.
124. Rodriguez Schmidt, R.; Hernandez Cifre, J.G.; Garcia de la Torre, J. Translational diffusion coefficients of macromolecules. *The European Physical Journal E* **2012**, *35*, 130.
125. Tanford, C. Physical chemistry of macromolecules. In *Physical chemistry of macromolecules*, Wiley: New York, USA, 1961.
126. Morris, G.A.; Adams, G.G.; Harding, S.E. On hydrodynamic methods for the analysis of the sizes and shapes of polysaccharides in dilute solution: A short review. *Food Hydrocolloids* **2014**, *42*, 318-334.
127. Pavlov, G.M. The concentration dependence of sedimentation for polysaccharides. *Eur. Biophys. J.* **1997**, *25*, 385-397.
128. Patel, T.R.; Winzor, D.J.; Scott, D.J. Analytical ultracentrifugation: A versatile tool for the characterisation of macromolecular complexes in solution. *Methods* **2016**, *95*, 55-61.
129. Schuck, P. Size-distribution analysis of macromolecules by sedimentation velocity ultracentrifugation and lamm equation modeling. *Biophysical Journal* **2000**, *78*, 1606-1619.
130. Brown, P.H.; Schuck, P. Macromolecular size-and-shape distributions by sedimentation veloxity analytical

ultracentrifugation. *Biophys. J.* **2006**, *90*, 4651-4661.

131. Harding, S.E. Analysis of polysaccharides by ultracentrifugation. Size, conformation and interactions in solution. In *Polysaccharides i: Structure, characterization and use*, Heinze, T., Ed. Springer Berlin Heidelberg: Berlin, Heidelberg, 2005; pp 211-254.

132. Lelievre, J.; Lewis, J.A.; Marsden, K. The size and shape of amylopectin: A study using analytical ultracentrifugation. *Carbohydrate Research* **1986**, *153*, 195-203.

Chapter II: Volumetric properties of Acacia gums

Highlights

- The volumetric properties, partial specific volume, v_s°, and partial specific adiabatic compressibility, β_s°, of A. gums and AGP fractions displayed an intermediate behaviour between globular proteins and linear polysaccharides.

- A. *senegal* and A. *seyal* showed similar values of v_s° (0.58 $cm^3.g^{-1}$). However, A. *seyal* showed lower β_s° (-12.2x10^{-11} and -13.2 x10^{-11} Pa^{-1}, respectively), suggesting a slightly more hydrated structure. In addition, the increase of the ionic strength up to 0.01 M did not show an important effect on the volumetric properties of A. *senegal*.

- The HIC-F1 fraction showed lower values of v_s° and β_s° (0.56 $cm^3.g^{-1}$ and -18.0x10^{-11} Pa^{-1}, respectively), and higher hydration number, n_h, (0.85 g H_2O/g AGP), suggesting a highly hydrated and semi flexible structure. On the other hand, the HIC-F2 and HIC-F3 fractions presented higher values of v_s° (0.59 and 0.65 $cm^3.g^{-1}$) and β_s° (-14.0 and -1.0x10^{-11} Pa^{-1}, respectively) and lower n_h (0.68 and 0.54 g H_2O/g AGP), suggesting a less hydrated and more flexible structure.

- The difference on the volumetric properties of AGPs was explained by their differences in the protein content, number of charges (contributed by charged sugars and amino acids) and polarity.

Flexibility and Hydration of Amphiphilic Hyperbranched Arabinogalactan-Protein from Plant Exudate: A Volumetric Perspective[1]

Verónica Mejia Tamayo [a], Michaël Nigen [a], Rafael Apolinar-Valiente [b], Thierry Doco [b], Pascale Williams [b], Denis Renard [c] and Christian Sanchez [a,]

[a] UMR IATE, UM-INRA-CIRAD-Montpellier Supagro, 2 Place Pierre Viala, F-34060.

[b] UMR SPO, INRA-UM, 2 Place Pierre Viala, F-34060 Montpellier Cedex, France.

[c] UMR BIA, INRA, F-44300 Nantes, France.

Abstract

Plant Acacia gum exudates are composed by glycosylated hydroxyproline-rich proteins, with a high proportion of heavily branched neutral and charged sugars in the polysaccharide moiety. These hyperbranched arabinogalactan-proteins (AGP) display a complexity arising from its composition, architecture and conformation, but also from its polydispersity and capacity to form supramolecular assemblies. Flexibility and hydration partly determined colloidal and interfacial properties of AGPs. In the present article, these parameters were estimated based on measurements of density and sound velocity and determination of volumetric parameters, e.g. partial specific volume (v_s°) and coefficient of partial specific adiabatic compressibility coefficient (β_s°). Measurements were done with Acacia *senegal*, Acacia *seyal* and fractions from the former separated according to their hydrophobicity by Hydrophobic Interaction Chromatography, i.e. HIC-F1, HIC-F2 and HIC-F3. Both gums presented close values of v_s° and β_s°. However, data on fractions suggested a less hydrated and more flexible structure of HIC-F3, in contrast to a less flexible and more hydrated structure of HIC-F2 and especially HIC-F1. The differences between the macromolecular fractions of A. *senegal* are significantly related to the fraction composition,

[1] Article published in Colloids and Surfaces, 2 (1), 11. doi:10.3390/colloids2010011

protein/polysaccharide ratio and type of amino acids and sugars, with a polysaccharide moiety mainly contributing to the global hydrophilicity and a protein part mainly contributing to the global hydrophobicity. These properties form the basis of hydration ability and flexibility of hyperbranched AGP from Acacia gums.

Keywords: Acacia gum; partial specific volume; adiabatic compressibility; hydration; flexibility

1. Introduction

Plant Acacia gum exudates from the trunk and branches of Acacia *senegal* and Acacia *seyal* trees are natural viscous fluids that are produced as a protection mechanism of trees [1,2]. Acacia gum exudates are used by humans since prehistoric times for their biological and health beneficial effects, as well as for their transport and interfacial physicochemical properties [2-4]. Acacia gum exudates contain structurally complex biopolymers and minor associated components such as minerals, traces of lipids and flavonoids, enzymes [2,4]. Acacia gum biopolymers are highly glycosylated hydroxyproline-rich arabinogalactan-peptide and arabinogalactan-proteins that belong to the glycoprotein superfamily [5-7]. Arabinogalactan-proteins (AGPs) have important biological functions since they are implicated in plant growth, development, signaling, and plant–pathogen interactions [8,9]. AGPs are basically composed of a protein core, which is decorated by arabinose and galactose-rich polysaccharide units with varying amounts of rhamnose, fucose and glucuronic acid [10,11]. Basically, the highly branched polysaccharidic structure consists of 1,3-linked β-D-galactopyranose monomers with side branches linked to the main chain mainly through substitution at O-6 position. Units of α-L-arabinofuranosyl and α-L-rhamnopyranosyl are distributed in the main and side chains while β-D-glucuronopyranosyl and 4-O-Methyl-β-D-glucuronopyranosyl are mostly end units [12]. In Acacia gums, various populations of hyperbranched AGPs coexist presenting slightly different sugar, amino acid and mineral composition, sugar to amino acid molar ratio, charge density, molar mass, size, shape and anisotropy [12-21].

When these AGPs are fractionated according to their polarity by hydrophobic interaction chromatography (HIC), three fractions are obtained [13,15]. These fractions have been named in the past arabinogalactan (AG), arabinogalactan-protein complex (AGP) and glycoproteins (GP), in the order of elution, to take into account their different protein content. However, since all fractions react to Yariv's reactant and contain arabinogalactan type II carbohydrate chains, they are formally AGPs. Then, to avoid any possible confusion, these fractions will be more rigorously named, in the order of elution, HIC-F1, HIC-F2 and HIC-F3 in the following. Using a combined experimental approach based on size exclusion chromatography (SEC-MALS), high resolution microscopic and small angle x-ray scattering (SAXS) and small neutron scattering (SANS) experiments, the structure of these fractions was recently considered [17-19,21,22]. These studies highlighted common and distinct features between fractions that can be summarized as follows. The sugar composition was closed between fractions, with however larger amount of charged sugars for HIC-F1 and larger amount of arabinose for HIC-F2 and HIC-F3. The amount of proteins increased in the order of polarity, with HIC-F1<HIC-F2<HIC-F3 and protein values of about 1%, 8-10% and 20-25%, respectively. All fractions were globally composed by three populations of AGPs, low M_w ($M_w < 7.5x10^5$ g.mol^{-1}), high M_w ($M_w > 7.5x10^5$ g.mol^{-1}) and supramolecular assemblies ($M_w > 2\text{-}3x10^6$ g.mol^{-1}). Supramolecular assemblies could be structurally self-similar and composed by interacting glycomodules [19,21]. A high amount of low M_w AGP was present in HIC-F1 while high amounts of high M_w AGP and assemblies were found in HIC-F2 and HIC-F3. All fractions displayed triaxial ellipsoidal shapes, with varying semi axis dimensions and anisotropies. Low M_w AGPs were in general more spheroidal and less anisotropic than the larger ones. HIC-F1 displayed an inner dense branched structure while HIC-F2 but especially HIC-F3 were more porous and expanded. Because of the presence of charged sugars and amino acids, all fractions were negatively charged with weak polyelectrolyte behavior. The solvent affinity of fractions, estimated from the inverse of the power-law exponent describing the intermediate q range of small angle scattering form factor, or alternatively by the exponent of the relationships between M_w and the intrinsic viscosity, coherently indicated that the solvent affinity of HIC fractions were intermediate between a poor affinity (0.33) and a good one (0.6).

This short summary points out that the complexity of plant exudates not only comes from the complex composition and architecture of individual AGPs but also from the structural

and physicochemical polydispersity, reinforced by interactions between macromolecules that induce the formation of supramolecular structures [10,15,18,19,22-27]. Apprehending this complexity is needed in order to better understand physicochemical properties of AGPs from plant exudates, especially solubility and interfacial properties that ultimately determine the practical use of gums in confectionaries, soft drinks and adhesive- or coating-based applications. In general, solubility and interfacial properties of biopolymers are determined both by intrinsic properties of macromolecules (composition, accessibility and spatial division of charged, polar and nonpolar atomic groups, chain density, molar mass, conformation, flexibility) and their ability to dynamically interact with the solvent. Many of their general dynamic properties can be described in terms of bulk quantities, for instance packing density, compressibility, or other coefficients of elasticity, which are typically applied to macroscopic systems [28]. Volumetric properties of biopolymers are directly related to their flexibility and hydration, then providing a convenient mean to assess these important molecular characteristics. In particular, the partial molar volume, V_s^o, and the partial molar adiabatic compressibility K_s^o are macroscopic thermodynamic observables which are particularly sensitive to the hydration properties of solvent exposed atomic groups, as well as to the structure, dynamics, and conformational properties of the solvent inaccessible biopolymer interior [29,30]. This has motivated many efforts to experimentally measure these quantities on small solutes (amino acids, sugars, minerals) and on biopolymers such as globular, fibrous and unfolded proteins [31-40], nucleic acids [33,35,41-43] and linear or branched polysaccharides [33,44-54].

In the present study, we reported the volumetric experimental characterization of hyperbranched charged arabinogalactan-proteins from Acacia gums. Specific objectives of the work were to qualitatively estimate the molecular flexibility of hyperbranched AGPs and their hydration ability. We characterized the two classically used total gums, i.e. Acacia *senegal* and Acacia *seyal* gums, and the three HIC fractions isolated from the former. Following a detailed analysis of volumetric data obtained on fractions, we estimated the flexibility and hydration characteristics of the three fractions of AGPs in dilute solutions. The results of the analysis shed light to the importance of the sugar composition and protein content on the hydration ability of AGPs but also on the intrinsic spatial structural heterogeneity, that determines macromolecular volume fluctuations, then the molecular flexibility.

2. Materials and methods

2.1. Materials

The experiments were carried out using commercially available Acacia *senegal* (lot OF 152413) and Acacia *seyal* (lot OF 110724) soluble powders, kindly provided by the Alland & Robert Company – Natural and Organic gums (Port Mort - France). The moisture, sugar and mineral content of the powders were previously reported elsewhere [20].

All reagents used were of analytical grade from Sigma Aldrich (St. Louis, MO, USA).

2.2. Methods

2.2.1. Chemical Analyses

Moisture content and ash of Acacia gum and HIC fraction samples were analyzed by the Hot Air Oven and Gravimetric methods (AOAC 925.10 and AOAC 923.03, respectively) Amino acid, neutral sugars and uronic acid compositions were determined as reported in Lopez et al (2015) [20]. Measures were duplicated.

2.2.2. Desalting of Acacia gums and HIC fractions

Acacia gum samples were prepared from a 10% (wt) dispersion of commercial Acacia *senegal* and Acacia *seyal* powders in ultrapure deionized water (18.2 mΩ). Dispersions were stirred overnight at room temperature (20–25°C) to allow complete hydration of Acacia gum molecules, followed by centrifugation at 12 000 rpm (20 °C) for 30 min to remove impurities. Dispersions were desalted by diafiltration against deionized water (18.2 mΩ) using a 1:3 (v/v) AG:water volume ratio, using an AKTA FLUX 6 system (GE Healthcare, Upsala, Sweden), with a transmembrane pressure of 15 psi. The membrane used was a Polysulfone Hollow fiber (GE Healthcare) with a nominal cut off of 30 kDa (63.5 cm L x 3.2 cm o.d., surface of 4800 cm^2). The sample was then centrifuged at 12 000 rpm (20 °C) for 30 min and freeze-dried for 72 h.

Macromolecular fractions, HIC-F1, HIC-F2 and HIC-F3 were obtained from A. *senegal* soluble powder via Hydrophobic Interaction Chromatography (HIC) according to the classical fractionation method used by Randall et al. (1989) [13] and Renard et al (2006) [15]. HIC-F1

and HIC-F2 followed the same diafiltration procedure as A. *senegal,* and were then atomized. The HIC-F3 fraction was concentrated using a rotavapor (until crystals appeared), extensively dialyzed (72 h), and freeze dried (72 h). The HIC-F3 fraction could not be desalted by dialfiltration because of excessive material losses during the process. Please note that freeze-drying of HIC-F3 was controlled to reach final sample moisture not below 10% (wt). Otherwise, about 50% of macromolecules become insoluble upon rehydration, as noted elsewhere [15,23].

2.2.3. Preparation of Acacia gum dispersions

Acacia gums and HIC fraction powders were dispersed and dialyzed against the solvent under constant agitation overnight at room temperature (1:5 AG:solvent volume ratio, 3.5 KDa Spectra/Por membrane) to reach isopotential equilibrium. Dispersions were centrifuged at 12 000 rpm (20 °C) for 30 min to remove impurities and degassed for 15 minutes to remove dissolved air (300 Ultrasonik bath, Ney, Yucaipa, CA, USA). The dialyzed solvent was used as reference in volumetric measurements.

The concentrations of Acacia gums and HIC fractions in dispersions were quantified using an Abbemat Refractometer (Anton Paar, Graz, Austria) and experimental refractive index increments (dn/dc) of 0.155, 0.151, 0.162, 0.160 and 0.145 $mL.g^{-1}$ for A. *senegal*, A. *seyal*, HIC-F1, HIC-F2 and HIC-F3, respectively. The repeatability of the instrument is $1x10^{-6}$. All measurements were performed at 25 °C and triplicated.

2.2.4. Size Exclusion chromatography (HPSEC)- Multi Angle Laser Light Scattering (MALLS)

Acacia gums and HIC fractions were characterized by multi-detector high performance size exclusion chromatography (HPSEC). HPSEC experiments were performed using a Shimadzu HPLC system (Shimadzu, Kyoto, Japan) coupled to 4 detectors: a Multi Angle Laser Light Scattering detector which operates at 18 angles (DAWN Heleos II, Wyatt, Santa Barbara, CA, USA), a differential refractometer (Optilab T-rEX, Wyatt, Santa Barbara, CA, USA), an on line Viscosimeter (VISCOSTAR II, Wyatt, Santa Barbara, CA, USA), and a UV VIS detector activated at 280 nm (SPD-20A, Shimadzu). The separation of macromolecules was performed on a column system composed of one Shodex OHPAK SB-G pre-column followed

by 4 columns in series (SHODEX OHPAK SB 803 HQ, SB 804 HQ, SB 805 HQ and OHPAK SB 806 HQ) for A. gums and HIC-F1 fraction, and 1 column (SHODEX OHPAK SB 805 HQ) for HIC-F2 and HIC-F3 fractions.

Acacia gums and HIC fractions based dispersions (1 $mg.cm^{-3}$) were injected and eluted using 0.1 M $LiNO_3$ (0.02% NaN_3 at 1 $cm^3.min^{-1}$ and 30°C. The data was analyzed using the dn/dc mentioned in the upper section and ASTRA software 6.1.2.84 (Wyatt Technologies, Santa Barbara, CA, USA).

2.2.5. Density and sound velocity measurements

Density and sound velocity of Acacia gum solutions were simultaneously determined at 25 °C using a DSA 5000M sonodensimeter (Anton Paar, France). The instrument is equipped with a density cell and a sound velocity cell, the repeatability of the instrument was $1x10^{-6}$ $g.cm^{-3}$ for density and 0.1 $m.s^{-1}$ for sound velocity. Measurements were triplicated. Averaged volumetric parameters were determined from the ensemble of measured points. Measurements were done on samples described above but also on additional samples not discussed in details in this paper, for instance arabic acid obtained from A. *senegal* gum upon acidification and extensive demineralization, and other AGP fractions stemming from various runs of classical hydrophobic interaction and/or ion-exchange chromatographies.

2.3. Theoretical treatment of density and sound velocity parameters

2.3.1 Partial specific volume

The partial specific volume (v_s°, $cm^3.g^{-1}$) of a solute is defined as the change on the volume (V) of the system that was caused by addition of an infinitesimal amount of the solute at constant pressure (P, Pa) and temperature (T, K) provided that the amount of the solvent (m_j, g) is kept constant (Eq. II.1) [33,55,56].

$$v_s^\circ = \left(\frac{\partial V}{\partial m_i}\right)_{P,T,m_j} \quad (i \neq j) \tag{II.1}$$

Literature suggests two main methods to obtain v_s°, the slope and the extrapolation [56]. The first one is used mainly in dispersions where differences between the density of solute and solution are important (Eq. II.2). The second one uses the apparent volume of dispersions

(Eq. II.3), since in highly diluted conditions apparent and partial specific volumes are similar [32,33,55-58].

$$v_s^\circ = \frac{1}{\rho_o}\left(1 - \frac{\rho-\rho_o}{C}\right) \quad \text{(II.2)}$$

where ρ_o and ρ are the density of the solvent and dispersion ($g.mL^{-1}$) and C is the concentration of the solute ($g.mL^{-1}$).

$$v_s^\circ = \frac{1}{\rho_o} \lim_{c\to 0} \frac{\rho-\rho_o}{C} \quad \text{(II.3)}$$

In order to determine v_s°, the intramolecular interactions between solute molecules have to be negligible. Furthermore, its value depends on the concentration range studied. For Acacia gums and its macromolecular fraction dispersions, v_s° was determined using the slope method in a range of concentrations between 20 and 70 $g.L^{-1}$, where repeatability and reproducibility of assays were reliable. Unpredictable variation of results was observed at gum concentrations below 20 $g.L^{-1}$, due mainly to interaction and aggregation phenomena.

2.3.2. Isoentropic compressibility coefficients

The adiabatic compressibility of the solute (K_s, $cm^3.g^{-1}.Pa^{-1}$) can be determined by the first derivative of the volume of the system with respect to its pressure at constant entropy (S) (Eq. II.4) [59]. It represents the apparent adiabatic compressibility caused by addition of an infinitesimal amount of the solute.

$$K_s = \beta_s V = -\left(\frac{\partial V}{\partial P}\right)_S \quad \text{(II.4)}$$

The adiabatic compressibility coefficient of the dispersion is related to the sound velocity by the Newton Laplace equation (Eq. II.5).

$$\beta_s = -\left(\frac{1}{V}\right)\left(\frac{\partial V}{\partial P}\right)_S = \frac{1}{\rho u^2} \quad \text{(II.5)}$$

where u is the sound velocity of the dispersion and ρ is the density of the solution. The partial specific adiabatic compressibility coefficient (β_s°) can be calculated from density and sound velocity measurements, using the following expression [49,50,56,60]:

$$\beta^\circ_s = \left(\frac{\beta_{so}}{v_s^\circ}\right) \lim_{c\to 0}\left[\frac{\beta/\beta_{so} - \Phi}{C}\right] \quad \text{(II.6)}$$

where β and β_{so} are the adiabatic compressibilities of the dispersion and solvent, respectively, and Φ is the apparent specific volume ($\Phi = (\rho\text{-}C)/\rho_o$).

2.3.3. Microscopic description of macroscopic volumetric data

In order to interpret less qualitatively macroscopic data in terms of microscopic phenomena, one need to separate each macroscopic variable into contributing components which can be ascribed to specific molecular "events" [61]. This can be done using the scaled particle theory that describes the process of introducing a solute molecule into a solvent according to two steps [62-65]. The first step corresponds to the creation of a cavity into the solvent able to accommodate the solute. The second step is the introduction into the cavity of a solute molecule which interacts with the solvent. In terms of partial molar volumes, this can be described according to [64,66]:

$$\bar{V}_s^{\circ} = \bar{V}_c + \bar{V}_l + \beta_{T0}RT \tag{II.7}$$

where $\bar{V}_s^{\circ}$ is the partial molar volume of the solute at infinite dilution, $\bar{V}_c$ is the partial molar volume change upon cavity formation, $\bar{V}_l$ is the partial molar volume change upon interactions of charged, polar and nonpolar atomic groups with the solvent (interaction volume), β_{T0} is the coefficient of isothermal compressibility of the solvent and RT is the energy of ideal gases. The term $\beta_{T0}RT$ is the ideal component of the partial molar volume resulting from the motion of the solute along the translational degrees of freedom. This parameter is small (about 1.1 $cm^3.mol^{-1}$ at 25°C) and can be neglected [65], especially in the case of biopolymers such as globular proteins or polysaccharides where partial molar volumes are larger than $\approx 10^4$-10^5 $cm^3.mol^{-1}$ [32,54]. Omitting for simplicity the bars onto the volume terms, the equation can be described as [38,61,64,65,67,68]:

$$V_s^{\circ} = V_c + V_l = V_M + V_T + V_l \tag{II.8}$$

$$V_s^{\circ} = V_{vdW} + V_{void} + V_T + n_h\left(V_h^0 - V_0^0\right) \tag{II.9}$$

where $V_M = (V_{vdW} + V_{void})$ is the intrinsic partial molar volume of the solute which corresponds to the spatial architecture of protein interior [59], a domain which water cannot penetrate, V_{vdW} is the van der Waals partial molar volume of the solute and V_{void} is the partial molar volume of voids into the solute due to imperfect atom packing; V_T is the

partial molar thermal volume that represents an "empty volume" around the solute molecules resulting from thermally induced mutual molecular vibrations and reorientations of the solute and the solvent [64,69,70]. It is related to the fact that the "cavity" of the solute molecule created by inserting the molecule into the solvent should be larger than its molecular volume, and this extra volume should be sensitive to temperature [38,70]. For molecules of arbitrary shapes, the thermal volume can be conveniently approximated as a layer of constant thickness Δ to the surface of the molecule [65]; and V_l the interaction volume is equal to n_h (V_h°-V_o°), with n_h the hydration number, i.e. the number of water molecules involved in the solute hydration shell, and V_h° and V_o° the partial molar volumes of water in the hydration shell and in the bulk state, respectively [61]. The term hydration shell refers to those water molecules which due to the presence of the solute, exhibit altered physicochemical characteristics when compared with bulk water [37]. V_l is the only term sensitive to hydration and its contribution is negative because $V_h^\circ < V_o^\circ$.

Regarding the partial molar adiabatic compressibility, K_s°, the relationship is [36,37,71]:

$$K_s^\circ = K_M + n_h\left(K_{sh}^\circ - K_{so}^\circ\right) + K_r \tag{II.10}$$

Where K_M is the intrinsic partial molar adiabatic compressibility of the solute, n_h is the hydration number, K_{sh}° and K_{so}° are the partial molar adiabatic compressibility of water in the hydration shell and bulk water, respectively, and K_r is a relaxation component which results from the redistribution of biopolymer conformational substrates due to pressure and temperature variations in the field of the ultrasonic waves [37]. The term K_M is proportional to the partial molar volume V_M according to [61]:

$$K_M = \beta_M V_M \tag{II.11}$$

Where: β_M is the coefficient of adiabatic compressibility of the biopolymer interior. This term is a measure of intra-macromolecular interactions that can be calculated from Equation II.11:

$$\beta_M = B_M \frac{V_M}{V_{vdW}} \tag{II.12}$$

where B_M is the coefficient of proportionality and $\frac{V_M}{V_{vdW}}$ is inverse of the molecular packing density ρ_M [41,61].

It is important to note from the two above equations that the values of the apparent molar volume and the apparent molar adiabatic compressibility of a solute are sensitive to both the intrinsic molecular characteristics of solutes, and the quantity and the quality of hydration. The quantity of hydration corresponds to the amount of solvating water molecules in the hydration shell (n_h). On the other hand, the quality of hydration is reflected in the values of the partial molar volume, V_h° and the partial molar adiabatic compressibility, K_{sh}°, of the hydration water, that inform on the ability of charged, polar and nonpolar chemical groups to alter its structure and physicochemical properties [35,37,64,72]. In other words, n_h indicates how much water molecules are perturbed by the solute and V_h° and K_{sh}° indicate how strong is the water molecule solute interaction.

3. Results

3.1. Biochemical and structural characteristics

The global biochemical composition of A. *seyal* and A. *senegal* gums and HIC fractions obtained from the latter, i.e. HIC-F1, HIC-F2 and HIC-F3 is presented in Table II.1. Classically, all AGPs from A. gums were composed of the same sugars: D-galactose, L-arabinose, L-rhamnose, D-glucuronic acid and 4-O-methyl glucuronic acid, galactose and arabinose being the main sugars present [4,13-15,20,73,74]. The molar ratio of Arabinose to Galactose (Ara/Gal) of A. *senegal* and A. *seyal* was 0.8 and 1.4, respectively. Meanwhile, the Ara/Gal ratio of A. *senegal* fractions was 0.69, 1.04 and 1.15, for HIC-F1, HIC-F2 and HIC-F3, respectively. These results were close to previously reported values for A. *senegal* fractions: 0.57 [15] and 1.25 [13] for HIC-F1; 0.75 [15] and 0.93 [13] for HIC-F2; and 0.76 [15] and 0.82 [13] for HIC-F3. The three HIC fractions have a similar amount of neutral sugars (Ara, Gal and Rha), however the HIC-F1 fraction has a higher uronic acid to neutral sugar ratio (0.28), as compared to HIC-F2 and HIC-F3 (0.19 and 0.17 respectively). A consequence of this is that the carbohydrate moiety of HIC-F1 is supposed to carry more negative charges than HIC-F3. This difference in charge density between HIC-fractions is certainly exacerbated by the difference in mineral contents between fractions. In particular, within fractions, HIC-F3 contained the larger amount of minerals (5%), which can be due both to difference in the applied demineralization treatment (see section 2) and to the higher content

in aspartic and glutamic amino acid residues (13.5%, 9.6% and 5.7% for HIC-F3, HIC-F2 and HIC-F1, respectively).

Table II.1. Biochemical composition of Acacia gums in dry basis (mean ± standard deviation)

Component (mg.g^{-1})	**A. *senegal***	**HIC-F1**	**HIC-F2**	**HIC-F3**	**A. *seyal***
Total Dry Matter	893.4 ± 4.0	921.6 ± 0.1	926.2 ± 1.0	921.9 ± 2.0	966.9 ± 2.5
Sugars[a]	944.4	961.3	918.3	813.0	978.0
Arabinose (%)[b]	30.2 ± 0.6	26.8 ± 1.3	35.6 ± 1.0	38.3 ± 2.1	48.5 ± 1.7
Galactose (%)[b]	40.5 ± 1.7	39.0 ± 0.8	34.4 ± 0.8	33.3 ± 1.8	34.2 ± 2.0
Rhamnose (%)[b]	12.4 ± 0.4	12.5 ± 0.1	13.7 ± 0.4	13.9 ± 1.0	3.2 ± 0.7
Glucuronic Acid (%)[b]	17.8 ± 1.7	20.3 ± 0.6	15.6 ± 0.6	13.7 ± 2.1	7.7 ± 0.4
4-O-Me-Glucuronic Acid (%)[b]	1.0 ± 0.1	1.4 ± 0.1	0.6 ± 0.1	0.7 ± 0.1	6.4 ± 0.6
Branching degree [d]	0.78	0.77	0.75	0.75	0.59
Proteins[c]	21.5 ± 0.9	4.9 ± 0.1	63.1 ± 1.2	137.7 ± 2.7	7.7 ± 0.0
	(27)[e]	(19) [e]	(27) [e]	(32) [e]	(29) [e]
Minerals	34.1 ± 0.1	30.5 ± 1.1	19.3 ± 1.1	49.3 ± 2.6	14.3 ± 2.5

(a) Total content of sugars calculated from the difference of proteins and minerals from 1000 mg.g^{-1}. (b) Sugar composition was determined by GC-MS. (c) Protein content was measured using the Kjeldhal method. (d) Determined on neutral sugars according to the equation DB = 2D/(2D + L), where D is the number of dendritic units or branched units linked at three or more sites and L is the number of linear units having two glycosidic linkages [20,75] (complementary data). (e) Percentage in nonpolar amino acids.

As expected, HIC-F3 showed a higher amount of proteins (14%) as compared to HIC-F1 (0.5%) and HIC-F2 (6.3%). These protein content, as determined twice by Kjeldhal method and close to that estimated from amino acid analysis (results not shown), were approximatively two times lower than values determined previously [15]. Likely, extensive desalting of fractions and losses of some protein rich AGP species during the semi-preparative fractionation could explain this discrepancy. This also suggests that part of proteins could be not associated with the protein core of AGPs but free. The amino acid composition of Acacia gums and its fractions is presented in the complementary data section. All gums showed a similar amino acid profile. As is common for most AGPs, hydroxyproline and serine are the dominant amino acids, with also significant amount of proline, threonine, histidine and leucine, which is in good agreement with the literature [4,13-15,20,76,77]. We also remarked that glutamic and aspartic acid amino acids are important with summed values of 10.1, 10.8,

5.7, 9.6 and 13.5, for, respectively, A. *senegal*, A. *seyal*, HIC-F1, HIC-F2 and HIC-F3. A main difference between the fractions is then the content of negatively-charged amino acids. Another difference is the higher Hyp content of HIC-F1 fraction (36.4%) as compared to HIC-F2 (28.8%), and HIC-F3 (19.2%). Importantly, the HIC-F1 fraction contained about 81% of polar and charged amino acids while this value was smaller for HIC-F2 (73%) and HIC-F3 (68%). The presence of only 19 to 32% of nonpolar amino acids in HIC fractions seriously questions about the current view of AGPs as kind of Janus biopolymers with a hydrophilic sugar moiety and a hydrophobic protein moiety. The subject is beyond the scope of the present study, however clustering of nonpolar amino acids in terminal regions of polypeptides, presence of secondary structures, weak energy interactions between amino acids and sugars in close proximity, amphiphilic helix-type structures of the galactan backbone and associative properties of macromolecules, all these characteristics must play a role in the subtle balance between polar and nonpolar properties of AGPs [15,19,78,79]. Nevertheless, due mainly to the higher protein content and percentage in nonpolar amino acids, the HIC-F3 fraction appeared as the less polar one.

In terms of basic structural parameters, *A. senegal* showed lower M_w ($6.8x10^5$ $g.mol^{-1}$) than A. *seyal* ($7.1x10^5$ $g.mol^{-1}$) but a larger polydispersity index (M_w/M_n) (Table II.2). In addition, A. *seyal* displayed a smaller intrinsic viscosity than A. *senegal*, then a smaller hydrodynamic volume, indicating a more compact conformation of the former. Comparable results are reported in literature [15,20,24,74,80,81]. Regarding the HIC fractions, HIC-F1, HIC-F2 and HIC-F3 showed M_w of $3.5x10^5$, $1.5x10^5$ and $1.6x10^6$ $g.mol^{-1}$, respectively as already reported [15]. The polydispersity index of HIC-F3 was higher (1.8) compared to HIC-F1 and HIC-F2 (1.4 and 1.3 respectively). On the other hand the density of fractions was not identical with a density decreasing in the order HIC-F1 > HIC-F2 > HIC-F3.

Combining biochemical composition and structural parameters allowed to deducing or calculating a number of basic parameters both for the polysaccharide and peptide/protein moieties that will be used in the following (Table II.3).

Table II.2. Structural parameters of Acacia gums and its fractions in aqueous solutions (1 g.L^{-1} at pH 5) obtained by high performance size exclusion chromatography (HPSEC) – multi angle light scattering (MALS)

	A. *senegal*	**HIC-F1**	**HIC-F2**	**HIC-F3**	**A. *seyal***
M_w (g.mol^{-1})	6.8x10^5	3.5x10^5	1.5x10^6	1.6x10^6	7.1x10^5
M_n (g.mol^{-1})	3.1x10^5	2.3x10^5	1.1x10^6	9.0x10^5	4.2x10^5
M_w/M_n	2.0	1.4	1.3	1.9	1.5
M_w<7.5x10^5 g.mol^{-1} (%)	86.0	93.0	12.3	22.7	80.0
M_w>7.5x10^5 g.mol^{-1} (%)	14.0	7.0	87.7	67.3	20.0
Density (g.cm^{-3})[a]	0.99766	0.99775	0.99759	0.99743	0.99747

(a) measured using sonodensitometry

Table II.3. Basic composition and structural parameters of Acacia gums and HIC fractions in aqueous solutions (1 g·L^{-1} at pH 5) as obtained from chemical analyses and HPSEC-MALS measurements.

Basic Molecular Characteristics	**HIC-F1**	**HIC-F2**	**HIC-F3**
AGP M_w (g·mol^{-1})	348300	1495000	1643000
Polysaccharide moiety M_w (g·mol^{-1})	346593	1400666	1416759
Average sugar residue M_w (g·mol^{-1})	173.2	169.3	168.2
Average sugar partial molar volume (cm^3·mol^{-1})	105.9	104.3	103.9
Average sugar van der Waals volume (Å^3)	136.9	133.8	133.0
Number of sugar residues	2001	8441	9375
Potential number of charged and polar interacting sites (Polysaccharide moiety)	6273	29,183	28,789
Protein moiety M_w (g·mol^{-1})	1707	94,335	226,241
Average amino acid residue M_w (g·mol^{-1})	127.3	128.2	129.5
Number of amino acid residues	13	736	1747
Charged and polar amino acids (%)	80	72	67
Hydrophobicity index [a]	−1.46	−1.01	−1.14
Potential number of charged and polar interacting sites (Protein moiety)	12	621	1391

(a) from the hydrophobicity scale proposed by Zhu et al. [82].

3.2. Volumetric properties

The partial specific volume, v_s°, partial adiabatic compressibility, $k_s^\circ = (\beta_s^\circ / v_s^\circ)$, and coefficient of partial specific adiabatic compressibility, β_s°, of A. *seyal*, A. *senegal* and its HIC fractions are presented in Table II.4. It is first noteworthy that all obtained k_s° or βs° values were negative, which indicates that the hydration contribution is more important than the intrinsic contribution for the entire population of AGPs [32,36,60,61]. For A. *senegal*, experiments were done at pH 5 in water, sodium acetate buffer 10 mM and $LiNO_3$ 100 mM. We did not remark an important effect of ionic strength. Thus, for instance, v_s^o and β_s^o were, respectively, in the range 0.5842 - 0.5940 $cm^3.g^{-1}$ and -12.0 – -12.3x10^{-11} Pa^{-1} (Table II.4). We however noted that v_s^o was the larger in $LiNO_3$ 100 mM (0.5940 $cm^3.g^{-1}$), suggesting a decrease of macromolecule hydration through partial shielding of charges. More globally, these results would indicate that the solvent ionic strength has little effect on the measured volumetric properties of A. *senegal* according to our experimental conditions. Regarding both total acacia gums, A. *seyal* displayed in acetate buffer 10 mM smaller v_s^o than A. *senegal* (0.5767 vs 0.5842 $cm^3.g^{-1}$) and more negative β_s^o value (-13.2 x10^{-11} vs -12.2 x10^{-11} Pa^{-1}) (Table II.4). This indicated that A. *seyal* was more hydrated in solution than A. *senegal* despite a smaller content in charged sugars (Table II.1). Possible reasons for these differences may be the larger mineral and protein content of A. *senegal* gum but also the higher arabinose content of A. *seyal*. Higher arabinose content promotes the formation of long arabinose chains that display important hydration properties [20]. Literature reported values of v_s° of 0.60 – 0.62 $cm^3.g^{-1}$ and 10^{-11} - 10^{-10} Pa^{-1} for neutral unmodified saccharides such as galactose and arabinose [33,36,56,83-85], which are the main sugars present in AGPs from Acacia gums. Additionally, values of v_s° around 0.61 – 0.62 $cm^3.g^{-1}$ and β_s° of -20x10^{-11} to -70x10^{-11} Pa^{-1} have been reported for modified dextran (SPD, DS, and CMD) of different M_w at 25°C [47]. Besides, v_s° values ranging from 0.40 to 0.553 $cm^3.g^{-1}$ and $\beta^\circ s$ of -3.5x10^{-11} to -16.4x10^{-11} Pa^{-1} have been reported for branched polysaccharides, such as dextran and oligodextran of different M_w at 25°C [47,49-52] and linear polysaccharides such as carragenans [54] and hyalunorate potassium salt [48]. Our values are therefore in good agreement with the literature.

Table II.4. Partial specific volume ($v_s°$, $cm^3.g^{-1}$), partial specific adiabatic compressibility ($k°s$, $cm^3.g^{-1}.Pa^{-1}$) and coefficient of partial specific adiabatic compressibility ($\beta_s°$, Pa^{-1}) obtained for A. *seyal* gum, A. *senegal* gum and its fractions HIC-F1, HIC-F2, HIC-F3. All measurements were done at 25°C using sodium acetate buffer (10 mM) unless specified under the table. HIC: Hydrophobic Interactions Chromatography.

Type of Acacia gum or fraction	$v_s°$ ($cm^3.g^{-1}$)	K_s (10^{11} x $cm^3.g^{-1}.Pa^{-1}$)	$\beta s°$ (10^{11} x Pa^{-1})
A. *seyal*	0.5767	-7.6	-13.2
A. *senegal* [a]	0.5870	-7.2	-12.2
A. *senegal*	0.5842	-7.1	-12.2
A. *senegal* [b]	0.5940	-7.5	-12.5
A. *senegal* [c]	0.5880	-7.3	-12.3
A. *senegal* [d]	0.5850	-7.0	-12.0
HIC-F1	0.5616	-10.3	-18.3
HIC-F2	0.5876	-8.5	-14.4
HIC-F3	0.6500	-0.7	-1.0

(a) solvent: H_2O. (b) solvent: $LiNO_3$ 100 mM. (c) desalted A. *senegal* (2.1% minerals). (d) dialyzed A. *senegal* (3.3% minerals).

If volumetric parameters were close for total Acacia gums (A. *senegal* and A. *seyal*), then the situation was clearly different for HIC fractions obtained from A. *senegal*. In this case, both $v_s°$ and $\beta_s°$ increased (became less negative for $\beta_s°$) from HIC-F1 to HIC-F3. These results show the clear effect of the differences in fraction biochemical composition, but especially of AGP hydrophobicity on volumetric properties, as results have already demonstrated for globular proteins [32]. As HIC-F1 the more polar AGP, according to their HIC elution order and protein content, it will be able to bind more water molecules, and therefore have a more hydrated and less flexible structure than HIC-F2 and HIC-F3. Conversely, HIC-F3 will have in theory a less hydrated and more flexible structure, as will be demonstrated in the discussion section. The increase of the v_s^o parameter in the fractions was apparently strongly correlated to the protein content since we know that the $v_s°$ of polysaccharides and globular proteins is in average of around 0.60 – 0.72 $cm^3.g^{-1}$ [32,33,61]. The effect of AGP protein content on v_s^o can be seen in Figure II.1, where data for total Acacia gums and HIC fractions, but also for other modified gum (arabic acid) and other batches from hydrophobic interaction chromatography or ion-exchange chromatography have been shown. Interestingly,

data for AGP formed a continuity from literature data obtained on glycoproteins containing from 7% to 98% proteins [86], suggesting the view that in solution, volumetric properties of AGP from Acacia gums are strongly (directly and indirectly) determined by their protein content.

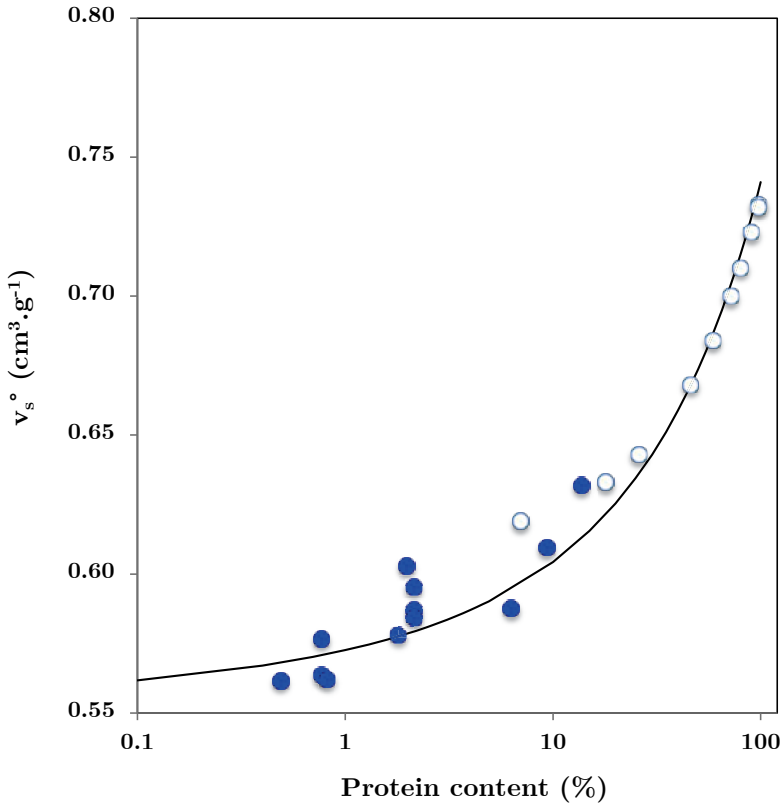

Figure II.1. Effect of protein content on the partial specific volume (v_s°, $cm^3 \cdot g^{-1}$) of A. gums (A. *senegal* and A. *seyal*), arabic acid and various molecular fractions (see Section 2) obtained from A. *senegal* gum by hydrophobic interaction chromatography or ion-exchange chromatography (blue circles) and various glycoproteins containing from 7 to 98% of proteins [86] (white circles). Continuous line is a guide to the eye (equation $v_s^\circ = 0.545 + 0.012\exp([\text{protein}]^{0.222})$).

4. Discussion

Hyperbranched AGPs from Acacia gums are structured macromolecules containing a protein core onto which massive sugar blocks and more linear sugar chains are connected [4]. Sugars are mainly neutral, however charged sugars and some amino acid residues contribute with charges that are at the basis of the polyelectrolyte nature of AGPs. Polar and charged residues provide hydrophilic properties to AGPs that are balanced by the nonpolar characteristics of about 20–30% of amino acids and the presence of methyl groups on

Rhamnose and 4-*O*-methyl glucuronic acids. The hydrophobicity of AGPs comes directly from their chemical composition, but also through their structural organization since both the polysaccharide and protein moieties contain a number of secondary structures (α and PPII helices, β-sheet structures, and turns) with specific hydrophilic/hydrophobic balances. Composition and structure of AGPs determine their behavior in solution, especially their flexibility and hydration, which can be approached through measurements of their volumetric properties. Volumetric parameters that were measured on A. *seyal*, A. *senegal* and its HIC fractions, i.e., partial specific volume, v_s°, and coefficient of partial specific adiabatic compressibility, β_s°, indicated that the protein content of AGPs was an important parameter and that hydration of macromolecules (negative values of β_s°) was in absolute value larger than the intrinsic compressibility (flexibility) contribution. In order to get a more general view of the volumetric behavior of AGPs, we then compared it to those of proteins and polysaccharides that we took from the literature [32,48,49,52,54,58,61,87]. Polysaccharides are charged linear polysaccharides salts (K- and Na-carageenans, K-hyaluronate) or branched dextran derivatives (sulfate-, sulfopropyl- and carboxymethyl dextrans) and neutral dextrans (various M_w). We also considered volumetric data obtained with nucleic acids [42,88]. For AGPs, we use data from total Acacia gums (A. *senegal* and *seyal*) and HIC fractions (Table II.4), and additional data not specifically discussed in this paper, for instance, arabic acid obtained from A. *senegal* gum upon acidification and extensive demineralization, and other AGP fractions stemming from various runs of classical hydrophobic interaction and/or ion-exchange chromatographies. Figure II.2 shows the coefficient of partial specific adiabatic compressibility $\beta^\circ_s = k_s^\circ/v_s^\circ$ (Pa^{-1}) as a function of partial specific volume $v_s^\circ = (V_s^\circ/M_w)$ ($cm^3 \cdot g^{-1}$).

A roughly linear tendency exists between β_s° and v_s° on the ensemble of data, with k_s° increasing with the increase of v_s°, as expected from the positive contribution of volume fluctuations (intrinsic flexibility) and the negative contribution of hydration [32,41,61]. The relationship between β_s° and v_s° could then be considered as a polarity-flexibility qualitative scale [32,41], delimiting three biopolymer groups from the highly polar and rigid charged polysaccharides and nucleic acids ($\beta_s^\circ < -20 \times 10^{-11}$ Pa^{-1}; $v_s^\circ < 0.56$ $cm^3 \cdot g^{-1}$) to the less polar and more flexible globular proteins (β_s° essentially positive; $v_s^\circ > 0.7$ $cm^3 \cdot g^{-1}$), as noted in Gekko and Hasegawa [32]. In this virtual polarity-flexibility scale of biopolymers, AGP

then display an intermediate behavior. Accordingly, fractions containing a larger amount of polysaccharides (HIC-F1; 97% polysaccharide, 0.5% protein) and less hydrophobic, according to the principle of the used separation technique, are closer to the linear and charged branched polysaccharides and nucleic acids (more hydration, lower flexibility), while fractions that are richer in protein (HIC-F3; 81% polysaccharide, 14 % protein) and more hydrophobic, are closer to the protein group (lower hydration, larger flexibility), with a β_s° value close to zero. This observation suggested again that hydration of fractions decreases in the order HIC-F3 < HIC-F2 < HIC-F1, a point that is confirmed in the next section. The fact that AGP data were close to those obtained for neutral dextrans, in line with a moderate hydration and flexibility of AGPs, demonstrates the weak polyelectrolyte characteristics of AGPs from Acacia gums [89]. These characteristics can explain that A. *senegal* gums dissolved in solvents of distinct ionic strengths or dissolved in the same solvent (pH 5 sodium acetate buffer), but containing different salt concentrations, display close β_s° and v_s° parameters (see Table II.4).

Finally, we determined for AGP data the linear relationship between β_s° and v_s° and we found an equation $\beta_s^\circ \approx 185 \times v_s^\circ - 129$ (R^2=0.93) that was closed to that obtained with a great number of globular proteins ($\beta_s^{\circ} \approx 195 \times v_s^\circ - 127$, R^2=0.85) [32]. We do not think that this result is fortuitous, but alternatively that it may indicate that globular proteins and (weakly) charged hyperbranched AGPs carry some common volumetric behavior, at least similar proportionality between volume and adiabatic compressibility parameters. If this assumption is correct, one could expect to treat in deeper details AGP volumetric data, as was previously done for globular proteins by Gekko and Noguchi [60] , Gekko and Hasegawa [32], Kharakoz and Sarvazian [36], but especially as reported by Chalikian and collaborators in a highly comprehensive series of articles [61,71,90,91].

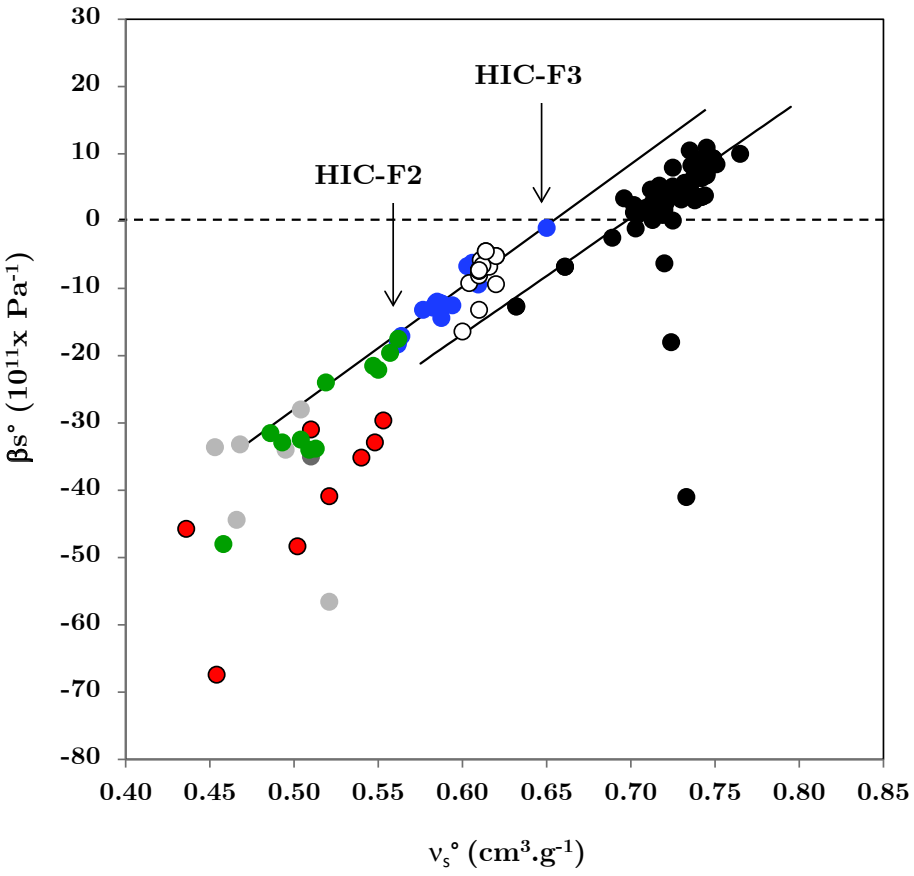

Figure II.2. Relationship at 25°C between the partial specific volume (v_s^0, $cm^3.g^{-1}$) and the coefficient of partial specific adiabatic compressibility (β_s^0, Pa-1) for A. gums (A. *senegal* and A. *seyal*), arabic acid and various molecular fractions (see Materials & Methods) obtained from A. *senegal* gum by hydrophobic interaction chromatography or ion-exchange chromatography (blue circles), various polysaccharides (neutral dextrans, white circles; charged dextran derivatives, red circles); Na- and K-carageenans, light gray circles, K hyaluronate, dark gray circle), various nucleic acids (green circle) and various globular proteins (black circles). Density and sound speed were measured in sodium acetate buffer (pH 5) for AGP. Vertical arrows points out HIC-F1 (left) and HIC-F3 (right) fractions. Continuous lines are linear regressions with equations (k_s^0 =185*ns-129) and (k_s^0 =195* ns-127) for globular proteins and AGP, respectively.

4.1. Microscopic description of AGP volumetric experimental data

The estimation of molar volumes (V_M, V_T, V_l, V_h°) and adiabatic compressibility (K_M, K_{sh}°, K_r) and hydration number (n_h) parameters was done on the AGP fractionated by HIC from A. *senegal* gum, i.e. HIC-F1, HIC-F2, HIC-F3. Despite the tedious fractionation, it was important to remember that HIC-fractions were more or less polydisperse (M_w/M_n: 1.3 - 1.9) and that the estimated volumetric parameters have to be considered as "average" of

macromolecules with similar polar properties but differing by their molar masses, size, shape and charge density [15]. We found by HPSEC-MALS, with a M_w of 7.5 x 10^5 g.mol^{-1} as a subjective limit between low and high M_w macromolecules, that HIC-F1, HIC-F2 and HIC-F3 were composed by about 7%, 88% and 67% of high M_w AGP. Keeping this limitation in mind, we first detailed the approach for HIC-F1 which presented the advantages to be the main specie in A. *senegal* gums (≈80-85%), then which largely determines its physicochemical properties, to contain very low amount of proteins (0.5%), that were neglected, and a high amount of low M_w AGP (93%).

4.2. Partial molar volumes of AGPs

Knowing that the experimental V_s° was 1.95x10^5 cm^3.mol^{-1} (Table II.5) and that the partial molar volume of bulk water at 25°C V_o° was 18 cm^3.mol^{-1}, for describing volumetric properties of HIC-F1 we needed to estimate V_M, V_T, V_l and V_h° (Eq. II.8 – II.10). We first tried to estimate the intrinsic partial molar volume $V_M = (V_{vdW} + V_{void})$. For a significant number of globular proteins, V_M represented about 80-95% of the experimental V_s° [61,92]. Taking an average value of 90%, the average V_M was 176296 cm^3.mol^{-1} (Table II.5). We then calculated the van der Waals volume V_{vdW} by an additivity scheme that was based on the Bondi approach [65,93-95]. We took into consideration the sugar composition, the presence of minerals and the contribution of covalent bonds (the branching characteristics of neutral sugars can be found Annex B). We obtained a final estimate for V_{vdW} of 143530 cm^3.mol^{-1}. We then calculated the partial molar volume of voids $V_{void} = (V_M - V_{vdW})$ as 32766 cm^3.mol^{-1}. The packing density of the molecule ($\rho_M = V_{vdW}/V_M$), as previously indicated, for HIC-F1 was 0.818 (Table 5). This is close to the maximum value for closely packed spheres (≈0.74) and the packing densities of organic crystals [41,59].

The packing density of HIC-F1 is close to the 0.87 value reported for nucleic acids [41], and for globular proteins is in the 0.72-0.78 range [38,61]. HIC-F1 is then tightly packed with voids (≈20% in average), which is an intrinsic property of hyperbranched polymers [96-99]. This view is consistent with the structure of HIC-F1 which is a thin ellipsoidal object with a dense outer shell and a highly dense porous central network, as indicated by the local fractal dimension of about 2.6 [17].

Table II.5. Volumetric parameters and hydration of HIC fractions (HIC-F1, HIC-F2 and HIC-F3) obtained from A. *senegal* gum by Hydrophobic Interaction chromatography (HIC). All measurements were done at 25°C using pH 5 acetate buffer 10 mM.

Partial molar volumes and related parameters	**HIC-F1**	**HIC-F2**	**HIC-F3**
$V_s°$ Experimental partial molar volume ($cm^3.mol^{-1}$)	195715	878462	1038047
V_M Intrinsic partial molar volume ($cm^3.mol^{-1}$)	176296	790616	934243
V_{vdw} vdW partial molar volume ($cm^3.mol^{-1}$)	143530	566467	548311
V_{void} void partial molar volume ($cm^3.mol^{-1}$)	32766	224149	385932
V_T thermal partial molar volume ($cm^3.mol^{-1}$)	50440	191573	192283
V_I interaction partial molar volume ($cm^3.mol^{-1}$)	-30852	-103727	-90771
V_{sh} Partial molar volume hydration water ($cm^3.mol^{-1}$)	16.298	16.320	16.333
Decrease of partial molar volume of hydration water (%)	9.5	9.3	9.3
Packing density ($Vvdw/V_M$)	0.81	0.72	0.60
Void volume (%)	18.6	28.4	40.2
Hydration number n_h (mole H_2O/mole AGP)	18128	61748	54444
Hydration number n_h (g_{H2O}/g_{AGP})	0.85	0.68	0.54
Hydration number n_h (molecule H_2O/per residue)	9.0	6.8	5.1
Hydration number n_h per polysaccharide moiety (gH_2O/g AGP)[a]	0.88	0.72	0.62
Hydration number n_h per interacting charged or polar site polysaccharide moiety ($g_{H2O}/g_{sugar\ residue}$)	8.5	6.6	5.8
Hydration number n_h per protein moiety (g_{H2O}/g_{AGP})[a]	0.44	0.36	0.31
Hydration number n_h per interacting charged or polar site protein moiety ($g_{H2O}/g_{amino\ acid\ residue}$)	3.9	3.6	3.4
Partial molar adiabatic compressibility and related parameters			
K_M ($cm^3.mol^{-1}.Pa^{-1}$) Intrinsic molar adiabatic compressibility	1.88E-05	1.00E-04	1.49E-04
β_M (Pa^{-1}) Intrinsic coefficient of adiabatic compressibility	1.06E-10	1.27E-10	1.60E-10
Partial molar compressibility hydration water ($cm^3.mol^{-1}.Pa^{-1}$)	5.20E-09	4.60E-09	5.30E-09
Partial specific compressibility hydration water (Pa^{-1})	2.91E-10	2.54E-10	2.95E-10
Decrease of partial molar adiabatic compressibility of hydration water (%)	37	45	36

(a) estimated values considering that polysaccharides bound twice as much water than proteins

The partial molar thermal volume V_T can be approximated from the product of the total solvent accessible surface area (SASA, $Å^2$) and the thickness of the thermal volume (Å) [61,68]. The SASA parameter for HIC-F1 was first estimated using the average solvent accessible surface areas of atoms of carbon and oxygen from various linear and weakly branched polysaccharides [100,101]. The used values for C, O and O^- were 10, 15.2 and 30.2 $Å^2$, respectively. We then obtained a total SASA estimate of about 84000 $Å^2$. To check if this value is in an acceptable magnitude, we first considered as a rough approach the surface area of a homogeneous oblate ellipsoid with the dimensions proposed for HIC-F1 with semi-axis (Å) 96x96x14 [17]. We found a surface area of ≈62000 $Å^2$. Since the surface of HIC-F1 is highly rough, an accessible surface area larger than 62000 $Å^2$ was not unreasonable. It may be of interest to note that, using with the M_w of HIC-F1 the power-law relationships SASA ≈ $5.3M_w^{0.76}$, found for oligomeric proteins with M_w up to $2x10^5$ $g.mol^{-1}$ [102,103], the SASA was 86000 $Å^2$. In order to calculate V_T, we needed to estimate the thickness (Δ) of the thermal volume. Values between 0.5 and 1 Å have been calculated on small solutes and proteins [61,64,68,69]. The parameter Δ has been shown to depend on the solute size, and values of around 1 have been calculated for large solute [91]. We then took a value of 1 Å. Multiplying the SASA estimation by 1 produced a thermal volume V_T of 84000 $Å^3$ or 50440 $cm^3.mol^{-1}$. If a Δ value of 0.65 had been taken, as calculated for globular proteins by Bano and Marek (2005)[68], a value of 54600 $Å^3$ or 33000 $cm^3.mol^{-1}$ should have been obtained. This should not change fundamentally the interpretation of our data, but obviously should impact the value of V_l, then of the hydration term (decrease).

Knowing V_s°, V_M and taking 84000 $Å^3$ for V_T, we obtained for HIC-F1 an interaction volume V_l of about -31000 $cm^3.mol^{-1}$ (Table II.5). We noted that V_l was close in absolute value to that of void volume V_{void}, as remarked previously for globular proteins [32]. V_l can be also estimated from the contribution of pentose and hexose type sugars. Thus, it was found that, on average, a monosaccharide in dilute solution such as arabinose or galactose contributed at 25°C to around -28 $cm^3.mol^{-1}$ to V_l and that a hydroxyl group OH contributed to -5 $cm^3.mol^{-1}$ [104]. We do not know the contribution to V_l of charged groups, but, based on the double solvent-accessible surface area of charged oxygen atoms as compared to uncharged ones, we supposed this contribution as the double than that of polar groups, i.e., -10 $cm^3.mol^{-1}$ to V_l. Multiplying this value by the number of sugar residues give a V_l value of around -30000 $cm^3.mol^{-1}$, close to the estimated one.

Using the different volumes, it was possible to find the hydration number of HIC-F1 in dilute conditions through the equation: $V_l = n_h\ (V_h^\circ - V_o^\circ)$. We needed however to know the water volume contraction that was induced by the solute-water interaction, then the partial molar volume of interacting water V_h°. Interactions between chemical groups and water induce generally a water volume contraction of about 5-10% for polar groups and 10-15% for charged groups [71]. A 10% increase in the density of hydration shell is commonly observed for biopolymers [41,105]. Taking an average value of 7.5% for polar groups and 12.5% for charged groups, $(V_h^\circ - V_o^\circ)$ was -1.7 $cm^3.mol^{-1}$ (9.3-9.5% water volume contraction). Then, n_h was in average 18130 H_20 molecules per HIC-F1 molecule or 0.85 g $H_2O.g^{-1}$ AGP (Table II.5).

The same analysis was done for the two other fractions HIC-F2 and HIC-F3. For these AGP, the amount of proteins cannot be longer neglected. However, in order to calculate the volumetric contribution of the protein part, we needed the protein M_w. Considering the percentages in proteins and the global M_w (Table II.1 and Table II.2), assuming a single averaged polypeptide, we get protein M_w values for HIC-F2 and HIC-F3 of around 95000 $g.mol^{-1}$ and 230000 $g.mol^{-1}$, respectively. Values comprised between 30000 and 250000 $g.mol^{-1}$ were proposed for the protein part of HIC-F2 [15,16,106] and a value of around 500000 $g.mol^{-1}$ was proposed for HIC-F3 [15]. High M_w values for the AGP protein cores probably indicated the presence of supramolecular structures, with many polypeptide chains in different glycoprotein modules [16,19]. Nevertheless, with these M_w values, we estimated the global protein contribution to V_s°, V_M and V_T using the approximate equations proposed for globular proteins [61]. Final calculations for HIC-F2 and HIC-F3 are indicated in Table II.5. We first noted that the V_l/V_{void} ratio, in absolute value, was smaller than unity, which was a clear difference with HIC-F1. This was mainly due to the increase of the void volume for HIC-F2 and HIC-F3 of 28.4% and 40.2%, respectively (Table II.5). This result can be connected to the above mentioned increase of AGP density from HIC-F1 to HIC-F3 (Table II.2), but also to previous microscopic experiments that showed a more open structure for HIC-F2, and especially HIC-F3, as noted in the introduction. The increase of V_{void} could be due both to the increase in the relative protein concentration (additive effect) and to more heterogeneous chain packing of massive sugar blocks and constrained proteins. Increasing the M_w of hyperbranched polymers have been shown to promote an increase of the volume of

voids [98,99,107,108]. In parallel, n_h decreased from HIC-F1 to HIC-F3 (as supposed from Figure II.2) with values around 0.85, 0.68 and 0.54 g $H_2O.g^{-1}$ AGP, respectively, in agreement with the charged, polar and nonpolar characteristics of the three fractions.

4.3. Partial molar adiabatic compressibility of AGPs

Having estimated the partial molar volumes and hydration numbers, we turn now to the determination of adiabatic compressibility, then to the flexibility of macromolecules. We used the modified version of the Eq. II.11:

$$k_s^\circ = k_M + n_h\left(K_{sh}^\circ - K_{so}^\circ\right)/M_w + k_r \qquad \text{(II.13)}$$

with the partial specific adiabatic compressibility k_s° ($cm^3.g^{-1}.Pa^{-1}$) equal to $k_s^\circ = K_s^\circ/\mathrm{M_w}$, the intrinsic partial specific adiabatic compressibility $k_M = K_M/\mathrm{M_w}$, and the relaxation term $k_r = K_r/\mathrm{M_w}$. The parameter K_r is of a few percent for globular proteins and almost zero for unfolded polypeptides and nucleic acids that are more hydrated than globular proteins, then less flexible [35,37,41,109]. It was neglected in the present analysis. We first considered HIC-F1 in some details, then HIC-F2 and HIC-F3.

The parameter k_M was estimated based on the partial molar adiabatic compressibility of hydrating water K_{sh}° predicted for charged and polar groups [71], and on the peculiar hydration properties of hyperbranched polymers. K_{sh}° of water solvating charged groups is smaller than that of bulk water (20-60% decrease) and the K_{sh}° of polar groups were between 80 and 110% of the bulk water value, depending on the chemical nature of other chemical groups in proximity. In addition, the compressibility of water in the hydration shell of the molecule is somewhat larger near apolar atoms [31,39]. For globular proteins, all these contributions resulted in a global ≈20-35% decrease of K_{sh}° [36,37,39,61,110]. This value can further decrease down to 50-60% for highly hydrophilic proteins or highly pressurized globular proteins, indicating that stronger solute-water interactions induced stronger perturbation of solvent adiabatic compressibility [110-112]. Stronger perturbation of hydrating water was also determined for highly branched polysaccharides as compared to linear ones or dendrimers, which can be due to strong water confinement within the hyperbranched architecture [113]. This can be probably related to the increased hydration of polar groups in close proximity to other polar groups [35,37,64,65]. Also, it is of interest to

note that the surface roughness of biopolymers can significantly impact, through the existence of grooves, the strength of solute-water hydration [114]. Based on these different arguments, we took for K_{sh}° average values of 3.30x10^{-9} cm^3.mol^{-1}.Pa^{-1} for charged groups (60% decrease) and 2.48 x 10^{-9} cm^3.mol^{-1}.Pa^{-1} for polar groups (30% decrease). We then obtained for HIC-F1 an average K_{sh}° value of 5.2x10^{-11} cm^3.mol^{-1}.Pa^{-1} or 29x10^{-11} Pa^{-1}, corresponding to a 37% decrease as compared to the bulk water (Table II.5). Please note that this value is larger than the 18x10^{-11} Pa^{-1} arbitrary value usually used for characterizing the adiabatic compressibility of strongly hydrogen-bonded hydrating water in the case of polysaccharides [45,47,50,51,54], but still of the same magnitude.

Using the assumed K_{sh}°, we then found for HIC-F1 an intrinsic partial specific adiabatic compressibility k_M of 5.4x10^{-11} cm^3.g^{-1}.Pa^{-1}, then a coefficient of adiabatic compressibility β_M of 10.6x10^{-11} Pa^{-1}, close to the 12 – 13x10^{-11} Pa^{-1} value found for ice [40,48,115-117]. This value is in the 3-10x10^{-11} Pa^{-1} range estimated for dextrans, carageenans and starch polysaccharides based on volumetric measurements [44-46,52], and confirmed the highly rigid nature of highly glycosylated AGPs. For globular proteins, ultrasonic measurements [31,36,61,118,119] and other experimental approaches or molecular dynamic simulations [28,110,120-124] have provided β_M values extrapolated at ambient pressure in the range 10–25x10^{-11} Pa^{-1}. Such value is considered as to be the most reliable value for globular proteins [38,40]. Since, $\beta_M = \frac{B_M}{\rho_M}$, the coefficient of proportionality B_M for HIC-F1 was 8.7x10^{-11} Pa^{-1}, which was notably smaller than the 18.3x10^{-11} Pa^{-1} value determined for globular proteins [61]. Consequently, the interior of HIC-F1 was less easily deformable than the interior of globular proteins, and then contributed to a less extent to the adiabatic compressibility. This can be in part related to the higher rigidity of sugar chains as compared to that of amino acid ones. It is known for long time that grafting glycan chains onto a protein resulted in a decrease of its flexibility [125]. Assuming that the B_M parameter was constant, we calculated the coefficients of adiabatic compressibility β_M for HIC-F2 and HIC-F3. We found, respectively, 12.7x10^{-11} Pa^{-1} and 16x10^{-11} Pa^{-1} for HIC-F2 and HIC-F3. Although all AGP were intrinsically rigid, the flexibility was increasingly larger for species containing more proteins, in relation to the increase in volume fluctuations. Armed with the β_M values, we calculated the adiabatic compressibility of hydrating water and we found that HIC-F2 and HIC-F3 hydration induced a decrease of K_{sh}° by 45% and 36%, respectively (Table II.5).

These results clearly suggested that the strength of solute-water molecule interactions, the quality of hydration, was not significantly different for the AGPs extracted from Acacia gum. this may connected to the observation that, within each class of neutral monosaccharides (pentoses and hexoses), the contraction of water caused by each polar group is more or less the same [104]. In parallel, this suggested that the hydration ability of AGP is mainly determined by the relative amount of charged, polar and nonpolar residues (the quantity of hydration) and the interior architecture of macromolecules.

4.4. Additional comments on the hydration properties of AGPs

The question of the hydration of AGPs has not been considered in details in the past, probably because it seemed obvious that Acacia gums are by nature highly hydrophilic [4]. Indeed, the affinity of AGPs for water provides an extremely favorable environment for binding water, which is mainly due to the carbohydrate component of AGPs and in part to their highly branched characteristic [126]. For instance, intramolecular (and intermolecular) voids could be occupied by water in a variety of metastable states, thus preventing the formation of the ideal ice structure [126]. In addition, hyperbranched macromolecules may induce the formation of a well-ordered network of interacting water molecules through the crowded environment between closely packed chains, as shown for phytoglycogen [113,127,128].

In the present study, we estimated hydration numbers of 0.85, 0.68, and 0.54 g $H_2O \cdot g^{-1}$ AGP for, respectively, HIC-F1, HIC-F2, and HIC-F3 (Table II.5). We remember that the "hydration number (n_h)" refers to water molecules involved in the hydration shell, and then with significant perturbation of its physicochemical properties. These values are in the range of the 0.6–1.2 g $H_2O \cdot g^{-1}$ values of interacting "bound" water experimentally measured on Acacia *senegal* gum by water adsorption experiments or DSC [4,126,129], validating *a posteriori* the approximations we used for calculations. More specifically, values around 0.6–0.7 g $H_2O \cdot g^{-1}$ were found for raw A. *senegal* gum and values around 0.9–1.2 g $H_2O \cdot g^{-1}$ were found for calcium or sodium salts of the gum, showing the role of minerals on molecule hydration. This range is common for polysaccharides and can be compared to the usual values found for globular proteins (0.3–0.5 g $H_2O \cdot g^{-1}$). Then, when considering that polysaccharides were bound in general twice water than proteins, the peptide or protein part

of HIC-F1, HIC-F2 and HIC-F3 contained approximatively 0.44, 0.36 and 0.31 g $H_2O \cdot g^{-1}$ protein (Table II.5), respectively, which is coherent with the content in polar and nonpolar amino acids and in line with reported values for proteins. On the other hand, n_h of the polysaccharide moieties was estimated as 0.88, 0.72, and 0.62 g $H_2O \cdot g^{-1}$ AGP, for, respectively, HIC-F1, HIC-F2, and HIC-F3 (Table II.5). This corresponded to n_h per sugar residue of, in average, 8.5, 6.6, and 5.8 g $H_2O \cdot g^{-1}$. Now, taking into account the 2.8 estimated averaged number of interacting polar and charged sites per sugar residue, n_h per interacting sites were in theory around 3.1, 2.4, and 2.1 for, respectively, HIC-F1, HIC-F2, and HIC-F3. These values can be compared to the 2.6–2.7 g H_2O per OH hydration number determined at 25 °C for arabinose and galactose, the two predominant sugars in Acacia gums [71], and more generally to the ~3 values that are usually found for monosaccharides and disaccharides in solution [127,130,131]. This result would indicate that the hydration shell of sugars that is involved in the hyperbranched structure of AGPs is not fundamentally different from that of isolated sugars. This is in clear contrast with (neutron scattering) results obtained on hyperbranched phytoglycogen, which revealed a n_h per polar sites of around 7, which was probably due to the crowded environment between the closely packed chains within the phytoglycogen particle and the existence of a well-ordered network of water molecules [113,127]. Thus, phytoglycogen can adsorb up to 2.6 g $H_2O \cdot g^{-1}$ polysaccharide [127].

Interestingly, like phytoglycogen, hyperbranched AGPs from Acacia gums may adsorb a maximum amount of 3–4 g $H_2O \cdot g^{-1}$ AGP, as determined from DSC experiments. This also indicated the formation of a three-dimensional network of AGP and water builds up as a structured entity [126]. We are then faced to an apparent contradiction, since sugars in AGPs displayed the same behavior than single sugars in solution, but a network of interacting water molecules seems to be created. One possible reason is that our estimate was based on the non-covalently bound polar and charged groups, without considering the likely existence of intramolecular hydrogen bonding between some of chemical groups. Strongly bound water is tightly associated with carbohydrate chains, which could form intramolecular hydrogen bonds within the highly cross-linked gum structure [126]. The presence of volume fluctuations in AGPs also suggests the existence of intramolecular hydrogen bonding. The question remains pending; however, higher n_h per interacting sites does not seem unreasonable for AGPs. Another possibility is that physicochemical properties of water hydrating Acacia gum, but not involved in hydration shell, is insufficiently perturbed to be probed using ultrasound

measurements. This point also deserves more investigation, using other complementary methods, such as DSC, neutron scattering, or dielectric spectroscopy.

5. Concluding Remarks

This paper reports the first volumetric characterization of hyperbranched arabinogalactan (AGP) from Acacia gum. These properties are to a great extent determined by hydration and flexibility of macromolecules, two molecular characteristics that can be probed using combined sound and density measurements and calculations of volumetric parameters, i.e., partial specific volume v_s° ($cm^3 \cdot g^{-1}$), and, for instance, coefficient of partial specific adiabatic compressibility β_s° (Pa^{-1}). We characterized both A. *senegal* and *seyal* gums and the three fractions that were obtained from the former by hydrophobic interaction chromatography (HIC). Fractions were named HIC-F1, HIC-F2, and HIC-F3, according to their order of elution, and then in the order of increased hydrophobicity.

For both total gums and HIC fractions, the adiabatic compressibility was negative, indicating that the hydration contribution was more important than the intrinsic molecular contribution. Changing the solvent quality did not markedly change the volumetric parameters of A. *senegal*, in line with the weak polyelectrolyte behavior of AGPs, excepted at high ionic strength where an increase of the v_s° parameter, then a decrease of hydration, was observed. In addition, the adiabatic compressibility (K_s°) of A. *senegal* was less negative than that of A. *seyal*, which is probably due to the larger arabinose content of the latter. Regarding HIC fractions, v_s° and K_s° were strongly dependent on their protein content, which in turn, largely determine their hydrophobicity. A larger protein content, like for HIC-F2 and HIC-F3, means a higher number of nonpolar amino acids and concomitantly a smaller number of polar and charged sugars, then a reduced hydration. Minerals contribute to this tendency through charge shielding. Thus, v_s° was larger and β_s° was less negative for the less polar HIC-F3. Plotting v_s° vs. β_s° with our AGP data and literature data obtained on globular proteins, polysaccharides and nucleic acids produced a curve that could be considered as a polarity-flexibility qualitative scale. In this curve, volumetric parameters of AGPs were intermediate between those of highly charged rigid polysaccharides and less polar more flexible globular proteins, highlighting the semi-rigid features of these hybrid protein-polysaccharide complexes. Due to this hybrid configuration, volumetric properties are better

balanced for AGPs than for polysaccharides and proteins, which must play an important role in the ability of these biopolymers to rapidly adapt to various polarity environments and to interact with both polar and nonpolar molecules.

Based on volumetric parameters, biochemical composition, and basic structural characteristics, we tentatively described macroscopic thermodynamic properties of HIC fractions through microscopic molecular characteristics. We obtained molecular parameters that were not previously described for AGP, such as, for instance, the packing density, then the percentage of interior voids, and the intrinsic adiabatic compressibility, and then the macromolecular flexibility. The volume of voids increased with the AGP molar mass and hydrophobicity from about 20% for HIC-F1 to 40% for HIC-F3. The high value obtained for the latter is probably due both to the larger amount of protein, the effect of this larger amount of protein in the global AGP architecture and the formation of AGP assembly through mainly protein-protein interactions. In parallel, the intrinsic AGP rigidity decreased from HIC-F1 to HIC-F3, which is in line with an increase in molecular volume fluctuations. The hydration number of fractions was estimated and reasonable values in the range 0.5–0.9 $H_2O \cdot g^{-1}$ AGP were found, with obviously the larger values being found for the more polar fraction, i.e., HIC-F1. The amount of interacting water clearly depended on the chemical composition of fractions, but apparently not on the strength of water-AGP interaction. Due to the calculation estimations, this point needs to be experimentally confirmed by alternative methods. Averaged n_h of sugar residues constituting AGP did not appear to be significantly different from that of single monosaccharide in solution, in the case where all free possible interacting sites are considered. However, the existence of intramolecular hydrogen bonding between sugar chains in close proximity that contribute to volume fluctuations, are rather in favor of larger effective n_h per sugar residue. This suggests the presence of a network of water molecules, which a part may display similar physicochemical properties than bulk water.

In the aggregate, despite some rough approximations, our results demonstrated that protein-rich high molar mass HIC-F3 was the more flexible and the less hydrated AGP in A. *senegal* gum, while protein-poor low molar mass HIC-F1 was the less flexible and the more hydrated AGP, the HIC-F2 fraction exhibiting an intermediate behavior. These results can be connected to the known physicochemical properties of Acacia gums, especially their solubility behavior and their interfacial properties. In particular, while Acacia gums solubilize easily in

water, through the major contribution of the polar HIC-F1, it is known that HIC-F3 is a molecule where the solubility is strongly sensitive to solvent polarity, but also to the minimum water concentration reached upon fraction dehydration, either by freeze-drying or spray-drying. Regarding interfacial properties, the higher surface activity of HIC-F3 among the three fractions [132] can be related both to the larger percentage of volume fluctuations and to the lower macromolecular hydration ability. In terms of futures prospects, the same analyses will be made on highly purified HIC-F2 and HIC-F3 fractions in order to better take into account the inherent AGP polydispersity. Also, the question of the effect of AGP self-assembly, a property that is shared by all AGPs, on volumetric properties of gums needs to be considered.

6. Acknowledgements

We gratefully acknowledge Tigran Chalikian for his help in part of the data treatment. This work was supported by the Alland&Robert Company and a Ph.D. grant (V. Mejia Tamayo) from the Equatorian research ministry (Senescyt).

7. Complementary Studies

Experiments were done in other types of Acacia gums and macromolecular fractions of A. *senegal*, arising from hydrophobic interaction chromatography (HIC) and interaction exchange chromatography (IEC) fractionation and acid precipitation (Arabic acid).

7.1. Biochemical properties and structural properties

The biochemical properties of the IEC-fractions of A. *senegal* are presented in Table II.6. These fractions, IEC-F1 and IEC-F2, were obtained by coupled Size Exclusion/ Ionic Exchange Chromatography (IEC) according to the procedure explained by Apolinar-Valiente et al (2019)[133]. Similarly to A. gums and HIC fractions, the IEC-fractions were composed of the same sugars, being Ara and Gal the main sugars present. Furthermore, the Ara/Gal ratio of the IEC-F1 and IEC-F2 fractions was 1.06 and 0.65, respectively, and, the negatively charged to neutral sugars ratio of IEC-F2 was higher compared to IEC-F1 (0.27 and 0.22,

respectively). In addition, the IEC-F2 presented a higher branching degree (0.79) than IEC-F1 (0.75).

The amount of protein found in the IEC-F1 fraction (9.36%) was considerably higher compared to the IEC-F2 fraction (1.98%). The protein content of IEC-F1 suggests the presence of the HIC-F2 and HIC-F3 fractions, since they have higher protein contents (6.3% and 13.8%, respectively). The IEC-F2 (4%) fraction presented a higher mineral content than IEC-F1 (2.4%), which can be explain by the fractionation process: IEC-F1 was eluted with water, meanwhile, IEC-F2 fraction was eluted using a solution of 2M NaCl.

Regarding the amino acid profile, the IEC fractions presented a similar profile as A. gums and HIC-fractions, being Hyp and Ser the mayor amino acids present (see Annex B). Furthermore, the Hyp and Ser summed value of IEC-F1 was higher than IEC-F2 (40% and 34%, respectively). In addition, both IEC fractions showed a similar value of polar and charged amino acids (72%).

Table II. 6. Biochemical properties of IEC fractions of A. *senegal* gum

Component ($mg.g^{-1}$)	**IEC-F1**	**IEC-F2**
Total Dry Matter	91.7 ± 0.2	91.8 ± 0.2
Sugars [a]	88.2	94.3
Arabinose (%)[b]	35.5 ± 1.4	26.1 ± 0.7
Galactose (%)[b]	33.5 ± 1.7	40.5 ± 0.4
Rhamnose (%)[b]	12.8 ± 0.7	12.4 ± 0.1
Glucuronic Acid (%)[b]	17.3 ± 0.4	19.8 ± 0.4
4-O-Me-Glucuronic Acid (%)[b]	1.1 ± 0.1	1.2 ± 0.2
Branching degree [d]	0.75	0.79
Proteins [c]	9.4 ± 0.1	1.8 ± 0.1
	(28) [e]	(28) [e]
Minerals	2.4 ± 0.3	4.0 ± 0.2

[a] Total content of sugars calculated from the difference of proteins and minerals from 1000 $mg.g^{-1}$
[b] Sugar composition was determined by GC-MS
[c] Protein content was measured using the Kjeldhal method
[d] Determined on neutral sugars according to the equation DB = 2D/(2D + L), where D is the number of dendritic units or branched units linked at three or more sites and L is the number of linear units having two glycosidic linkages[20,75]
[e] Percentage in nonpolar amino acids calculated according to Zhu et al (2016) [82]

The structural properties of the IEC fractions of A. *senegal* are presented in Table II.7. The IEC-F1 fraction contained mainly molecules of high M_w (97%), which might suggest that the

HIC-F2 and a part of HIC-F3 are present in this fraction. Furthermore, its higher M_w ($3.1x10^6$ g.mol^{-1}) suggests the presence of supramolecular assemblies (M_w> 2-$3x10^6$ g.mol^{-1}). On the other hand, the IEC-F2 fraction presented a low M_w ($5.3x10^5$ g.mol^{-1}) and was formed mainly of low M_w molecules (81%). In addition, the IEC-F1 fraction presented lower polydispersity index than IEC-F2 (1.2 and 1.9, respectively). Conversely, the intrinsic viscosity and R_h of IEC-F1 was higher (87.9 mL.g^{-1} and 34 nm, respectively) than the IEC-F2 fraction (28.2 mL.g^{-1} and 12.6 nm, respectively).

Table II. 7 Structural properties of the IEC fractions obtained from A. *senegal,* obtained by high performance size exclusion chromatography (HPSEC)-Multi angle light scattering (MALS) at 25°C

	IEC-F1	**IEC-F2**
M_w (g.mol^{-1})	$3.1x10^6$	$5.3x10^5$
M_n (g.mol^{-1})	$2.6x10^6$	$2.9x10^5$
M_w/M_n	1.2	1.8
M_w<$7.5x10^5$ g.mol^{-1} (%)	3	81
R_h (nm)	34.8	12.4
[η] (mL.g^{-1})	90.2	27.8
Density (g.cm-**3**)[a]	0.99726	0.99742

(a) Obtained from the extrapolation of the density in function of gum concentration

The combination of the biochemical and structural properties of A. gums and IEC fractions allowed the calculation of the basic composition and structural properties calculated of the polysaccharide and protein moiety (Table II.8). The potential number of charged and polar and non-polar sites was calculated in the same way as for the HIC fractions (section 4.2.).

The IEC-F1 fraction presented a higher number of charges compared to IEC-F2 (50377 and 9375, respectively). Furthermore, the charge density among the macromolecular fractions of A. *senegal* increases as follows: HIC-F1 < IEC-F2 < HIC-F2 < HIC-F3 < IEC-F1. In addition, taking into account the amount of non-polar interacting sites, the IEC-F1 fraction has a higher hydrophobicity than IEC-F2 (342 and 12, respectively). Interestingly, this amount is similar as HIC-F3 (354), which also suggests its presence in the IEC-F1 fraction. In a general way, the hydrophobicity of the HIC and IEC fractions is as follows: HIC-F1 <

IEC-F2 < HIC-F2 < IEC-F1 < HIC-F3. These results show that the fractionation processes HIC and IEC are able to separate the macromolecular fractions in terms of size, charge and hydrophobicity.

Table II. 8. Basic composition and structural parameters of A. gums and IEC fractions in aqueous solutions (1 g.L^{-1}) as obtained from biochemical analyses and HPSEC-MALS measurements

	A. *seyal*	**A. *senegal***	**IEC-F1**	**IEC-F2**
M_w (g.mol^{-1})	700500	645500	3100000	529900
Sugars (%)	97.80	94.71	88.208	92.56
Proteins (%)	0.77	2.15	9.36	1.8
Polysaccharide moiety M_w (g.mol^{-1})	695106	631622	2809840	520362
Average sugar residue M_w (g.mol^{-1})	167.8	175.1	170.4	173.3
Number of sugar residues	4142	3606	16490	3003
Average total free OH/residue	2.52	2.96	3.05	3.12
Potential number of charged and polar interacting sites (polysaccharide moiety)	10449	10678	50377	9375
Protein moiety M_w (g.mol^{-1})	5394	13878	290160	9538
Average amino acid residue M_w (g.mol^{-1})	126.6	128.1	129.3	128.0
Number of amino acid residues	43	108	2244	75
Charged and polar amino acids (%)	71.5	79.6	72.3	72.4
Non-polar amino acids (%)	28.5	26.8	27.7	27.6
Hydrophobicity index [a]	-1.07	-1.18	-1.39	-1.15
Number of interaction sites	0.81	0.85	0.85	0.84
Potential number of charged and polar interacting sites (protein moiety)	35	92	1915	63
Potential number of non-polar interacting sites (protein moiety)	8	16	329	12

(a) From the hydrophobicity scale proposed by Zhu et al [82]

7.2. Volumetric properties

The partial specific volume (v_s°) and partial specific adiabatic compressibility coefficient (β_s°) of the IEC fractions obtained from A. *senegal* are presented in Table II.9. The IEC-F1 fraction presented higher values of v_s° and β_s° (0.6095 cm^3.g^{-1} and -9.42x10^{-11} Pa^{-1},

respectively) than A. *senegal* (0.584 $cm^3.g^{-1}$ and -12.2x10^{-11} $cm^3.g^{-1}$, respectively). These results suggest a higher flexibility of IEC-F1 as compared to A. *senegal*, HIC-F1 and HIC-F2. Since molecule flexibility has been associated with good interfacial properties [134], this fraction should have better interfacial properties than HIC-F2. On the other hand, the IEC-F2 fraction presented a similar value of $v_s°$ and $\beta_s°$ (0.583 $cm^3.g^{-1}$ and -12.9x10^{-11} Pa^{-1}, respectively) than A. *senegal*, thus suggesting similar flexibility and interfacial properties.

Table II. 9. Partial specific volume ($v_s°$) and coefficient of partial specific adiabatic compressibility ($\beta_s°$) of the additional HIC, IEC fractions and Arabic acid obtained from A. *senegal*

Gum or fraction	$v_s°$ ($cm^3.g^{-1}$)	$\beta s°$ (x10^{11} Pa^{-1})
IEC-F1	0.6095	-9.42
IEC-F2	0.5823	-12.9

8. Complementary Information

8.1. Branching degree of A. gums

Table C.1: Branching degree of A. gums, HIC and IEC fractions of A. *senegal*

Gum or fraction	D	L	Branching degree
A. *seyal*	34.7	47.9	0.59
A. *senegal*	41.1	22.9	0.78
HIC-F1	38.5	23.1	0.77
HIC-F2	39.5	23.4	0.77
HIC-F3	36.0	24.0	0.75
IEC-F1	41.2	27.6	0.75
IEC-F2	46.0	25.1	0.79

(a) Branching degree was calculated according to Holter et al (1997)[75], using the equation: DB= 2D/(2D+L), where: D is the fraction of dendritic monomeric units and L is the fraction of linear monomeric units. (b) Values of D and L were obtained by methylation analysis, according to the procedure explained by Lopez et al (2015)[20].

8.2. Amino acid composition of A. gums and macromolecular fractions

Table C.2. Amino acid composition of Acacia gums and macromolecular fractions obtained using Hydrophobic Interaction (HIC) and Ionic Exchange (IEC) Chromatography in dry basis (mean ± standard deviation)

Amino acid ($mg.g^{-1}$)	A. *senegal*	HIC-F1	HIC-F2	HIC-F3	IEC-F1	IEC-F2	A. *seyal*
Alanine	0.49 ± 0.04	0.04 ± 0.01	0.77 ± 0.06	3.10 ± 0.17	2.53 ± 0.00	0.30 ± 0.03	0.22 ± 0.01
Arginine	0.31 ± 0.05	0.05 ± 0.01	0.48 ± 0.12	2.59 ± 0.07	2.41 ± 0.00	0.21 ± 0.05	0.12 ± 0.00
Aspartic Acid	1.24 ± 0.04	0.11 ± 0.02	2.28 ± 0.15	9.36 ± 0.27	7.35 ±0.17	0.87 ± 0.03	0.49 ± 0.04
Cysteine	0.00 ± 0.00	0.08 ± 0.01	0.22 ± 0.15	0.90 ± 0.05	0.00 ± 0.00	0.00 ± 0.00	0.00 ± 0.00
Glutamic Acid	0.92 ± 0.01	0.12 ± 0.02	2.16 ± 0.24	6.56 ± 0.11	4.94 ± 0.09	0.87 ± 0.10	0.28 ± 0.003
Glycine	0.79 ± 0.004	0.13 ± 0.01	1.51 ± 0.07	4.42 ± 0.08	4.25 ± 0.09	0.56 ± 0.02	0.25 ± 0.07
Histidine	1.37 ± 0.60	0.29 ± 0.03	3.07 ± 0.24	7.40 ± 0.45	9.08 ± 0.26	1.02 ± 0.02	0.27 ± 0.07
Hydroxyproline	6.26 ± 0.52	1.47 ± 0.16	13.3 ± 0.36	22.66 ± 0.79	25.25 ± 0.09	4.32 ± 0.05	2.13 ± 0.19
Isoleucine	0.31 ± 0.02	0.00 ± 0.00	0.51 ± 0.03	2.61 ± 0.03	2.07 ± 0.09	0.19 ± 0.02	0.13 ± 0.01
Leucine	1.83 ± 0.04	0.31 ± 0.04	4.18 ± 0.04	10.91 ± 0.05	10.11 ± 0.17	1.40 ± 0.01	0.60 ± 0.03
Lysine	0.63 ± 0.02	0.06 ± 0.01	1.04 ± 0.09	5.34 ± 0.22	5.75 ± 0.17	0.38 ± 0.01	0.12 ± 0.03
Phenylalanine	0.82 ± 0.05	0.07 ± 0.02	2.14 ± 0.02	6.58 ± 0.07	4.71 ± 0.09	0.70 ± 0.03	0.21 ± 0.01
Proline	1.61 ± 0.14	0.27 ± 0.04	3.42 ± 0.07	8.17 ± 0.17	7.70 ± 0.09	1.14 ± 0.02	0.56 ± 0.001
Serine	2.50 ± 0.05	0.60 ± 0.06	5.69 ± 0.23	12.05 ± 0.41	13.67 ± 0.26	1.91 ± 0.02	0.95 ± 0.03
Threonine	1.42 ± 0.02	0.33 ± 0.04	3.46 ± 0.09	7.22 ± 0.13	7.93 ± 0.00	1.14 ± 0.01	0.34 ± 0.02
Tyrosine	0.31 ± 0.04	0.04 ± 0.01	0.28 ± 0.03	1.73 ± 0.09	2.18 ± 0.02	0.11 ± 0.02	0.14 ± 0.02
Valine	0.71 ± 0.00	0.07 ± 0.01	1.63 ± 0.04	6.22 ± 0.03	4.60 ± 0.09	0.60 ± 0.03	0.31 ± 0.16
Total amino acids	**21.52 ± 1.64**	**4.04 ± 0.50**	**46.14 ± 2.03**	**117.82 ± 3.19**	**114.53 ± 1.68**	**15.74 ± 0.47**	**7.12 ± 0.69**

9. References

1. Williams, P.A.; Philips, G.O. Gum arabic. In *Handbook of hydrocolloids*, G. O. Philips, P.A.W., Ed. Boca Raton: CRC Press: 2000; pp 155-168.
2. Nussinovitch, A. *Plant gum exudates of the world: Sources, distribution, properties and aplication*. CRC Press: Boca Raton (USA), 2010.
3. Verbeken D.; Dierckx S.; K., D. Exudate gums: Occurence, production, and applications. *Applied Microbiology Biotechnology* **2003**, *63*, 10-21.
4. Sanchez, C.; Nigen, M.; Mejia Tamayo, V.; Doco, T.; Williams, P.; Amine, C.; Renard, D. Acacia gum: History of the future. *Food Hydrocolloids* **2018**.
5. Akiyama, Y.; Eda, S.; Kato, K. Gum arabic is a kind of arabinogalactan protein. *Agric. and Biol. Chem.* **1984**, *48*, 235-237.
6. Tan, L.; Showalter, A.M.; Egelund, J.; Hernandez-Sanchez, A.; Doblin, M.S.; Bacic, A. Arabinogalactan-proteins and the research challenges for these enigmatic plant cell surface proteoglycans. *Frontiers in Plant Sci.* **2012**, *3*, 1-10.
7. Lamport, D.T.A.; Várnai, P. Periplasmic arabinogalactan glycoproteins act as a calcium capacitor that regulates plant growth and development. *New Phytologist* **2013**, *197*, 58-64.
8. Liu, C.; Mehdy, M.C. A nonclassical arabinogalactan protein gene highly expressed in vascular tissues, agp31, is transcriptionally repressed by methyl jasmonic acid in arabidopsis. *Plant Physiology* **2007**, *145*, 863-874.
9. Ellis, M.; Egelund, J.; Schultz, C.J.; Bacic, A. Arabinogalactan-proteins: Key regulators at the cell surface? *Plant Physiol* **2010**, *153*, 403-419.
10. Showalter, A.M. Arabinogalactan-proteins: Structure, expression and function. *Cell. Mol. Life Sci.* **2001**, *58*, 1399-1417.
11. Qu, Y.; Egelund, J.; Gilson, P.R.; Houghton, F.; Gleeson, P.A.; Schultz, C.J.; Bacic, A. Identification of a novel group of putative arabidopsis thaliana β-(1,3)-galactosyltransferases. *Plant Molecular Biology* **2008**, *68*, 43-59.
12. Anderson, D.M.W.; Stoddart, J.F. Studies on uronic acid materials. Part xv. The use of molecular-sieve chromatography on acacia *senegal* gum (gum arabic). *Carbohydrate Research* **1966**, *2*, 104-114.
13. Randall, R.C.; Phillips, G.O.; Williams, P.A. Fractionation and characterization of gum from acacia *senegal*. *Food Hydrocolloids* **1989**, *3*, 65-75.
14. Islam, A.M.; Phillips, G.O.; Sljivo, A.; Snowden, M.J.; Williams, P.A. A review of recent developments on the regulatory, structural and functional aspects of gum arabic. *Food Hydrocolloids* **1997**, *11*, 493-505.
15. Renard, D.; Lavenant-Gourgeon, L.; Ralet, M.C.; Sanchez, C. Acacia *senegal* gum: Continuum of molecular species differing by their protein to sugar ratio; molecular weight and charges. *Biomacromolecules* **2006**, 2637-2649.
16. Mahendran, T.; Williams, P.; Phillips, G.; Al-Assaf, S.; Baldwin, T. New insights into the structural characteristics of the arabinogalactan-protein (agp) fraction of gum arabic. *Journal of Agricultural and Food Chemistry* **2008**, 9269-9276.
17. Sanchez, C.; Schmitt, C.; Kolodziejczyk, E.; Lapp, A.; Gaillard, C.; Renard, D. The acacia gum arabinogalactan fraction is a thin oblate ellipsoid: A new model based on small-angle neutron scattering and ab initio calculation. *Biophysical Journal* **2008**, *94*, 629-639.
18. Renard, D.; Garnier, C.; Lapp, A.; Schmitt, C.; Sanchez, C. Structure of arabinogalactan-protein from acacia gum: From porous ellipsoids to supramolecular architectures. *Carbohydrate Polymers* **2012**, *90*, 322-332.
19. Renard, D.; Lavenant-Gourgeon, L.; Lapp, A.; Nigen, M.; Sanchez, C. Enzymatic hydrolysis studies of arabinogalactan-protein structure from acacia gum: The

self-similarity hypothesis of assembly from a common builiding block. *Carbohydrate Polymers* **2014**, *112*, 648-661.

20. Lopez-Torrez, L.; Nigen, M.; Williams, P.; Doco, T.; Sanchez, C. Acacia *senegal* vs. Acacia *seyal* gums – part 1: Composition and structure of hyperbranched plant exudates. *Food Hydrocolloids* **2015**, *51*, 41-53.

21. Renard, D.; Garnier, C.; Lapp, A.; Schmitt, C.; Sanchez, C. Corrigendum to "structure of arabinogalactan-protein from acacia gum: From porous ellipsoids to supramolecular architectures" [carbohydr. Polym. 90 (2012) 322–332]. *Carbohydrate Polymers* **2013**, *97*, 864-867.

22. Renard, D.; Lepvrier, E.; Garnier, C.; Roblin, P.; Nigen, M.; Sanchez, C. Structure of glycoproteins from acacia gum: An assembly of ring-like glycoproteins modules. *Carbohydrate Polymers* **2014**, *99*, 736-747.

23. Ray, A.K.; Bird, P.B.; Iacobucci, G.A.; Clark, B.C. Functionality of gum arabic. Fractionation, characterization and evaluation of gum fractions in citrus oil emulsions and model beverages. *Food Hydrocolloids* **1995**, *9*, 123-131.

24. Idris, O.H.M.; Williams, P.A.; Phillips, G.O. Characterisation of gum from acacia *senegal* trees of different age and location using multidetection gel permation chromatography. *Food Hydrocolloids* **1998**, 379-388.

25. Dror, Y.; Cohen, Y.; Yerushalmi-Rozen, R. Structure of gum arabic in aqueous solution. *J. of Polym. Sci. Pol. Phys.* **2006**, *44*, 3265-3271.

26. Wang, Q.; Burchard, W.; Cui, S.W.; Huang, X.Q.; Philips, G.O. Solution properties of conventional gum arabic and a matured gum arabic (acacia (sen) super gum). *Biomacromolecules* **2008**, *9*, 1163-1169.

27. Al-Assaf, S.; Sakata, M.; McKenna, C.; Aoki, H.; Phillips, G.O. Molecular associations in acacia gums. *Structural Chemistry* **2009**, *20*, 325-336.

28. Kharakoz, D.P. Protein compressibility, dynamics, and pressure. *Biophysical Journal* **2000**, 511-525.

29. Chalikian, T.V.; Breslauer, K.J. On volume changes accompanying conformational transitions of biopolymers. *Biopolymers* **1996**, *39*, 619 - 626.

30. Scharnagl, C.; Reif, M.; Friedrich, J. Stability of proteins: Temperature, pressure and the role of the solvent. *Biochimica et Biophysica Acta (BBA) - Proteins and Proteomics* **2005**, *1749*, 187-213.

31. Gavish, B.; Gratton, E.; Hardy, C.J. Adiabatic compressibility of globular proteins. *Proc. Natl. Acad. Sci. USA* **1983**, *80*, 750-754.

32. Gekko, K.; Hasegawa, Y. Compressibility-structure relationship of globular proteins. *Biochemistry* **1986**, *25*, 6563 - 6571.

33. Durchschlag, H. Specific volumes of biological macromolecules and some other molecules of biological interest. In *Thermodynamic data for biochemistry and biotechnology*, Hinz, H.-J., Ed. Springer: Berlin, 1986; pp 45 - 128.

34. Gekko, K. Hydration-structure-function relationships of polysaccharides and proteins. *Food Hydrocolloids* **1989**, *3*, 289-299.

35. Sarvazyan, A., P. Ultrasonic velocimetry of biological compounds. *Annu. Rev. Biophys. Biophys. Chem* **1991**, *20*, 321 - 342.

36. Kharakoz, D.P.; Sarvazyan, A., P. Hydrational and intrinsic compressibilities of globular proteins. *Biopolymers* **1993**, *33*, 11 - 26.

37. Chalikian, T.V.; Sarvazyan, A., P.; Breslauer, K.J. Hydration and partial compressibility of biological compounds. *Biophysical Chemistry* **1994**, *51*, 89 - 109.

38. Chalikian, T.V.; Filfil, R. How large are the volume changes accompanying protein transitions and binding? *Biophysical Chemistry* **2003**, *104*, 489-499.

39. Dadarlat, V.M.; Post, C.B. Decomposition of protein experimental compressibility into intrinsic and hydration shell contributions. *Biophysical Journal* **2006**, *91*, 4544-4554.

40. Gekko, K. Volume and compressibility of proteins. In *High pressure bioscience: Basic concepts, applications and frontiers*, Akasaka, K.; Matsuki, H., Eds. Springer Netherlands: Dordrecht, 2015; pp 75-108.

41. Buckin, V.A.; Kankiya, B.I.; Sarvazyan, A., P.; Uedaira, H. Acoustical investigation of poly(da)-poly(dt), poly[d(a-t)]-poly[d(at)], poly (a).Polyflj) and DNA

hydration in dilute aqueous solutions. *Nucleic Acids Res.* **1989**, *17*, 4189-4203.

42. Chalikian, T.V.; Sarvazyan, A., P.; Plum, S.G.E.; Breslauer, K.J. Influence of base composition, base sequence, and duplex structure on DNA hydration: Apparent molar volumes and apparent molar adiabatic compressibilities of synthetic and natural DNA duplexes at 25°c. *Biochemistry* **1994**, *33*, 2394-2401.

43. Chalikian, T.V.; McGregor, J.R.B. Nucleic acid hydration: A volumetric perspective. *Phys. of Life Rev.* **2007**, *4*, 91-115.

44. Myahara, Y.; Shio, H. The adiabatic compressibility of starch sols. *Nippon kagaku zasshi* **1952**, *73*, 1-2.

45. Shiio, H.; Yoshihashi, H. Measurement of the amount of bound water by ultrasonic interferometer. Ii. Polyvinyl alcohol and its partially substituted acetates. *The Journal of Physical Chemistry* **1956**, *60*, 1049-1051.

46. Itoh, K. Adiabatic compressibility of polysaccharides. *Nippon kagaku zasshi* **1956**, *77*, 1594-1595.

47. Nomura, H.; Miyahara, Y. Partial specific compressibility of polystyrene. *Journal of Applied Polymer Science* **1964**, *8*, 1643-1649.

48. Suzuki, Y.; Uedaira, H. Hydration of potassium hyaluronate. *Bulletin of the Chemical Society of Japan* **1970**, *43*, 1892-1894.

49. Gekko, K.; Noguchi, H. Physicochemical studies of oligodextran. I. Molecular weight dependence of intrinsic viscosity, partial specific compressibility and hydrated water *Biopolymers* **1971**, *10*, 1513 -1524.

50. Gekko, K.; Noguchi, H. Hydration behavior of ionic dextran derivatives. *Macromolecules* **1974**, *7*, 224 - 229.

51. Kawaizumi, F.; Nishio, N.; Nomura, H.; Miyahara, Y. Calorimetric and compressibility study of aqueous solutions of dextran with special reference to hydration and structural change of water. *Polymer Journal* **1981**, *13*, 209 - 213.

52. Nomura, H.; Onoda, M.; Miyahara, Y. Preferential solvation of dextran in water - ethanol mixtures. *Polymer Journal* **1982**, *14*, 249-253.

53. Davies, A.; Gormally, J.; Wyn-Jones, E.; Wedlock, D.J.; Phillips, G.O. A study of factors influencing hydration of sodium hyaluronate from compressibility and high precision densimetric measurements. *Biochem. J.* **1983**, *213*, 363 - 369.

54. Gekko, K.; Mugishima, H.; Koga, S. Compressibility, densimetric and calorimetric studies of hydration of carrageenans in the random form. *Int. J. Biol. Macromol.* **1985**, *7*, 57 -63.

55. Kupke, D.W. Density and volume change measurements. In *Physical principles and techniques of protein chemistry, part c*, Leach, S.J., Ed. Academic Press: 1973; pp 3 - 75.

56. Hoiland, H. Partial molar volumes of biochemical model compounds in aqueous solution. In *Thermodynamic data for biochemistry and biotechnology*, Hinz, H.-J., Ed. Springer-Verlag Berlin Heidelberg: 1986; pp 17 - 44.

57. Chalikian, T.V.; Sarvazyan, A.P.; Breslauer, K.J. Partial molar volumes, expansibilities, and compressibilities of .Alpha.,.Omega.-aminocarboxylic acids in aqueous solutions between 18 and 55.Degree.C. *The Journal of Physical Chemistry* **1993**, *97*, 13017-13026.

58. Gekko, K.; Yamagami, K. Flexibility of food proteins as revealed by compressibility. *Journal Agricultural Food Chemisty* **1991**, *39*, 57 - 62.

59. Taulier, N.; Chalikian, T.V. Compressibility of protein transitions. *Biochimica et Biophysica Acta (BBA) - Protein Structure and Molecular Enzymology* **2002**, *1595*, 48-70.

60. Gekko, K.; Noguchi, H. Compressibility of globular proteins in water at 25 °c. *The Journal of Physical Chemistry* **1979**, *83*, 2706 -2714.

61. Chalikian, T.V.; Totrov, M.; Abagyan, R.; Breslauer, K.J. The hydration of globular proteins as derived from volume and compressibility measurements: Cross correlating thermodynamic and structural data. *Academic Press* **1996**, *260*, 588 - 603.

62. Pierotti, R.A. A scaled particle theory of aqueous non aqueous solutions. *Chem. Rev.* **1976**, *76*, 717 - 726.

63. Reiss, H. Scaled particle methodsin the statistical thermodynamics of fluids. *Adv. Chem. Phys.* **1965**, *9*, 1-84.

64. Kharakoz, D.P. Volumetric properties of proteins and their analogs in diluted water solutions. *Biophysical Chemistry* **1989**, *34*, 115-125.

65. Kharakoz, D.P. Partial volumes of molecules of arbitrary shape and the effect of hydrogen bonding with water. *Journal of Solution Chemistry* **1992**, *21*, 569-595.

66. Pierotti, R.A. The solubility of gases in liquids. *J. Phys. Chem.* **1963**, *67*, 1840-1845.

67. Kauzmann, W. Some factors in the interpretation of protein denaturation. *Advanced Protein Chemistry* **1959**, *14*, 1 - 63.

68. Bánó, M.; Marek, J. How thick is the layer of thermal volume surrounding the protein? *Biophysical Chemistry* **2006**, *120*, 44-54.

69. Edward, J.T.; Farrell, P.G. Relation between van der waals and partial molal volumes of organic molecules in water. *Can. J. Chem.* **1975**, *53*, 2965-2970.

70. Voloshin, V.P.; Medvedev, N.N.; Smolin, N.; Geiger, A.; Winter, R. Exploring volume, compressibility and hydration changes of folded proteins upon compression. *Physical Chemistry Chemical Physics* **2015**, *17*, 8499-8508.

71. Chalikian, T.V. Structural thermodynamics of hydration. *The Journal of Physical Chemistry B* **2001**, *105*, 12566-12578.

72. Kharakoz, D.P. Volumetric properties of proteins and their analogues in diluted water solutions. 2. Partial adiabatic compressibilities of amino acids at 15-70.Degree.C. *The Journal of Physical Chemistry* **1991**, *95*, 5634-5642.

73. Anderson, D.M.W.; Bridgeman, M.M.E.; Farquhar, J.G.K.; McNab, C.G.A. The chemical characterization of the test article used in toxicological studies of gum arabic (acacia senegal (l.) willd). *International Tree Crops Journal* **1983**, *2*, 245-254.

74. Flindt, C.; Alassaf, S.; Phillips, G.; Williams, P. Studies on acacia exudate gums. Part v. Structural features of acacia *seyal*. *Food Hydrocolloids* **2005**, *19*, 687-701.

75. Hölter, D.; Burgath, A.; Frey, H. Degree of branching in hyperbranched polymers. *Acta Polym.* **1997**, *48*.

76. Gashua, I.B.; Williams, P.A.; Yadav, M.P.; Baldwin, T.C. Characterisation and molecular association of nigerian and sudanese acacia gum exudates. *Food Hydrocolloids* **2015**, *51*, 405-413.

77. Osman, M.E.; Menzies, A.R.; Williams, P.A.; Phillips, G.O.; Baldwin, T.C. The molecular characterisation of the polysaccharide gum from acacia *senegal*. *Carbohydrate Research* **1993**, *246*, 303-318.

78. Chen, C.-G.; Pu, Z.-Y.; Moritz, R.L.; Simpson, R.J.; Bacic, A.; Clarke, A.E.; Mau, S.-L. Molecular cloning of a gene encoding an arabinogalactan-protein from pear (pyrus communis) cell suspension culture. *Proc. Natl. Aca. Sci.* **1994**, *91*, 10305-10309.

79. Goodrum, L.J.; Patel, A.; Leykam, J.F.; Kieliszewski, M.J. Gum arabic glycoprotein contains glycomodules of both extensin and arabinogalactan-glycoproteins. *Phytochemistry* **2000**, *54*, 99-106.

80. Al-Assaf, S.; Phillips, G.; Williams, P. Studies on acacia exudate gums: Part ii. Molecular weight comparison of the vulgares and gummiferae series of acacia gums. *Food Hydrocolloids* **2005**, *19*, 661-667.

81. Sanchez, C.; Renard, D.; Robert, P.; Schmitt, C.; Lefebvre, J. Structure and rheological properties of acacia gum dispersions. *Food Hydrocolloids* **2002**, *16*, 257-267.

82. Zhu, C.; Gao, Y.; Li, H.; Meng, S.; Li, L.; Francisco, J.S.; Cheng Zeng, X. Characterizing hydrophobicity of amino acid side chains in a protein environment via measuring contact angle of a water nonodroplet on planar peptide network. *PNAS* **2016**, *113*, 12946-12951.

83. Shahidi, F.; P., F.; Edward, J.T. Partial molar volumes of organic compounds in water. Iii. Carbohydrates. *Journal of Solution Chemistry* **1976**, *5*, 807 - 816.

84. Banipal, P.K.; Banipal, T.S.; LArk, B.S.; Ahluwalia, J.C. Partial molar heat capacities and volumes of some mono-, di- and tri-saccharides in water at 298.15, 308.15 and 318.15 k. *J. Che.Soc., Faraday Trans* **1997**, *93*, 81 - 87.

85. Perkins, S.J.; Miller, A.; Hardingham, T.E.; Muir, H. Physical properties of the hyaluronate binding region of proteoglycan

from pig laryngeal cartilage. *Journal of Molecular Biology* **1981**, *150*, 69-95.

86. Durchschlag, H. Determination of the partial specific volume of conjugated proteins. *Colloid & Polymer Science* **1989**, *267*, 1139 - 1150.

87. Tamura, Y.; Gekko, K.; Yoshioka, K.; Vonderviszt, F.; Namba, K. Adiabatic compressibility of flagellin and flagelar filament of *salmonella typhimurium*. *Biochimica et Biophysica Acta* **1997**, *1335*, 120 - 126.

88. Chalikian, T.V.; Völker, J.; Srinivasan, A.R.; Olson, W.K.; Breslauer, K.J. The hydration of nucleic acid duplexes as assessed by a combination of volumetric and structural techniques. *Biopolymers* **1999**, *50*, 459-471.

89. Vandevelde, M.C.; Fenyo, J.C. Estimation of the charge density of arabic acid by potentiometry and dye binding. *Polym. Bull.* **1987**, *18*, 47-51.

90. Chalikian, T.V. On the molecular origins of volumetric data. *J. Phys. Chem. B* **2008**, *112*, 911-917.

91. Patel, N.; Dubins, D.N.; Pomes, R.; Chalikian, T.V. Size dependence of cavity volume: A molecular dynamics study. *Biophys Chem* **2012**, *161*, 46-49.

92. Chen, C.R.; Makhatadze, G.I. Protein volume: Calculating molecular van der waals and void volume in proteins. *BMC Bioinformatics* **2015**, *16*, 101-106.

93. Bondi, A. Van der waals volumes and radii. *J. Phys. Chem.* **1964**, *68*, 441-451.

94. Spillane, W.J.; Birch, G.G.; Drew, M.G.B.; Bartolo, I. Correlation of computed van der waals and molecular volumeswith apparent molar volumes (amw) for amino acid, carbohydrate and sulfamate tastant molecules. Relationship between corey-pauling-koltun volumes (vcpk) and computed volumes. *Chem. Soc. Perkin Trans* **1992**, *2*.

95. Batsanov, S.S. Van der waals radii of elements. *Inorganic Mat.* **2001**, *37*, 871-885.

96. Carl, W. A monte carlo study of model dendrimers. *J. Chem. Soc. Faraday Trans.* **1996**, *92*, 4151-4154.

97. Lin, S.-T.; Maiti, P.K.; Goddard, W.A. Dynamics and thermodynamics of water in pamam dendrimers at subnanosecond time scales. *J. Phys. Chem. B* **2005**, *109*, 8663-8672.

98. Li, T.; Honk, K.; Porcar, L.; Verduzco, R.; Butler, P.D.; Smith, G.S.; Liu, Y.; Wei-Ren Chen, W.R. Assess the intramolecular cavity of a pamam dendrimer in aqueous solution by small-angle neutron scattering. *Macromolecules* **2008**, *41*, 8916-8920.

99. Maiti, P.K. Pamam dendrimer: A ph controlled nanosponge. *Can. J. Chem.* **2017**, *95*, 991-998.

100. Kaliannan, P.; Gromiha, M.M.; Elanthiraiyan, M. Solvent accesibility studies on polysaccharides. *Int. J. Biol. Macromol.* **2001**, *28*, 135-141.

101. Kaliannan, P.; Gromiha, M.M.; Ramamurthi, K.; Elanthiraiyan, M. Solvent accesibility studies on glycosaminoglycans. *Biophysical Chem.* **1998**, *74*, 135-141.

102. Miller, S.; Lesk, A.M.; Janin, J.; Chothia, C. The accesible surface area and stability of oligomeric proteins. *Nature* **1987**, *328*, 834-836.

103. Janin, J.; Miller, S.; Chothia, C. Surface, subunit interfaces and interior of oligomeric proteins. *Mol. Biol.* **1988**, *204*, 155-164.

104. Chalikian, T.V.; Breslauer, K.J. Thermodynamic analysis of biomolecules: A volumetric approach. *Current Opinion in Structural Biology* **1998**, *8*, 657-664.

105. Svergun, D.I.; Richard, S.; Koch, M.H.J.; Sayers, Z.; Kuprin, S.; Zaccai, G. Protein hydration in solution: Experimental observation by x-ray and neutron scattering. *PNAS* **1998**, *95*, 2267-2272.

106. Qi, W.; Fong, C.; Lamport, T.A. Gum arabic glycoprotein is a twisted hairy rope. A new model based on o-galactosylhydroxyproline as the polysaccharide attachment site. *Plant Physiology* **1991**, *96*, 848-855.

107. Maiti, P.K.; Tahir, C.T.; T., L.S.; Williamm, A.G.I. Effect of solvent and ph on the structure of pamam dendrimers. *Macromolecules* **2005**, *38*, 979-991.

108. Maiti, P.K.; Cagin, T.; Wang, G.; Goddard, W.A. Structure of pamam dendrimers: Generations 1 through 11. *Macromolecules* **2004**, *37*, 6236-6254.

109. Sarvazyan, A., P.; Hemmes, P. Relaxational contributios to protein

compressibility from ultasonic data. *Biopolymers* **1979**, *18*, 3015-3024.

110. Marchi, M. Compressibility of cavities and biological water from voronoi volumes in hydrated proteins. *J. Phys. Chem. B.* **2003**, *107*, 834-836.

111. Scharnagl, R.M.; Friedrich, J. Local compressibilities of compressibilities: Comparison of optical experiments and simulations for horse heart cytochrome-c. *Biophysical J.* **2005**, *89*, 64-75.

112. Smolin, N.; Winter, R. A molecular dynamics simulation of snase and its hydration shell at high temperature and high pressure. *Biochim. Biophys. Acta* **2006**, *1764*.

113. Grossutti, M.; Dutcher, J.R. Correlation between chain architecture and hydration water structure in polysaccharides. *Biomacromolecules* **2016**, *17*, 1198-1204.

114. Kuhn, L.A.; Siani, M.A.; Pique, M.E.; Fisher, C.L.; Getzoff, E.D.; Tainer, J.A. The interdependence of protein surface topography and bound water molecules revealed by surface accessibility and fractal density measures. *J. Mol. Biol.* **1992**, *228*, 13-22.

115. Smith, A.H.; Lawson, A.W. The velocity of sound in water as a function of temperature and pressure. *J. Chem. Phys.* **1954**, *22*, 351-359.

116. Leadbetter, A.J. The thermodynamic and vibrational properties of h₂o ice and d₂o ice. *Proceedings of the Royal Society of London. Series A, Mathematical and Physical Sciences* **1965**, *287*, 403-425.

117. Chen, Y.-C. *Review of thermal properties of snow, ice and sea ice*; 1981; pp 1-35.

118. Jacobson. On the adiabatic compressibility of aqueous solutions. *Arkh. Kemi* **1950**, *2*, 177-210.

119. Priev, A.; Almagor, A.; Yedgar, S.; Gavish, B. Glycerol decreases the volume and compressibility of protein interior. *Biochemistry* **1996**, *35*, 2061 - 2066.

120. Edwards, C.; Palmer, S.B.; Helliwell, J.R.; Glover, D.; Harris, G.W.; Moss, D.S. Thermal motion in proteins estimated using laser-generated ultrasound and young's modulus measurements. *Acta Crystallogr.* **1990**, *A46*, 315-320.

121. Morozov, V.N.; Morozova, T.Y. Elasticity of globular proteins. The relation between mechanics, thermodynamics and mobility. *J. Biomol. Struct. Dyn.* **1993**, *11*, 459-481.

122. Paci, E.; Velikson, B. On the volume of macromolecules. *Biopolymers* **1996**, 785-797.

123. Mori, K.; Seki, Y.; Yamada, Y.; Matsumoto, H.; Soda, K. Evaluation of intrinsic compressibility of proteins by molecular dynamics simulations. *J. Chem. Phys.* **2006**, *125*.

124. Li, H.; Yamada, H.; Akasaka, K. Effect of pressure on individual hydrogen bonds in proteins: Basic pancreatic trypsin inhibitor. *Biochemistry* **1998**, *37*.

125. Wormald, M.R.; Petrescu, A.J.; Pao, Y.-L.; Glithero, A.; Elliot, T.; Dwek, R.A. Conformational studies of oligosaccharides and glycopeptides: Complementarity of nmr, x-ray crystallography, and molecular modelling. *Chem. Rev.* **2002**, *102*, 371-386.

126. Phillips, G.O.; Takigami, S.; Takigami, M. Hydration characteristics of the gum exudate from *acacia senegal*. *Food Hydrocolloids* **1996**, *10*, 11-19.

127. Nickels, J.D.; Atkinson, J.; Papp-Szabo, E.; Stanley, C.; Diallo, S.O.; Perticaroli, S.; Baylis, B.; Mahon, P.; Ehlers, G.; Katsaras, J., *et al.* Structure and hydration of highly-branched, monodisperse phytoglycogen nanoparticles. *Biomacromolecules* **2016**, *17*, 735-743.

128. Ramadugu, S.K.; Chung, Y.-H.; Xia, J.; Margulis, C.J. When sugars get wet. A comprehensive study of the behavior of water on the surface of oligosaccharides. *J. Phys. Chem. B* **2009**, *113*, 11003-11015.

129. Hatakeyama, T.; Uetake, T.; Hatakeayama, H. Frezeeing bound water restrained by gum arabic. In *Gums and stabilizers for the food industry*, Philips, P.A.W.G.O., Ed. RSC Publishing: Cambridge (UK), 2010; Vol. 15, pp 69-75.

130. Lupi, L.; Comez, L.; Paolantoni, M.; Perticaroli, S.; Sassi, P.; Morresi, A.; Ladanyi, B.M.; Fioretto, D. Hydration and aggregation in mono- and disaccharide aqueous solutions by gigahertz-to-terahertz light scattering and molecular dynamics simulations. *J. Phys. Chem. B* **2012**, *116*, 14760-14767.

131. Perticaroli, S.; Nakanishi, M.; Pashkovski, E.; Sokolov, A.P. Dynamics of hydration water in sugars and peptides solutions. *J. Phys. Chem. B* **2013**, *117*, 7729-7736.

132. Castellani, O.; Al-Assaf, S.; Axelos, M.; Phillips, G.O.; Anton, M. Hydrocolloids with emulsifying capacity. Part 2 – adsorption properties at the n-hexadecane–water interface. *Food Hydrocolloids* **2010**, *24*, 121-130.

133. Apolinar-Valiente, R.; Williams, P.; Nigen, M.; Tamayo, V.M.; Doco, T.; Sanchez, C. Recovery, structure and physicochemical properties of an aggregate-rich fraction from acacia senegal gum. *Food Hydrocolloids* **2019**, *89*, 864-873.

134. Razumovsky, L.; Damodaran, S. Surface activity-compressibility relationship of proteins at the air-water interface. *Langmuir* **1999**, *15*, 1392-1399.

Chapter III: Hydrodynamic Properties of Arabinogalactan-proteins from Acacia gums

Highlights

- AGPs were roughly classified using its weight-average molar mass into 'small AGPs' (M_w<7.5x10^5 g.mol^{-1}), 'large AGPs' (M_w>7.5x10^5 g.mol^{-1}) and 'AGP-based aggregates' (M_w<2x10^6 g.mol^{-1}).

- Three main phenomena were involved in the increase of the viscosity at low gum concentrations: the polyelectrolyte effect, adsorption on the capillary wall and presence of supramolecular assemblies.

- At charge neutralization, intrinsic viscosities [η] of 15, 45 and 60 mL.g^{-1} and hydrodynamic radii (R_H) of below 10 nm, from 10-40 nm and >50 nm were considered as characteristic values for 'small AGPs', 'large AGPs' and 'AGP-based aggregates', respectively. These results would suggest the existence of a basic "hydrodynamic unit".

- Using a combination of dynamic light scattering (DLS) and diffusion ordered nuclear magnetic resonance spectroscopy (DOSY-NMR), macromolecular populations with mean R_H significantly lower than the usually reported value of 9 nm were seen. Comparison of R_H measured by DLS and NMR highlighted the presence of AGP aggregates, especially in water.

- The use of a viscosity increment (ν) corresponding to a hard sphere (2.5) lead to overestimations of the hydration number, n_h. Based on approximated AGP dimensions, experimental ν in the range of 10-50 were estimated. Thus, n_h values corresponding to the bound water in the first hydration layer were obtained.

Hydrodynamic properties of Arabinogalactan-proteins from Acacia gums [1]

Veronica Mejia Tamayo[a], Michaël Nigen[a], Rafael Apolinar-Valiente[b], Thierry Doco[b], Pascale Williams[b], Denis Renard[c], Christian Sanchez[a]

[a] UMR IATE, UM-INRA-CIRAD-Montpellier Supagro, 2 Place Pierre Viala, F-34060 Montpellier Cedex, France.
[b] UMR SPO, INRA-UM, 2 Place Pierre Viala, F-34060 Montpellier Cedex, France.
[c] UMR BIA, INRA, F-44300 Nantes, France.

Abstract

Acacia gums are weakly charged, amphiphilic, hyperbranched arabinogalactan-proteins (AGP). They have a natural variability resulting from their differences in composition, size and conformation, polarity, polydispersity and self-assembly ability. In this article, we studied the main dynamic volumetric (hydrodynamic properties) solution properties of A. gums exudates. The study was carried out using the main species, A. *senegal*, A. *seyal* and the macromolecular fractions of the former obtained using hydrophobic interaction and ionic exchange chromatography (HIC and IEC fractions, respectively). The principal findings evidenced that three main phenomena were involved in the increase of the reduced viscosity at low gum concentration, the polyelectrolyte effect, adsorption of the gum on the capillary glass wall and presence of supramolecular assemblies or AGP aggregates. These factors were especially important in salt-free dispersions. The intrinsic viscosity, ($[\eta]$), and hydrodynamic radius (R_H) of all A. gums and macromolecular fractions were reduced with the increase of ionic strength of solvent, due to a reduction of solvent polarity, shielding of AGP charges and size of aggregates. The presence of a macromolecular population with R_H between 4-9 nm was evidenced using a combination of dynamic light scattering (DLS) and diffusion ordered nuclear magnetic spectroscopy (DOSY-NMR). Using $[\eta]$ at charge neutralization and

[1] Article prepared to be published in Colloids and Interfaces

viscosity increments (ν) in the range 10-50, hydration numbers (n_h) in the range of 0.1-1.1 g H_2O/g AGP were found for A. gums and HIC fractions. These results were close to that found using ultrasound and density measurements.

Keywords: Acacia gums, plant exudates, Arabinogalactan-proteins, hydrodynamic properties, intrinsic viscosity, hydrodynamic radius

1. Introduction

Acacia gum is the gummy exudate produced by the trunk and branches of Acacia *senegal* and Acacia *seyal* trees [1,2]. A. gums are composed by an ensemble of hyperbranched, amphiphilic, weakly charged arabinogalactan-protein type macromolecules (AGPs)[3]. They are composed of about 90% sugars, i.e. D-galactose, L-arabinose, L-rhamnose, glucuronic acid and 4-O-methylglucuronic acid [2,4], around 1-3% of proteins (0.2–0.4% of nitrogen) and 3-5% minerals [2]. Small amount of polyphenols and lipids are also present. The chemical structure of AGP's includes a backbone of 1-3 linked β–D-galactopyranosyl units, side chains being formed of two or five 1,3-linked β-D-galactopyranolsyl units joint to the main chain by 1,6 linkages. Both chains have units of α-L-arabinofuranosyl, α-L-rhamnopyranosyl, β-D-glucuronopyranosyl and 4-O-methyl-β-D-glucoronopyranosyl, being the last two end units [2,5-9]. A. gum is defined as a continuum of AGPs differing in sugar, amino acid and mineral composition, charge density, molar mass, size, shape and anisotropy [8-16]. The variability of Acacia gums properties arise not only from its origin and composition, but also from differences in their structural properties and inter and intra molecular interactions. In particular, it is known that AGP-based aggregates are often present in A. gums [2,17-19]. The presence of these aggregates is expected to modify flow properties of A. gum dispersions at high gum concentration but especially interfacial properties.

A. gums are extensively used in the food industry mainly due to their low viscosity up to 20-30% concentration and ability to form and stabilize oil-in-water emulsions [7]. Since these properties are related to intrinsic macromolecular characteristics such as molecular volume, flexibility and hydration, *static* volumetric properties, *i.e.* partial specific volume (v_s°) and adiabatic compressibility coefficient (β_s°), were studied in the precedent chapter. Thus, we demonstrated experimentally the different partial specific volumes and compressibilities of

the various AGP populations found in A. *senegal* gum and we estimated hydration numbers in the range 0.6 – 0.9 g H_2O/g AGP. These results could be used in part to explain physicochemical properties of gums. However, in practical situations of use A. gums dispersions are mixed, homogenized, pumped, and then, we may question about the effect of flow on macromolecule hydration. Fortunately, the volumetric characteristics of *moving* hydrated biomolecules, which are the hydrodynamic parameters of the molecule [20,21], can also be studied using their intrinsic viscosity ($[\eta]$), translational diffusion coefficient (D_T) and sedimentation coefficient (S_o). They allow access to complementary molecular properties such as hydrodynamic volume, conformation in dilute conditions, and dynamic interaction properties, which can also be linked to flexibility and hydration and thus physicochemical properties. Describing and linking static and dynamic volumetric properties is *a priori* interesting to provide a clearer picture of biopolymer functionality.

The hydrodynamic properties of A. gums have been scarcely studied, thus few information about the intrinsic viscosity, hydrodynamic radius and conformation of the HIC-fractions can be found in literature. In a general way, A. *senegal* has a higher $[\eta]$ than A. *seyal* (8-40 and 9-18 $mL.g^{-1}$, respectively) and lower hydrodynamic radius R_H (10-15 and 17 nm, respectively) [8,12,14,22-31]. Regarding HIC-fractions, HIC-F1 presented a lower $[\eta]$ and R_H (16-18 $mL.g^{-1}$ and 9-11 nm, respectively) than HIC-F2 (71-74 $mL.g^{-1}$ and 23-34 nm, respectively) and HIC-F3 (30-103 $mL.g^{-1}$ and 16-28 nm, respectively) [8,10,11,14,15,28,32]. Comparing data from different authors appears essentially difficult because of different experimental conditions, for instance different ionic strength of dispersions, when measuring intrinsic viscosity or hydrodynamic radius. In addition, polydispersity of gums render difficult if not impossible the rigorous measurement of the latter.

In the present article, we report the characterization of hydrodynamic and structural properties of A. *senegal*, A. *seyal* and AGP fractions of the former separated using hydrophobic interaction chromatography (HIC) and ionic exchange chromatography (IEC), as a function of the solvent ionic strength. The main objective of the study was to determine and compare intrinsic viscosity ($[\eta]$), sedimentation and translational diffusion coefficients (S_o and D_T, respectively), and hydrodynamic radius (R_H) of A. gums and fractions using different complementary techniques. These techniques encompass capillary viscometry, size exclusion chromatography coupled to multiangle laser light scattering and refractometry, low

field nuclear magnetic resonance spectroscopy, dynamic light scattering and analytical ultracentrifugation. In addition, macromolecular hydration was estimated from the intrinsic viscosity data and results were in reasonable agreement with those found using ultrasound measurements provided that anisotropy of AGP are takan into account.

2. Materials and Methods

2.1. Materials

The experiments were done using soluble powders of Acacia *senegal* (lot OF 152413) and Acacia *seyal* (lot OF110724), provided by Alland & Robert Company – Natural and Organic gums (Port Mort, France). Moisture, sugar and mineral content were reported elsewhere (Lopez et al, 2015)[12].

Macromolecular fractions of A. *senegal*, HIC-F1, HIC-F2 and HIC-F3, were obtained by colleagues of our team via hydrophobic interaction chromatography, following the fractionation process used by Randall et al (1989)[14] and Renard et al (2006)[8]. The HIC-F1 and HIC-F2 fractions were diafiltrated (AKTAFLUX 6 system, GE Healthcare, Upsala Sweden) and spray-dried (B-290 BUCHI, Labortechnik AG, Switzerland). The HIC-F3 fraction did not followed the diafiltration and spray drying steps to prevent the huge loss of materials and to avoid excessive dehydration and formation of insoluble AGPs [8,33]. Hence, it was concentrated using a rotavapor (461 BUCHI Water bath, Labortechnik AG, Switzerland), extensively dialyzed and freeze dried (Alpha 2-4 LSC, Bioblock Scientific, France). Freeze-drying was controlled to avoid excessive dehydration and avoid the formation of insoluble AGP [8,33]. AGPs from A. *senegal* (OF 152413) were also separated based on their charge density and hydrodynamic volume via ionic exchange chromatography with the recovery of two fractions, IEC-F1 and IEC-F2, that were diafiltratated and spray-dryed.

The biochemical characterization and amino acid profile of A. gums and HIC-fractions has already been discussed in a previous publication [34], for the IEC-fractions please see the supplementary studies of Chapter II. However, a summary is presented in Tables III.1 and III.2.

Table III.1. Summary of the biochemical composition of A. gums and AGP fractions

Gum or fraction	Ara/Gal	Charged /neutral sugar ratio	Branching degree	Proteins (%)	Minerals (%)
Acacia gums					
A. *seyal*	1.4	0.2	0.6	0.8	1.4
A. *senegal*	0.8	0.1	0.8	2.2	3.4
AGP fractions					
HIC-F1	0.7	0.3	0.8	0.5	3.1
HIC-F2	1.0	0.2	0.8	6.3	1.9
HIC-F3	1.2	0.2	0.8	13.8	4.9
IEC-F1	1.1	0.3	0.8	9.4	2.4
IEC-F2	0.7	0.2	0.8	1.6	4.0

* Data was taken from Mejia et al (2018) and Complementary studies of Chapter II.

Table III.2. Summary of the polar, non-polar and charged amino acids present in A. gums and AGP fractions

Gum or fraction	Charged (%)	Polar (%)	Non polar (%)	Hyp + Ser (%)	Glu + Asp (%)
Acacia gums					
A. *seyal*	47.9	27.4	28.5	43.3	10.8
A. *senegal*	49.9	29.7	26.8	40.7	10.0
AGP fractions					
HIC-F1	52.0	36.4	18.8	51.2	5.7
HIC-F2	48.4	30.8	27.4	41.2	9.6
HIC-F3	45.8	28.6	31.9	29.5	13.5
IEC-F1	47.8	32.4	27.7	34.0	10.7
IEC-F2	48.8	30.1	27.6	39.6	11.1

* Data extracted from the amino acid composition of A. gums and AGP fractions (supplementary) information of Chapter II)

2.2. Methods

2.2.1. Sample preparation

A. gum samples were prepared by dispersion of the freeze dried or spray dried powder in the desired solvent and kept overnight under constant stirring to allow complete hydration.

Dispersions were centrifuged to remove insoluble material (12 000 rpm, 30 min, 20°C). Dispersions were degassed to remove dissolved air (300 Ultrasonik bath, Ney, Yucaipa, CA, USA) and if needed the pH was controlled to 5 or 7, using 0.1 M HCl and 0.1 M NaOH, depending on the solvent used.

2.2.3. Determination of the Refractive Index Increment

The refractive index increment (dn/dc) of A. gums, HIC and IEC fractions was determined by measurements of the refractive index of A. gums dispersions (w/w), prepared in a similar way as explained in section 2.2.1. The refractive index was measured using an Abbemat Refractometer (Anton Paar, France). Measurements were performed at 25 °C and triplicated. The solvents used were water (pH 5), 0.01M sodium acetate buffer (pH 5), and 0.1M, 0.3M and 0.5M $LiNO_3$ (pH 7), that are all the solvent we used in studying A. gums. The dn/dc was obtained by linear regression of the refractive index versus A. gum concentration.

2.2.4. Size Exclusion chromatography (HPSEC) - Multi Angle Light Scattering (MALS)

The structural properties of A. *senegal*, A. *seyal,* HIC and IEC fractions of the former were characterized by multi-detector high performance size exclusion chromatography (HPSEC). The experiments were performed using a Shimadzu HPLC system (Shimadzu, Japan) coupled to four detectors, a Multi Angle Laser Light Scattering (DAWN Heleos II, Wyatt, Santa Barbara, CA, USA), a differential refractometer (Optilab T-rEX, Wyatt, Santa Barbara, CA, USA), an on-line viscometer (VISCOSTAR II, Wyatt, Santa Barbara, CA, USA) and a UV detector activated at 280 nm (SPD-20A, Shimadzu, Japan).

The separation of A. *senegal*, A. *seyal*, HIC-F1 and IEC-F2 fractions was performed on a column system composed of a pre-column Shodex OHPAK SB-G and four in-series columns: SHODEX OHPAK SB 803 HQ, SB 804 HQ, SB 805 HQ and OHPAK SB 806 HQ. Meanwhile, the separation of the HIC-F2, HIC-F3 and IEC-F1 fractions was done using only the SHODEX OHPAK 805 column due to their large molar mass and hyperbranched properties responsible of unusual elution phenomena using the four in-series column configuration.

Aqueous dispersions of A. gums, HIC and IEC fractions of approximately 1 $g.L^{-1}$ were injected and eluted using 0.1, 0.3 and 0.5 M (pH 7) $LiNO_3$ (0.02% NaN_3) as mobile phase (1

$cm^3.min^{-1}$, 25°C). Data were analyzed using the dn/dc determined experimentally and ASTRA software 6.1.2.84 (Wyatt Technologies, Santa Barbara, CA). A. gums were analyzed considering their weight-averaged molar masses, M_w. A gum was considered to have a low molar mass if its $M_w < 7.5x10^5$ $g.mol^{-1}$, to have a high molar mass if its $M_w > 7.5x10^5$ $g.mol^{-1}$ and to have supramolecular assemblies if its $M_w >$ 2-3 x 10^6 $g.mol^{-1}$ [10,13,34]. These limits are subjective but allow to simply classifying gums.

2.2.5 Capillary viscosimetry

The dynamic viscosity (η, mPa.s) of A. gums, HIC and IEC fractions in water (pH 5), 0.01 M sodium acetate buffer (pH 5) and 0.1 M $LiNO_3$ (pH 7) was measured using a capillary micro-viscometer LOVIS 2000M (Anton Paar, Graz, Austria). According to literature, the viscosity of A. *senegal* measured in aqueous dispersions remains practicaly constant in the pH range of 5–9 [35,36], therefore the difference in pH between water and sodium acetate buffer (pH 5) and 0.1 M $LiNO_3$ (pH 7) was not considered as significant. Temperature was kept at 25°C and was controlled using a built-in Peltier thermostat. Measurements were performed using a glass capillary (1.59 mm of diameter) and a steel ball (1 mm of diameter and density of 7.69 $g.cm^{-3}$). Dispersions were centrifuged (12 000 rpm, 30 min, 20°C) to eliminate insoluble material and large air bubbles, then degassed for 15 min to eliminate dissolved air (300 Ultrasonik bath, Ney, Yucaipa, CA, USA). Measurements were at least duplicated.

2.2.6. Dynamic Light Scattering (DLS)

The translational diffusion coefficient (D_T, $m^2.s^{-1}$) of A. gums, HIC and IEC fractions was determined using a 100 mW HeNe laser NICOMP nano Z (Z3000) equipment (PSS, Florida, USA). The wavelength used was 660 nm and a 10 mm square quartz cell was used to contain the sample. The equipment was set to operate in 'photon counting' mode. Fitting of the autocorrelation function was done using the cumulants method according to the following relation [37]:

$$g^{(1)}(\tau) = \exp(-\Gamma\tau) \quad \text{(III.1)}$$

$$\Gamma = k^2 D_T \quad \text{(III.2)}$$

where $g^{(1)}$ is the intensity of the signal (photon count), τ is the decay time (s) and Γ is the decay constant. Data were further analyzed using the NICOMP 2.0 software, which analyzed

data using a modified version of the cumulants method (non-linear least squares). This method allowed the qualitative discrimination of up to three molecule or particle populations.

Initial measurements were performed at different A. *senegal* concentrations in sodium acetate buffer (pH 5). However, an increase of the hydrodynamic radius, R_H, was seen at gum concentrations below 5 $g.L^{-1}$ and above around 10 $g.L^{-1}$ (complementary data C III.1), thus suggesting formation of supramolecular assemblies. The study of the effect of concentration on the hydrodynamic radius of A. gums was out of the scope of this study and was not performed in water and 0.1M $LiNO_3$. Measurements for A. *seyal*, HIC and IEC fractions were performed only at 5 $g.L^{-1}$ in all the used solvents.

In order to have an indication about biopolymer and particle anisotropy, the effect of the scattering angle was studied using three different angles (90°, 120° and 150°). However, no important dependence was seen in the hydrodynamic volume when considering *filtrated samples*. Therefore, the rest of the measurements were performed only in filtrated dispersions (0.25 µm, VWR, USA) at a scattering angle of 90°. Measurements were performed at 25°C and at least triplicated.

2.2.7. Diffusion Ordered Nuclear Magnetic Resonance Spectroscopy (DOSY-NMR)

The diffusion translational coefficient (D_T, $m^2.s^{-1}$) of A. gums, HIC and IEC fractions was determined using an Avance III-600 MHz NMR spectrometer (BRUKER, Leipzig, Germany), combined with a TXI cryoprobe. The instrument was equipped with a cooling system BCU I BRUKER to keep the probe and samples at constant temperature (25 °C). The equipment capability allows measurements of D_T values down to a minimum of 10^{-11} $m^2.s^{-1}$, which corresponded to a maximum R_H in D_20 solvent of about 20 nm.

Measurements were performed in dispersions of 5 $g.L^{-1}$ prepared in deuterium dioxide (D_2O), 0.01 M sodium acetate buffer/D_2O and 0.1 M lithium nitrate/D_2O. Dispersions were centrifuged (12 000 rpm, 30 min, 20°C) to eliminate insoluble material and air bubbles and if needed pH was corrected using DCl (0.1 N) and NaOD (0.1 N). Measurements were duplicated.

2.2.8 Analytical Ultracentrifugation (AUC)

The coefficient of sedimentation (S_o, Svedberg unit = 10^{-13} s) of A. gum, HIC and IEC macromolecular fractions was determined by Analytic Ultracentrifugation XLI (rotor Anti-50, Beckman Coulter Instruments, Palo Alto, USA) at 35 000 rpm and 25°C. The equipment had a double canal cell of 12 mm of optic path equipped with sapphire windows (Nanolytics, Postdam, DE). Measurements were performed using the sedimentation velocity method (AUC-SV). This method will be further explained in section 3.4. Data acquisition was done in integrated absorbance and interference optics and analyzed using the Redate v 1.0.1 software.

3. Theoretical treatment of data

3.1 Intrinsic viscosity

3.1.1. Definitions and determination

The viscosity of a solution η (mPa.s) is a measure of the resistance to flow [38,39] . Provided the fluid behaves as a Newtonian fluid, it can be measured using a capillary viscosimeter, where its value is determined from the flow time of a fixed volume of the liquid [38,40,41]. The effect of the dispersed macromolecule in the dispersion is given by the relative viscosity η_{rel} (dimensionless) or the specific viscosity η_{sp} (dimensionless) [38,39,42,43]:

$$\eta_{rel} = \frac{\eta}{\eta_o} \tag{III.3}$$

$$\eta_{sp} = \eta_{rel} - 1 = \frac{\eta - \eta_o}{\eta_o} \tag{III.4}$$

where η and η_o are the dynamic viscosity of the dispersion and solvent, respectively. The reduced viscosity (η_{red}) is the relation between the specific viscosity and the concentration (C, $cm^3.g^{-1}$) of the dispersion [38,39,42,43]:

$$\eta_{red} = \frac{\eta_{sp}}{C} \tag{III.5}$$

The intrinsic viscosity, $[\eta]$ ($mL.g^{-1}$), is a measure of the hydrodynamic volume (V_H) occupied by a molecule in solution, in the limit of infinite dilution [44-46]. It can be obtained from the extrapolation of the reduced viscosity η_{red} at infinite dilution since its value depends only on the molecular dimensions [38,45,47]:

$$[\eta] = \lim_{C \to 0} \eta_{red} = \lim_{C \to 0} \frac{\eta - \eta_o}{\eta_o C} \tag{III.6}$$

Several models have been developed to determine $[\eta]$, one of the most commonly used it the one developed by Huggins in 1942 [39,47-50]:

$$\eta_{red} = [\eta] + k_H\, C\, [\eta]^2 \quad \text{(III.7)}$$

where k_H is the Huggins constant (dimensionless), which depends on the form of the molecule and intermolecular interactions (quality of the solvent) [48,50].

In contrast with most neutral polymers, the reduced viscosity η_{red} of polyelectrolytes tends to increase with the decrease of polymer concentration, an effect also known as 'polyelectrolyte effect' [40,44,51-57]. This behavior has been suggested to be the effect of the increase of the electrostatic repulsions on the solute molecules (polyelectrolyte effect) [40,44,52,53,57-59] and alternatively to the adsorption of the polymer on the walls of the glass capillary [41,54,60]. The latter has been found to account for around 1-2% of errors in the determination of [η], hence in some studies it is often neglected [41]. We will show in the present paper that surface effects are not negligible with AGPs.

Due to the increase of the reduced viscosity at low concentrations, the use of the Huggins equation (III.7) to estimate the intrinsic viscosity results problematic. However, several mathematical models have been proposed to calculate the intrinsic viscosity of polyelectrolyte dispersions. Among them, the model of Yang takes into account the interactions between the solute and the wall of the capillary glass [54].

$$\frac{\eta_{sp}}{C} = \frac{[1+[\eta]\,C]\left[1+\left(k\,C/C_a+C\right)\right]-1}{C} \quad \text{(III.8)}$$

where k (dimensionless) describes the degree of adsorption of the solute, it can be positive or negative (see below) and C_a ($g.mL^{-1}$) is the concentration at which half of the available sites of the glass capillary wall are occupied by the solute. Furthermore, if the reduced viscosity of the dispersion as a function of the concentration shows an upward bending form, the solute is adsorbed in the capillary glass ($k>0$). Conversely, a downward bending form indicates a slip flow behavior, then a repulsion of the solute from the capillary wall ($k<0$) [41,54,60].

3.2. Translational diffusion coefficient

The translational diffusion coefficient (D_T) can be obtained via dynamic light scattering measurements (DLS) and diffusion ordered nuclear magnetic resonance spectroscopy (DOSY-NMR). In the DLS method, D_T is obtained by measuring the change of the intensity of the scattered light in time (correlation curve) as impacted by the Brownian motion of the objects. Meanwhile, in the DOSY-NMR method, D_T is measured by using the change of the

signal due to the Brownian movement of the molecules due to an applied gradient pulse [61,62].

Using the Stokes-Einstein equation, it is possible to access the hydrodynamic radius (R_H) of a molecule [21,42,59,63]:

$$D_T = \frac{k_B T}{f} = \frac{k_B T}{6 \pi \eta R_H} \quad \text{(III.9)}$$

where f is the frictional coefficient of a spherical particle of the same mass and (anhydrous) volume, defined by the Stokes equation $f = 6 \pi \eta N_A R_H$, where k_B is the Boltzmann constant (1.38×10^{-23}, $m^2.Kg.s^{-2}.K^{-1}$), T is the absolute temperature (K), η is the dynamic viscosity of the solvent ($mPa.s^{-1}$).

3.3. Sedimentation coefficient

The sedimentation coefficient, S, can be obtained via analytical ultracentrifugation using two methods, the sedimentation equilibrium (AUC-SE) and sedimentation velocity (AUC-SV) [64-66]. In the AUC-SE method, the ultracentrifugation is performed at lower speeds to allow the equilibrium between the centrifugal migration and diffusion, in other words when the concentration distribution remains constant over time [65,67]. The utilization of this method results more problematic due to the constraints of attaining the equilibrium that can take long measuring times [64,67]. In the AUC-SV method, the sedimentation coefficient is determined by measuring the movement of the boundary formed as the molecules move towards the bottom of the cell once a centrifugal field is applied [42,68,69]. This method is highly dependent on the hydrodynamic volume of molecules as large molecules will sediment faster [64,66,68].

The extrapolation of the sedimentation coefficient to zero concentration, S_o, is done to correct the non-ideality effects (e.g. charge of the molecule, diffusion and sedimentation variability depending on the polydispersity of the dispersion) and to eliminate the strong concentration dependence of S [42,68,70-72]. The following relations are the most used:

$$S = S_o(1 - k_s C) \quad \text{(III.10)}$$

$$\frac{1}{S} = \frac{1}{S_o}(1 + k_s C) \quad \text{(III.11)}$$

where k_s is the Gralen parameter ($cm^3.g^{-1}$), which is used for corrections due to the non-ideality of the system.

4. Results

4.1. Refractive Index Increment

The refractive index increments (dn/dc, $mL.g^{-1}$) of A. gums, HIC and IEC fractions of A. *senegal* measured in water, sodium acetate buffer and $LiNO_3$ are presented in Table III.3. No significant variation on the dn/dc of A. *senegal* obtained in water, sodium acetate buffer (0.01 M) and lithium nitrate (0.1 M) was seen (0.154, 0.155 and 0.155 $mL.g^{-1}$, respectively) and the same was true for A. *seyal*. Then, for the HIC and IEC fractions, the dn/dc was only determined in acetate buffer (0.01 M). On the other hand, when the ionic strength of lithium nitrate was increased to 0.3 M and 0.5 M, a decrease of the dn/dc of all A. gums, HIC and IEC fractions was clearly seen. This behavior suggested a predominant effect of the solute in salt-free solutions. In contrast, as salt is added, the solvent has a more important impact on the dn/dc. Similar behavior has been reported for dextran aqueous solutions [73].

The dn/dc value depends on the nature of the molecule, solvent and wavelength. For polysaccharides in aqueous solutions, values ranging from 0.14-0.16 $mL.g^{-1}$ are found in literature [68]. Meanwhile, for unmodified proteins, dn/dc values are in the range from 0.16 to 0.20 $mL.g^{-1}$ [73,74]. Furthermore, for A. gums, values around 0.14 $mL.g^{-1}$ (0.1 M $NaNO_3$, 30°C) [75], 0.141 $mL.g^{-1}$ (0.2 M NaCl, 25°C) [76] and 0.145 $mL.g^{-1}$ (0.1 M $LiNO_3$, 30°C) [8,12] are the most commonly reported. Therefore our results are in good concordance with the literature.

Table III.3 Experimental refractive index increment (dn/dc) of Acacia gums and AGP fractions of A. *senegal* at different ionic strength. All measurements were performed at 25°C.

Gum or fraction	Solvent	Ionic strength (M)	dn/dc ($mL.g^{-1}$)
A. *senegal*	Water	--	0.154
	Sodium acetate buffer	0.01	0.155
	Lithium nitrate	0.10	0.155
		0.30	0.147
		0.50	0.147
A. *seyal*	Sodium acetate buffer	0.01	0.151
	Lithium nitrate	0.10	0.154
		0.30	0.133
		0.50	0.131
HIC-F1	Sodium acetate buffer	0.01	0.162
	Lithium nitrate	0.30	0.149
		0.50	0.147
HIC-F2	Sodium acetate buffer	0.01	0.160
	Lithium nitrate	0.30	0.142
		0.50	0.141
HIC-F3	Sodium acetate buffer	0.01	0.145
	Lithium nitrate	0.30	0.144
		0.50	0.141
IEC-F1	Sodium acetate buffer	0.01	0.158
	Lithium nitrate	0.30	0.144
		0.50	0.141
IEC-F2	Sodium acetate buffer	0.01	0.155
	Lithium nitrate	0.30	0.139
		0.50	0.139

4.2. Structural properties

The molar masses, weight (M_w) and number (M_n) averaged, polydispersity index (M_w/M_n) and percentage of molecules with $M_w < 7.5x10^5$ $g.mol^{-1}$ of A. gums and AGP fractions from A. *senegal* measured at 0.1, 0.3 and 0.5 M $LiNO_3$ using HPSEC-MALS are presented in Table III.4. The structural properties of A. gums and AGP fractions measured at 25°C in 0.1 M $LiNO_3$ have been already discussed in Mejia Tamayo et al (2018) [34] (see Chapter II). However, a summary is presented in the following.

At ionic strength of 0.1 M, A. *senegal* and A. *seyal* are composed of mainly low M_w molecules (86% and 80%, respectively) with M_w of $6.8x10^5$ and $7.0x10^5$ $g.mol^{-1}$, respectively. In addition, A. *senegal* presented a higher polydispersity index (M_w/M_n) than A. *seyal* (2.0 and 1.5, respectively). Regarding the HIC fractions, HIC-F1 was composed mainly of low M_w molecules (97%) with a low polydispersity index (1.4). In contrast, the HIC-F2 and HIC-F3 fractions were composed mainly of molecules of high M_w (88% and 67%, respectively) with polydispersity index of 1.3 and 1.9, respectively. Furthermore, HIC-F1, HIC-F2, HIC-F3 presented a M_w of $3.5x10^5$, $1.5x10^6$ and $1.6x10^6$ $g.mol^{-1}$, respectively. Similar molar mass distributions of A. *seyal,* A. *senegal* and the HIC-fractions of the latter have been shown in other studies using size exclusion chromatography (SEC) techniques coupled with similar detectors [8,12,77].

Concerning IEC-fractions, IEC-F1 and IEC-F2 presented M_w of $3.1x10^6$ and $5.3x10^5$ $g.mol^{-1}$, respectively. Thus, the IEC-F1 fraction was formed mainly of supramolecular aggregates (97%). Conversely, the IEC-F2 fraction was formed mainly of low M_w molecules (80%), indicating the presence of the HIC-F1 fraction. Based on the amino acid profile and sugar content, it has been roughly estimated that IEC-F1 may be composed of approximately 70% of HIC-F3 and 30% of HIC-F2. Presence of aggregates in A. gums has been observed over a large range of concentrations using size exclusion chromatography (SEC), static light scattering, SANS and SAXS [2,11,13,17,18,26-28,32]. The formation of these aggregates can be explained by the self-association capability of arabinogalactan-proteins [2,78].

The increase of the ionic strength from 0.1 M to 0.5 M caused an apparent increase in the molar mass of some systems (A. *seyal*, HIC-F3 and IEC-F1). Furthermore, the amount of molecules of low M_w of A. *seyal*, HIC-F3 and IEC-F1 was reduced by 7%, 5% and 3%, respectively. These results suggest further ionic strength-induced AGP aggregation, that can be explained in part by the lower polarity of some of AGPs, for instance in the HIC-F3 fraction, due to the presence of non-polar sugar residues and hydrophobic amino acids [2,8,13]. For the opposite reasons, the low self-aggregation tendency of HIC-F1 [2,8,13] can explain the constant behavior of A. *senegal* and IEC-F2 with the increasing ionic strength.

Table III.4 Molar weight-averaged mass (M_w), molar number-averaged mass (M_n), polydispersity index (M_w/M_n) and percentage of molecules with Mw < $7.5x10^5$ $g.mol^{-1}$ of A. gums and AGP fractions eluted in 0.1, 0.3 and 0.5 M LiNO3 at 25°C. A. gums and its fractions were prepared in deionized water at 1 $g.L^{-1}$

Gum or fraction	Ionic Strength (M)	M_w ($g.mol^{-1}$)	M_n ($g.mol^{-1}$)	M_w/M_n	$M_w < 7.5x10^5$ $g.mol^{-1}$ (%)
A. *seyal*	0.1	$7.0x10^5$	$4.5x10^5$	1.5	80
	0.3	$8.4x10^5$	$4.9x10^5$	1.7	73
	0.5	$8.4x10^5$	$4.7x10^5$	1.8	73
A. *senegal*	0.1	$6.8x10^5$	$3.3x10^5$	2.0	86
	0.3	$6.5x10^5$	$3.3x10^5$	2.2	83
	0.5	$7.5x10^5$	$3.3x10^5$	2.3	83
HIC-F1	0.1	$3.5x10^5$	$2.4x10^5$	1.4	97
	0.3	$3.7x10^5$	$2.5x10^5$	1.5	96
	0.5	$3.5x10^5$	$2.4x10^5$	1.4	97
HIC-F2	0.1	$1.5x10^6$	$1.2x10^6$	1.3	12
	0.3	$1.6x10^6$	$1.2x10^6$	1.3	12
	0.5	$1.5x10^6$	$1.1x10^6$	1.3	15
HIC-F3	0.1	$1.6x10^6$	$8.8x10^5$	1.9	33
	0.3	$1.9x10^6$	$1.0x10^6$	1.9	28
	0.5	$1.9x10^6$	$1.0x10^6$	1.9	28
IEC-F1	0.1	$3.1x10^6$	$2.6x10^6$	1.2	3
	0.3	$3.9\ x10^6$	$3.2x10^6$	1.2	0
	0.5	$3.9\ x10^6$	$3.1x10^6$	1.3	0
IEC-F2	0.1	$5.3x10^5$	$2.9x10^5$	1.8	80
	0.3	$5.7x10^5$	$3.2x10^5$	1.8	80
	0.5	$5.8x10^5$	$3.4x10^5$	1.7	80

4.3. Dynamic viscosity

The reduced viscosity of A. gums, HIC and IEC fractions, dispersed in water, sodium acetate or $LiNO_3$ buffers, as a function of macromolecule concentration, is presented in Figure III.1. For all gums and AGP fractions, the curves corresponding to measurements in water showed an upward bending form at gum concentrations lower than approximately 10 $g.L^{-1}$, the effect being particularly strong below 5 $g.L^{-1}$. Furthermore, the increase seen in A. *seyal* dispersions was less important as compared to A. *senegal*. When the ionic strength was increased to 0.01 M (sodium acetate buffer) and 0.1 M ($LiNO_3$), the upward bending form of the curve was strongly reduced but not completely eliminated. Please note that addition of only 0.01 M of

salt had a very important effect on the viscosity, demonstrating again the weak polyelectrolyte characteristics of AGP from Acacia gums. Interestingly, for HIC-F3 and IEC-F1, a downward bend curve was also seen, suggesting slipping phenomena at the capillary wall [54]. Although these effects will be discussed later, it is important to remark that adsorption on the capillary glass was clearly indirectly remarked during the experiments. This effect was especially important with HIC-F2 and IEC-F1, since sometimes gum adsorption caused blockage of the steel ball used in the measurements.

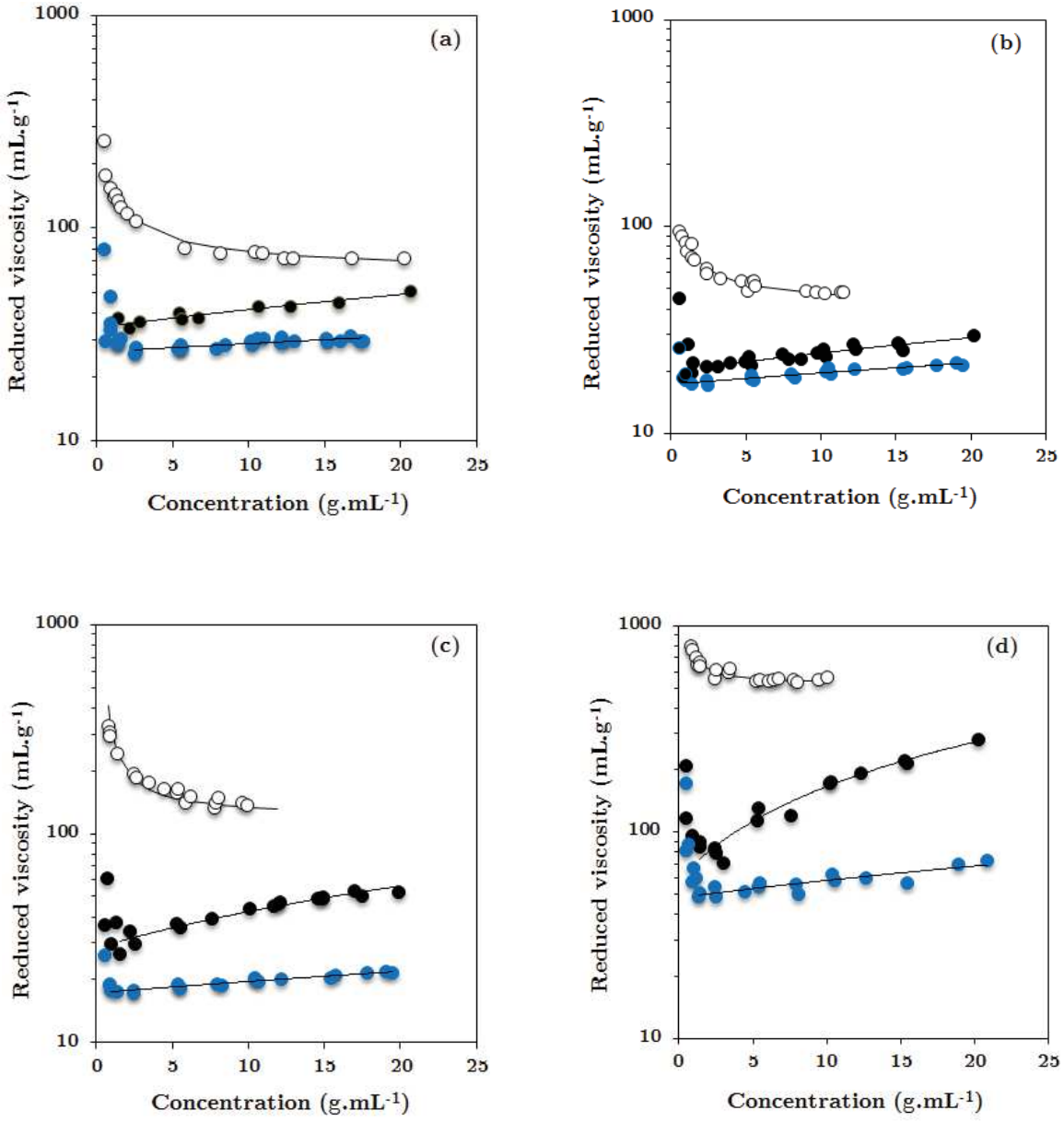

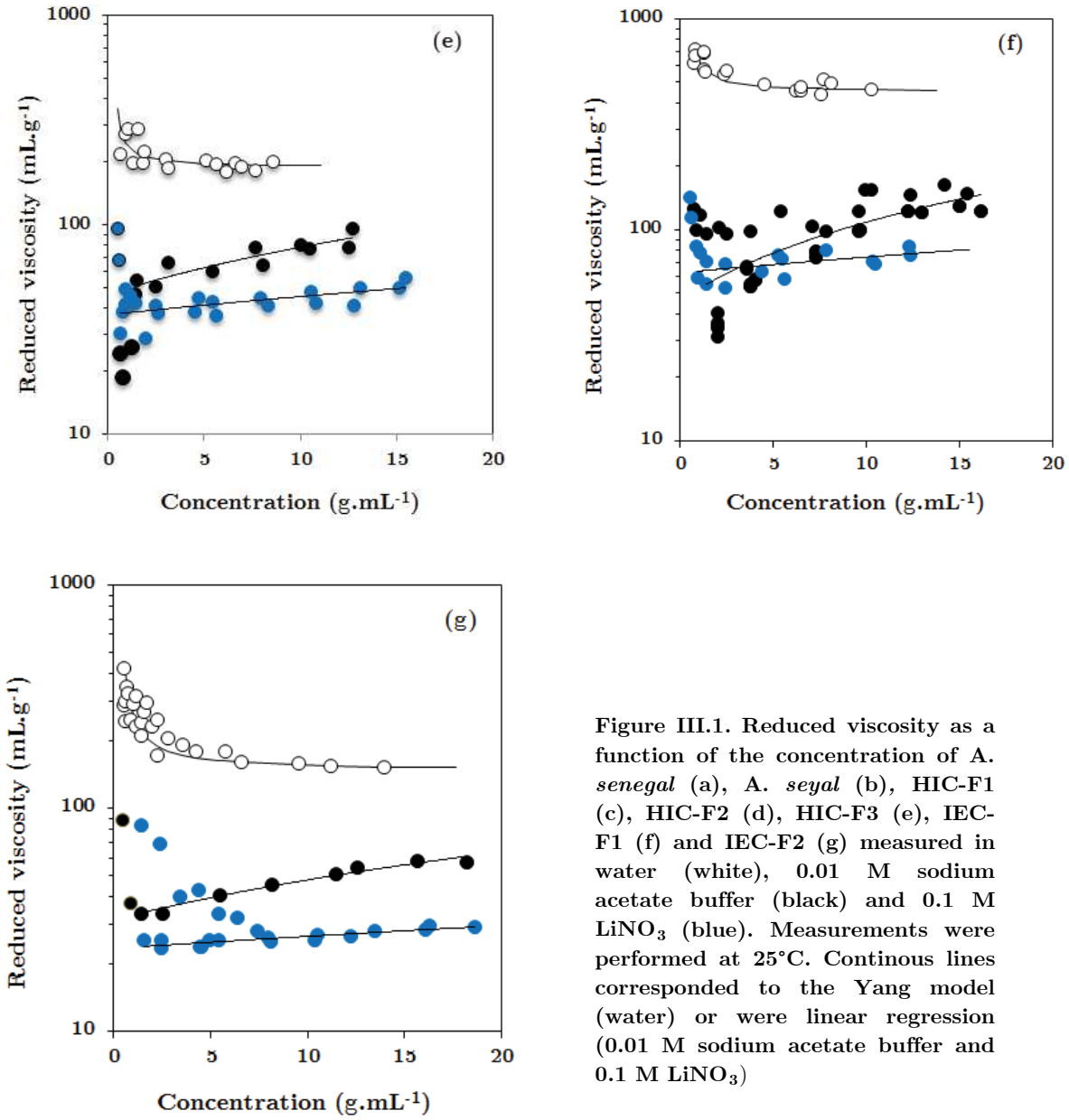

Figure III.1. Reduced viscosity as a function of the concentration of A. *senegal* (a), A. *seyal* (b), HIC-F1 (c), HIC-F2 (d), HIC-F3 (e), IEC-F1 (f) and IEC-F2 (g) measured in water (white), 0.01 M sodium acetate buffer (black) and 0.1 M $LiNO_3$ (blue). Measurements were performed at 25°C. Continous lines corresponded to the Yang model (water) or were linear regression (0.01 M sodium acetate buffer and 0.1 M $LiNO_3$)

The increase of η_{red} with the decreasing gum concentration has been suggested to be the effect of two main phenomena: the polyelectrolyte effect (including the primary, secondary and tertiary electroviscous effects) [79,80] and the adsorption of the solute on the capillary glass wall [41,54,81].

The polyelectrolyte effect is described by theories of polyelectrolyte hydrodynamics as purely electrostatic in nature, then it is caused mainly by intermolecular forces although intramolecular effects cannot be excluded [82]. Since charged macromolecules are surrounded by an electrical double layer, the interactions between the electrical double layers result in a repulsion effect. This repulsive force leads to a larger effective hydrodynamic volume of the

particles and, hence, to an increase in viscosity [82-84]. This effect is sometimes called the second-order electroviscous effect [83], in relation to the secondary electroviscous effect described for rigid particles [80,85].

Intramolecular repulsion/attractive forces may also have an effect and increase/decrease hydrodynamic volume of the polymer. As salt is added to the dispersion, the number of interacting sites is occupied, hence reducing the solute-solvent interactions and as a consequence the hydrodynamic volume is reduced [52,86,87]. The mechanism of this shrinking has been explained as a competition between the solvent and solute to form hydrogen bonds with the polar groups of the molecule [88]. The increase/decrease in the reduced viscosity due to expansion/shrinking mechanism is also commonly observed with hyperbranched polyelectrolytes, for instance green tea polysaccharides or polysterene-graft-poly(2-vinylpyridine) copolymers [89,90]. While this phenomenon may play a role in the observed increase of viscosity at reduced gum concentrations, the expansion of the macromolecule seems not to be the cause of the large increase in viscosity of Acacia gum when the ionic strength of the solvent is reduced, as shown by static light scattering [91].

The second effect that may explain the increase of η_{red} with the decreasing gum concentration is the adsorption of the polymer on the silica present on the surface of the glass capillary wall. As a consequence, the effective diameter of the glass capillary is reduced, thus changing its flow time and viscosity (Figure III.2) [41,54,58,60]. Depending on the nature of the adsorbed molecule and its interaction with the solvent, the viscosity will increase or decrease (slipping phenomena) [41].

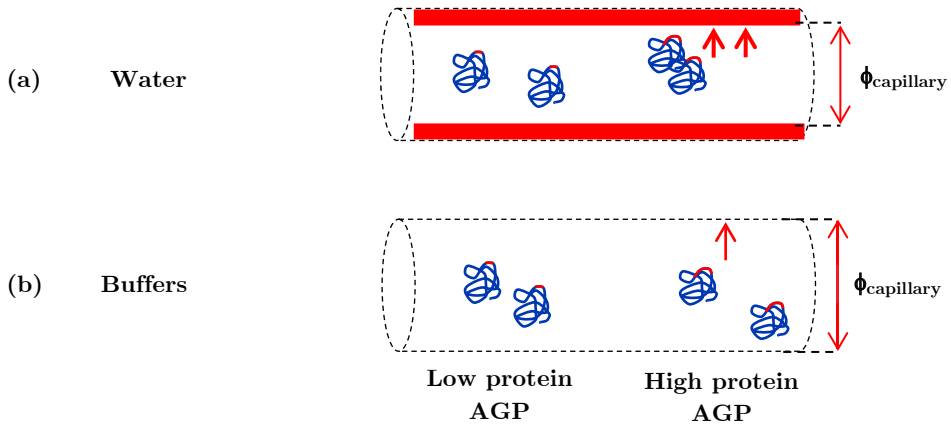

Figure III.2. Representation of the effect of the adsorption of A. gum on the hydrodynamic radius, R_H, in (a) water and (b) buffers. In water, non-polar molecules are less "soluble" and will adsorb easily although in buffers, non-polar molecules are more "soluble" and will adsorb to a less extent.

Since AGPs are weak polyelectrolytes due to the presence of uronic acids and charged amino acids, one can be inclined to think that this phenomenon dominates the increase of the viscosity at low gum concentrations. However, the upward bend form of the curve was seen even after the ionic strength of the solvent was increased (Fig. III.1). Similar behavior was also reported for neutral polymers, e.g. polystyrene in toluene, benzene and methyl ethyl ketone [81,92-94]. Therefore, the polyelectrolyte effect alone fails to explain the increase of η_{red}. Furthermore, it emphasizes the probably major effect of the molecular adsorption.

The adsorption effect was clearly evidenced for A. gums and AGP fractions, but especially in measurements performed in salt-free dispersions with HIC-F2 and IEC-F1 (Figure III.1), due to the need of exhaustive cleaning of the glass capillary, as it has been reported in other studies [41]. Upon increase of the ionic strength, the increase of η_{red} was diminished, but the cleaning of the capillary glass still needed specific attention. This adsorption behavior is due to the good adsorption properties of A. gums, since AGPs are able to reduce the interfacial tension of solid-liquid interfaces due mainly to their protein moiety [95]. Furthermore, experiments performed in A. gums and β-casein solutions have shown that the molecule with lower polarity tends to adsorb first [96]. It is important to note that HIC-F2 and IEC-F1 displayed a peculiar behavior, with a strong adsorption and higher reduced viscosities in the entire concentration range (Figure III.1). This behavior was believed to be caused both by

the higher protein concentration (6.3 and 9.4 %wt, respectively) and the presence of macromolecules with high M_w and AGP-based aggregates. Then, the presence of aggregates, as demonstrated by DLS (section 5.1), probably played also a role on the increase of the reduced viscosity in dilute conditions. The increase of viscosity of A. gums solutions due to the presence of supramolecular assemblies was studied by Li et al (2009). It was suggested that in the dilute regime, AGPs are associated forming clusters [97]. As previously explained, based on their protein content, HIC-F2, HIC-F3 and IEC-F1 are the less polar AGP fractions (Table III.1), then they are prone to self-assembly in salt-free conditions. It was then expected that the HIC-F3 fraction will display a similar behavior as HIC-F2 and IEC-F1. Surprisingly, that was not the case (see Figure III.1 e). We believe that the different drying process followed by HIC-F3 is the main reason for this difference. This fraction was freeze dried meanwhile HIC-F2 and IEC-F1 were spray dried. It is known that spray drying of A. gums enhances their capacity to form aggregates [98].

Finally, a downward form type of curve was also observed in measurements performed in 0.01 M (sodium acetate buffer) and 0.1 M ($LiNO_3$) using HIC-F3 and IEC-F1 (Fig III.1). Slipping phenomena at the capillary wall is due to the displacement of particles away from solid boundaries, leaving a liquid layer, which has apparent lower viscosity than the bulk viscosity [99]. These effects arise from steric, hydrodynamic, viscoelastic and chemical forces and constraints acting on the disperse phase immediately adjacent to the walls [99]. Large dispersed particles favor slipping so that we can assume that AGP aggregates are also involved in these apparent phenomena.

4.3.1 Intrinsic Viscosity

The reduced viscosity of A. gums and AGP fractions in salt-free dispersions were fitted to the Yang model (Eq. III.8) because it was assumed that the adsorption was the dominating effect in the increase of η_{red}. Since electrostatics effects were not considered, values obtained have to be considered as qualitative. For measurements performed in solvents with ionic strengths of 0.01 and 0.1 M, the intrinsic viscosity was determined using the slope of the linear portion of the curve of η_{red} respect to the concentration. In this region, $[\eta]$ is considered as a variable of the molecular state and is independent of the used model [44,100]. The results are presented in Table III.5.

Table III.5 Intrinsic viscosity ([η], mL.g^{-1}) of A. gums, HIC and IEC fractions at different ionic strengths. Measurements were done at 25°C.

Solvent	H_2O [a]	Sodium acetate [a] 0.01 M	$LiNO_3$ 0.1 M		$LiNO_3$ [b] 0.3 M	$LiNO_3$ [b] 0.5 M	Limit [η] [c]	Corrected limit [η]
			[a]	[b]				
Acacia gums								
A. *senegal*	54.0	34.3	26.5	29.8	24.5	24.0	23.0	16.0
A. *seyal*	41.0	22.4	18.2	23.8	17.7	17.7	17.0	15.0
AGP fractions								
HIC-F1	105.0	29.0	18.9	22.1	18.9	18.5	16.5	14.0
HIC-F2	444.0	63.5	48.3	64.3	46.9	45.9	43.0	47.0
HIC-F3	180.0	59.0	36.9	54.7	42.2	41.7	35.0	49.7
IEC-F1	400.0	74.5	63.0	90.2	65.5	63.5	60.0	60.0
IEC-F2	136.0	32.3	23.7	27.8	21.7	20.5	20.0	13.0

a: estimated from capillary viscometry measurements

b: measured using differential capillary viscometry (on line size exclusion chromatography system)

c: estimated from $[\eta] = I^{½}$ (Fuoss law)

In all the solvents and ionic strengths studied, A. *senegal* presented a higher [η] than A. *seyal,* in relation with the different chemical composition (Table III.1) and more compact conformation of A. *seyal* [12,23]. In measurements done in water, HIC-F2, HIC-F3 and IEC-F1 presented higher [η] (444, 180 and 400 $mL.g^{-1}$, respectively), than HIC-F1 and IEC-F2 (105 and 136 $mL.g^{-1}$, respectively), and the tendency remained the same when the ionic strength of the dispersion was increased. This behavior was expected based on their polarity (Table III.1), higher M_w (Table III.4), and presence of AGP aggregates.

The similarity of [η] of HIC-F2 and IEC-F1 evidenced the presence of HIC-F2 in the latter as it was previously seen using HPSEC-MALS measurements (Table III.4). Conversely, the HIC-F1 and IEC-F2 fractions showed higher values of [η] than A. *senegal* (54 $mL.g^{-1}$). However, since they are the main fractions of A. *senegal*, a similar [η] was expected. The higher values obtained could be explained either by the dehydration underwent by these two fractions, inducing further molecular aggregation (although it was not confirmed by DLS) or to chemical changes of some interfacial residues, resulting in improved adsorption properties or hydration of biopolymers.

In a general way, [η] decreased with the increase of the ionic strength, which was previously observed with A. senegal gum [101], and it is the known effect of ionic strength on the hydrodynamic volume of polyelectrolytes. The addition of only 0.01 M of salt (sodium acetate) caused a 2-fold reduction on the [η] of A. *senegal* and A. *seyal*. Meanwhile, reductions of up to 3-7 folds were found for the AGP fractions, being more important for HIC-F2 and IEC-F1. It seems then that upon fractionation, AGP fractions become more sensitive to changes on the ionic strength. More generally, it appears that AGPs separated from A. gums using a number of processing conditions are not exactly the same than AGP in gums. At higher ionic strengths, [η] reached an almost constant value since the difference between 0.3 and 0.5 M ($LiNO_3$) was minimal, suggesting the shielding of the charges of A. gums and AGP fractions around 0.5 M $LiNO_3$. However, even at 0.5 M, total shielding was not effectively reached. It can be noted that intrinsic viscosity values measured by capillary viscometry in 0.1M $LiNO_3$ were smaller than those measured using differential capillary viscometry (on line chromatography detector, HPSEC-MALS). The smaller capillary diameter of the latter could explain this small discrepancy. Literature shows a wide range of [η] values depending on the solvent and its ionic strength. For A. *senegal*, [η] in the range

from 8 to 60 mL.g^{-1} have been reported upon measurements in water and salt concentrations up to 1 M [8,22,23,27,29-31,102,103]. For A. *seyal*, [η] between 13 and 17 mL.g^{-1} have been reported in salt concentrations up to 1 M [12,23,24]. For HIC-F1 and HIC-F2, [η] of 16–18 and 71–87 mL.g^{-1}, respectively, have been reported at salt concentration of 0.05 M [8,32]. For the three populations of HIC-F3, [η] of 103, 64 and 20 mL.g^{-1} have been reported (0.05 M) [8]. Therefore, our results are close with the values found in literature for A. gums and HIC-fractions.

The intrinsic viscosity at total charge neutralization, limit [η], was estimated from the Fuoss law ($[\eta] = I^{-½}$) that describes the relationship of the intrinsic viscosity with the ionic strength, at low polyelectrolyte concentrations [52,55-57,82,86,104,105]. Then, the intrinsic viscosity was further corrected to take into account the polydispersity of A. gums and AGP fractions. Corrections were done according to the amount of low and high molar mass (M_w) AGPs present in each gum (Table III.4). Thus, intrinsic viscosities of 15 and 50 mL.g^{-1} were hypothesized for low M_w AGPs ($M_w < 7.5x10^5$ g.mol^{-1}) and high M_w AGPs ($M_w > 7.5x10^5$ g.mol^{-1}) from which experimental [η] were corrected. Please note that the values chosen corresponded to the limit [η] of HIC-F1 and HIC-F2 since the first fraction is formed mainly by smaller AGPs (93% of low M_w molecules) and HIC-F2 is formed mainly of large AGPs (88%). In the aggregate, values around 15, 45 and 60 mL.g^{-1} could be considered as characteristic values for 'small AGPs', 'large AGPs' and 'AGP aggregates', respectively. These values, multiple of 15 or possibly 5 numbers, possibly suggest the presence of a nominal hydrodynamic unit.

4.4. Translational diffusion coefficient

The translational diffusion coefficient (D_T, m^2.s) of A. gums, HIC and IEC fractions was determined in solvents with different ionic strengths using dynamic light scattering (DLS) and diffusion ordered nuclear magnetic resonance spectroscopy (DOSY-NMR).

The DLS method is based on the fluctuation of the intensity of the light over the time, $g^{(1)}(\tau)$, when a particle suspended in a liquid interacts with a laser light. Providing that particles follow a Brownian motion (Rayleigh theory), D_T can be calculated through the Stokes-Einstein equation (Eq. III.9). This measured scattered light is highly impacted by polymer charges, concentration, polydispersity and presence of supramolecular assemblies

[106-108]. Furthermore, theoretical developments have found that the scattering intensity is directly proportional to the hydrodynamic radius to the power of six ($I(q) \sim R_H^6$) [108]. Then, the determination of R_H is strongly influenced by the presence of aggregates. This was evidenced especially in measurements done in salt-free dispersions and with HIC-F2, HIC-F3 and IEC-F1 fractions, as shown below.

On the other hand, the operating principle of the DOSY method is based on the fluctuation of the intensity of the encoded magnetization phase at the beginning of the experience, where there is no diffusion. A gradient pulse is applied to the solution and depending on its intensity and time (delay), the molecules experiment a change in their displacement due to their Brownian motion. By measuring the attenuation of the signal, the individual translational diffusion coefficient, D_T, can be calculated [61,62]. Since the equipment used in the study had a detection limit around 10^{-11} $m^2.s^{-1}$, which probed molecules with a maximum hydrodynamic radius of about 20 nm according to our experimental conditions, aggregates were not in theory taken into account by the measurement. Therefore, using both DLS and this DOSY-NMR method should allow to better discriminate the different AGP populations present in A. gums, as well as to define more accurately the R_H of the non-aggregated AGPs.

4.4.1. Dynamic light scattering (DLS)

The translational diffusion coefficient, D_T, of A. gums, HIC and IEC fractions was obtained from the recorded autocorrelation curve. The decay rate of the normalized intensity was fitted to the correlation time using the cumulants method. The intensity signal of small molecules decays more rapidly because these molecules tend to move faster. In the same way, presence of large molecules will slow the decay of the signal [108]. Measurements were performed at a scattering angle of 90°. The effect of the scattering angle on A. *senegal* and A. *seyal* dispersions was studied and no important differences in the R_H obtained at scattering angles of 120° and 160° were seen on *filtered dispersions*, highlighting the anisotropy of the larger AGP aggregates. Therefore, the rest of the gum measurements were performed only at 90° on *filtered dispersions*.

The autocorrelation curves of A. gums, HIC and IEC fractions measured in deionized water and 0.1 M sodium acetate buffer are presented in Figure III.3. The larger hydrodynamic volume and the presence of supramolecular assemblies in HIC-F2, HIC-F3 and IEC-F1dispersions induced a slower decay of the autocorrelation curves as compared to A. gums,

HIC-F1 and IEC-F2 fractions. As already explained, presence of aggregates in HIC-F2, HIC-F3 and IEC-F1 was already observed in HPSEC-MALS measurements (see section 4.2). Furthermore, when the ionic strength was increased, the signal decay rate of all gums was increased. Since for flexible polyelectrolytes, the increase of ionic strength promotes a *decrease* of the translational diffusion coefficient [109,110], then a smaller signal decay rate, our results suggest a decrease of the amount of aggregates, then a decrease of the hydrodynamic volume of AGPs. This further suggests a possible involvement of electrostatic and 'hydrophobic' interactions in the formation of these AGP assemblies.

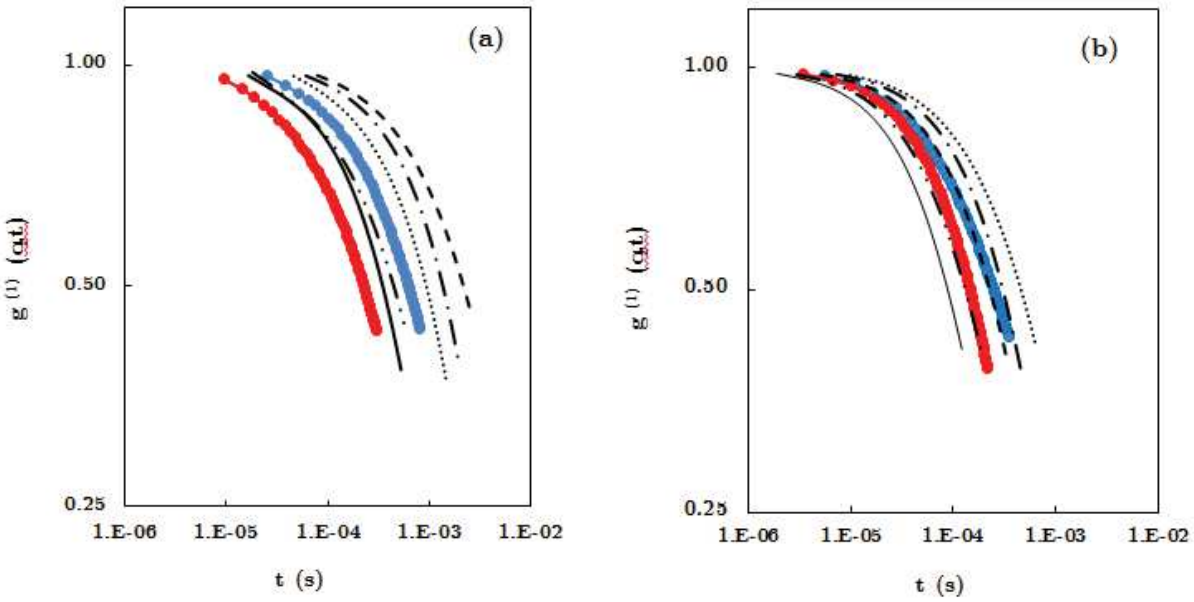

Figure III.3. Autocorrelation function curves of A. *senegal* (blue line), A. *seyal* (red line), HIC-F1 (black line), HIC-F2 (dashed line), HIC-F3 (dotted line), IEC-F1 (dash dot line) and IEC-F2 (dash dot dot line). Measurements were performed using dynamic light scattering (DLS) in 5 g.L^{-1} dispersions prepared in water (a) and sodium acetate buffer 0.01M (b).

4.4.2. Diffusion ordered nuclear magnetic resonance spectroscopy (DOSY-NMR)

The dependence of translational diffusion coefficient, D_T, of A. gums, HIC and IEC fractions with the ionic strength of the solvent is presented in Figure III.4. The increase of the ionic strength to 0.1 M did not have an important effect on the D_T of A. *senegal* and A. *seyal*. However for the HIC and IEC fractions, the increase of the ionic strength to 0.01 M resulted in an increase of the translational diffusion coefficient. Using the same method, similar results

with the decrease of polymer ionization have been found recently on small weak polyelectrolytes [111]. The explanation proposed by the authors was a decrease of chain dimensions with the decrease of charge density. Further experiments with A. gums are needed to decipher what happens since we found the opposite behavior using DLS and that, in addition to the different methods capability, different solvent (D_20 *vs* H_2O) and different sample preparation methods were used (unfiltered *vs* filtered dispersions). Further increase of the ionic strength did not have an important impact on the D_T. This behavior shows again the weak polyelectrolyte character of A. gums and AGP fractions.

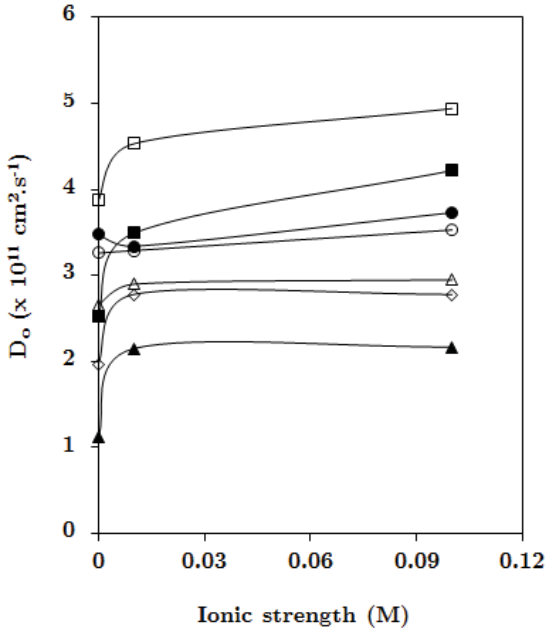

Figure III.4. Dependence of the translation diffusion coefficient (D_T) with the ionic strength of A. *senegal* (white circle), A. *seyal* (black circle), HIC-F1 (white square), HIC-F2 (white triangle), HIC-F3 (white diamond), IEC-F1 (black triangle) and IEC-F2 (black square). Measurements were done using diffusion ordered nuclear magnetic resonance spectroscopy (DOSY) in 5 g.L^{-1} dispersions prepared in D_2O. Continuous lines are a guide to the eye.

4.5. Sedimentation coefficient

The sedimentation coefficients (S, Svedberg units = 10^{-13} s) of A. gums, HIC and IEC fractions were first classically corrected to standard solvent conditions, $S_{20,w}$, to eliminate the effect of temperature, density and viscosity of the solvent [72]. The correction was done using the properties of water at 20°C:

$$S_{20,w} = S\left(\frac{\rho_{H2O}\, v_s^{\circ}}{1-\rho_o\, v_s^{\circ}}\right)\left(\frac{\eta_o}{\eta_{H2O}}\right) \qquad \text{(III.12)}$$

where ρ_o and ρ_{H2O} are the densities of solvent and water (20°C) and η_o and η_{H2O} are the viscosities of solvent and water (20°C). It is important to remark that this correction was done to allow the comparison with data from literature.

The concentration dependence of $S_{20,w}$ of A. *senegal,* A. *seyal* and AGP fractions in 0.01 M (sodium acetate), 0.1 M ($LiNO_3$) and 0.5 M ($LiNO_3$) is presented in Figure III.5. For all gums and ionic strengths studied, an increase on $S_{20,w}$ was seen with the decreasing gum concentration. This behavior has been explained due to an increase of the viscosity as concentration is increased [112], then to hydrodynamic effects due to the higher number of macromolecules. Similar behavior has been reported for other biomolecules, for instance: dextran[112], wheat amylopectin[68,72]; carboxymethylchitin (CMCT)[113], lactodendrimers (LDs)[114] and β-glucan [115]. Interestingly, at a ionic strength of 0.01 M we remarked a more rapid decrease on $S_{20,w}$ of HIC-F1 and HIC-F2. This behavior might be explained by aggregation induced by the different dehydration treatment (spray drying) of these fractions compared to A. *senegal* and A. *seyal* (freeze drying) (See Materials and Methods).

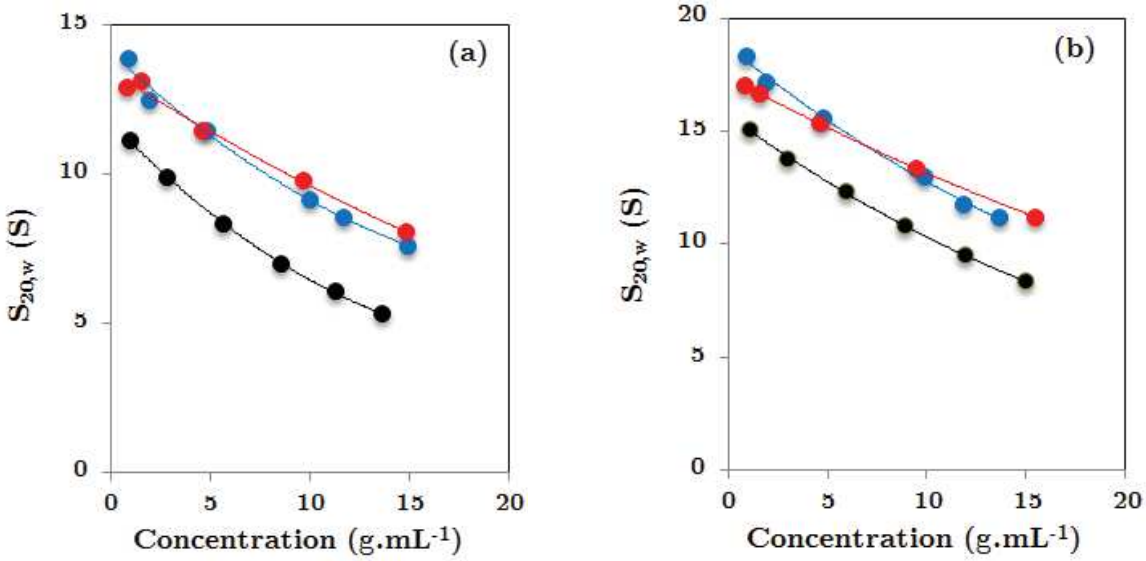

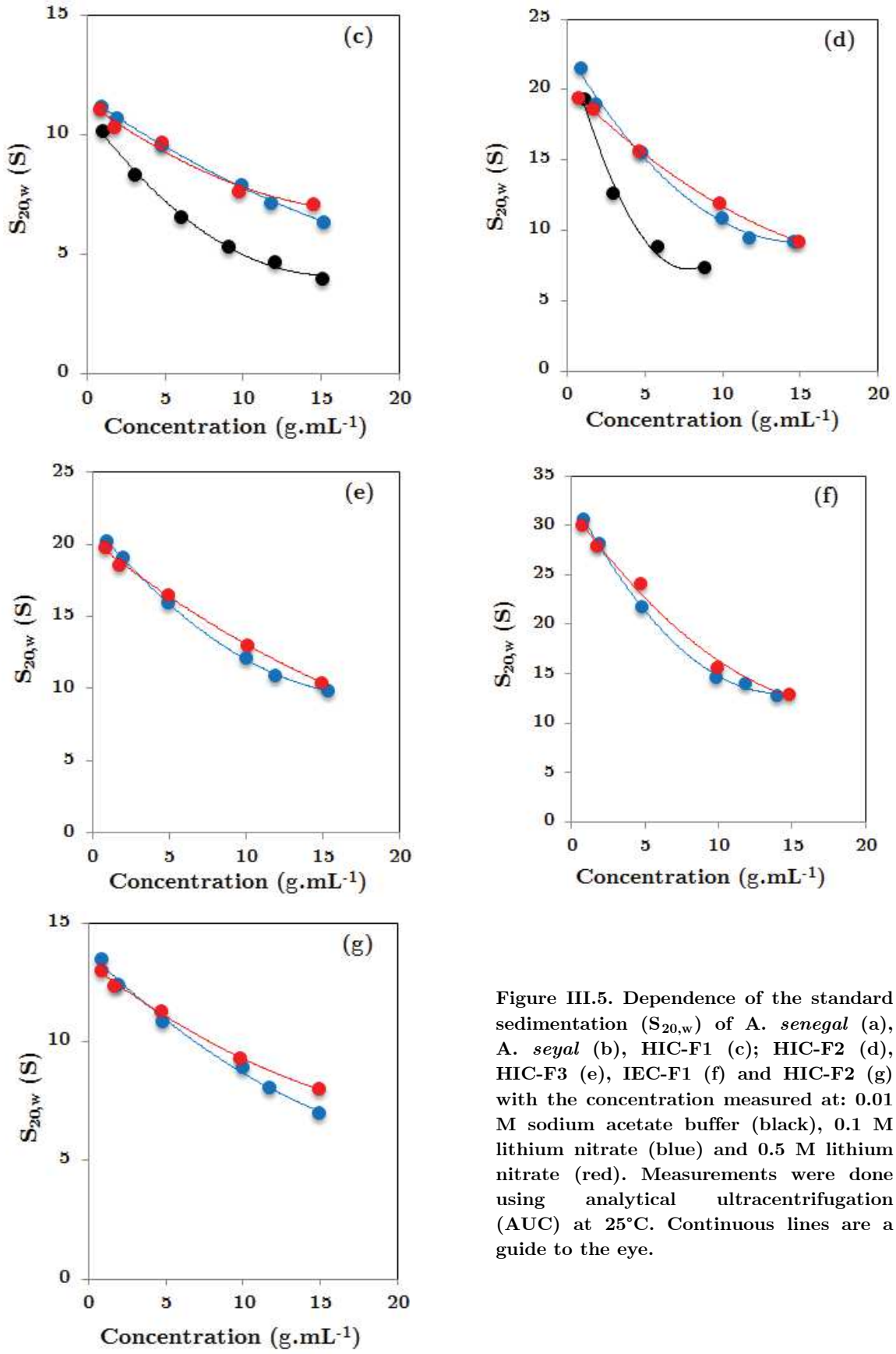

Figure III.5. Dependence of the standard sedimentation ($S_{20,w}$) of A. *senegal* (a), A. *seyal* (b), HIC-F1 (c); HIC-F2 (d), HIC-F3 (e), IEC-F1 (f) and HIC-F2 (g) with the concentration measured at: 0.01 M sodium acetate buffer (black), 0.1 M lithium nitrate (blue) and 0.5 M lithium nitrate (red). Measurements were done using analytical ultracentrifugation (AUC) at 25°C. Continuous lines are a guide to the eye.

Addition of salt classically increased the sedimentation coefficients, $S_{20,w}$, accounting for the additional friction effect due to charges [116]. Further increase of the ionic strength to 0.5 M (lithium nitrate), had a less important effect.

The standard sedimentation coefficients, $S_{20,w}$, of A. gums and AGP fractions were fitted to the Gralen equation (Eq. III.11) to obtain the sedimentation coefficients at zero concentration, S_o, and the results are presented in Table III.6. This form of the Gralen equation was chosen because it gave better correlation coefficients (R^2 ~0.99).

Table III.6. Sedimentation coefficient extrapolated at zero concentration (S_o) and Gralen parameter (k_s) of A. gums and AGP fractions at 0.01 M (sodium acetate), 0.1 M ($LiNO_3$) and 0.5 M ($LiNO_3$) ionic strength. Data were fitted to Eq. III.13.

Gum or fraction	S_o (S)			k_s (mL.g^{-1})		
	0.01 M	**0.10 M**	**0.50 M**	**0.01 M**	**0.10 M**	**0.50 M**
Acacia gums						
A. *seyal*	16.5	19.2	17.7	62.6	52.1	36.7
A. *senegal*	12.6	14.4	13.8	95.8	44.2	46.8
AGP fractions						
HIC-F1	11.4	11.9	11.3	123.0	56.2	43.2
HIC-F2	22.5	23.1	20.4	243.2	111.1	82.3
HIC-F3		22.0	21.3		81.5	67.1
IEC-F1		33.8	33.7		121.6	109.3
IEC-F2		14.3	13.5		67.1	45.9

At all ionic strengths, A. *seyal* presented higher S_o than A. *senegal*, which can be mainly explained by its higher M_w (Table III.2). Regarding the AGP fractions at 0.1 M, the high M_w fractions, HIC-F2, HIC-F3 and IEC-F1, showed higher values of S_o (23.1, 22 and 33.8 S, respectively) than HIC-F1 and IEC-F2 (11.9 and 14.3 S, respectively). Further increase of the salt concentration to 0.5 M did not have a large impact on the sedimentation coefficients, suggesting efficient charge screening. A similar trend was reported by Gillis et al (2016) for A. *senegal* dispersions when the ionic strength was increased from 0.1 to 0.5 M [30]. We noted however that the values we found at 0.5 M were systematically slightly lower than at 0.1 M for all systems, suggesting some salt-induced aggregation of AGP. This can be related to the M_w reported at different ionic strengths in Table III.4.

The Gralen parameter, k_s, of A. gums and AGP fraction decreased with the increase of the ionic strength. This effect was more important for A. *senegal*, HIC-F1 and HIC-F2 which showed a decrease of more than 50% when the ionic strength was increased from 0.01 to 0.1 M. Therefore, a clear effect of the charges of the molecule, then, a decrease of the non-ideality of the system due to charge screening was observed, as expected.

5. Discussion

The physicochemical properties and conformation of biopolymers greatly depend on their interactions with water through their volumetric properties [117-120]. For instance, their ability to form and stabilize an interfacial layer is related to their polarity and the formation of a viscoelastic structure. Another example is the aggregation of biopolymers that involves a dehydration of molecules and formation of supramolecular assemblies [121,122].

Static volumetric properties of AGPs from Acacia gums, including their hydration, have been estimated using ultrasonic measurements (see Chapter II). Based on viscometric, translational diffusion and sedimentation coefficients, we then studied the hydrodynamic properties of AGPs. More specifically, we calculated and compared the hydrodynamic volumes and radius of macromolecules and tried to estimate their conformation in solution as well as to extract their hydration numbers.

5.1 Hydrodynamic radius

The hydrodynamic (R_H, nm) or viscosimetric radius (R_η nm) of A. *senegal*, A. *seyal* and HIC-fractions, which are not necessarily equivalent, have not been studied in great details in the literature. Available data differ and sometimes are contradictory depending on the solvent and ionic strength used in the determination. The combination and comparison of data obtained by different methods, e.g. viscometry, DLS, DOSY-NMR and AUC methods will allow the estimation of a more accurate hydrodynamic radius.

The hydrodynamic radius obtained from the intrinsic viscosity is a sphere equivalent radius, known as viscosimetric radius or R_η. It can be determined from measures of capillary and differential viscometry using the Einstein relation [45]:

$$R_\eta = \left(\frac{[\eta]\, M_v}{10\, \pi/3\, N_A}\right)^{1/3} \qquad \text{(III.13)}$$

where M_v is the volume-average molar mass ($g.mol^{-1}$) and N_A is the Avogadro's number ($6.022x10^{23}$ $molecules.mol^{-1}$).

On the other hand, R_H obtained from the translational diffusion coefficient, D_T, were calculated using the Stokes-Einstein equation (Eq. III.9). The results are summarized in Table III.7.

The differences on R_H obtained by the different methods were especially important in deionized water. For instance, values of 8, 18 and 50 nm were obtained for A. *senegal* using DOSY-NMR, viscometry and DLS methods, respectively (Table III.7). For HIC-F2, values of 8, 47 and 79 nm were obtained. In our opinion, these results clearly showed the different limitations of methods but also the effect of AGP-based aggregates. As a whole, the lower R_H obtained by DOSY-NMR experiments can be explained by its relative insensitivity to the presence of aggregates. On the other hand, the larger R_H difference between viscometric and DLS methods is due to the larger impact of aggregates on the DLS method [123], as previously explained (section 4.3). Results obtained by DLS will be discussed later in more details.

As the ionic strength of the solvent increased, the R_H of A. gums, HIC and IEC fractions was reduced. This reduction is related to the decrease of solvent polarity and screening of charges, that decrease hydration, then AGP hydrodynamic volume, and of the size of aggregates. At ionic strengths higher than 0.1 M, the R_H obtained from the different methods (except DOSY-NMR) were similar. Thus, for the following discussion, we will use a R_H averaged over the 0.1 to 0.5 M ionic strength range. Since R_H values obtained by DOSY-NMR method were significantly smaller, there were not taken into account in the averaged R_H value, but they will be discussed later.

Table III.7. Hydrodynamic radius (R_H or R_η nm) of A. gums, HIC and IEC at different ionic strengths (25°C). R_η was determined from the intrinsic viscosity [η]; R_H was determined from the translational diffusion coefficient (D_T)

	Water			Sodium acetate buffer 0.01 M				$LiNO_3$ 0.1 M				$LiNO_3$ 0.3 M	$LiNO_3$ 0.5 M	Average	Limit
	a	b	c	a	b	c	d	a	b	d	e	e	e		
Acacia gums															
A. *senegal*	8	18	50	7	15	15	18	6	14	16	15	14	14	15	12
A. *seyal*	6	16	20	6	14	13	17	6	13	14	14	13	13	13	13
AGP fractions															
HIC-F1	6	18	8	5	12	8	12	4	10	11	11	10	10	10	9
HIC-F2	8	47	70	8	25	17	24	7	23	24	25	23	22	23	22
HIC-F3	11	36	50	8	25	17		8	21	23	24	24	23	23	25
IEC-F1	20	58	70	10	33	30		10	31	32	35	34	34	33	33
IEC-F2	9	23	35	6	14	13		5	13	14	13	13	12	13	10

* Average R_H was obtained using the values in the 0.1-0.5 M ionic strength range. Limit R_H was obtained at charge neutralization and taking into account the polydispersity of AGPs. (a) Diffusion ordered nuclear resonance magnetic chromatography (DOSY-NMR). (b) Capillary viscometry. (c) Dynamic light scattering (DLS). (d) Analytical ultracentrifugation (AUC). (e) Differential capillary viscometer detector coupled to size exclusion chromatography (HP-SECMALS).

In a general way, A. *senegal* presented a slightly higher R_H than A. *seyal* (15 and 13 nm, respectively). Regarding the HIC-fractions, HIC-F1 presented a lower R_H than HIC-F2 and HIC-F3 (10, 23 and 23 nm, respectively). In addition, it is important to remark that the ratio R_η/R_H, that is sensitive to particle anisotropy, increased with the increase of the ionic strength, except for the HIC-F1 fraction, demonstrating a decrease of particle anisotropy. This result highlights the importance of AGP based aggregates on the R_H estimated by DLS. A survey of literature showed R_H values of 11 - 16 nm for A. *senegal* [8,14,26,30], 17 nm for A. *seyal* [26], 9 - 11 nm for HIC-F1 [8,14], 23 - 34 nm for HIC-F2 [8,11,14,15] and 16 -28 nm for HIC-F3 [8,10,14]. Therefore our results are in reasonable agreement with the literature but provide a most robust picture. Regarding the original IEC-F1 and IEC-F2 fractions, we found R_H of 33 and 13 nm, respectively. This further shows the aggregated characteristic of IEC-F1 since it is composed mainly by AGP present in HIC-F2 and HIC-F3 fractions.

The limit R_H was obtained from the intrinsic viscosity at total charge neutralization and taking into account gum polydispersity. We were able to obtain three R_H values, ~10, ~25 and ~35 nm, which corresponded roughly to 'small AGP', 'large AGP' and 'AGP-based aggregates'. This is probably fortuitous but all these values are multiples of 5, a subunit dimension largely found when imaging AGP from A. *senegal* gum [13].

5.1.1. Hydrodynamic radius obtained from Dynamic Light Scattering

The hydrodynamic radius, R_H, obtained by DLS was estimated using two different methods. First, the z-average values shown in Table III.7 were calculated assuming a classical Gaussian distribution (cumulant method). The use of this method is questionable for polydisperse dispersions, especially in water, but allows a first qualitative description of structural differences between the studied dispersions. Then, dispersion polydispersity was taken into account by applying a more complex mathematical treatment (non-linear least square method, NICOMP algorithm). This treatment produced up to three molecular populations. The results are presented in Table III.8.

Table III.8. Hydrodynamic radius (R_H) of A. gums and AGP fractions obtained from dynamic light scattering (DLS). Measurements were done in 5 g.L^{-1} at 25°C.

Solvent	Water	Sodium Acetate 0.01 M	Lithium nitrate 0.1 M
Acacia gums			
A. *senegal*	6/28/150 (50)	7/50 (15)	13/75 (11)
A. *seyal*	12/50 (20)	8/32 (13)	
AGP fractions			
HIC-F1	5/25 (8)	5/28 (8)	
HIC-F2	9/35/150 (70)	6/18/30 (17)	
HIC-F3	4/17/125 (50)	7/18/100 (17)	
IEC-F1	17/75/250 (70)	17/75 (30)	
IEC-F2	6/18/49 (35)	6/19/38 (13)	

* R_H values corresponding to different AGP populations were obtained using the non-linear least square method of correlation function treatment (NICOMP method). Values in parenthesis were obatined using a Gaussian distribution (z-average values)

In measurements performed in water, A. *senegal* showed a mean intensity-average R_H of 50 nm (z-average). Meanwhile, the NICOMP analysis showed the presence of three macromolecular populations around 6, 28 and 150 nm. Taking into account the scattered light intensity, the percentage of AGP in the largest population was above 40% for all assays we did. Increase of the ionic strength of the solvent caused a reduction of the mean R_H, mainly due to the decrease of particle hydrodynamic volume [52,86,87] and reduction of the size of AGP-based aggregates. Similar behavior was seen with A. *seyal* and AGP fractions. Interestingly, the increase of the ionic strength did not have an important effect on HIC-F1. This behavior can be explained due to its low protein content and low self-assembly capacity [2]. It is important however to remark the presence of large AGP-based aggregates in HIC-F2, HIC-F3 and IEC-F1. The presence of this population can be explained by their high propensity to self-assembly due to its moderate to low polarity and high protein content [2,8,13]. Another reason of the reduction of R_H is the effect of the masking of the charges when salt is added. As the ionic strength is increased, the molecular charges are masked and the intramolecular forces are increased, hence the hydrodynamic volume is reduced [57,82]. In a general way, four macromolecular populations with R_H in the range of <10, 10-20, 30-40 and >50 nm were identified. The two first populations corresponded to 'small AGPs', the

third one corresponded to 'large AGPs' and the last population corresponded to 'AGP-based aggregates'.

Now we wish to comment more specifically the presence of AGP populations with R_H as small as about 5 nm, that were detected using both DLS (first population) and DOSY-NMR (Table III.7). This small macromolecular population was present also in A. *seyal* and all AGP fractions except for the aggregated IEC-F1. The R_H was not modified by the increase of the ionic strength. In addition, preliminary experiments using a capillary electrophoresis method coupled to Taylor dispersion analysis revealed presence of molecules with R_H around 1 nm. This result needs to be confirmed but it highlights the presence of very small macromolecules or molecules in A. gums.

5.2 Gyration radius

The gyration radius (R_G, nm) of A. gums, HIC and IEC fractions at different ionic strengths (from 0.1 to 0.5 M $LiNO_3$) was obtained from HPSEC-MALS measurements and is presented in Table III.9. It is important to remark that due to the method sensitivity only molecules with R_G higher than 10 nm can be analyzed. The R_G was measured on about 50%, 35%, 12% and 25% of the molecules present in A. *senegal*, A. *seyal*, HIC-F1 and IEC-F2, respectively (Table III.9). For HIC-F2, HIC-F3 and IEC-F1 fractions, the percentage of molecules involved in the R_G calculation ranged from 69-92%, 43-71% and 10-100%, respectively, according to the ionic strength (Table III.9). Hence, the R_G calculated was 'overestimated' for some samples as only part of molecules was considered for its calculation.

The increase of the ionic strength of the solvent did not have apparently an effect on R_G values. The limit R_G was corrected in a similar way as done for $[\eta]$ and R_H, to take into account the polydispersity. In general, A. *senegal* presented a higher R_G than A. *seyal* (16 and 14 nm, respectively). Among the AGP-fractions, HIC-F3 and IEC-F1 presented higher R_G (33 and 43 nm, respectively) than HIC-F1, HIC-F2 and IEC-F2 (14, 27 and 16 nm, respectively). For A. gums, reported R_G values are: 12-31 nm for A. *senegal* [8,12,24,26], 17-30 nm for A. *seyal* [12,24,26,124], 8–11 nm for HIC-F1 [8,125], 30-45 nm for HIC-F2 [8,11,15,125] and 20 – 103 nm for HIC-F3 [8,10,125]. Our results are in these ranges. In a similar way to R_H values, three groups of R_G values, 15, 30 and 45 nm, corresponding to 'small AGPs', 'large AGPs' and 'AGP-based aggregates' were identified.

Table III.9. Gyration radius (R_G, nm) of A. gums, HIC and IEC at 0.1, 0.3 and 0.5 M ($LiNO_3$). Measurements were performed in HPSEC-MALS (25°C).

Gum or fraction	Ionic strength (M)			Average R_G	Limit R_G
	0.1	0.3	0.5		
Acacia gums					
A. *senegal*	21 (46%)	22 (50%)	19 (60%)	21	16
A. *seyal*	14 (37%)	14 (40%)	15 (35%)	14	14
AGP fractions					
HIC-F1	15 (16%)	15 (11%)	14 (12%)	15	14
HIC-F2	27 (73%)	27 (69%)	27 (92%)	27	27
HIC-F3	32 (43%)	33 (71%)	33 (68%)	31	33
IEC-F1	41 (70%)	45 (100%)	43 (77%)	43	43
IEC-F2	19 (25%)	19 (30%)	18 (24%)	19	16

*Values in parenthesis correspond to the percentage of molecules taken into account in the calculation. Corrected R_G was calculated taking into account the polydispersity

5.3. Conformational Analysis

The size and conformation of a polyelectrolyte molecule is defined by its polarity (hydrophobic or hydrophilic), charge density, the ionic strength of the dispersion, the length of the molecule, the branching characteristics and the interactions with the solvent [20,126]. Polysaccharides and branched biomolecules can present a wide range of conformations from highly rigid rods to random coils [20]. The main hydrodynamic properties, intrinsic viscosity, sedimentation and translational diffusion coefficients, and gyration radius can be related to the molar mass as a power law according to the following relationships [39,45,59]:

$$[\eta]_w = K_\eta M_w^{a_\eta} \quad \text{(III.14)}$$

$$R_G = K_G M_w^{a_G} \quad \text{(III.15)}$$

$$S_{20,w} = K_s M_w^{a_S} \quad \text{(III.16)}$$

$$D_{20,w} = K_D M_w^{-a_D} \quad \text{(III.17)}$$

Where a_η, a_G, a_S and a_D are the static and hydrodynamic coefficients and K_η, K_G, $K_{S\ 20,w}$ and K_D are the corresponding constants. These parameters depend on the molecular conformation, molar mass distribution, anisotropy, temperature and solute-solvent interactions [11,39,59]. They can take values comprised between 0 and 2 depending on the shape of the molecule and the equation used [11,42,45,86]. Using these parameters molecules

are roughly classified in homogeneous spheres, random coils and rigid rods. Classical values are $a_\eta = 0$ and $a_G = a_S = a_D = 0.33$ for a sphere, $a_\eta = 0.5 - 0.8$ and $a_G = a_S = a_D = 0.5 - 0.6$ for random coils and $a_\eta = 1.8$ and $a_G = a_S = a_D = 1$ for rods [11,42,45,86].

The conformation analysis of A. gums and HIC-fractions has been previously studied by colleagues of our group, Renard et al (2006, 2012 and 2014), Sanchez et al (2008) and Lopez-Torres (2015) [8,10,11,32]. However, in these studies the HPSEC-MALS column configuration used was either two or four columns in series. As already explained in the Materials and Methods (section 2.2.4), we used different configurations depending on the M_w of the gum, one column for gums with a larger M_w (HIC-F2, HIC-F3 and IEC-F1) and 4 columns for gums with low M_w (A. *senegal*, A. *seyal*, HIC-F1 and IEC-F2). This was supposed to minimize abnormal elution effects usually occurring with large M_w hyperbranched polymers. In addition, the HIC-F3 used in the study of Renard et al. (2014) [10] contained an important quantity of insoluble material, which in our case was controlled by the dehydration process used (see Materials and Methods). In the following, we explore the effect of these changes on the estimated conformation of A. gums and AGP fractions.

The a_η and a_G coefficients and the fractal dimension (d_f) of A. gums and AGP fractions at different ionic strengths are presented in Tables III.10 and III.11. The increase of the ionic strength from 0.1 to 0.5 M ($LiNO_3$) did not influence the a_η and a_G coefficients of A. gums and AGP fractions. Hence, the conformation of AGPs was not modified in this range of ionic strength. This behavior can be explained due to the hydrophilic moiety of A. gums. Studies performed on hydrophilic and hydrophobic polyelectrolytes have shown that polyelectrolytes based on hydrophilic polymers are not easily compacted into a globular conformation. Furthermore, they are able to maintain its chain conformation up to a ionic strengths of 5 M [126].

For all A. gums and fractions, a_η varied over the M_w range (Table III.10) suggesting the presence of more than one conformation. Similar observations were reported for A. *senegal* and A. *seyal* by Lopez-Torres et al. (2015)[12] and for HIC-F2 by Renard et al (2012) [11]. However, for HIC-F1 and HIC-F3 only one conformation was reported by Sanchez et al (2008)[32] and Renard et al. (2014)[10].

Table III.10. Kuhn-Mark-Houwink-Sakurada parameter (a_η) of A. gums and AGP fractions obtained at ionic strength of 0.1, 0.3 and 0.5 M ($LiNO_3$).

Range (x 10^5 g.mol^{-1})	Gum or fraction	0.1 M	0.3 M	0.5 M
	A. *senegal*	0.44	0.39	0.37
1.5 – 5.0	HIC-F1	0.39	0.33	0.35
	IEC-F2	0.39	0.35	0.31
2.0 – 10.0	A. *seyal*	0.26	0.25	0.24
5.0 - 15.0	A. *senegal*	0.67	0.68	0.67
5.5 – 10.0	HIC-F1	0.49	0.51	0.48
5.0 – 10.0	HIC-F2	0.91	0.79	0.87
5.0 – 15.0	HIC-F3	0.86	0.87	0.71
5-0 – 15.0	IEC-F2	0.76	0.72	0.71
15.0 – 50.0	A. *senegal*	0.41	0.44	0.36
10.0 – 25.0	A. *seyal*	0.39	0.37	0.47
10.0 – 30.0	HIC-F2	0.33	0.30	0.32
10.0 – 50.0	HIC-F3	0.33	0.35	0.36
2.0 – 100.0	IEC-F1	0.45	0.42	0.42
15.0 – 40.0	IEC-F2	0.37	0.45	0.47

*a_η was obtained from the slope of the double logarithmic plot of the intrinsic viscosity in function of the weight-average molar mass measured using HPSEC-MALS.

The [η] vs. M_w of A. *seyal* displayed two slopes with a_η values of ~0.25 for AGPs showing a M_w lower than 10^6 g.mol^{-1} (around 95% of AGPs of whole gum) and 0.37-0.47 for high M_w AGPs ($M_w > 10^6$ g.mol^{-1} corresponding to around 5% of AGPs) (Table III.10). For A. *senegal* gum, three a_η coefficients were identified according to the M_w with values of 0.37-0.44 for AGPs with M_w ranging from 1.5–5.0 x10^5 g.mol^{-1}, 0.67-0.68 for AGPs with M_w ranging from 5.0-15 x10^5 g.mol^{-1} and 0.36-0.44 for AGPs with M_w higher than 15 x10^5 g.mol^{-1} (Table III.10). a_η values around 0.4 - 0.8 for A. *senegal* [12,27,28,31,127,128] and 0.3 - 0.4 for A. *seyal* [12] were previously reported for A. gums. Therefore, our results are in good accordance with literature and with hyperbranched polymers. Indeed, similar a_η values were found for other hyperbranched polymers as dextran derivatives (0.5 - 0.6)[129,130], β-glucan (0.2)[131], copolyester with different branching degree (0.2- 0.6)[132], hyperbranched poly-L-lysine (0.5), methacrylate-type hyperbranched glycopolymers (0.2-0.3)[133] and polycarbosilanes (0.1-0.4)

[134]. A. *seyal* presented lower a_η value than A. *senegal* reflecting a less anisotropic and more compact structure as previously described by Lopez-Torrez et al. (2015)[12]. The three M_w ranges observed for A. *senegal* were also identified with its HIC and IEC fractions (Table III.10). However, some slight differences in the a_η coefficients were evidenced according to the fractions considered. For $M_w<5.0x10^5$ g.mol^{-1}, HIC-F1 and IEC-F2 fractions displayed an a_η coefficient of 0.3-0.4 in agreement with the hyperbranched, dense and compact structure of low M_w AGPs described by Sanchez et al. (2008) [32]. In the second M_w range ($5.0<M_w<15x10^5$ g.mol^{-1}), a_η coefficients between 0.49 and 0.91 were found. Hence, the conformation of these AGPs was certainly more anisotropic and elongated than that of low M_w AGPs. Moreover, it could be noted that the richest fractions in proteins, HIC-F2 and HIC-F3, presented higher a_η coefficients than HIC-F1 and IEC-F2 fractions. A higher a_η coefficient could be associated to a less branched, smaller chain density or more anisotropic structure. The branching degree of carbohydrate blocks of A. *senegal* as well as its HIC and IEC fractions were identical with a value of 0.8 (Table III.1). Hence, this indicates that AGPs from HIC-F2 and HIC-F3 with M_w ranging from 5.0 to $15x10^5$ g.mol^{-1} presented a more anisotropic structure with certainly a lower carbohydrate blocks density on the protein backbone. For AGPs with M_w upper than 10-15 $x10^5$ g.mol^{-1}, a_η coefficient decreased with values ranging from 0.30 to 0.47 (Table III.10). The decrease of a_η could be especially associated to the increase of the branching degree and the presence of aggregates [132,135]. IEC-F1 that contained only AGPs with M_w upper than 10-$15x10^5$ g.mol^{-1} with identical branching degree as the other fractions from A. *senegal* (Table III.1) showed a_η value around 0.42. Hence, the decrease of the a_η coefficient in this M_w range was certainly due to the presence of aggregates and not to the increase of the branching degree.

The conformation of AGPs was also studied using the a_G coefficient obtained from the R_G vs. M_w conformation plots of A. gums and AGP fractions. Before to discuss the results, it is important to remind that only AGPs presenting a R_G above 10 nm were considered for this analysis (that concerned only a percentage of AGP according to the considered fraction, see Table III.9), and that R_G, and then a_G coefficient, are greatly influence by the presence of aggregates. For all samples, a_G coefficient was constant over the M_w studied that indicates the presence of only one kind of conformation. a_G values of 0.5–0.6 were found for A. *senegal*, A. *seyal*, HIC-F2 and IEC-F2, 0.3-0.5 for HIC-F3 and IEC-F1 and 0.7 for HIC-F1 (Table III.11). Our results are in accordance with previous studies showing a_G values of 0.3–1.2 for

A. *senegal* [12,27,76,136], 0.4-0.7 for A. *seyal* [12], 0.4–0.9 for HIC-F2 [11] and 0.3–0.6 for HIC-F3. The finding of only one a_G coefficient appeared in contradiction with the results obtained with the Kuhn-Mark-Houwink-Sakurada (KMHS) plots for which several conformations were evidenced. The absence of a_G coefficient for M_w lower than $5x10^5$ $g.mol^{-1}$ was due to a R_G lower than 10 nm in this molar mass range. The difference observed for M_w upper than $5x10^5$ $g.mol^{-1}$ could be explained by the presence and the abnormal elution of AGP based aggregates that co-eluted with lower molar mass AGPs and greatly contributed to the light scattering signals. This hypothesis was evidenced by the analysis of a_G coefficient of A. *senegal* fractions. The a_G coefficient of HIC-F1, that mainly contained low molar mass AGPs and was devoid of aggregates, was around 0.71 in 5-10 $x10^5$ $g.mol^{-1}$ molar mass range. These results confirmed the presence of elongated and more anisotropic AGPs in this molar mass range as previously described using KMHS plots for A. *senegal* and its fractions. The elongated and more anisotropic AGPs also shown in HIC-F3 and HIC-F2 using KMHS plots were not evidenced using the R_G vs. M_w conformation plots, especially for HIC-F3. For these fractions, the presence of AGPs based aggregates was established for M_w upper than $10x10^5$ $g.mol^{-1}$ using the KMHS plots. Hence, the absence of a_G coefficient corresponding to elongated AGPs in 5-10 $x10^5$ $g.mol^{-1}$ molar mass range was attributed to the co-elution of aggregates that contributed to the light scattering signals. Based on this consideration, it appeared difficult to use the a_G coefficient to characterize the AGPs conformation. However, it could be used as qualitative information about the aggregation state of the sample considering that more the sample was aggregated, more the a_G coefficient was lower for a same molar mass range. Based on this assumption and on the a_G coefficient, A. *senegal* and its fractions can be classified in the following order HIC-F3<IEC-F1<HIC-F2<A. *senegal*<IEC-F2<HIC-F1. This order is directly related to the AGP protein content, then to the propensity of protein rich AGPs to self-associate and form aggregates.

Table III.11. Kuhn-Mark-Houwink-Sakurada parameter (a_G) and fractal dimension (d_f) of A. gums and AGP fractions obtained at 0.1, 0.3 and 0.5 M ($LiNO_3$).

Gum or fraction	M_w range ($x10^{-5}$ g.mol^{-1})	Ionic strength (M)	a_G	d_f
A. *senegal*	5.0 – 50.0	0.1	0.52	1.9
		0.3	0.52	1.9
		0.5	0.51	2.0
A. *seyal*	7.0 – 25.0	0.1	0.64	1.6
		0.3	0.67	1.5
		0.5	0.78	1.3
HIC-F1	5.0 – 10.0	0.1	0.71	1.4
		0.3	0.69	1.4
		0.5	0.71	1.4
HIC-F2	5.0 – 30.0	0.1	0.51	2.0
		0.3	0.47	2.1
		0.5	0.47	2.1
HIC-F3	5.0 – 50.0	0.1	0.32	3.1
		0.3	0.31	3.2
		0.5	0.29	3.4
IEC-F1	20.0 – 60.0	0.1	0.36	2.8
		0.3	0.48	2.1
		0.5	0.43	2.3
IEC-F2	5.0 – 40.0	0.1	0.61	1.6
		0.3	0.61	1.6
		0.5	0.60	1.7

*Fractal dimension was obtained from $d_f = {}^1/_{a_G}$.

Using the a_G coefficient, the fractal dimension was calculated through the following relation: $d_f = {}^1/_{a_G}$. As previously discussed for a_G, the calculated d_f values considered only a part of AGPs according the fractions and was greatly influenced by the presence of aggregates in the samples. The fractal dimension, d_f, is defined as a measure of the self-similarity (e.g. monomers and cluster units) of an object. It depends on the mass and number of similar objects on a unit of length (e.g. the gyration radius, R_G) [137]. Fractal dimensions around 1.5 were found for A. *seyal*, HIC-F1 and IEC-F2, around 2 for A. *senegal* and HIC-F2 and around 3 for HIC-F3 and IEC-F1 (Table III.11). In general, higher d_f values (around 3) suggests a dense and spherical structure [45,137], for instance globular proteins and dendrimers. Values around 2 are characteristic of branched molecules [45]. Meanwhile, lower d_f values (1.1–2.0) are found for more elongated molecules [45,137]. In line with this, HIC-F3 and IEC-F1 are expected to have a dense, compact and ramified structure due to the

presence of aggregates. A. *senegal* and HIC-F2 are expected to have a less dense and more branched structure. Meanwhile, A. *seyal*, HIC-F1 and IEC-F2 are expected to display a more linear conformation. Interestingly, A. *senegal* has a higher fractal dimension, thus a more ramified structure than A. *seyal* which is in good agreement with its higher branching degree (78% and 59%) as reported by Lopez-Torres et al (2015) [12]. Reported d_f values for A. gums and HIC-fractions are: 1.5–2 and 1.4–2.6 for A. *senegal and* A. *seyal* and around 2.0 for the HIC-fractions [10-12,32]. Our results are in good agreement with literature, except for fractions HIC-F1 and HIC-F3. The difference in HIC-F1 values can be explained both by the small population analyzed (11%) and the consideration of only the elongated AGPs (M_w>5x10^5 g.mol^{-1}) of this fraction for the d_f calculation. For HIC-F3, the difference was explained by the presence of AGPs based aggregates in this fraction.

By fitting the sedimentation and translational diffusion coefficients (S_o and D_T, respectively) and their respective weight-averaged molar masses according to a power law function, the global a_S and a_D coefficients of A. gums, HIC and IEC fractions were obtained (Figure III.6). A coefficient a_S of 0.47 (R^2 = 0.943) corresponding to a random coil conformation was obtained for experiments performed using 0.1 M $LiNO_3$ (Figure III.6 a). The increase of the ionic strength from 0.1 M to 0.5 M of the solvent did not impact the conformation of AGPs as the a_S coefficient was 0.46 in 0.5 M $LiNO_3$. Using the translational diffusion coefficient, it is interesting to note that a_D was lower with a value of 0.36 (R^2 = 0.984) corresponding to a conformation close to that of a sphere (Figure III.6 b). The difference observed between a_S and a_D coefficients was due to the specificity of the DOSY-NMR method which only measured the D_T of small AGPs, excluding the D_T of elongated high molar mass AGPs and AGPs based aggregates.

Using the combination of conformational coefficients obtained using different methods and several fractions from A. *senegal* gums, the AGPs from A. *senegal* gum can be categorized in 'small AGPs' adopting a compact and less anisotropic structure (1.5–5.0 x10^5 g.mol^{-1}), 'large AGPs' adopting more elongated and anisotropic structure (5–12 x10^5 g.mol^{-1}) and 'AGP-based aggregates' adopting a compact structure (12–50 x10^5 g.mol^{-1}).

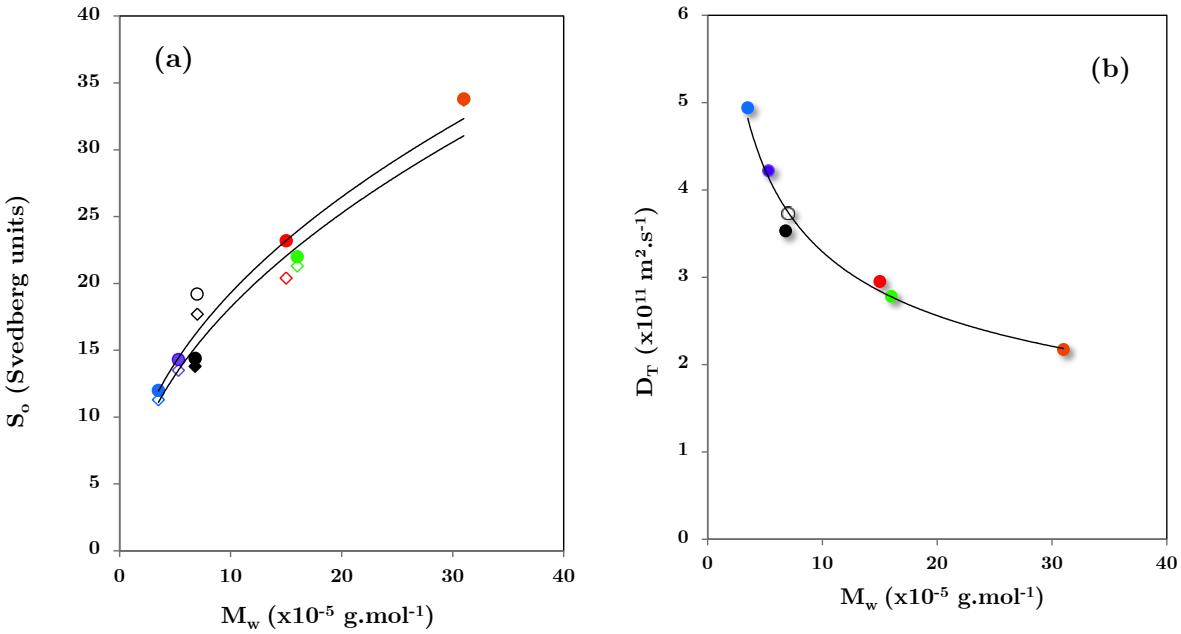

Figure III. 6. Sedimentation coefficient extrapolated at zero concentration, S_o (a) and translational diffusion coefficient, D_T (b) in function of the weight-averaged molar mass (M_w) of A. *seyal* (white), A. *senegal* (black), HIC-F1 (blue), HIC-F2 (red), HIC-F3 (green), IEC-F1 (orange) and IEC-F2 (purple). Measurements were performed at 0.1 M (circle) and 0.5 M (diamond) $LiNO_3$. The data were fitted to: $So = 6.738M_w^{0.457}$ ($R^2 = 0.937$) for 0.1 M, $So = 6.154\ M_w^{0.471}$ ($R^2 = 0.943$) for 0.5 M and $D_T = 7.593M_w^{-0.363}$ ($R^2 = 0.984$). Translational diffusion coefficient was measured by DOSY-NMR.

5.4. Hydration

As detailed in the general introduction (Chapter I), solute hydration is generally described as a mixture of two main water species, bulk water and bound water. The latter refers to all water molecules which physicochemical properties are perturbed by the presence of the solute. In the same way, bulk water refers to water with unperturbed physicochemical properties [120]. Moreover, strongly perturbed water molecules are generally located in the first hydration layer [120]. It is important here to recall that the term 'hydration' refers both to the number of molecules in the hydration shell, known as hydration number, n_h (quantitative aspect), and the strength of solute-water interactions (qualitative aspect) [34,138]. Quantitative and qualitative aspects are taken into consideration in theoretical description of volumetric experiments (see Chapter II). The hydration number, n_h, can be estimated from the analysis of intrinsic viscosity. It is related to the swollen volume through the relationship:

$$n_h = \frac{V_{sw} - v_s^\circ}{\rho_o} \qquad \text{(III.18)}$$

where V_{sw} is the volume of a macromolecule dissolved in a solution per unit of anhydrous mass of the macromolecule [39], v_s° is the partial specific volume and ρ_o is the density of the solvent. This relation holds in theory for hard homogeneous particles. Since AGPs are semi-flexible and inhomogeneous, the values calculated in the following will be discussed in terms of comparison.

The intrinsic viscosity can be described using two main structural contributions, the viscosity increment and the swollen hydrated volume of the molecule [39]:

$$[\eta] = \nu . V_{sw} \tag{III.19}$$

where ν is the viscosity increment (dimensionless). Therefore, n_h can be related to the intrinsic viscosity by:

$$n_h = (\rho_o)\left(\frac{[\eta]}{\upsilon} - v_s^\circ\right) \tag{III.20}$$

The viscosity increment is known as Einstein or Simha-Saito parameter. It depends mainly on the particle shape or anisotropy. For hard impenetrable homogeneous spheres, it takes a value of 2.5 and for anisotropic objects is a function of the axial ratio [40,59,70,139].

In a first rough approach, we take a hard sphere viscosity increment. This is usually done in a great number of articles dealing with protein or polysaccharide hydration regardless of the shape of the molecule. Using a $\nu = 2.5$, hydration numbers n_h were around 7-10 g H_2O/g AGP for A. *senegal*, A. *seyal*, HIC-F1 and IEC-F2, then those gums or fractions containing majoritarily low molar mass AGP and low protein content, and around 15-25 g H_2O/g AGP for HIC-F2, HIC-F3 and IEC-F1, then gums or fractions containing in majority large molar mass AGP and AGP aggregates and higher protein content (Tabl.III.12). These values are supposed to describe the number of water molecules in the first hydration layer. In our opinion, they are very high. Using the same methods and approach, Masuelli (2013) found still higher n_h value, namely 50 g H_2O/g AGP [31] for A. *senegal* gum. The huge discrepancy with our result can be explained in part by the solvent used in the last study, water, instead of 0.1M $LiNO_3$. However, if we take our intrinsic viscosity result in water, 54 $mL.g^{-1}$, we found a n_h of around 20 g H_2O/g AGP, a value still far from the published result. The difference in the gum batch may have an effect but the most likely explanation for this discrepancy is the gum adsorption onto capillary wall that was took into consideration in the present study. In addition, it is worth noting that with a viscosity increment of 2.5, highly

hydrophilic polysaccharides such as xanthan, hyalunoran and hylan display hydration numbers of around 2, 3 and 10 g H_2O/g polymer, respectively [140].

Table III.12. Hydration number (n_h, g H_2O/g AGP) and viscosity increment of A. gums and AGP fractions

Gum or fraction	n_h [a]	ν [b]	n_h	n_h [f]	ν (exp)
Acacia gums					
A. *senegal*	10		1.0[c]	0.8	11
A. *seyal*	7		1.0[d]	0.9	10
AGP fractions					
HIC-F1	7	11	1.0[c]	0.9	10
HIC-F2	19	40	0.6	0.7	37
HIC-F3	14	50	0.1	0.5	42
IEC-F1	24		0.4[e]	0.6	51
IEC-F2	9		0.7[c]	0.8	9

(a) Hydration number calculated using a viscosity increment of 2.5 (hard impenetrable sphere) and the intrinsic viscosity measured by capillary viscometry in 0.1M $LiNO_3$ solvent, (b) Viscosity increments calculated (ELLIPS2 software) from the following triaxial ellipsoid dimensions: 96x96x7 Å for HIC-F1 [32], 580x86x12 Å for HIC-F2 [11] and 538x82x8 Å for HIC-F3 [10], (c) Hydration numbers calculated using a viscosity increment of 11 for small M_w AGP and 45 for large M_w (d) Hydration number calculated using a virtual viscosity increment of 11, (e) Hydration number calculated using a virtual viscosity increment of 60, (f) Hydration numbers taken from Mejia Tamayo et al. (2018)[34] (HIC-F1, HIC-F2 and HIC-F3) or estimated (italic numbers) from the known molecular composition of fractions.

In fact, the main problem with these different n_h is not their intrinsic values, but the fact that values contain also the contribution of AGP anisotropy, flexibility, shape irregularity and surface roughness. As already explained, a viscosity increment ν value of 2.5 is valid only for hard impenetrable homogeneous spheres. However, it was proposed that A. gums have ellipsoidal shapes [10,11,32]. Larger ν values have been reported for anisotropic objects (oblate or prolate ellipsoids) of similar hydrodynamic volume [40,139]. In addition, studies of the intrinsic viscosity of molecules with irregular shapes have shown a difference of 20-120% higher than molecules with equivalent regular (spheroid) shapes [141]. Since we further estimated in Chapter II that AGP are probably semi-flexible, we can conclude that the use of a viscosity increment of 2.5 to calculate the hydration number of an AGP is objectively questionable.

Unfortunately, we do not know how the flexibility and irregularity of a hyperbranched object impact the ν parameter. However, based on experimental small angle scattering

measurements of shape factors and their fitting by theoretical ellipsoidal functions, we were able to propose approximate anisotropic structural models for HIC-F1, HIC-F2 and HIC-F3 fractions[10,11,32]. The reported dimensions for HIC-F1, HIC-F2 and HIC-F3 were 96x96x7, 580x86x12 and 538x82x8 Å, respectively [10,11,32]. It is important to note that these dimensions, especially those of HIC-F2 and HIC-F3 are *averaged* dimensions of large AGP and aggregates, explaining probably the high value of the major dimensions. Nevertheless, armed with these values, we calculated the theoretical ν parameter of equivalent hard impenetrable homogeneous triaxial ellipsoids using the ELLIPS2 software developed by Garcia de la Torre & Harding (2013)[142]. Thus, viscosity increments of around 11, 40 and 50 were obtained for HIC-F1, HIC-F2 and HIC-F3, respectively (Table III.12). Using these values, we found hydration numbers of around 1.0, 0.6 and 0.1 g H_2O/g AGP. We also tried to estimate n_h values for the other gum systems using a ν of 11 for small M_w AGP, 45 for large M_w AGP (average between 40 and 50) and 60 for AGP aggregates. The estimated n_h values were around 1.0 g H_2O/g AGP for A. gums and 0.4 g H_2O/g AGP for IEC-F1, which seems in line with the high content of HIC-F1 fraction in A. *senegal* gum and the aggregated characteristics of IEC-F1.

Information regarding the hydration properties of A. gums is scarce. However, using calorimetric methods, hydration values between 3–6 g H_2O/ g AGP were found for A. *senegal* by Takigami et al (1995) [140]. This is higher than the values we estimated and correspond to ν values of 4-8, which are also compatible with anisotropic objects having smaller aspect ratios. More work is clearly needed to decipher the hydration number of AGP from A. gums. However, we think that n_h around 0.5-1.0 g H_2O/ g AGP is consistent with the hyperbranched nature of AGPs but also to the simultaneous presence of protein and polysaccharide moieties. In addition, we noted that n_h values estimated for HIC fractions were really close or in the range to those estimated from volumetric experiments and reported in Table III.12, i.e. 0.9, 0.7 and 0.5 g H_2O/g AGP for HIC-F1, HIC-F2 and HIC-F3, respectively. Now, using these n_h values and estimated n_h for the other gum systems (Table III.12), we found viscosity increments of around 10 for small M_w AGP systems (A. *senegal*, A. *seyal*, HIC-F1 and IEC-F2) and values around 40-50 for large M_w AGP systems (HIC-F2, HIC-F3 and IEC-F1). This is really close to the values estimated from the supposed dimensions of HIC fractions.

6. Conclusions

This study reports the characterization of hydrodynamic properties of A. gums and the main macromolecular fractions from A. *senegal* obtained using hydrophobic interaction and ionic exchange chromatographies. The combination of viscometry, size exclusion chromatography, dynamic light scattering, diffusion ordered nuclear magnetic spectroscopy and analytical ultracentrifugation provided a complementary description of the main species present in A. gums, thus allowing more reliable results to be obtained. The analysis was focused on intrinsic viscosity and hydrodynamic radius, hydration number and molecular conformation.

The intrinsic viscosity and hydrodynamic radius of A. gums and AGP fractions was reduced with addition of salt due to screening of charges and reduction of the polarity of the solvent, thus reduction of hydrodynamic volume of AGP and AGP aggregates. In addition, during experiments, adsorption of AGPs on the capillary glass wall decrease. At charge neutralization, intrinsic viscosities of about 15, 45 and 60 $mL.g^{-1}$ and hydrodynamic radius of below 10 nm, from 10-40 nm and >50 nm can be considered as characteristic values for 'small AGPs' ($M_w < 7.5x10^5$ $g.mol^{-1}$), 'large AGPs' ($M_w > 7.5x10^5$ $g.mol^{-1}$) and 'AGP-based aggregates' ($M_w > 2\text{-}3x10^6$ $g.mol^{-1}$), respectively. The combination of dynamic light scattering (DLS) and diffusion ordered nuclear magnetic spectroscopy (DOSY-NMR) allowed the identification of macromolecular populations with mean R_H below 9 nm. Moreover, this population showed to be insensitive to changes on the ionic strength of the solvent and adopt a spherical shape. The conformational analysis showed that 'small AGP's' and 'AGP-based aggregates' are likely to adopt a more spherical shape. Meanwhile, 'large AGPs' are more likely to adopt a more extended and anisotropic shape.

The hydration number, n_h, of A. gums and AGP fractions was obtained from measurements of the intrinsic viscosity and their respective viscosity increment, ν. In most studies, a ν of 2.5 corresponding to a hard impenetrable sphere is used. We showed that use of such value leads to an overestimation of n_h and was not compatible with the anisotropic, semi-flexible and surface heterogeneity characteristics of AGPs. Using the AGPs dimensions that we estimated in previous studies and viscosity increment values calculated using ELLIPS2 software, hydration numbers of 1.0, 0.6 and 0.1 g H_2O/g AGP were found for HIC-F1, HIC-F2 and HIC-F3 fractions, respectively. This could correspond to n_h of around 1 g H_2O/g AGP for A. *senegal*. Probably, the n_h of A. *seyal* is also in this range, considering both its

composition and structure. The rough estimation of HIC fraction hydration was however close to hydration values estimated from volumetric data, 0.9, 0.6 and 0.5 g H_2O/g AGP confirming that the n_h parameter mainly corresponds to the number of water molecules in the first hydration layer. Using these n_h values, viscosity increments comprised between 10-50 were found, in relation with the anisotropic shape, flexibility and irregularity of AGPs from A. gums.

7. Complementary data

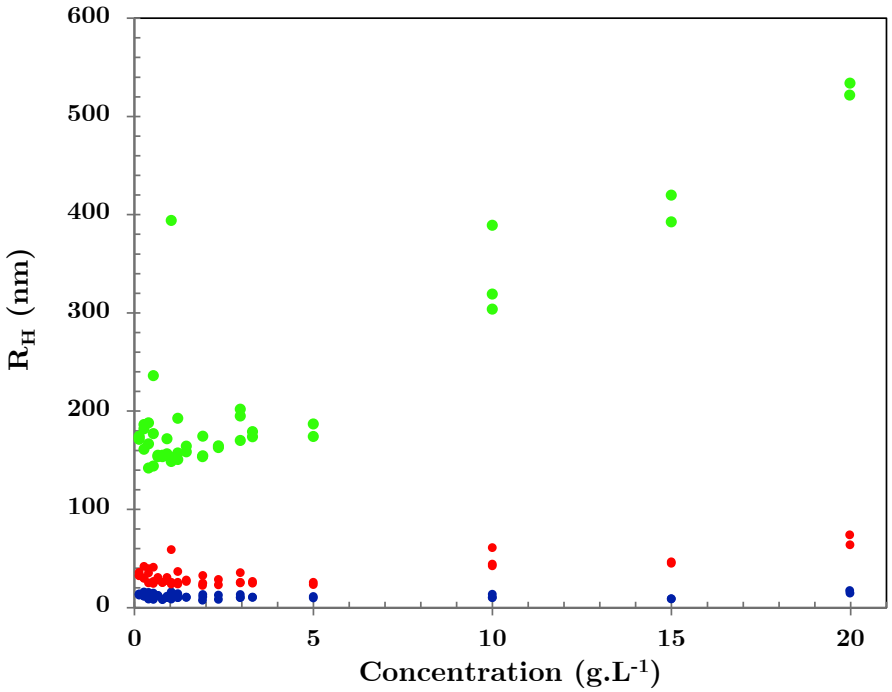

Figure C.1. Mean hydrodynamic radius (z-average, R_H) as function of the concentration of A. *senegal*. Data were analyzed using the NICOMP method allowing the determination of three molecular populations: peak 1 (blue), peak 2 (red) and peak 3 (green). Measurements were performed at 25 °C.

8. References

1. Williams, P.A.; Philips, G.O. Gum arabic. In *Handbook of hydrocolloids*, G. O. Philips, P.A.W., Ed. Boca Raton: CRC Press: 2000; pp 155-168.
2. Sanchez, C.; Nigen, M.; Mejia Tamayo, V.; Doco, T.; Williams, P.; Amine, C.; Renard, D. Acacia gum: History of the future. *Food Hydrocolloids* **2018**.
3. Akiyama, Y.; Eda, S.; Kato, K. Gum arabic is a kind of arabinogalactan protein. *Agric. and Biol. Chem.* **1984**, *48*, 235-237.
4. Williams, P.A. Structural characteristics and functional properties of gum arabic. In *Gum arabic*, The Royal Society of Chemistry: 2012; pp 179-187.
5. Williams, P.A.; Phillips, G.O.; Randall, R.C. Structure-function relationships of gum arabic. In *Gums and stabilisers for the food industry 5* Phillips, G.O.; Williams, P.A.; Wedlock, D.J., Eds. IRL Press: Oxford, 1990; pp 25-36.
6. Ali, B.H.; Ziada, A.; Blunden, G. Biological effects of gum arabic: A review of some recent research. *Food and Chemical Toxicology* **2009**, *47*, 1-8.
7. Verbeken D.; Dierckx S.; K., D. Exudate gums: Occurence, production, and applications. *Applied Microbiology Biotechnology* **2003**, *63*, 10-21.
8. Renard, D.; Lavenant-Gourgeon, L.; Ralet, M.C.; Sanchez, C. Acacia *senegal* gum: Continuum of molecular species differing by their protein to sugar ratio; molecular weight and charges. *Biomacromolecules* **2006**, 2637-2649.
9. Anderson, D.M.W.; Stoddart, J.F. Studies on uronic acid materials. Part xv. The use of molecular-sieve chromatography on acacia *senegal* gum (gum arabic). *Carbohydrate Research* **1966**, *2*, 104-114.
10. Renard, D.; Lepvrier, E.; Garnier, C.; Roblin, P.; Nigen, M.; Sanchez, C. Structure of glycoproteins from acacia gum: An assembly of ring-like glycoproteins modules. *Carbohydrate Polymers* **2014**, *99*, 736-747.
11. Renard, D.; Garnier, C.; Lapp, A.; Schmitt, C.; Sanchez, C. Structure of arabinogalactan-protein from acacia gum: From porous ellipsoids to supramolecular architectures. *Carbohydrate Polymers* **2012**, *90*, 322-332.
12. Lopez-Torrez, L.; Nigen, M.; Williams, P.; Doco, T.; Sanchez, C. Acacia *senegal* vs. Acacia *seyal* gums – part 1: Composition and structure of hyperbranched plant exudates. *Food Hydrocolloids* **2015**, *51*, 41-53.
13. Renard, D.; Garnier, C.; Lapp, A.; Schmitt, C.; Sanchez, C. Corrigendum to "structure of arabinogalactan-protein from acacia gum: From porous ellipsoids to supramolecular architectures" [carbohydr. Polym. 90 (2012) 322–332]. *Carbohydrate Polymers* **2013**, *97*, 864-867.
14. Randall, R.C.; Phillips, G.O.; Williams, P.A. Fractionation and characterization of gum from acacia *senegal*. *Food Hydrocolloids* **1989**, *3*, 65-75.
15. Mahendran, T.; Williams, P.; Phillips, G.; Al-Assaf, S.; Baldwin, T. New insights into the structural characteristics of the arabinogalactan-protein (agp) fraction of gum arabic. *Journal of Agricultural and Food Chemistry* **2008**, 9269-9276.
16. Islam, A.M.; Phillips, G.O.; Sljivo, A.; Snowden, M.J.; Williams, P.A. A review of recent developments on the regulatory, structural and functional aspects of gum arabic. *Food Hydrocolloids* **1997**, *11*, 493-505.
17. Dror, Y.; Cohen, Y.; Yerushalmi-Rozen, R. Structure of gum arabic in aqueous solution. *J. of Polym. Sci. Pol. Phys.* **2006**, *44*, 3265-3271.
18. Al-Assaf, S.; Sakata, M.; McKenna, C.; Aoki, H.; Phillips, G.O. Molecular associations in acacia gums. *Structural Chemistry* **2009**, *20*, 325-336.
19. Grein-Iankovski, A.; Ferreira, J.G.L.; Orth, E.S.; Sierakowski, M.-R.; Cardoso, M.B.; Simas, F.F.; Riegel-Vidotti, I.C. A comprehensive study of the relation between structural and physical chemical properties of acacia gums. *Food Hydrocolloids* **2018**, *85*, 167-175.
20. Pavlov, G.M. The concentration dependence of sedimentation for polysaccharides. *Eur. Biophys. J.* **1997**, *25*, 385-397.
21. Tanford, C. Physical chemistry of macromolecules. In *Physical chemistry of macromolecules*, Wiley: New York, USA, 1961.
22. Cozic, C.; Picton, L.; Garda, M.-R.; Marlhoux, F.; Le Cerf, D. Analysis of arabic gum: Study of degradation and water desorption processes. *Food Hydrocolloids* **2009**, *23*, 1930-1934.
23. Flindt, C.; Alassaf, S.; Phillips, G.; Williams, P. Studies on acacia exudate gums. Part v. Structural features of acacia

seyal. *Food Hydrocolloids* **2005**, *19*, 687-701.

24. Hassan, E.A.; Al-Assaf, S.; Phillips, G.O.; Williams, P.A. Studies on acacia gums: Part iii molecular weight characteristics of acacia *seyal* var. Seyal and acacia *seyal* var fistula. *Food Hydrocolloids* **2005**, *19*, 669-677.
25. Elmanan, M.; Al-Assaf, S.; Phillips, G.O.; Williams, P.A. Studies on acacia exudate gums: Part vi. Interfacial rheology of acacia *senegal* and acacia *seyal*. *Food Hydrocolloids* **2008**, *22*, 682-689.
26. Gashua, I.B.; Williams, P.A.; Yadav, M.P.; Baldwin, T.C. Characterisation and molecular association of nigerian and sudanese acacia gum exudates. *Food Hydrocolloids* **2015**, *51*, 405-413.
27. Idris, O.H.M.; Williams, P.A.; Phillips, G.O. Characterisation of gum from acacia *senegal* trees of different age and location using multidetection gel permation chromatography. *Food Hydrocolloids* **1998**, 379-388.
28. Sanchez, C.; Renard, D.; Robert, P.; Schmitt, C.; Lefebvre, J. Structure and rheological properties of acacia gum dispersions. *Food Hydrocolloids* **2002**, *16*, 257-267.
29. Vandevelde, M.-C.; Fenyo, J.-C. Macromolecular distribution of acacia senegal gum (gum arabic) by size exclusio chromatography. *Carbohyd. Polym.* **1985**, *5*, 251-273.
30. Gillis, R.B.; Adams, G.G.; Alzahrani, Q.; Harding, S.E. A novel analytical ultracentrifugation based approach to the low resolution structure of gum arabic. *Biopolymers* **2016**, *105*, 618-625.
31. Masuelli, M. Hydrodynamic properties of whole arabic gum. *American Journal of Food Science and Technology* **2013**, *1*, 60-66.
32. Sanchez, C.; Schmitt, C.; Kolodziejczyk, E.; Lapp, A.; Gaillard, C.; Renard, D. The acacia gum arabinogalactan fraction is a thin oblate ellipsoid: A new model based on small-angle neutron scattering and ab initio calculation. *Biophysical Journal* **2008**, *94*, 629-639.
33. Ray, A.K.; Bird, P.B.; Iacobucci, G.A.; Clark, B.C. Functionality of gum arabic. Fractionation, characterization and evaluation of gum fractions in citrus oil emulsions and model beverages. *Food Hydrocolloids* **1995**, *9*, 123-131.
34. Mejia Tamayo, V.; Nigen, M.; Apolinar-Valiente, R.; Doco, T.; Williams, P.; Renard, D.; Sanchez, C. Flexibility and hydration of amphiphilic hyperbranched arabinogalactan-protein from plant exudate: A volumetric perspective. *Colloids and Interfaces* **2018**, *2*, 11.
35. Riddell, G.L.; Davies, C.W. A study of gum arabic. Part i. Viscosity and adsorption measurements. *Journal of Physical Chemistry* **1931**, *35*, 2722-2731.
36. Thomas, A.W.; Murray, H.A. A physico-chemical study of gum arabic. *The Journal of Physical Chemistry* **1927**, *32*, 676-697.
37. Bryant, G.; Thomas, J.C. Improved particle size distribution measurement using multiagle dynamic light scattering. *Langmuir* **1995**, *11*, 2480-2485.
38. Harding, S.E. The intrinsic viscosity of biological macromolecules. Progress in measurement, interpretation and application to structure in dilute solution. *Progress in Biophysics and Molecular Biology* **1997**, *68*, 207-262.
39. Harding, S.E. Dilute solution viscometry of food biopolymers. In *Fuctional properties of food macromolecules*, 2nd ed.; Aspen Pub: MA, USA, 1998; pp 1-49.
40. Jamieson, A.M.; Simha, R. Newtonian viscosity of dilute, semidilute, and concentrated polymer solutions. In *Polymer physics*, 2010; pp 17-87.
41. Cheng, R.; Shao, Y.; Liu, M.; Qian, R. Effect of adsorption on the viscosity of dilute polymer solution. *European Polymer Journal* **1998**, *34*, 1613-1619.
42. Morris, G.A.; Adams, G.G.; Harding, S.E. On hydrodynamic methods for the analysis of the sizes and shapes of polysaccharides in dilute solution: A short review. *Food Hydrocolloids* **2014**, *42*, 318-334.
43. Cui, S.W. *Food carbohidrates: Chemistry, physical properties, and applications*. 1st edition ed.; CRC Press: 2005; p 411.
44. Wolf, B.A. Polyelectrolytes revisited: Reliable determination of intrinsic viscosities. *Macromolecular Rapid Communications* **2007**, *28*, 164-170.
45. Burchard, W. Solution properties of branched macromolecules In *Branched polymers ii*, Roover, J., Ed. Springer Berlin Heidelberg: Berlin, Heidelberg, 1999; pp 113-194.
46. Simha, R. Effect of concentration on the viscosity of dilute solutions. *Journal of Research of the National Bureau of Standards* **1949**, *42*, 409-418.
47. Rao, M.V.S. Viscosity of dilute to moderately concentrated polymer solutions. *Polymer* **1993**, *34*, 592-596.
48. Desbrieres, J. Viscosity of semiflexible chitosan solutions: Influence of

concentration, temperature, and role of intermolecular interactions. *Biomacromolecules* **2002**, *3*, 342-349.

49. Huggins, M.L. The viscosity of dilute solutions of long-chain molecules. Iv. Dependence on concentration. *Journal of the American Chemical Society* **1942**, *64*, 2716-2718.
50. Yang, J.T. The viscosity of macromolecules in relation to molecular conformation. In *Advances in protein chemistry*, Anfinsen, C.B.; Anson, M.L.; Bailey, K.; Edsall, J.T., Eds. Academic Press: 1962; Vol. 16, pp 323-400.
51. Cohen, J.; Priel, Z. Viscosity of dilute polyelectrolyte solutions: Temperature dependence. *The Journal of Chemical Physics* **1990**, *93*, 9062-9068.
52. Fuoss, R.M.; Strauss, U.P. Electrostatic interaction of polyelectrolytes and simple electrolytes. *Journal of Polymer Science* **1948**, *3*, 602-603.
53. Ghimici, L.; Nichifor, M.; Wolf, B.A. Ionic polymers based on dextran: Hydrodynamic properties in aqueous solution and solvent mixtures. *The Journal of Physical Chemistry B* **2009**, *113*, 8020-8025.
54. Yang, H.; Zheng, Q.; Cheng, R. New insight into "polyelectrolyte effect". *Colloids and Surfaces A: Physicochemical and Engineering Aspects* **2012**, *407*, 1-8.
55. Nagasawa, M. Thermodynamic and hydrodynamic properties of polyelectrolytes *J. Polymer Sci.* **1975**, 1-49.
56. Zhang, H.; Wang, H.; Wang, J.; Guo, R.; Zhang, Q. The effect of ionic strenght on the viscosity of sodium alginate solution. *Polymers for Advanced Technologies* **2001**, *12*, 740-745.
57. Rubinstein, M.; Colby, R.H.; Dobrynin, A.V. Dynamics of semidilute polyelectrolyte solutions. *Phys Rev Lett* **1994**, *73*, 2776-2779.
58. Zhong, D.; Huang, X.; Yang, H.; Cheng, R. New insights into viscosity abnormality of sodium alginate aqueous solution. *Carbohydrate Polymers* **2010**, *81*, 948-952.
59. Elias, H.G. Viscosity of dilute solutions. In *Macromolecules, volume 3: Physical structures and properties*, Wiley VCH: 2008; pp 395-425.
60. Cai, Z.; Dai, J.; Yang, H.; Cheng, R. Study on the interfacial properties of viscous capillary flow of dilute acetic acid solutions of chitosan. *Carbohydrate Polymers* **2009**, *78*, 488-491.
61. Rogerson, A.K. New techniques in diffusion-ordered nmr spectroscopy. University of Manchester, 2013.
62. Gilard, V.; Trefi, S.; Balayssac, S.; Delsuc, M.A.; Gostan, T.; Malet-Martino, M.; Martino, R.; Prigent, Y.; Taulelle, F. Chapter 6 - dosy nmr for drug analysis a2 - holzgrabe, ulrike. In *Nmr spectroscopy in pharmaceutical analysis*, Wawer, I.; Diehl, B., Eds. Elsevier: Amsterdam, 2008; pp 269-289.
63. Lelievre, J.; Lewis, J.A.; Marsden, K. The size and shape of amylopectin: A study using analytical ultracentrifugation. *Carbohydrate Research* **1986**, *153*, 195-203.
64. Schuck, P. Size-distribution analysis of macromolecules by sedimentation velocity ultracentrifugation and lamm equation modeling. *Biophysical Journal* **2000**, *78*, 1606-1619.
65. Lebowitz, J.; Lewis, M.S.; Schuck, P. Modern analytical ultracentrifugation in protein science: A tutorial review. *Protein Science* **2009**, *11*, 2067-2079.
66. Brown, P.H.; Schuck, P. Macromolecular size-and-shape distributions by sedimentation veloxity analytical ultracentrifugation. *Biophys. J.* **2006**, *90*, 4651-4661.
67. Patel, T.R.; Winzor, D.J.; Scott, D.J. Analytical ultracentrifugation: A versatile tool for the characterisation of macromolecular complexes in solution. *Methods* **2016**, *95*, 55-61.
68. Harding, S.E. Analysis of polysaccharides by ultracentrifugation. Size, conformation and interactions in solution. In *Polysaccharides i: Structure, characterization and use*, Heinze, T., Ed. Springer Berlin Heidelberg: Berlin, Heidelberg, 2005; pp 211-254.
69. Stafford, W.F. Boundary analysis in sedimentation transport experiments: A procedure for obtaining sedimentation coefficient distributions using the time derivative of the concentration profile. *Analytical Biochemistry* **1992**, *203*, 295-301.
70. Harding, S.E. On the hydrodynamic analysis of macromolecular conformation. *Biophysical Chemistry* **1995**, *55*, 69-93.
71. Harding, S.E. Sedimentation analysis of polysaccharides. In *Analytical ultracentrifugation in biochemistry and polymer science*, S. E. Harding, A.J.R.a.J.C.H., Ed. Royal Society of Chemistry: Cambridge, UK, 1992; pp 495-516.
72. Harding, S.E. Challenges for the modern analytical ultracentrifuge analysis of polysaccharides. *Carbohydrate Research* **2005**, *340*, 811-826.

73. Theisen, A.; Johann, C.; Deacon, M.P.; Harding, S.E. *Refractive increment data - book for polymer and biomolecular scientists*. Nottingham University Press: Nottingham, UK, 2000.
74. Zhao, H.; Brown, P.H.; Schuck, P. On the distribution of protein refractive index increments. *Biophys. J.* **2011**, *100*, 2309-2317.
75. Grein, A.; da Silva, B.C.; Wendel, C.F.; Tischer, C.A.; Sierakowski, M.R.; Moura, A.B.D.; Iacomini, M.; Gorin, P.A.J.; Simas-Tosin, F.F.; Riegel-Vidotti, I.C. Structural characterization and emulsifying properties of polysaccharides of acacia mearnsii de wild gum. *Carbohydrate Polymers* **2013**, *92*, 312-320.
76. Wang, Q.; Burchard, W.; Cui, S.W.; Huang, X.Q.; Philips, G.O. Solution properties of conventional gum arabic and a matured gum arabic (acacia (sen) super gum). *Biomacromolecules* **2008**, *9*, 1163-1169.
77. Al-Assaf, S.; Phillips, G.; Williams, P. Studies on acacia exudate gums: Part ii. Molecular weight comparison of the vulgares and gummiferae series of acacia gums. *Food Hydrocolloids* **2005**, *19*, 661-667.
78. Showalter, A.M. Arabinogalactan-proteins: Structure, expression and function. *Cell. Mol. Life Sci.* **2001**, *58*, 1399-1417.
79. Natraj, V.; Chen, S.B. Primary electroviscous effect in a suspension of charged porous spheres. *Journal of Colloid and Interface Science* **2002**, *251*, 200-207.
80. Russel, W.B. Low-shear limit of the secondary electroviscous effect. *Journal of Colloid and Interface Science* **1976**, *55*, 590-604.
81. Chen, J.; Shao, Y.; Yang, Z.; Yang, H.; Cheng, R. Analysis of viscosity abnormalities of polyelectrolytes in dilute solutions. *Chinese Journal of Polymer Science* **2011**, *29*, 750-756.
82. Antonietti, M.; Briel, A.; Förster, S. Intrinsic viscosity of small spherical polyelectrolytes: Proof for the intermolecular origin of the polyelectrolyte effect. *The Journal of Chemical Physics* **1996**, *105*, 7795-7807.
83. Yamanaka, J.; Araie, H.; Matsuoka, H.; Kitano, H.; Ise, N.; Yamaguchi, T.; Saeki, S.; Tsubokawa, M. Revisit to the intrinsic viscosity-molecular weight relationship of ionic polymers. 5. Further studies on solution viscosity of sodium poly(styrenesulfonates). *Macromolecules* **1991**, *24*, 6156-6159.
84. Antonietti, M.; Briel, A.; Förster, S. Quantitative description of the intrinsic viscosity of branched polyelectrolytes. *Macromolecules* **1997**, *30*, 2700-2704.
85. Rattanakawin, C.; Hogg, R. Viscosity behavior of polymeric flocculant solutions. *Minerals Engineering* **2007**, *20*, 1033-1038.
86. Smidsrød, O. Solution properties of alginate. *Carbohydrate Research* **1970**, *13*, 359-372.
87. Morikawa, A. Comparison of properties among dendritic and hyperbranched poly(ether ether ketone)s and linear poly(ether ketone)s. *Molecules* **2016**, *21*.
88. Rossky, P.; Karplus, M. Solvation. A molecular dynamics study of a dipeptide in water. *Journal of the American Chemical Society* **1979**, *101*, 1913-1937.
89. Yang, L.; Fu, S.; Zhu, X.; Zhang, L.M.; Yang, Y.; Yang, X.; Liu, H. Hyperbranched acidic polysaccharide frm green tea. *Biomacromolecules* **2010**, *11*, 3395-3405.
90. Kee, R.A.; Gauthier, M. Arborescent polystyrene-graft-poly(2-vinylpyridine) copolymers: Synthesis and enhanced polyelectrolyte effect in solution. *Macromolecules* **2002**, *35*, 6526-6532.
91. Swenson, H.A.; Kaustinen, H.M.; Kaustinen, O.A.; Thompson, N.S. Structure of gum arabic and its configuration in solution. *Journal of Polymer Science Part A-2: Polymer Physics* **1968**, *6*, 1593-1606.
92. Kawai, T.; Saito, K. Anomalous viscosity behavior of polymer solutions at very low concentrations. *Journal of Polymer Science* **1957**, *XXVI*.
93. Öhrn, O.E. Preliminary report on the influence of adsorption on capillary dimensions of viscometers. *Journal of Polymer Science* **1955**, *17*, 137-140.
94. Streeter, D.J.; Boyer, R.F. Viscosities of extremely dilute polystyrene solutions. *Journal of Polymer Science* **1954**, *14*, 5-14.
95. Randall, R.C.; Phillips, G.O.; Williams, P.A. The role of the proteinaceous component on the emulsifying properties of gum arabic. *Food Hydrocolloids* **1988**, *2*, 131-140.
96. Damodaran, S.; Razumovsky, L. Competitive adsorption and thermodynamic incompatibility of mixing of β-casein and gum arabic at the air–water interface. *Food Hydrocolloids* **2003**, *17*, 355-363.
97. Li, X.; Fang, Y.; Al-Assaf, S.; Phillips, G.O.; Nishinari, K.; Zhang, H. Rheological study of gum arabic solutions: Interpretation based on molecular self-

association. *Food Hydrocolloids* **2009**, *23*, 2394-2402.

98. Al-Assaf, S.; Philips, G.O. Characterization of agp's in acacia gums. *Food Ingredients Journal of Japan* **2006**, *3*, 189-197.
99. Barnes, H.A. A review of the slip (wall depletion) of polymer solutions, emulsions and particle suspensions in viscometers: Its cause, character, and cure. *Journal of Non-Newtonian Fluid Mechanics* **1995**, *56*, 221-251.
100. Eckelt, J.; Knopf, A.; Wolf, B.A. Polyelectrolytes: Intrinsic viscosities in the absence and in the presence of salt. *Macromolecules* **2008**, *41*, 912-918.
101. Giannouli, P. Effect of polymeric cosolutes on calcium pectinate gelation. Part 3. Gum arabic and overview. *Carbohydrate Polymers* **2004**, *55*, 367-377.
102. Mothé, C.G.; Rao, M.A. Rheological behavior of aqueous dispersions of cashew gum and gum arabic: Effect of concentration and blending. *Food Hydrocolloids* **1999**, *13*, 501-506.
103. Alain, M.; McMullen, J.-N. Molecular weight of acacia. *International Journal of Pharmaceutics* **1985**, *23*, 265-275.
104. Chien, H.; Isihara, C.H.; Isihara, A. Intrinsic viscosity of polyelectrolytes in salt solutions. *Polymer Journal* **1976**, *8*, 288-293.
105. Dobrynin, A.V.; Rubinstein, M. Theory of polyelectrolytes in solutions and at surfaces. *Progress in Polymer Science* **2005**, *30*, 1049-1118.
106. Buhler, E.; Rinaudo, M. Structural and dynamical properties of semirigid polyelectrolyte solutions: A light-scattering study. *Macromolecules* **2000**, *33*, 2098-2106.
107. Geddes, R.; Harvey, J.D.; Wills, P.R. The molecular size and shape of liver glycogen. *Biochem. J.* **1977**, *163*, 201-209.
108. Lim, J.; Yeap, S.; Che, H.; Low, S.C. Characterization of magnetic nanoparticle by dynamic light scattering. *Nanoscale Research Letters* **2013**, *8*, 381.
109. Drifford, M.; Dalbiez, J.P. Dynamics of polyelectrolyte solutions by light scattering. *Journal de Physique Lettres* **1985**, *46*, 311-319.
110. Sedlák, M. What can be seen by static and dynamic light scattering in polyelectrolyte solutions and mixtures? *Langmuir* **1999**, *15*, 4045-4051.
111. Dolce, C.; Meriguet, G. Ionization of short weak polyelectrolytes: When size matters. *Colloid Polym Sci* **2017**, *295*, 279-287.
112. Setford, S.J. Measurement of native dextran synthesis and sedimentation properties y analytical ultracentrifugation. *Journal of Chemica Technology and Biotecnology* **1999**, *74*, 17-24.
113. Pavlov, G.M.; Korneeva, E.V.; Vikhoreva, G.A.; Harding, S.E. Hydrodynamic and molecular characteristics of carboxymethylchitin in solution. *Polymer Science* **1998**, *40*, 1275-1281.
114. Pavlov, G.M.; Korneeva, E.V.; Jumel, K.; Harding, S.E.; Meijer, E.W.; Peerlings, H.W.I.; Stoddart, J.F.; Nepogodiev, S.A. Hydrodynamic properties of carbohydrate-coated dendrimers. *Carbohydrate Polymers* **1999**, *38*, 195-202.
115. Igarashi, O.; Sakurai, Y. Studies on the non-starchy polysaccharides of the endosperm of naked barley

part i. Preparation of the water soluble β-glucans from naked barley endosperm and their properties. *Agricultural and Biological Chemistry* **1965**, *29*, 678-686.

116. Nagasawa, M.; Eguchi, Y. Charge effect in sedimentation. I. Polyelectrolytes. *The Journal of Physical Chemistry* **1967**, *71*, 880-888.
117. Hu, X.; Kaplan, D.; Cebe, P. Dynamic protein−water relationships during β-sheet formation. *Macromolecules* **2008**, *41*, 3939-3948.
118. Huang, W.; Krishnaji, S.; Tokareva, O.R.; Kaplan, D.; Cebe, P. Influence of water on protein transitions: Thermal analysis. *Macromolecules* **2014**, *47*, 8098-8106.
119. Hatakeyama, T.; Nakamura, K.; Hatakeyama, H. Determination of bound water content in polymers by dta, dsc and tg. *Thermochimica Acta* **1988**, *123*, 153-161.
120. Laage, D.; Elsaesser, T.; Hynes, J.T. Water dynamics in the hydration shells of biomolecules. *Chemical Reviews* **2017**, *117*, 10694-10725.
121. Chandler, D. Hydrophobicity: Two faces of water. *Nature* **2002**, *417*, 491.
122. Sun, Q. The physical origin of hydrophobic effects. *Chemical Physics Letters* **2017**, *672*, 21-25.
123. Xu, M.; Yan, X.; Cheng, R.; Yu, X. Investigation into the solution properties of hyperbranched polymer. *Polymer International* **2001**, *50*, 1338-1345.
124. Siddig, N.; Osman, M.; Alassaf, S.; Phillips, G.; Williams, P. Studies on acacia exudate gums, part iv. Distribution of molecular components in in relation to. *Food Hydrocolloids* **2005**, *19*, 679-686.

125. Renard, D.; Lavenant-Gourgeon, L.; Lapp, A.; Nigen, M.; Sanchez, C. Enzymatic hydrolysis studies of arabinogalactan-protein structure from acacia gum: The self-similarity hypothesis of assembly from a common builiding block. *Carbohydrate Polymers* **2014**, *112*, 648-661.
126. Pavlov, G.M.; Okatova, O.V.; Gavrilova, I.I.; Ul'yanova, N.N.; Panarin, E.F. Sizes and conformations of hydrophilic and hydrophobic polyelectrolytes in solutions of various ionic strengths. *Polymer Science Series A* **2013**, *55*, 699-705.
127. Anderson, D.M.W.; Rahman, S. Studies on uronic acid materials. Part xx. The viscosity molecular weight relationship for acacia gums. *Carbohydrate Research* **1967**, *4*, 298-304.
128. Vandevelde, M.C.; Fenyo, J.C. Macromolecular distribution of acacia senegal gum (gum arabic) by size exclusion chromatography. *Carbohydrate Polymers* **1985**, *5*, 251-273.
129. Senti, F.R.; Hellman, N.; Ludwig, N.H.; Babcock, G.E.; Tobin, R.; Glass, C.A.; Lamberts, B.L. Viscosity, sedimentation and light-scattering properties of fractions of an acid-hydrolyzed dextran. *Journal of Polymer Science* **1955**, *XVII*, 527-546.
130. Ioan, C.E.; Aberle, T.; Burchard, W. Structure properties of dextran. 2. Dilute solution. *Macromolecules* **2000**, *33*, 5730-5739.
131. Hu, T.; Huang, Q.; Wong, K.; Yang, H.; Gan, J.; Li, Y. A hyperbranched β-d-glucan with compact coil conformation from lignosus rhinocerotis sclerotia. *Food Chemistry* **2017**, *225*, 267-275.
132. Möck, A.; Burgath, A.; Hanselmann, R.; Frey, H. Synthesis of hyperbranched aromatic homo- and copolyesters via the slow monomer addition method. *Macromolecules* **2001**, *34*, 7692-7698.
133. Muthukrishnan, S.; Mori, H.; Müller, A.H.E. Synthesis and characterization of methacrylate-type hyperbranched glycopolymers via self-condensing atom transfer radical copolymerization. *Macromolecules* **2005**, *38*, 3108-3119.
134. Filipov, A.P.; Belyaeva, E.V.; Tarabukina, E.B.; Amirova, A.I. Behaviour of hyperbranched polymers in solution. *Polymer Science* **2011**, *53*, 107-117.
135. Bello-Perez, L.A.; Roger, P.; Colonna, P.; Paredes-Lopez, O. Laser light scattering of high amylose and high amylopectin materials, stability in water after microwave dispersion. *Carbohydrate Polymers* **1998**, *37*, 383-394.
136. Picton, L.; Bataille, I.; Muller, G. Analysis of a complex polysaccharide (gum arabic) by multi-angle laser light scattering coupled on-line to size exclusion chromatography and flow field flow fractionation. *Carbohydrate Polymers* **2000**, *42*, 23-31.
137. Pavlov, G.M. Size and average density spectra of macromolecules obtained from hydrodynamic data. *Eur. Biophys. J.* **2007**, *22*, 171-180.
138. Chalikian, T.V.; Sarvazyan, A., P.; Breslauer, K.J. Hydration and partial compressibility of biological compounds. *Biophysical Chemistry* **1994**, *51*, 89 - 109.
139. Simha, R. The influence of brownian movement on the viscosity of solutions. *The Journal of Physical Chemistry* **1940**, *44*, 25-34.
140. Takigami, S.; Takigami, M.; Phillips, G.O. Effect of preparation method on the hydration characteristics of hylan and comparison with another highly cross-linked polysaccharide, gum arabic. *Carbohydrate Polymers* **1995**, *26*, 11-18.
141. Daghooghi, M.; Borazjani, I. The effects of irregular shape on the particle stress of dilute suspensions. *J. Fluid Mech.* **2018**, *839*, 663-692.
142. Garcia de la Torre, J.; Harding, S.E. Hydrodynamic modelling of protein conformation in solution: Ellips and hydro. *Biophys. J.* **2013**, *5*, 195-206.

Chapter IV: Effects of Temperature on the structure and solution properties of Arabinogalactan-proteins from Acacia gum exudates

Highlights

- The thermogravimetric analysis showed a two-stage process for all A. gums and fractions, with a first stage related to dehydration and a second stage corresponding to AGP degradation. However, a second intermediate stage was seen for HIC-F3, due to further dehydration (possibly of the protein moiety) or alternatively to degradation of uronic acids. A. *seyal* showed a lower transition temperature than A. *senegal,* suggesting a higher sensitivity for dehydration. These results are in line with the lowest flow activation energy found for A. *seyal*. In addition, the transition temperatures in HIC fractions increased in the order of their polarity HIC-F1>HIC-F2>HIC-F3, confirming the important role of the protein moiety in the global affinity for solvent.

- The structural and hydrodynamic properties of A. gums and HIC fraction marginally changed in the temperature range 25–50°C. We think that this behavior is mainly caused by both the weak polyelectrolyte and the hyperbranched characteristics of AGPs.

- The volumetric properties, partial specific volume and partial specific adiabatic compressibility, of A. gums and HIC fractions increased with the increase of temperature. This behavior was explained mainly due to changes on the thermal

volume, increase of volume fluctuations (expansion of voids) and, to a less extent, weakening of the hydrogen bonds and loss of water molecules from the hydration layer.

- An expansibility coefficient around $5x10^{-4}$ $cm^3.g^{-1}.K^{-1}$ was calculated for A. gums and HIC fractions, which is a typical value found for proteins and more generally for biopolymers.

Effects of Temperature on the Structure and Solution Properties of Arabinogalactan-proteins from Acacia gum exudates[1]

Veronica Mejia Tamayo[a], Michaël Nigen[a], Rafael Apolinar-Valiente[b], Thierry Doco[b], Pascale Williams[b], Denis Renard[c], Christian Sanchez[a]

[a] UMR IATE, UM-INRA-CIRAD-Montpellier Supagro, 2 Place Pierre Viala, F-34060 Montpellier Cedex, France.

[b] UMR SPO, INRA-UM, 2 Place Pierre Viala, F-34060 Montpellier Cedex, France.

[c] UMR BIA, INRA, F-44300 Nantes, France.

Abstract

Acacia gums are widely used in the industry due to their good interfacial properties: e. g. formation and stabilization of emulsions, and their ability to form low viscosity dispersions at concentrations up to around 20-30 (%wt). These properties depend to a great extent on the molar mass, flexibility and hydration of arabinogalactan-protein-type biopolymers composing gums, which defined their so called volumetric properties.

In the present article, we studied principally the effects of the temperature on the partial specific volume (v_s°), adiabatic compressibility coefficient (β_s°), intrinsic viscosity ($[\eta]$) and hydrodynamic radius (R_H) of arabinogalactan – protein (AGP) biopolymers from Acacia gum exudates. However, the effect of the increase of the ionic strength on the intrinsic viscosity was also studied. The study was performed with A. *senegal*, A. *seyal* and the macromolecular fractions of the former obtained from hydrophobic interaction chromatography (HIC), named according to their elution order and decreasing polarity as HIC-F1, HIC-F2 and HIC-F3. In addition, we studied the thermal stability of the different systems in the powdered state by thermogravimetric analysis (TGA). The thermal treatment of A. gums showed a two-event process. The first event, corresponding to a first

[1] Article in preparation for Colloids and Interfaces

transition temperature was found around 70°C, corresponding to the loss of bound water. However, A. *seyal* showed a lower transition temperature (64°C) than A. *senegal* (69°C), which suggests a higher sensitivity to the dehydration of the former. HIC-F1 showed a higher transition temperature (70°C) than HIC-F2 and HIC-F3 (65°C and 60°C, respectively), suggesting a lower strength of interaction with the solvent of the less polar HIC-F3 fraction. In addition, an intermediate event around 170°C was observed for this fraction, suggesting the loss of remaining water or decomposition of carboxylic groups. The increase of the temperature had little effect on the structural and hydrodynamic properties of A. gums, where reductions of less than 10% of measured parameters were observed. On the other hand, the main volumetric parameters, v_s° and β_s°, increased with the increasing temperature. The temperature-induced evolution of volumetric parameters did not depend on the AGP polarity, but rather to the expansion of thermal volume and inner volume fluctuations. A. gums showed a partial expansibility (E°) around of $5x10^{-4}$ $cm^3.g^{-1}.K^{-1}$, a value typically found for globular proteins and polysaccharides.

Keywords: Acacia gum, Arabinogalactan-proteins, partial specific volume, expansibility coefficient, intrinsic viscosity, hydrodynamic radius.

1. Introduction

Acacia gum (A. gum) is one of the most used gums in the industry due to its interesting functional properties, e. g. formation and stabilization of emulsions, and their ability to form low viscosity dispersions at concentrations up to around 20–30 % (wt), which is not the case for other commonly used gums. A. gum is defined as the dried exudate of the branches and trunk of the *Acacia senegal* (L) Willdenow and *Acacia seyal* (Fam. Leguminosae) trees [1-3]. A. gums are composed of hyperbranched, slightly acidic, amphiphilic arabinogalactan-protein (AGP) macromolecules [4]. They are formed of different populations of AGP differing in sugar, protein and mineral composition, charge

density, molar mass, size and anisotropy [5-8]. In addition, supramolecular entities (aggregates) are always present in gums, due to the high self-assembly propensity of AGPs [1,6,9-13]. Basically, AGPs are composed of a polysaccharide moiety composed of D-galactose, L-arabinose, L-rhamnose, D-glucuronic and 4-O-methylglucuronic acids [1,14], being galactose (Gal) and arabinose (Ara) the main sugars [1,5,8,15-18]. The AGP seminal chemical structure includes a backbone of 1-3 linked β-D-galactopyranosyl units bound to side chains formed of two or five 1-3 linked β-D-galactopyranosyl units joined to the main chain at the 1, 6 position. Units of α-L-arabinofuranosyl and α-L-rhamnopyranosyl are distributed along the main and side chains; meanwhile β-D-glucuronopyranosyl and 4-O-methyl-β-D-glucuronopyranosyl units are found most likely as end units [1,19-21]. The protein moiety is composed of more or less the same amino acids, being serine and hydroxyproline the main amino acids present [1,5,8,16,18].

For historical and use reasons, A. *senegal* gum has been more extensively studied than A. *seyal* gum. Thus, it was mainly fractionated using hydrophobic interaction chromatography (HIC), producing mainly three fractions, HIC-F1, HIC-F2 and HIC-F3, named according to their elution order and increasing hydrophobicity index [5,8]. These three fractions differ mainly in their protein content (around 1%, 10% and up to 25%, respectively), molar mass weight average M_w (around $3x10^5$, in the range of $1\text{-}40x10^5$ and $3\text{-}30x10^5$ $g.mol^{-1}$, respectively) and hydrodynamic radii R_H (9, 23-35 and 16-28 nm, respectively) [1,5,7,22]. In addition, these HIC fractions were found to differ on their volumetric compressibility or flexibility and hydration number (n_h) in close relation to their polarity [23]. Thus, the HIC-F1 fraction displays the lowest flexibility and higher hydration number (0.85 g H_2O/g AGP) while the HIC-F3 fraction is characterized by the higher flexibility and lowest hydration number (0.54 g H_2O/g AGP). The HIC-F2 fraction displays an intermediate behaviour with a n_H of 0.67 g H_2O/g AGP. These results are coherent with the inverse relationship observed for all biopolymers between volumetric compressibility and hydration. It is important to note here that these volumetric properties play a fundamental role in determining functional properties of biopolymers, especially interfacial properties but also viscosimetric behavior [24-27].

It is important to recall that hydration water can be categorized into two main groups, bound and bulk water. The former corresponds to water molecules which physicochemical properties are perturbed by the presence of the solute. Meanwhile, bulk water refers to water molecules that do no interact with the solute or that interact but without changes in their physicochemical properties [28,29]. Few information regarding the hydration properties of A. gums is available. Most studies were performed only on A. *senegal* and using differential calorimetry (DSC) methods. In general, bound water around 0.6-1.2 g H_2O/ g AGP have been estimated [1,23,30,31].

One way to better understand solution properties of AGP dispersions is to change their physicochemical environment, for instance ionic strength, pH or temperature. In the present study, we choose to change mainly temperature. However, the combination of the increase of temperature and ionic strength on the intrinsic viscosity of A. *senegal* and A. *seyal*, was also studied. Thus, the main objective of this study was to determine the influence of the increase of temperature on the volumetric properties, v_s° and β_s°, structure (molar masses, polydispersity) and hydrodynamic properties (intrinsic viscosity, dynamic viscosity and hydrodynamic radius) of A. gums and HIC fractions. The volumetric properties were studied using ultrasound and density measurements. The structural properties were studied using size exclusion chromatography (HPSEC-MALS), and hydrodynamic properties were studied using viscometry techniques. In addition, the thermal stability of A. gums was followed using thermogravimetric analysis (TGA). Our results highlighted the importance of hydrostatic and hydrodynamic volumetric properties of the different types of AGPs on the functional properties of A. gums. Furthermore, a different temperature behavior of these properties was emphasized.

2. Materials and Methods

2.1. Materials

The study was done using Acacia *senegal* (lots OF 110676 and OF 152413) and Acacia *seyal* (lot OF 110724) soluble powders, donated by the Alland & Robert Company – Natural and Organic gums (Port Mort - France).

Macromolecular fractions HIC-F1, HIC-F2 and HIC-F3 of A. *senegal* (OF 152413) were obtained using Hydrophobic Interaction Chromatography (HIC) following the fractionation process described elsewhere [5,8]. The HIC-F1 and HIC-F2 fractions were diafiltrated (AKTA FLUX 6 system, GE Healthcare, Upsala, Sweden), then spray-dried (B-290 BUCHI, Labortechnik AG, Switzerland). The HIC-F3 fraction was concentrated in a rotavapor (461 BUCHI Water bath, Labortechnik AG, Switzerland) and extensively desalted by dialysis against deionized water, centrifuged (12 000 rpm, 30 min, 20°C) and freeze dried (Alpha 2-4 LSC, Bioblock Scientific, France). The freeze-drying process was controlled to avoid formation of insoluble material as noted elsewhere [5,32].

The biochemical characterization of A. gums and HIC fractions has already been discussed in a previous publication [23]. However, a summary is presented in Tables IV.1 and IV.2.

Table IV. 1. Summary of the main biochemical properties of A. gums and HIC fractions

Gum or fraction	**Ara/Gal**	**Uronic acids (%)**	**Branching degree**	**Proteins (%)**	**Minerals (%)**	**Humidity (%)**
Acacia gums						
A. *seyal*	1.4	14.1	0.6	0.8	1.4	3.3
A. *senegal*	0.8	18.8	0.8	2.2	3.4	10.7
HIC fractions						
HIC-F1	0.7	21.7	0.8	0.5	3.1	7.8
HIC-F2	1.0	16.2	0.8	6.3	1.9	7.4
HIC-F3	1.2	14.4	0.8	13.8	4.9	7.8

Table V.2. Summary of the polar, non-polar and charged amino acids present in A. gums and HIC fractions

Gum or fraction	Charged (%)	Polar (%)	Non polar (%)	Hyp + Ser (%)	Glu + Asp (%)
Acacia gums					
A. *seyal*	47.9	27.4	28.5	43.3	10.8
A. *senegal*	49.9	29.7	26.8	40.7	10.0
AGP fractions					
HIC-F1	52.0	36.4	18.8	51.2	5.7
HIC-F2	48.4	30.8	27.4	41.2	9.6
HIC-F3	45.8	28.6	31.9	29.5	13.5

All reagents used were of analytical grade from Sigma Aldrich (St. Louis, MO, USA).

2.2. Methods

2.2.1. Desalting of Acacia gums and HIC fractions

A. gums were prepared by dispersing the commercial powders of A. *senegal* and A*. seyal* (10%wt) in ultrapure deionized water (18 mΩ). Dispersions were stirred overnight and centrifuged to remove impurities and insoluble material (12 000 rpm, 30 min, 20°C). Dispersions were diafiltrated and freeze dried following the same procedures as previously explained for HIC-F1 and HIC-F2 or HIC-F3.

2.2.2. Sample preparation

A. gum samples were prepared by dispersion of the freeze dried or spray dried powder in the desired solvent and kept overnight under constant stirring to allow complete hydration. Dispersions were centrifuged to remove insoluble material (12 000 rpm, 30 min, 20°C). Dispersions were degassed to remove dissolved air (300 Ultrasonik bath, Ney, Yucaipa, CA, USA) and if needed the pH was controlled to 5 or 7, depending on the solvent used. The solvents used were water (pH 5), 0.01M sodium acetate buffer (pH 5), and 0.1M $LiNO_3$ (pH 7).

2.2.3. Density and sound velocity

Density and sound velocity of A. gums and HIC-fractions aqueous dispersions were determined simultaneously using a DSA 5000M sonodensimeter (Anton Paar, Graz, Austria). Temperature was varied from 5-70°C and was controlled by a built-in Peltier system. The sample concentration was varied from 20–70 $g.L^{-1}$ and dispersions were dialyzed against the solvent (3.5 KDa, Spectra/Pore) overnight under constant stirring, centrifuged (12 000 rpm, 20°C, 30 min) and degassed for 15 min (300 Ultrasonik bath, Ney, Yucaipa, CA, USA) to remove dissolved air (300 Ultrasonik bath, Ney, Yucaipa, CA, USA). Measurements were triplicated.

2.2.4. Capillary viscosimetry

The dynamic viscosity (η) of A. gum and HIC-fraction aqueous dispersions was determined using a capillary microviscometer LOVIS 2000M (Anton Paar, Graz, Austria). Temperature was varied from 25-50°C and was controlled by a built-in Peltier system. Measurements were performed using a glass capillary (1.59 mm of diameter) and a steel ball (1 mm of diameter). Dispersions were kept overnight under constant agitation, centrifuged (12 000 rpm, 20°C and 30 min) and degassed 15 min (300 Ultrasonik bath, Ney, Yucaipa, CA, USA) to remove dissolved air (300 Ultrasonik bath, Ney, Yucaipa, CA, USA). Measurements were at least duplicated.

2.2.5. Size Exclusion Chromatography (HPSEC) - Multi Angle Light Scattering (MALS)

A. gums and HIC fractions were characterized using a HPLC system (Shimadzu, Kyoto Japan) coupled to 4 detectors: a DAWN Heleos multi angle light scattering (Wyatt, Santa Barbara, CA, USA), an Optilab T-rEX differential refractometer (Wyatt, Santa Barbara, CA, USA), an on-line Viscostar viscometer (Santa Barbara, CA, USA) and a SPD-20A UV-Vis detector activated at 280 nm (Shimadzu, Kyoto, Japan). Molecule separation was achieved on a Shodex (OHPAK SB-G) pre-column system coupled to a 4-column system (SHODEX OHPAK SB 803 HQ, SB 804 HQ, SB 805 HQ and 806 HQ). Fractions with an important proportion of high M_w, HIC-F2, HIC-F3, were analyzed using only the

SHODEX OHPAK SB 805 HQ column, to avoid or reduce abnormal elution phenomena known to occur with hyperbranched macromolecules.

A. gum aqueous dispersions of 1 $g.L^{-1}$ were injected and eluted using 0.1 M $LiNO_3$ (0.02 % NaN_3) as a carrier. Temperature was varied from 25-45°C. Data were analyzed using the refractive index increments (dn/dc) previously obtained (Chapter III, section 4.1) and ASTRA software (version 6.1.2.84) of Wyatt Technologies (Santa Barbara, CA, USA). A. gums were analyzed considering their weight-averaged molar mass (M_w): a gum was considered to have a low molar mass if $M_w < 7.5x10^5$ $g.mol^{-1}$, to have a high molar mass if its $M_w > 7.5x10^5$ $g.mol^{-1}$ and to have supramolecular assemblies if its $M_w >$ 2-3 x 10^6 $g.mol^{-1}$ [7,9,23]

2.2.6. Thermogravimetric Analysis (TGA)

Thermal stability of A. gums and HIC fractions was studied using a TGA 2 Star System (Mettler Toledo, Schwerzenbach, Switzerland). The instrument was equipped with a high sensitivity (0.1 µg) ultra-micro balance (Mettler Toledo, Schwerzenbach, Switzerland). Samples were analyzed in powder form (initial humidity around 8-10%wt) using an alumina pan. Temperature was increased from 25–300°C at a constant rate of 10°C per minute. To avoid errors due to diffusion, measurements were performed in samples of 7-8 mg of A. gums and HIC fractions, under constant air flow (50 $cm^3.min^{-1}$), and duplicated.

3. Results and discussion

3.1. Thermogravimetric Analysis

In order to study changes on the physicochemical behavior of A. gums and HIC fractions when temperature is increased, we first studied their thermal stability in their powder form. Since A. gums and HIC powders have already been subjected to a dehydration process (either spray or freeze drying), the remaining water in the powders corresponds only to firmly bound water. Therefore, it will provide an indication of how this water category behaves as temperature is increased.

The thermally induced changes of A. *senegal*, A. *seyal* and HIC fractions of the former were studied by thermogravimetric analysis (TGA) in the range of temperature from 25 to 300°C. The results are presented in Figure IV.2. Thermal changes affecting A. gums and HIC fractions followed a two-stage process. The first stage was seen between 25 and 150°C, and the second stage was seen from 150 to 300°C. The first stage is a dehydration usually attributed to the loss of bound water [33-36]. Meanwhile, the second stage is attributed to the degradation of the molecule, due to mainly to depolymerization and decomposition [33,36]. The end of the second weight loss event was at higher temperatures and was not recorded in the experiment. However, weight losses of more than 50% were seen at 300°C. Literature shows similar thermal behavior of A. gums [33,35,37,38] and other polysaccharides (e.g. cashew gum, tragancanth gum, xantan gum, sodium alginate, and others) [35,37,39]. Furthermore, for the first transition stage, a temperature range of 33 - 100°C was reported for A. gums by Mothé and Rao (2000)[37] and Zohuriaan et al (2004) [35], from 20-200°C by Cozic et al (2009)[33], and from 30–150°C by Daoub et al (2014)[38]. Regarding the second event, transition temperatures of 252°C and 260°C were reported, respectively, by Mothé and Rao (2004)[37] and Daoub et al (2014)[38], in the range 223-378°C by Zohuriaan et al (2004) [35] and from 200-600°C by Cozic et al (2009)[33]. Therefore, the temperature ranges corresponding to the first and second mass loss events we found were previously observed for Acacia gums.

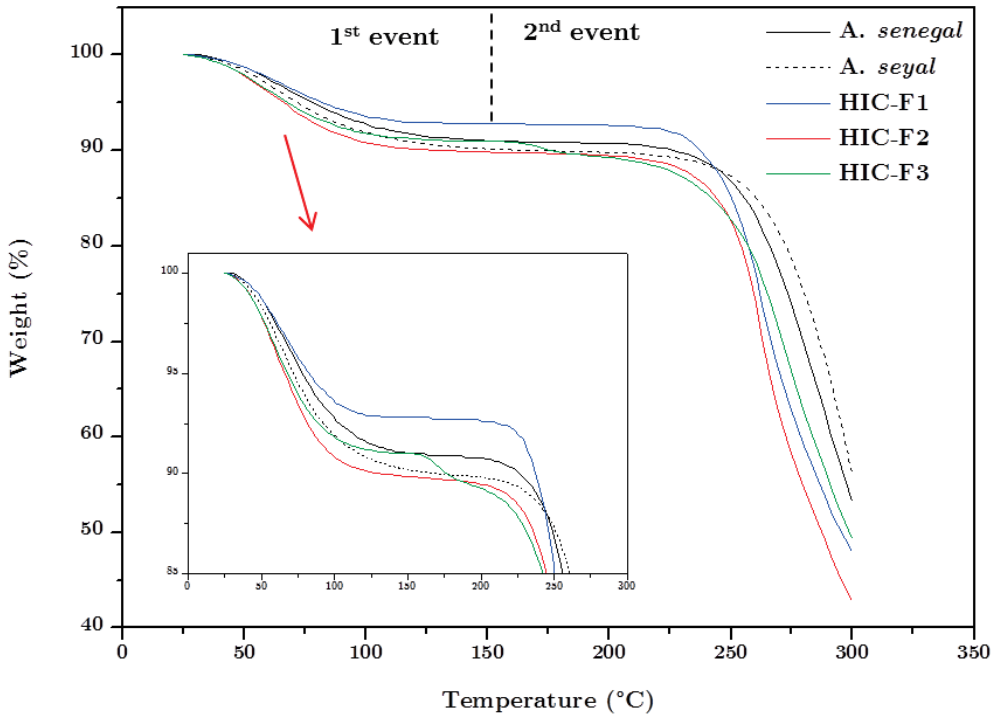

Figure IV.1 TG curves of A. *senegal* (black line), A. *seyal* (dash black line), HIC-F1 (blue line), HIC-F2 (red line) and HIC-F3 (green line). Measurements were performed using 7-8 mg of A. gum powders under air at a heating rate of 10°C.min^{-1}. Inset highlights the first dehydration stage to show the double transition displayed by the HIC-F3 fraction.

Regarding in more details Figure IV.1, we can observed different thermal behaviors among A. gums and HIC fractions. For instance, A. *senegal* gum lost less water than A. *seyal*. The HIC-F1 fraction experienced as well a smaller weight loss while the dehydration of HIC-F2 and HIC-F3 fractions was stronger. Interestingly, the latter showed an additional transition temperature in the 150-180°C range.

To gain more insight about these thermal behaviors, we analyzed the differential thermogravimetric (DTG) curves of A. *senegal*, A. *seyal* and HIC fractions, which are presented in Figure IV.2. A large peak, with a maximum in the range between 60 and 70°C was seen for all AGP systems. As noted above, the HIC-F3 fraction showed however a second smaller peak with a maximum around 170°C. The first peak corresponded to the loss of bound water, which can be associated to the polysaccharide part of AGPs, which is

dominant for all systems. The origin of the second peak observed with HIC-F3 is less clear. It may correspond to an additional dehydration event or alternatively to the second stage, the degradation of the molecule. Literature suggests that water vaporization occurs at temperatures up to 300°C (e.g. gelatin, xanthan, guar, PO seeds, chitosan) [40-44]. In addition, depending on how tight bound water is attached to the solute molecule, dehydration can occur in two or more stages [36]. Furthermore, thermal studies done in proteins of gluten have shown transition temperatures around 175-211°C [45,46]. On the other hand, studies performed with alginate have suggested temperatures of 178-190°C as the degradation temperature of carboxylic groups [47]. Hence, it is possible that the extra peak seen in HIC-F3 is the result of evaporation of water bound to the protein moiety not removed in the first event and/or the degradation of the carboxylic groups.

The onset, offset, transition temperatures and amount of loss bound water of A. gums and HIC fractions of A. *senegal* obtained from the DTG curves (Figure IV.2) are presented in Table IV.3. The onset and offset temperatures represent the range of temperature in which the thermal event is taking place. For this study, the onset temperature, T_{on}, has been defined as the temperature at which at least 0.1% of the mass is lost and the offset temperature, T_{off}, as the temperature at which less than 0.1% of the mass is lost. The first and second transition temperatures (T_1 and T_2, respectively) are the temperatures corresponding to the peaks on the DTG curve. The amount of bound water, W_b, was calculated using the following expression:

$$W_b = \frac{W_{lost}}{W_o} \qquad \text{(IV.1)}$$

where W_{lost} is the weight lost at the offset temperature and W_o is the initial weight of the sample.

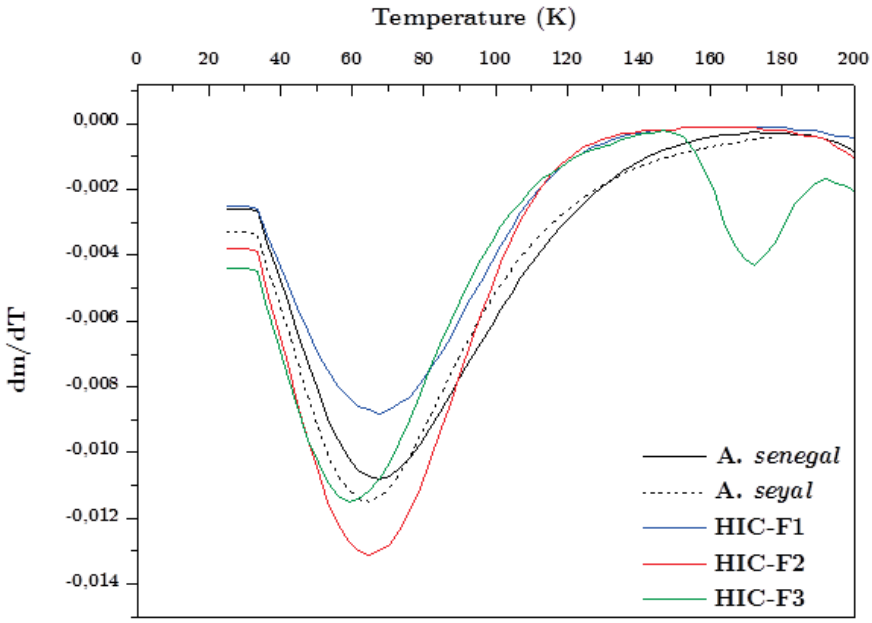

Figure IV.2. DTG curves of A. *senegal* (black solid line), A. *seyal* (black dash line), HIC-F1 (blue line), HIC-F2 (red line) and HIC-F3 (green line). Measurements were performed using 7-8 mg of A. gums powders under air at heating rate of 10°C.min^{-1}.

For all gums, the T_{on} was found at 28°C. Meanwhile the offset temperature varied for each gum. A. *senegal* showed a higher T_{off} than A. *seyal* (146 and 140°C, respectively). However, the three fractions, HIC-F1, HIC-F2 and HIC-F3, displayed a same smaller T_{off} (around 130°C). The large difference in T_{off} between A. *senegal* and the three AGP fractions suggests that fractionation of AGP, involving drying, produced more heat sensitive biopolymers. The origin of this "extra" heat sensitivity is not a different polydispersity as shown by HPSEC-MALS measurements (see section 3.2), and remains unclear. It could be due to a weaker polarity of some chemical groups, conformational changes of AGP or AGP aggregation.

For both A. gums, the loss of bound water was identical at around 0.10 g H_2O/g AGP. Thus, all the water present in the powders was lost. A. *senegal* showed a higher first transition temperature, T_1, than A. *seyal* (69 and 64°C, respectively). The larger T_1 of the former suggests a stronger strength of interaction of AGP with water. Its larger proportion of uronic acids compared to A. *seyal* (19 and 14 % w/w, respectively) and higher number

of charges could explain the different T_1. On the other hand, DSC studies performed on linear hyperbranched and dendrimer molecules have shown that transition temperatures increased with the branching degree of the molecule [48,49]. The branching degree of A. gums was obtained from the number of branched and linear units with two glycosidic linkages [18,23]. A. *senegal* presented a higher branching degree than A. *seyal* (0.78 and 0.54, respectively), therefore possibly contributing to the lower T_1 found for A. *seyal*.

Regarding HIC-fractions, HIC-F1 showed a higher first transition temperature (70°C) as compared to HIC-F2 and HIC-F3 (65 and 60°C, respectively). The higher transition temperature of HIC-F1 suggests a higher water affinity and presence of stronger hydrogen bonds. Since in addition, this fraction is largely (about 85%) the most concentrated fraction in A. *senegal*, this is mainly responsible for the high sorption ability of this gum. The lower transition temperatures of HIC-F2 and HIC-F3 suggest the presence of weaker hydrogen bonds, probably due to the larger protein concentration of these fractions, therefore allowing water molecules to escape easily. Interestingly, the results are comparable to the volumetric properties of the HIC-fractions, since due to its higher protein content, the HIC-F3 fraction has the lower hydration number (0.54 g H_2O/g AGP) as compared to HIC-F1 and HIC-F2 (0.85 and 0.68 g H_2O/g AGP, respectively) (See Chapter IV). TGA results then confirmed that polarity of fractions increased in the order HIC-F1 > HIC-F2 > HIC-F3, in relation with the order of elution during HIC experiments. Additionally, this suggested that TGA experiments on powders can be used to predict the polarity behavior of AGP.

Table IV. 3. Onset, Offset, Transition temperatures and weight loss of A. gums the HIC fractions of A. *senegal*. Measurements were performed in A. gums powders under constant air flow at a heating rate of 10°C.min^{-1}

Gum or fraction	Onset Temperature (°C)	Offset temperature (°C)	Transition T_1 (°C)	Weight loss at T_1 (g H_2O/g AGP)	Transition T_2 (°C)	Weight loss at T_2 (g H_2O/g AGP)
A. *seyal*	30.7 ± 0.0	145.9 ± 1.6	64.2 ± 1.1	0.10 ± 0.08		
A. *senegal*	30.7 ± 0.0	140.2 ± 5.9	68.7 ± 1.6	0.09 ± 0.02		
HIC-F1	30.7 ± 0.0	127.0 ± 2.8	70.3 ± 0.0	0.08 ± 0.04		
HIC-F2	30.7 ± 0.0	124.1 ± 4.9	64.6 ± 0.1	0.09 ± 0.07		
HIC-F3	30.7 ± 0.0	127.9 ± 3.3	59.9 ± 1.3	0.09 ± 0.01	171.3 ± 1.03	0.12 ± 0.2

3.2. Structural and hydrodynamic properties as determined by HPSEC-MALS

3.2.1. Basic structural and hydrodynamic properties

The effect of the temperature on the main structural properties, i.e. weight-average (M_w) and number-average (M_n) molar masses, polydispersity index (M_w/M_n), intrinsic viscosity ($[\eta]$), hydrodynamic (R_H) and gyration (R_G) radii, and percentage of molecules with $M_w < 7.5x10^5$ g.mol^{-1}, of A. gums and HIC fractions is presented in Table IV.4. It is important to note that due to the sensitivity of the multi-angle laser light scattering detector, R_G was calculated only for macromolecules with a R_G higher than 10 nm. This is particularly important for gums with low M_w, for instance HIC-F1, where only 9–13 % of molecules were taken into account.

At 25°C, as previously discussed (see Chapter II), A. *seyal* displayed a higher molar mass than A. *senegal* (Table IV.4). However, A. *senegal* showed higher polydispersity, higher content of molecules with $M_w>7.5x10^5$ g.mol^{-1}, intrinsic viscosity, hydrodynamic and gyration radii. Among the HIC fractions, HIC-F1 showed lower M_w, and lower R_H and R_G than HIC-F2 and HIC-F3. On the other hand, HIC-F2 presented a higher intrinsic viscosity and higher proportion of molecules with $M_w>7.5x10^5$ g.mol^{-1} than HIC-F1 and HIC-F3. Similar structural and hydrodynamic parameters were previously described for A. gums and HIC fractions in several studies [5-7,22].

The structural properties of all A. gums and HIC fractions remained practically constant over the studied temperature range, 25-45°C. When changes were detected, they displayed a variation of less than 10%. For instance, a small decrease of the intrinsic viscosity of A. *seyal*, HIC-F2 and HIC-F3 was observed. This decrease (54.7 mL.g^{-1} at 25°C to 50.5 mL.g^{-1} at 45°C) was coupled to an increase of R_H (23 nm at 25°C to 31 nm at 45°C) for HIC-F3, mainly due to a small increase in M_w ($16.4x10^5$ g.mol^{-1} at 25°C to $17.1x10^5$ g.mol^{-1} at 45°C) and polydispersity (1.9 at 25°C to 2.1 at 45°C). Then, the obvious conclusion of this study by HPSEC-MALS was that temperature between 25 and 45°C marginally modified the structure of A. gums and HIC fractions.

Table IV.4. Temperature dependence of the weight-averaged (M_w) and number-averaged (M_n) molar masses, polydispersity index (M_w/M_n), percentage of molecules with $M_w<7.5x10^5$ g.mol^{-1}, intrinsic viscosity ([η]), hydrodynamic (R_H) and gyration (R_G) radii of A. gums and HIC fractions. Data were obtained using HPSEC-MALS in 0.1 M $LiNO_3$ solvent.

	Gum or fraction	25°C	30 °C	35°C	40°C	45°C
M_w (x10^{-5} g.mol^{-1})	A. *seyal*	7.0	7.3	6.8	7.4	7.4
	A. *senegal*	6.8	6.5	6.6	6.6	6.5
	HIC-F1	3.5	3.6	3.4	3.5	3.4
	HIC-F2	15.0	14.5	14.6	14.6	15.0
	HIC-F3	16.4	16.2	16.8	17.6	17.1
M_n (x10^{-5} g.mol^{-1})	A. *seyal*	4.5	4.4	4.5	4.3	4.3
	A. *senegal*	3.3	3.3	3.2	3.3	3.1
	HIC-F1	2.4	2.5	2.3	2.4	2.2
	HIC-F2	11.7	10.9	11.6	11.0	10.8
	HIC-F3	9.0	9.0	9.6	9.7	8.0
M_w/M_n	A. *seyal*	1.5	1.7	1.5	1.7	1.7
	A. *senegal*	2.0	2.0	2.1	2.0	2.1
	HIC-F1	1.4	1.4	1.5	1.5	1.6
	HIC-F2	1.3	1.3	1.3	1.3	1.4
	HIC-F3	1.9	1.8	1.8	1.8	2.1
$M_w<7.5x10^5$ g.mol^{-1} (%)	A. *seyal*	80	78	80	79	79
	A. *senegal*	86	85	85	84	85
	HIC-F1	93	93	93	92	92
	HIC-F2	12	16	13	16	17
	HIC-F3	33	32	30	29	31
[η] (mL.g^{-1})	A. *seyal*	23.8	22.7	23.6	22.7	22.3
	A. *senegal*	29.8	28.7	29.8	30.8	30.2
	HIC-F1	22.1	22.9	22.6	22.7	22.5
	HIC-F2	67.3	62.7	64.2	62.7	64.0
	HIC-F3	54.7	55.7	55.9	52.8	50.7
R_H (nm)	A. *seyal*	13	13	13	13	13
	A. *senegal*	13	13	13	14	13
	HIC-F1	10	11	10	10	10
	HIC-F2	24	24	24	24	24
	HIC-F3	23	23	23	26	31
R_G (nm)	A. *seyal*	14 (16%)	14 (26%)	14 (19%)	14 (22%)	14 (22%)
	A. *senegal*	21 (46%)	21 (48%)	22 (44%)	22 (45%)	21 (43%)
	HIC-F1	13 (13%)	14 (10%)	15 (9%)	14 (10%)	14 (11%)
	HIC-F2	27 (73%)	28 (66%)	27 (76%)	27 (76%)	27 (75%)
	HIC-F3	32 (43%)	33 (42%)	33 (50%)	32 (50%)	32 (50%)

*Dispersions were prepared in deionized water at 1 g.L^{-1} and eluted in 0.1 M ($LiNO_3$). Values into parenthesis correspond to the percentage of analyzed molecules.

3.2.2. Conformational analysis

The influence of temperature from 25 to 45°C on the conformation of A. gums and HIC fractions in solution was studied using the power law relationships between the intrinsic viscosity or gyration radius and the molar mass as the following[50-52]:

$$[\eta]_w = K_\eta M_w{}^{a_\eta} \quad \text{(IV.2)}$$

$$R_G = K_G M_w{}^{a_G} \quad \text{(IV.3)}$$

Where a_η and a_G are known as the hydrodynamic and static coefficients and K_η and K_G are the corresponding constants. They depend on the structural conformation, molar mass, anisotropy, temperature and solute-solvent interactions. In general, classical values of a_η and a_G are 0 and 0.33 for a sphere, between 0.5-0.8 and 0.5-0.6 for a random coil and 1.8 and 1 for rods [6,52-54].

The a_η and a_G coefficients of A. gums and HIC fractions from A. *senegal* for temperature ranging from 25°C to 45°C are presented in Tables IV.5 and IV.6. The a_η and a_G values of A. gums and HIC fractions were constant reflecting the stable conformation of AGPs in this range of temperature (25°C to 45°C). The a_η coefficient of A. gums and HIC fractions varied over the M_w range (Table IV.5) suggesting the presence of more than one conformation. A. *seyal* was characterized by two slopes with a_η values of 0.3 for AGPs showing a M_w lower than 10^6 g.mol^{-1} (around 95% of AGPs of whole gum) and 0.4-0.5 for higher M_w AGPs ($M_w > 10^6$ g.mol^{-1} corresponding to around 5% of AGPs) (Table IV.5). A. *senegal* displayed three a_η coefficients according to the M_w, with values of 0.4-0.5 for AGPs with M_w ranging from 1.5–5.0 x10^5 g.mol^{-1}, 0.7-0.8 for AGPs with M_w ranging from 5-12 x10^5 g.mol^{-1} and 0.5-0.6 for AGPs with M_w higher than 12x10^5 g.mol^{-1} (Table IV.5). These values were in accordance with those previously reported for A. *senegal* (0.4 - 0.8)[10,11,55-58] and A. *seyal* (0.3-0.4) [55]. A. *seyal* presented lower a_η value than A. *senegal* reflecting a less anisotropic and more compact structure as previously described by Lopez-Torrez et al. (2015)[55]. The three M_w ranges observed for A. *senegal* were also identified with its HIC fractions (Table IV.5). For M_w<5.0x10^5 g.mol^{-1}, AGPs displayed an a_η coefficient of 0.4-0.5 in agreement with the hyperbranched, dense and compact structure

of low M_w AGPs described by Sanchez et al. (2008)[22]. In the second M_w range ($5.0<M_w<12x10^5$ g.mol^{-1}), a_η coefficients between 0.4 and 1 were determined. Hence, these AGPs presented certainly a more anisotropic and elongated conformation than low M_w AGPs. AGPs with M_w upper than $12x10^5$ g.mol^{-1} showed a_η coefficient ranging from 0.3 to 0.5 (Table IV.5) highlighting a more isotropic conformation of these molecules. As previously discussed in chapter III, the low a_η coefficient in this third M_w range could be attributed to the self-assembly properties of the AGPs and the presence of aggregates that are known to decrease the a_η coefficient, especially for hyperbranched polymers [59,60].

Table IV.5. Temperature dependence of the Kuhn-Mark-Houwink-Sakurada coefficient (a_η) of A. gums and HIC fractions.

M_w range ($x10^5$ g.mol^{-1})	Gum or fraction	25 °C	30 °C	35°C	40°C	45°C
1.5 - 5.0	A. *senegal*	0.5	0.4	0.4	0.5	0.5
	HIC-F1	0.4	0.4	0.4	0.4	0.4
2.0 – 10.0	A. *seyal*	0.3	0.3	0.3	0.3	0.3
5.0 - 12.0	A. *senegal*	0.7	0.7	0.8	0.7	0.7
	HIC-F1	0.6	0.5	0.5	0.6	0.4
	HIC-F2	1.0	0.9	0.9	0.9	1.0
	HIC-F3	0.7	0.7	0.7	0.8	0.7
12.0 - 50.0	A. *senegal*	0.5	0.6	0.5	0.5	0.5
	HIC-F2	0.3	0.4	0.3	0.3	0.4
	HIC-F3	0.4	0.4	0.5	0.5	0.5
10.0 – 25.0	A. *seyal*	0.5	0.5	0.4	0.4	0.4

The conformation of A. gums and HIC fractions from A. *senegal* according to temperature was also studied using the R_G vs. M_w conformation plots. Before to discuss the results, it is important to remind that only AGPs presenting a R_G above 10 nm were considered for this analysis (that concerned only a percentage of AGPs that varied according to the considered fraction, see Table IV.4), and that R_G, and then a_G coefficient, are greatly

influence by the presence of aggregates. For all samples, a_G coefficient was constant over the M_w studied that indicates the presence of only one kind of conformation. A. *senegal*, A. *seyal*, HIC-F1, HIC-F2 and HIC-F3 presented a_G coefficient 0.5-0.6, 0.6, 0.6-0.7, 0.5 and 0.3, respectively, in the range of temperature studied. These results are in accordance with previous studies showing a_G values of 0.3–1.2 for A. *senegal* [11,55,61,62], 0.4-0.7 for A. *seyal* [55], 0.4–0.9 for HIC-F2 [6] and 0.3–0.6 for HIC-F3. The finding of only one a_G coefficient appeared in contradiction with the results obtained via the Kuhn-Mark-Houwink-Sakurada (KMHS) plots for which several conformations were evidenced. The absence of a_G coefficient for M_w lower than $5x10^5$ $g.mol^{-1}$ was due to a R_G lower than 10 nm in this molar mass range. The difference observed for M_w upper than $5x10^5$ $g.mol^{-1}$ could be explained by the presence and the abnormal elution of AGP based aggregates that co-eluted with lower molar mass AGPs and greatly contributed to the light scattering signals. This hypothesis was evidenced by the analysis of a_G coefficient of A. *senegal* fractions. The a_G coefficient of HIC-F1, that mainly contained low molar mass AGPs and was almost devoid of aggregates, was 0.6-0.7 in 5-10 $x10^5$ $g.mol^{-1}$ molar mass range. Hence, these results confirmed the presence of elongated and more anisotropic AGPs in this molar mass range, as previously described using KMHS plots for A. *senegal*, HIC-F2 and HIC-F3 fractions. The elongated and more anisotropic AGPs also shown in HIC-F3 and HIC-F2 using KMHS plots were not evidenced using the R_G vs. M_w conformation plots, especially for HIC-F3. For these fractions, the presence of AGPs based aggregates was established for M_w upper than $12x10^5$ $g.mol^{-1}$ using the KMHS plots. Hence, the absence of a_G coefficient corresponding to elongated AGPs in the 5-10$x10^5$ $g.mol^{-1}$ molar mass range for HIC-F2 and HIC-F3 was attributed to the co-elution of aggregates that greatly contributed to the light scattering signals and inducing the decrease of a_G coefficient.

In conclusion, this study revealed that temperature marginally modified the structural parameters and conformation of AGPs in A. gums. Using the conformational coefficients (a_η and a_G) determined on HIC fractions from A. *senegal* gums, the AGPs from A. *senegal* gum can be categorized in 'small AGPs' adopting a compact and less anisotropic structure (1.5–5.0 $x10^5$ $g.mol^{-1}$), 'large AGPs' adopting more elongated and anisotropic structure (5–

12 x10^5 g.mol^{-1}) and 'AGP-based aggregates' adopting a compact structure (12–50 x10^5 g.mol^{-1}).

Table IV.6. Temperature dependence of a_G for A. gums and HIC fractions.

Gum or fraction	M_w range (x10^5 g.mol^{-1})	Temperature (°C)	a_G
A. *seyal*	5.0 – 20.0	25	0.6
		30	0.6
		35	0.6
		40	0.6
		45	0.6
A. *senegal*	5.0 – 30.0	25	0.5
		30	0.6
		35	0.6
		40	0.6
		45	0.6
HIC-F1	5.0 – 10.0	25	0.7
		30	0.7
		35	0.7
		40	0.6
		45	0.6
HIC-F2	5.0 – 40.0	25	0.5
		30	0.5
		35	0.5
		40	0.5
		45	0.5
HIC-F3	8.0 – 40.0	25	0.3
		30	0.3
		35	0.3
		40	0.3
		45	0.3

3.3. Temperature dependence of intrinsic and dynamic viscosity as determined by capillary viscometry

The main objective of the study was to explore the effect of temperature on the dynamic viscosity of A. gums and HIC fractions in diluted conditions. The dynamic viscosity, η, of A. *senegal* and A. *seyal* was measured using capillary viscometry. The temperature was varied from 25-50°C and measurements were performed in salt-free dispersions (pH 5), 0.01 M (sodium acetate buffer, pH 5) and 0.1 M (lithium nitrate buffer, pH 7) salts. However, we also first determined from viscosity data the intrinsic viscosity, $[\eta]$, and calculated hydrodynamic radii, R_H. Our purpose was to obtain these data in water but also to compare those obtained in salt solution with data obtained by HPSEC-MALS. In the latter experiment, gum dispersions are ultra diluted and molecules are filtered and can adsorbed onto column gels, which can impact the measured parameters.

3.3.1. Intrinsic viscosity and hydrodynamic radius

The intrinsic viscosity, $[\eta]$, is defined as the hydrodynamic volume (V_H) of a molecule in a dispersion, measured at infinite dilution [52,63,64]. It can be obtained from extrapolation of the reduced viscosity:

$$[\eta] = \lim_{C\to 0} \eta_{red} = \lim_{C\to 0} \frac{\eta - \eta_o}{\eta_o C} \quad \text{(IV.4)}$$

where η and η_o are the dynamic viscosities of solute and solvent ($mL.g^{-1}$) and C is the concentration of solute ($g.mL^{-1}$).

As already explained in the previous chapter (section 4.3), the intrinsic viscosity of A. gums in salt-free dispersions is influenced by two main phenomena, electrostatic repulsion due to the electrical double layer present at the surface of AGPs (polyelectrolyte effect) and adsorption of macromolecules on the glass capillary wall. As a consequence of the polyelectrolyte effect, the effective hydrodynamic volume of the polymer chain is increased [65,66], then the measured viscosity. The adsorption onto the capillary glass wall is also able to impact the measured viscosity due to a reduction of the internal diameter of the

capillary as the product is adsorbed [67-69]. Finally, experiments performed at 25 °C have shown that adsorption was especially important in fractions with high protein content and containing AGP-based aggregates, which are present in salt-free dispersions (for more information, please refer to chapter III, section 4.3.1). Then, in latter, [η] was calculated using the equation proposed by Yang (2012) [67]:

$$\frac{\eta_{sp}}{C} = \frac{[1+[\eta]\,C]\left[1+\left(k\,C/C_a+C\right)\right]-1}{C} \quad \text{(IV.5)}$$

where η_{sp} is the specific viscosity of the dispersion, C_a is the concentration where half of the available sites in the capillary wall are occupied and k is a constant that describes the degree of adsorption of the gum in the capillary wall (if $k > 0$, the gum is adsorbed; if $k<0$, the gum is expelled from the capillary wall inducing slipping effects).

On the other hand, in dispersions prepared in solvents with 0.01 M (sodium acetate) and 0.1 M ($LiNO_3$) ionic strength, it was assumed that the predominant phenomenon was the polyelectrolyte effect. Since salt was added to the dispersion, the charges present were screened. Then, [η] was measured from the initial slope of the reduced viscosity, η_{red}, in function of the concentration [63,70]. The intrinsic viscosities obtained are presented in Figure IV.3.

At all temperatures and ionic strengths studied, A. *senegal* presented a higher intrinsic viscosity [η] than A. *seyal*. This result is in good agreement with the different composition (lower polarity), branching (lower branching index) (Tables IV.1 and IV.2) and structural conformation (more compact) of the latter [17,55]. We observed that intrinsic viscosities obtained by viscometry were 10-15% lower than values obtained using HPSEC-MALS. This difference can be due to the increase adsorption of molecules onto the thinner walls of the differential capillary viscosimetric detector, or alternatively to AGP aggregation in highly dilute conditions. For both A. gums, [η] decreased with the increase of the ionic strength. A first important remark is that the decrease is not due to the different pH of buffers since the viscosity of A. gums is practically constant between pH 5 and 7 [1]. More consistently, this behavior can be explained by the screening of charges present on the molecule as salt is added (polyelectrolyte behavior) [71-74]. It can be noted that 0.01 M of

salt is sufficient to strongly decrease the viscosity of gum dispersions, in line with their weak polyelectrolyte characteristics. The effect of the screening of charges on the hydrodynamic properties and conformation has been extensively discussed in the previous chapter (section 4.3.1). Hence, only the temperature effect will be discussed in the following.

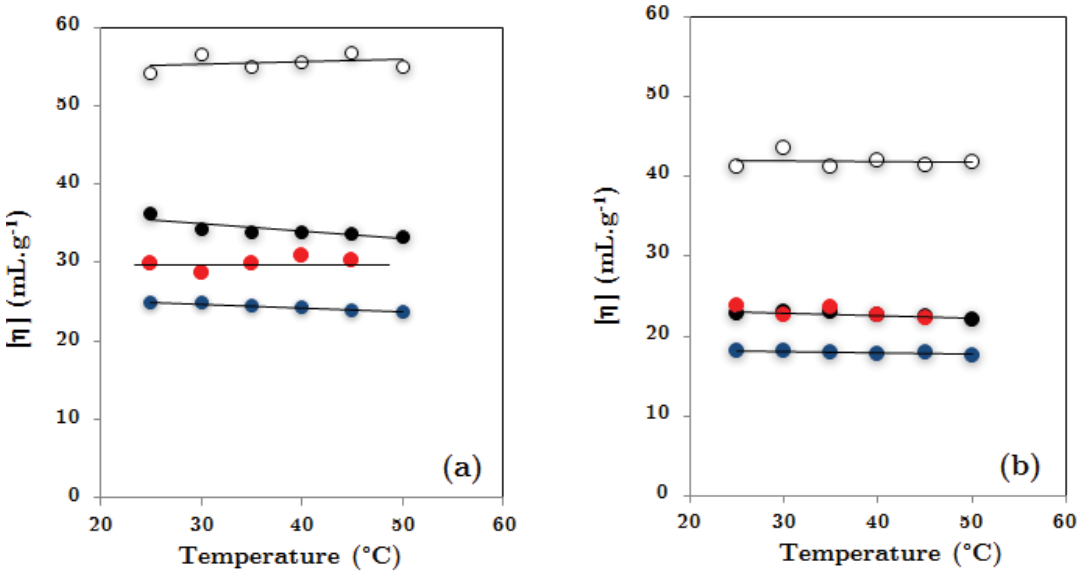

Figure IV.3. Dependence of the intrinsic viscosity ([η]) with temperature of A. *senegal* (a) and A. *seyal* (b) measured in: water (white), sodium acetate buffer 0.01M (black), and lithium nitrate 0.1 M (blue). Data obtained in lithium nitrate 0.1 M using differential capillary viscometric detector in HPSEC-MALS are also shown (red).

The increase of temperature did not have an important impact on the intrinsic viscosities of A. *senegal* and A. *seyal* measured in salt-free dispersions (Figure IV.5). Meanwhile, a small decrease (<10%) was seen when the ionic strength was increased. Small changes in the hydrodynamic volume (V_H), thus the intrinsic viscosity, with the increasing temperature have been referred in literature as a typical polyelectrolyte behavior [67,69]. On one hand, it has been reported that [η] of flexible polymers are temperature independent in good solvents where their chains are extended [75,76], like for instance xanthan (in the range 20-80°C), sodium alginate [67,69], κ-carrageenan and sodium

carboxymethyl cellulose (CMC) [77]. As well, it has been suggested that hyperbranching plays also an important role by stabilizing the macromolecule structure when temperature is applied [75]. For instance, the hydrodynamic volume of stiff hyperbranched β-glucan did not change at temperatures up to 120°C [78]. On the other hand, a decrease of intrinsic viscosity with the temperature was observed for hyperbranched polyglycerols [79]. It is then difficult at present to draw a general thermal behavior of hyperbranched macromolecules since it must depend on the chemical composition and architecture of molecules, especially the branching degree and the extent of intramolecular interactions. Although our results are consistent with a number of polyelectrolyte and hyperbranched biopolymer behaviors, it contradicts the findings of Masuelli (2013) [56]. In the same temperature range (25-50°C) and using deionized water, this author found a 30% reduction of the intrinsic viscosity of A. *senegal*. The difference in the results can be explained since in the study of Masuelli, i) adsorption of gum onto capillary walls was not taken into consideration, ii) [η] was obtained using the Hugging's equation which is not well suited for describing the behavior of polyelectrolytes, especially in water where the polyelectrolyte effect and presence of aggregates play a more important role (Chapter III, section 4.3.1).

The equivalent sphere hydrodynamic radius, R_η, of A. *senegal* and A. *seyal* was obtained from the intrinsic viscosity, [η], using the following equation:

$$R_\eta = \left\{[\eta]\frac{3}{10\,\pi}\left(\frac{M_v}{N_A}\right)\right\}^{\frac{1}{3}} \qquad \text{(IV.6)}$$

where M_v is the volume-averaged molar mass ($g.mol^{-1}$) and N_A is the Avogadro's number ($6.022x10^{23}$ $molecules.mol^{-1}$). The results are presented in Table IV.7.

With all temperatures and ionic strengths studied, A. *senegal* presented a close but systematically higher R_η than A. *seyal*. Reported hydrodynamic radius of 11-16 nm and 17 nm were found for A. *senegal* [5,8,13] and A. *seyal* [13], respectively. As expected, the R_η of both A. gums decreased by about 25% with the increase of the ionic strength. In addition, the increase of temperature did not change the R_η of A. gums, as found using HPSEC-MALS (see Table IV.4).

Table IV.7. Sphere equivalent hydrodynamic radius (R_η, nm) of A. *senegal* and A. *seyal* in the temperature range of 25-50°C. Measurements were performed using capillary viscometry. Dispersions were prepared in deionized water, sodium acetate buffer (0.01 M) and lithium nitrate (0.1 M).

Gum or fraction	Temperature (°C)	Ionic Strength (M)		
		0	0.01	0.1
A. *senegal*	25	16	14	13
	30	17	14	13
	35	17	14	13
	40	17	14	13
	45	17	14	13
	50	17	14	12
A. *seyal*	25	15	13	12
	30	16	13	12
	35	16	13	12
	40	16	13	12
	45	16	13	12
	50	16	13	12

3.3.2. Dynamic viscosity and flow activation energy

In the temperature range of 25–50°C, as expected, the viscosity of both gums decreased with the increasing temperature. As well, the increase of the ionic strength caused a reduction of the viscosity. The same behavior was seen up to gum concentrations of 20 $g.L^{-1}$. The decrease of viscosity with temperature can be explained by a decrease of solute-solvent interactions when temperature is increased [80]. Meanwhile, the decrease of viscosity with the ionic strength can be explained as the result of neutralization of charges present in the molecule as salt is added [71], as discussed above. For all ionic strengths and concentrations studied, the logarithm of the viscosity showed a linear relation with the inverse of the temperature, indicating that no conformational changes or order-disorder transition occurred in the selected temperature range. However, only the curves corresponding to 5 $g.L^{-1}$ dispersion of A. *senegal* and A. *seyal* are shown in Figure IV.4.

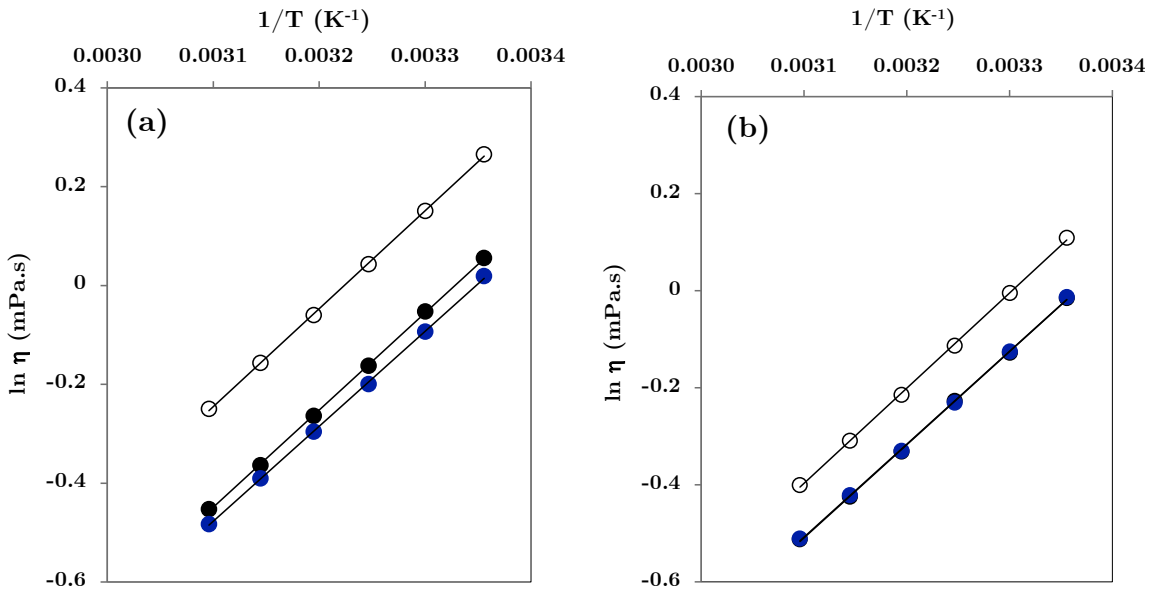

Figure IV. 4. Representation of the logarithm of the dynamic viscosity in function of the inverse of the temperature of a 5 g.L^{-1} dispersion of A. *senegal* (a) and A. *seyal* (b). Measurements were done in deionized water (white), 0.1 M sodium acetate (black) and 0.1 M lithium nitrate (blue).

This linearity is generally associated to a reduced range of temperature and concentrations [81]. However, by using the linear portion of this curve, the flow activation energy can be determined through the following relation [82,83]:

$$\eta = A \exp\left(\frac{E_a}{RT}\right) \quad \text{(IV.7)}$$

where E_a (kJ.mol^{-1}) is the flow activation energy, A (dimensionless) is the pre exponential factor (independent from temperature), R (8.31 kJ.K^{-1}mol^{-1}) is the ideal gas constant and T (K) is the absolute temperature. The flow activation energy is defined as the energy needed for moving a molecule from a static position to a new position induced by flow or the energy required by a molecule to escape the influence of its neighboring molecules [84,85]. For polymers, this energy is related to both attractive forces between the molecule and the solvent and entropic considerations. It then depends on the nature of the solvent (quality), intramolecular interactions, branching and rigidity of the polymer branches and backbone [83,86]. Its value depends on the thermodynamic and hydrodynamic parameters or structural changes occurring as the temperature is raised [57].

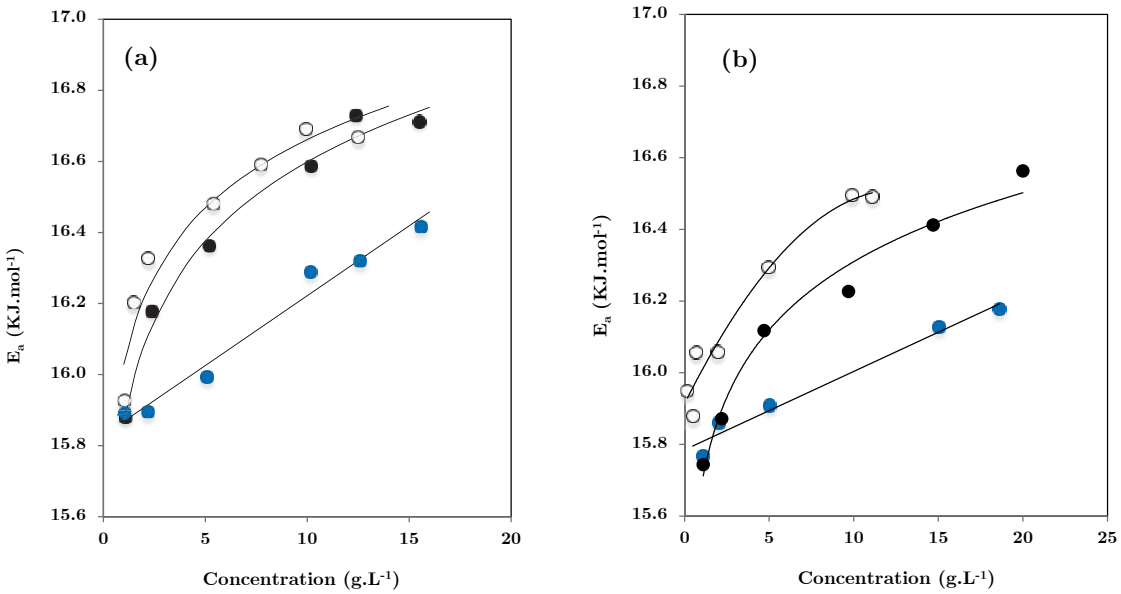

Figure IV.5. Flow activation energy (E_a) as a function of the concentration of A. *senegal* (a) and A. *seyal* (b) measured in: water (white), sodium acetate buffer 0.01M (black), and lithium nitrate 0.1 M (blue). E_a was obtained using the Arrhenius form equation (Eq. IV.7). Measurements were performed in the temperature range of 25-50°C.

For both gums, the flow activation energy increased with gum concentration and decreased with the increase of the ionic strength of the solvent (Figure IV.5). E_a values were low and in the same range (15.8-16.8 kJ.mol^{-1}) than that found previously with Acacia gum (15 kJ.mol^{-1}, then the same value than water) [87] or other exudate gums (15.9-17.2 kJ.mol^{-1}) [88]. Low E_a values of flow indicate few inter- and intra- interactions between polysaccharide and/or protein chains in the concentration range investigated.

Interestingly, E_a values obtained in deionized water and sodium acetate buffer (0.01 M) showed a non-linear relationship with the concentration, essentially below a gum concentration of 5 g.L^{-1}. Meanwhile, the ones obtained in lithium nitrate (0.1 M) displayed a linear relationship. The form of the curve depends on the structure of the polymer and its interactions with the solute [86]. A linear relationship indicates a Newtonian viscosity dependence with the temperature [86] but also that there is only one type of rheological unit involved in gum flow [89]. On the other hand, the non-linear concave downward profile indicated that more than one type of rheological unit was involved in gum flow, or

in other words than a concentration dependent dispersion structure prevailed. An increased effective hydrodynamic volume of AGP species in highly diluted conditions (< 5 g.L^{-1}) and low ionic strength, possibly due to AGP aggregates, were detected by DLS measurements (Chapter III, section 4.4.1), and this could be partly at the origin of the non-linear behavior.

These results showed clearly an effect of charges since at lower ionic strengths, biopolymer-water interactions are more important. Thus, a higher amount of energy is necessary to move the molecules. In addition, A. s*eyal* showed lower values E_a than A. *senegal*, which might be explained by its less hydrophilic nature (See Tables IV.1 and IV.2), but also its lower branching degree, more compact structure, and lower charge content (both glucuronic acids and charged amino acids). In addition, E_a values are sensitive to the flexibility of the polymer. Then, a higher E_a corresponds to lower chain flexibility [86]. Using acoustic methods we were able to determine that A. *senegal* has a higher flexibility than A. *seyal* as evidenced by its higher values of partial specific volume and adiabatic compressibility [23]. Therefore, the flow activation energy results are also quite well correlated with volumetric results.

3.4. Effect of temperature on volumetric (hydrostatic) properties

3.4.1. Basic theoretical aspects

The main volumetric properties (hydrostatic) are the partial specific volume, ($v_s°$, mL.g^{-1}) and the partial specific adiabatic compressibility coefficient ($\beta_s°$, Pa^{-1}). These properties can be related to hydration and flexibility of the molecule [90]. Then, they can be used to access important functional properties of Acacia gums (e.g. interfacial properties). They have already been extensively described in Chapter II (see section 2.3), however a summary of the main concepts is presented in the following.

The partial specific volume is defined as the change in the volume of the system due to the addition of a small quantity of solute [91-93]. It can be obtained from measurements of density and sound velocity, using the expression:

$$v_s^\circ = \frac{1}{\rho_0} \lim_{c \to 0} \frac{\rho - \rho_o}{C} \quad \text{(IV.8)}$$

where ρ_o and ρ are the densities of the solvent and dispersion ($g.mL^{-1}$) and C ($g.mL^{-1}$) is the concentration of the solute.

The partial specific adiabatic compressibility (k_s, $mL.g^{-1}.Pa^{-1}$) is defined as the change on the volume of the system respect to its pressure caused by the addition of a molecule of solute [93-96]. It is related to the volume of the system by the partial adiabatic coefficient ($\beta_s = K_s/V$) which can be calculated from measurements of density (ρ) and sound velocity (u) through the Newton Laplace relation:

$$\beta = \frac{1}{\rho u^2}. \quad \text{(IV.9)}$$

The partial specific adiabatic compressibility (β_s°, Pa^{-1}) coefficient can be obtained by extrapolation at zero concentration of the relationship [80]:

$$\beta^\circ_s = \left(\frac{\beta_{so}}{v_s^\circ}\right) \lim_{c \to 0} \left[\frac{{}^{\beta}/_{\beta_{so}} - \Phi}{C}\right] \quad \text{(IV.10)}$$

where β_{so} and β are the adiabatic coefficients of the solvent and dispersion and Φ is the apparent specific volume ($\Phi = (\rho\text{-}C)/\rho_o$).

Regarding the partial specific volume, v_s° can be essentially described as a sum of three main contributions, the intrinsic contribution (v_M), the thermal volume (v_T) and the interaction volume contribution (v_l) [95-97] :

$$v_s^\circ = v_M + v_T + v_l \quad \text{(IV.11)}$$

The intrinsic contribution refers to the volume of the molecule itself which is not accessible to the solvent [98]. It is constituted by the van der Waals volume and the volume of voids inside the solute molecule due to imperfect macromolecular packing [23,99-101]. The thermal volume refers to a layer of constant thickness (Δ) around the solute molecule created by the solute when the molecule is placed in the solvent [102]. Formerly, it represents the void present between the surface of the molecule and water molecules of the first hydration shell. The interaction volume contribution refers to solute-solvent interactions [23,29,101]. It is the only parameter describing the affinity of solute for the

solvent. To better understand this contribution, first we have to recall the two main types of water involved in the hydration, bulk and bound water. As already explained in the introduction, bulk water refers to water which physicochemical properties are not influenced by the presence of the solute. Meanwhile, bound water refers to water with properties are more or less perturbed by the solute depending on the strength of their interactions [28,29]. The strength depends on the type of solute chemical groups and is a function of the distance of water molecules respect to the solute [103]. Thus, theoretical layers around the solute molecule can be distinguished (known also as hydration shells). Generally, it is assumed that perturbations induced by the solute are mostly limited to the first hydration shell [29,104], which for charged molecules is around 2-3 Å [29]. However, recent studies performed on lactose and proteins using terahertz spectroscopy have found that the perturbations might extent up to 10 Å [105,106]. The interaction volume contribution represents a decrease in the solvent volume due mainly to the electrostriction effect, resulting from the hydration of charged groups [102]. Polar groups also contribute to the interaction volume but to a less extent. Mathematically, v_I it is represented by the relation:

$$v_I = n_h(V_h^o - V_o^o) \tag{IV.12}$$

where n_h is the number of water molecules in the first hydration shell, V_h° and V_o° are the partial specific volumes of water in the hydration shell and in bulk water, respectively [90]. Then, hydration of a molecule can be described by the amount of water molecules (quantity) and the strength of the solute/solvent interactions (quality of the solvent) [23].

Regarding the partial specific adiabatic compressibility, k_s°, the relationship is mainly [97,107,108]

$$k_s^\circ = k_M + n_h(k_{sh}^\circ - k_{so}^\circ)/M_w \tag{IV.13}$$

Where k_s° is the partial specific adiabatic compressibility ($cm^3.g^{-1}.Pa^{-1}$), k_M the intrinsic partial specific adiabatic compressibility, n_h the hydration number (g H_2O/g AGP), k_{sh}° and k_{so}° are the partial molar adiabatic compressibility of water in the hydration shell and bulk water, respectively.

3.4.2. Temperature effect on the partial specific volume ($v_s°$) and adiabatic compressibility coefficient ($\beta_s°$)

The dependence of the partial specific volume ($v_s°$) and partial adiabatic compressibility coefficient ($\beta_s° = k_s°/v_s°$) of A. *seyal*, A. *senegal* and HIC fractions (HIC-F1, HIC-F2 and HIC-F3) with temperature in the 5-70°C range is presented in Figure IV.6.

The $v_s°$ of all A. gums and HIC fractions increased linearly with the increasing temperature. We noted that the slope of this linear function did not depend on the gum type nor the AGP type. This increase is believed to be mainly the effect of the expansion of the thermal volume, v_T, i.e. the "empty volume" at the interface between the molecule and the solvent resulting from thermally induced mutual molecular vibrations and reorientations of the solute and the solvent [76,] [102], due in part to interfacial dehydration [39]. The expansion of voids inside molecules has also a significant but smaller effect [102]. The decrease of the solute–solvent interactions and loosening of water molecules from solvation layers, due to weakening of the hydrogen bonds with the increasing temperature, impacts marginally the observed volume increase. This major contribution of thermal volume expansion is universal and can explain that similar $v_s°$ curves were found in literature for neutral sugars [109,110], native globular proteins [90,111-115] , nucleic bases and nucleosides [108,116], amino acids [98], amino acid side chains analogues [98,112] and peptides [112]. In addition, the simulated linear increase of thermal volume with temperature in the 5-70°C temperature range for proteins [102] may explain the linear dependence of $v_s°$ that we experimentally observed.

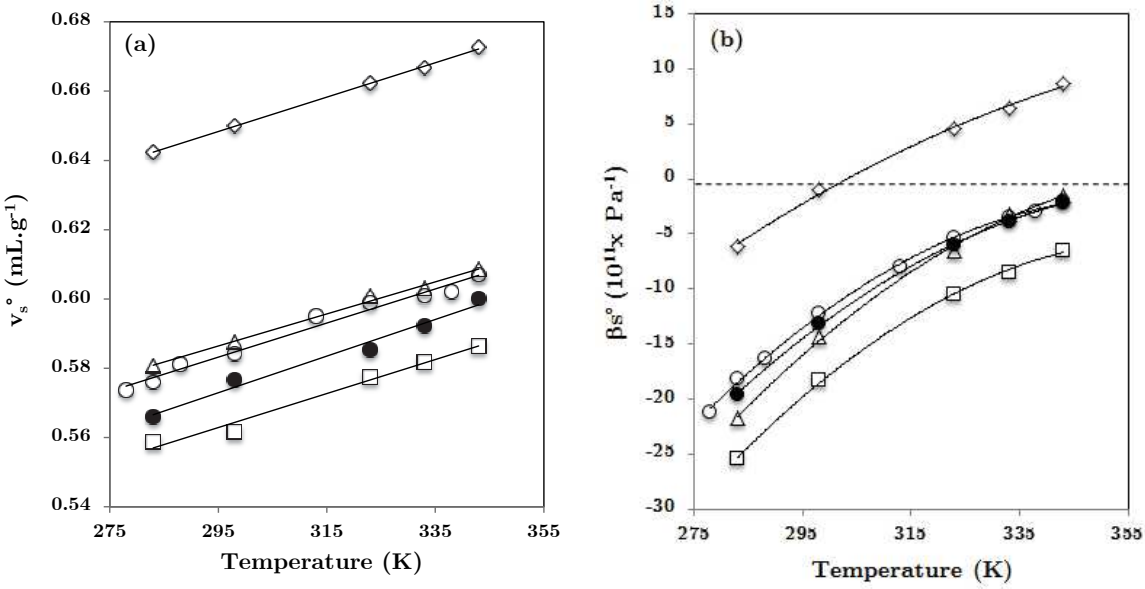

Figure IV. 6. Effect of the temperature on the partial specific volume ($v_s°$) and partial adiabatic specific compressibility coefficient ($\beta_s°$) of A. *senegal* (white circle) and its HIC-fractions: HIC-F1 (square), HIC-F2 (triangle), HIC-F3 (diamond) and A. *seyal* (black circle). All measurements were done at 25°C using sodium acetate buffer (10 mM).

In a similar way, the partial adiabatic compressibility coefficient $\beta_s°$ increased (become less negative) with the temperature. This parameter is negative because the hydration contribution overcomes the intrinsic molecular contribution, especially the contribution of inner volume fluctuations (internal voids) [117]. It is important to note here that while $v_s°$ increased following a linear function, $\beta_s°$ increased following a nonlinear function. The difference can be explained by analyzing the equation IV.13. In this equation, the intrinsic term k_M is supposed not to be affected by the temperature for globular proteins because their interior is solid like [23, 29]. For HIC fractions, we found k_M values in the range 11-16 10^{-11} Pa^{-1}, demonstrating as well their interior rigidity. Thus, we can assumed that the nonlinear temperature dependence of $\beta_s°$ is mainly determined by the hydration contribution n_h $(k_{sh}° - k_{so}°)$ or $(n_h k_{sh}° - n_h k_{so}°)$. In the case of charged molecules, the nonlinear temperature dependence of the adiabatic compressibility can be explained by the nonlinear adiabatic compressibility of bulk water ($k_{so}°$) with temperature, which exhibits a minimum around 60°C [29]. In addition, the compressibility of water molecules in the

hydration shell of charged atomic groups is strongly reduced, due to strong electrostatic fields which cause them to behave like water under high pressure[29]. The consequence of this effect is a linear increase of the water compressibility with increasing temperature. Thus, the temperature dependence of charged solutes represents a difference between a linear term corresponding to water in the hydration shell and the nonlinear term corresponding to bulk water. This results in the nonlinear temperature dependence of β_s°. This behavior was repeatedly demonstrated for globular proteins [29,115,118].

The β_s° parameter was negative on the entire temperature range for the majority of the systems, the only exception coming from the HIC-F3 fraction which β_s° became positive at temperatures close to 30°C. Positive values of β_s° are characteristic of proteins, since in these biomolecules the contribution of internal volume fluctuations overcomes the hydration contribution [96,117,119,120]. The temperature at which β_s° is 0, can be seen as an equilibrium temperature for these two effects [121] (the cavity or packing of the molecule and the solute-solvent interactions), highlighting again the low polarity of the HIC-F3 fraction.

3.4.3. Partial specific expansibility coefficient of A. gums and HIC fractions

The isobaric thermal expansibility (E) is defined as the variation on the volume of the dispersion with respect to the temperature of the system at constant pressure [108,116,122-125]. The expansibility of a dispersion depends on the expansibility of its components, thus on the volume of solute and solvent [124,126]. If we extrapolate E_T to concentrations close to 0, the volume of the system equals the partial specific volume, then the partial specific thermal expansibility (E°, $cm^3.g^{-1}.K^{-1}$) can be calculated from the derivative of the partial specific volume respect to the temperature [108,127,128]:

$$E^\circ = \left(\frac{\partial v_s^\circ}{\partial T}\right)_P \qquad \text{(IV.14)}$$

The partial specific expansibility coefficients ($E^\circ = (\partial v_s^\circ/dT)$) of A. *seyal*, A. *senegal* and the HIC fractions of the latter obtained from the slope of the curves of v_s° related to temperature (Figure IV.6) are presented in Table IV.8. The E° of A. gums and HIC-fractions is in the range of $5x10^{-4}$ $cm^3.g^{-1}.K^{-1}$. Literature shows values of E° of $5.7x10^{-4}$, 4.3

x10^{-4} $cm^3.g^{-1}.K^{-1}$ and 4.7 x10^{-4} for arabinose, galactose and glucose, respectively [110]; 3.5-5.0 x10^{-4} $cm^3.g^{-1}.K^{-1}$ for native globular proteins (e.g. lysozyme, bovine serum albumin) [90,91,107,121]; 4.3-7.7 x10^{-4} $cm^3.g^{-1}.K^{-1}$ for peptides [129]; from 4.9-7.4 x10^{-4} $cm^3.g^{-1}.K^{-1}$ for most amino acids (except proline, glycine and methionine)[98]; and, 3.6–17 x10^{-4} $cm^3.g^{-1}.K^{-1}$ for nucleic bases and nucleosides [116]. Therefore our values are close to values found for neutral sugars, the most abundant sugars in AGP from A. gums. However, it is important to remark that the E° of A. gums falls also within the native globular proteins range. This might suggest that the temperature influence on the partial specific volume does not depends greatly on the composition but on the solute-water interactions as proposed by Voloshin et al (2015) [102]. In addition, the positive values of E°, shows the overcome of the intrinsic contribution to the hydration contribution as temperature is increased. A. *seyal* showed a slightly higher value of E° as compared to A. *senegal* (5.3x10^{-4} and 4.9x10^{-4} $cm^3.g^{-1}.K^{-1}$, respectively), suggesting that temperature has a greater effect on the structure of A. *seyal* than in A. *senegal*. This result might suggest that the structure of A. *seyal* is stabilized by weaker hydrogen bonds, as temperature is increased these hydrogen bonds break and as water molecules are released due to its increased chain flexibility the molecule swells more than A. *senegal*.

Regarding the HIC fractions, HIC-F1 and HIC-F3 showed similar E° as A. *senegal* (4.90x10^{-4} and 4.96x10^{-4} $cm^3.g^{-1}.K^{-1}$, respectively). Meanwhile, HIC-F2 showed the lowest E° of all A. gums (4.63x10^{-4} $cm^3.g^{-1}.K^{-1}$). The similarity between the E° values of HIC-F1 and A. *senegal* can be explained because it is formed mainly of the HIC-F1 fraction (~80%). However, the differences between HIC-F2 and HIC-F3 might be explained by its amino acid content. Thus, the $v_s°$ of charged amino acids increases more slowly with temperature than non-polar groups [98]. Since the HIC-F3 fraction contains a higher amount of non-polar amino acids than the HIC-F2 fraction (32% and 27%, respectively), and a higher protein content, it displays a more rapid increase of $v_s°$ with the increasing temperature. Furthermore, recent studies have shown that serine is able to form hydrogen bonds even when the temperature is increased (up to 77°C) [130]. This behavior is explained by the fact that the –COOH group of this amino acid participates in the formation of hydrogen bonds with water molecules [130].

Table IV.8. Partial specific isobaric thermal expansibility coefficient (E°) of A. gums and HIC-fractions. E° values were calculated from the slope of the partial specific volume ($v_s°$) against temperature. All measurements were done at 25°C using sodium acetate buffer (0.01 M).

Gum or fraction	E° (x10^4 $cm^3.g^{-1}.K^{-1}$)
A. *seyal*	5.28
A. senegal	4.92
HIC-F1	4.90
HIC-F2	4.63
HIC-F3	4.96

4. Conclusions

In this article we studied the thermal stability behavior in dried state of A. *senegal*, A. *seyal* and the fractions of the former, HIC-F1, HIC-F2 and HIC-F3, obtained via hydrophobic interaction chromatography, and the effect of increasing temperature on their volumetric, hydrodynamic and structural properties in diluted aqueous dispersions.

Using thermogravimetric measurements, we found that A. *seyal* presented a lower transition temperature, T_1, than A. *senegal* (64 and 69°C), which can be explained due to the presence of weaker hydrogen bonds, which allows water molecules to be released easily. Regarding HIC-fractions, HIC-F1 showed a higher water affinity and stronger hydrogen bonds, as evidenced by its higher transition temperature (70°C) compared to HIC-F2 and HIC-F3 (65 and 60°C). The lowest transition temperature of HIC-F3 can be explained due to its lower polarity and weaker hydrogen bonds with water. In addition, a second transition temperature was detected for HIC-F3 at 172°C, which is likely to be due to water strongly bound to the protein moiety or degradation of carboxylic groups.

The increase of temperature did not have a noticeable impact on the hydrodynamic properties and conformation of A. gums and HIC-fractions. This behavior has been observed in other polyelectrolytes and hyperbranched macromolecules. The hyperbranched

characteristics of A. gums might have a stabilizing effect on the conformation and hydrodynamic volume. The flow activation energy E_a of A. *seyal* was lower than A. *senegal*, which is line with the lower transition temperatures obtained using thermogravimetric analysis. The concentration dependence of E_a was linear at high ionic strength but nonlinear at low ionic strength and in water, suggesting a concentration dependent structure of dispersions, especially at concentrations below 5 $g.L^{-1}$. The formation of AGP aggregates in highly diluted conditions was expected at the origin of the observed behavior.

The volumetric properties, v_s° and β_s°, of A. gums and HIC fractions increased with the increase of temperature. The increase of v_s° was linear, which is mainly due to increase of the thermal volume and expansion of internal molecular voids. On the other hand, the increase of β_s° was nonlinear, which is mainly a consequence of the weakening of water-AGP hydrogen bonds and release of water molecules in the bulk, and the difference between the linear temperature dependence of water molecules in the hydration shell and that of bulk water. The analysis of the temperature behavior of v_s° allowed the calculation of another volumetric property, the partial specific expansibility coefficient (E°). The E° of A. gums and HIC fractions was in the order of $5x10^{-4}$ $cm^3.g^{-1}.K^{-1}$, which is the same range than values found for small solutes (neutral sugars, amino acids, peptides) and macromolecules (globular proteins, polysaccharides and nucleic acids). This suggests a universal effect of temperature on volumetric properties of biomolecules.

5. Acknowledgments

This work was supported by the Alland&Robert Company and a Ph.D. grant (V. Mejia Tamayo) from the Equatorian research ministry (Senescyt).

6. References

1. Sanchez, C.; Nigen, M.; Mejia Tamayo, V.; Doco, T.; Williams, P.; Amine, C.; Renard, D. Acacia gum: History of the future. *Food Hydrocolloids* **2018**.
2. Williams, P.A.; Philips, G.O. Gum arabic. In *Handbook of hydrocolloids*, G. O. Philips, P.A.W., Ed. Boca Raton: CRC Press: 2000; pp 155-168.
3. FAO. Gum arabic. Food and Nutrition Paper 52 1999
4. Akiyama, Y.; Eda, S.; Kato, K. Gum arabic is a kind of arabinogalactan protein. *Agric. and Biol. Chem.* **1984**, *48*, 235-237.
5. Renard, D.; Lavenant-Gourgeon, L.; Ralet, M.C.; Sanchez, C. Acacia *senegal* gum: Continuum of molecular species differing by their protein to sugar ratio; molecular weight and charges. *Biomacromolecules* **2006**, 2637-2649.
6. Renard, D.; Garnier, C.; Lapp, A.; Schmitt, C.; Sanchez, C. Structure of arabinogalactan-protein from acacia gum: From porous ellipsoids to supramolecular architectures. *Carbohydrate Polymers* **2012**, *90*, 322-332.
7. Renard, D.; Lepvrier, E.; Garnier, C.; Roblin, P.; Nigen, M.; Sanchez, C. Structure of glycoproteins from acacia gum: An assembly of ring-like glycoproteins modules. *Carbohydrate Polymers* **2014**, *99*, 736-747.
8. Randall, R.C.; Phillips, G.O.; Williams, P.A. Fractionation and characterization of gum from acacia *senegal*. *Food Hydrocolloids* **1989**, *3*, 65-75.
9. Renard, D.; Garnier, C.; Lapp, A.; Schmitt, C.; Sanchez, C. Corrigendum to "structure of arabinogalactan-protein from acacia gum: From porous ellipsoids to supramolecular architectures" [carbohydr. Polym. 90 (2012) 322–332]. *Carbohydrate Polymers* **2013**, *97*, 864-867.
10. Sanchez, C.; Renard, D.; Robert, P.; Schmitt, C.; Lefebvre, J. Structure and rheological properties of acacia gum dispersions. *Food Hydrocolloids* **2002**, *16*, 257-267.
11. Idris, O.H.M.; Williams, P.A.; Phillips, G.O. Characterisation of gum from acacia *senegal* trees of different age and location using multidetection gel permation chromatography. *Food Hydrocolloids* **1998**, 379-388.
12. Dror, Y.; Cohen, Y.; Yerushalmi-Rozen, R. Structure of gum arabic in aqueous solution. *J. of Polym. Sci. Pol. Phys.* **2006**, *44*, 3265-3271.
13. Gashua, I.B.; Williams, P.A.; Yadav, M.P.; Baldwin, T.C. Characterisation and molecular association of nigerian and sudanese acacia gum exudates. *Food Hydrocolloids* **2015**, *51*, 405-413.
14. Williams, P.A. Structural characteristics and functional properties of gum arabic. In *Gum arabic*, The Royal Society of Chemistry: 2012; pp 179-187.
15. Anderson, D.M.W.; Bridgeman, M.M.E.; Farquhar, J.G.K.; McNab, C.G.A. The chemical characterization of the test article used in toxicological studies of gum arabic (acacia senegal (l.) willd). *International Tree Crops Journal* **1983**, *2*, 245-254.
16. Islam, A.M.; Phillips, G.O.; Sljivo, A.; Snowden, M.J.; Williams, P.A. A review of recent developments on the regulatory, structural and functional aspects of gum arabic. *Food Hydrocolloids* **1997**, *11*, 493-505.
17. Flindt, C.; Alassaf, S.; Phillips, G.; Williams, P. Studies on acacia exudate gums. Part v. Structural features of acacia *seyal*. *Food Hydrocolloids* **2005**, *19*, 687-701.
18. Lopez-Torres, L. Characterization of acacia gums (a. *Senegal* and a. *Seyal*) and development of heat induced acacia gum/potato protein microparticles. Supagro, Montpellier, 2017.
19. Anderson, D.M.W.; Stoddart, J.F. Studies on uronic acid materials. Part xv. The use of molecular-sieve

chromatography on acacia *senegal* gum (gum arabic). *Carbohydrate Research* **1966**, *2*, 104-114.

20. Williams, P.A.; Phillips, G.O.; Randall, R.C. Structure-function relationships of gum arabic. In *Gums and stabilisers for the food industry 5* Phillips, G.O.; Williams, P.A.; Wedlock, D.J., Eds. IRL Press: Oxford, 1990; pp 25-36.

21. Ali, A.; Maqbool, M.; Ramachandran, S.; Alderson, P.G. Gum arabic as a novel edible coating for enhancing shelf-life and improving postharvest quality of tomato (solanum lycopersicum l.) fruit. *Postharvest Biology and Technology* **2010**, *58*, 42-47.

22. Sanchez, C.; Schmitt, C.; Kolodziejczyk, E.; Lapp, A.; Gaillard, C.; Renard, D. The acacia gum arabinogalactan fraction is a thin oblate ellipsoid: A new model based on small-angle neutron scattering and ab initio calculation. *Biophysical Journal* **2008**, *94*, 629-639.

23. Mejia Tamayo, V.; Nigen, M.; Apolinar-Valiente, R.; Doco, T.; Williams, P.; Renard, D.; Sanchez, C. Flexibility and hydration of amphiphilic hyperbranched arabinogalactan-protein from plant exudate: A volumetric perspective. *Colloids and Interfaces* **2018**, *2*, 11.

24. Hu, X.; Kaplan, D.; Cebe, P. Dynamic protein−water relationships during β-sheet formation. *Macromolecules* **2008**, *41*, 3939-3948.

25. Huang, W.; Krishnaji, S.; Tokareva, O.R.; Kaplan, D.; Cebe, P. Influence of water on protein transitions: Thermal analysis. *Macromolecules* **2014**, *47*, 8098-8106.

26. Hatakeyama, T.; Nakamura, K.; Hatakeyama, H. Determination of bound water content in polymers by dta, dsc and tg. *Thermochimica Acta* **1988**, *123*, 153-161.

27. Bano, M.; Marek, J.; Stupak, M. Hydrodynamic parameters of hydrated macromolecules: Monte carlo calculation. *Physical Chemistry Chemical Physics* **2004**, *6*, 2358-2363.

28. Laage, D.; Elsaesser, T.; Hynes, J.T. Water dynamics in the hydration shells of biomolecules. *Chemical Reviews* **2017**, *117*, 10694-10725.

29. Chalikian, T.V.; Sarvazyan, A., P.; Breslauer, K.J. Hydration and partial compressibility of biological compounds. *Biophysical Chemistry* **1994**, *51*, 89 - 109.

30. Phillips, G.O.; Takigami, S.; Takigami, M. Hydration characteristics of the gum exudate from *acacia senegal*. *Food Hydrocolloids* **1996**, *10*, 11-19.

31. Hatakeyama, T.; Uetake, T.; Hatakeayama, H. Frezeeing bound water restrained by gum arabic. In *Gums and stabilizers for the food industry*, Philips, P.A.W.G.O., Ed. RSC Publishing: Cambridge (UK), 2010; Vol. 15, pp 69-75.

32. Ray, A.K.; Bird, P.B.; Iacobucci, G.A.; Clark, B.C. Functionality of gum arabic. Fractionation, characterization and evaluation of gum fractions in citrus oil emulsions and model beverages. *Food Hydrocolloids* **1995**, *9*, 123-131.

33. Cozic, C.; Picton, L.; Garda, M.-R.; Marlhoux, F.; Le Cerf, D. Analysis of arabic gum: Study of degradation and water desorption processes. *Food Hydrocolloids* **2009**, *23*, 1930-1934.

34. Bothara, S.B.; Sinngh, S. Thermal studies on natural polysaccharide. *Asian Pacific Journal of Tropical Biomedicine* **2012**, S1031 - S1035.

35. Zohuriaan, M.J.; Shokrolahi, F. Thermal studies on natural and modified gums. *Polymer testing* **2003**, *23*, 575-579.

36. Hatakeyama, H.; Hatakeyama, T. Interaction between water and hydrophilic polymers. *Thermochimica Acta* **1998**, *308*, 3-22.

37. Mothé, C.G.; Rao, M.A. Thermal behavior of gum arabic in comparison with cashew gum. *Thermochimica Acta* **2000**, *357-358*, 9-13.

38. Daoub, R.M.A.; Elmubarak, A.H.; Misran, M.; Hassan, E.A.; Osman, M.E. Characterization and functional properties of some natural *acacia* gums. *Journal of the Saudi Society of Agricultural Sciences* **2016**.

39. Iqbal, M.S.; Massey, S.; Akbar, J.; Ashraf, C.M.; Mashid, R. Thermal analysis of some natural polysaccharides materials by isoconversional method. *Food Chemistry* **2013**, *140*, 178-182.

40. Bagchi, S.; Jayaram Kumar, K. Studies on water soluble polysaccharides from pithecellobium dulce (roxb.) benth. Seeds. *Carbohydrate Polymers* **2016**, *138*, 215-221.

41. Srivastava, A.; Mishra, V.; Singh, P.; Srivastava, A.; Kumar, R. Comparative study of thermal degradation behavior of graft copolymers of polysaccharides and vinyl monomers. *Journal of Thermal Analysis and Calorimetry* **2012**, *107*, 211-223.

42. Iqbal, M.S.; Akbar, J.; Saghir, S.; Karim, A.; Koschella, A.; Heinze, T.; Sher, M. Thermal studies of plant carbohydrate polymer hydrogels. *Carbohydrate Polymers* **2011**, *86*, 1775-1783.

43. Dhawade, P.; Jagtap, R. Characterization of the glass transition temperature of chitosan and its oligomers by temperature modulated differential scanning caorimetry. *Advances in Applied Science Research* **2012**, *3*, 1372-1382.

44. Apostolov, A.A.; Fakirov, S.; Vassileva, E.; Patil, R.D.; Mark, J.E. Dsc and tga studies of the behavior of water on native and crosslinked gelatin. *Journal of Applied Polymer Science* **1999**, *71*, 465-470.

45. Mohamed, A.; Finkenstadt, V.L.; Gordon, S.H.; Biresaw, G.; Palmquist, D.E.; Rayas-D., P. Thermal properties of pcl/gluten bioblends characterized by tga, dsc, sem, and infrared-pas. *Journal of Applied Polymer Science* **2008**, *110*, 3256-3266.

46. Micard, V.; Morel, M.-H.; Bonicel, J.; Guilbert, S. Thermal properties of raw and processed wheat gluten in relation with protein aggregation. *Polymer* **2001**, *42*, 477-485.

47. Kulig, D.; Zimoch-Korzycka, A.; Jarmoluk, A.; Marycz, K. Study on alginate–chitosan complex formed with different polymers ratio. *Polymers* **2016**, *8*, 167.

48. Morikawa, A. Comparison of properties among dendritic and hyperbranched poly(ether ether ketone)s and linear poly(ether ketone)s. *Molecules* **2016**, *21*.

49. Borde, B.; Bizot, H.; Vigier, G.; Buleon, A. Calorimetric analysis of the structural relaxation in partially hydrated amorphous polysaccharides. I. Glass transition and fragility. *Carbohyd. Polym.* **2001**, *48*, 83-96.

50. Elias, H.G. Viscosity of dilute solutions. In *Macromolecules, volume 3: Physical structures and properties*, Wiley VCH: 2008; pp 395-425.

51. Harding, S.E. Dilute solution viscometry of food biopolymers. In *Fuctional properties of food macromolecules*, 2nd ed.; Aspen Pub: MA, USA, 1998; pp 1-49.

52. Burchard, W. Solution properties of branched macromolecules In *Branched polymers ii*, Roover, J., Ed. Springer Berlin Heidelberg: Berlin, Heidelberg, 1999; pp 113-194.

53. Morris, G.A.; Adams, G.G.; Harding, S.E. On hydrodynamic methods for the analysis of the sizes and shapes of polysaccharides in dilute solution: A short review. *Food Hydrocolloids* **2014**, *42*, 318-334.

54. Smidsrød, O. Solution properties of alginate. *Carbohydrate Research* **1970**, *13*, 359-372.

55. Lopez-Torrez, L.; Nigen, M.; Williams, P.; Doco, T.; Sanchez, C. Acacia *senegal* vs. Acacia *seyal* gums – part 1: Composition and structure of hyperbranched plant exudates. *Food Hydrocolloids* **2015**, *51*, 41-53.

56. Masuelli, M. Hydrodynamic properties of whole arabic gum. *American Journal of Food Science and Technology* **2013**, *1*, 60-66.

57. Anderson, D.M.W.; Rahman, S. Studies on uronic acid materials. Part xx. The viscosity molecular weight relationship for acacia gums. *Carbohydrate Research* **1967**, *4*, 298-304.

58. Vandevelde, M.-C.; Fenyo, J.-C. Macromolecular distribution of acacia senegal gum (gum arabic) by size exclusio chromatography. *Carbohyd. Polym.* **1985**, *5*, 251-273.

59. Möck, A.; Burgath, A.; Hanselmann, R.; Frey, H. Synthesis of hyperbranched aromatic homo- and copolyesters via the slow monomer addition method. *Macromolecules* **2001**, *34*, 7692-7698.

60. Bello-Perez, L.A.; Roger, P.; Colonna, P.; Paredes-Lopez, O. Laser light scattering of high amylose and high amylopectin materials, stability in water after microwave dispersion. *Carbohydrate Polymers* **1998**, *37*, 383-394.

61. Wang, Q.; Burchard, W.; Cui, S.W.; Huang, X.Q.; Philips, G.O. Solution properties of conventional gum arabic and a matured gum arabic (acacia (sen) super gum). *Biomacromolecules* **2008**, *9*, 1163-1169.

62. Picton, L.; Bataille, I.; Muller, G. Analysis of a complex polysaccharide (gum arabic) by multi-angle laser light scattering coupled on-line to size exclusion chromatography and flow field flow fractionation. *Carbohydrate Polymers* **2000**, *42*, 23-31.

63. Wolf, B.A. Polyelectrolytes revisited: Reliable determination of intrinsic viscosities. *Macromolecular Rapid Communications* **2007**, *28*, 164-170.

64. Simha, R. Effect of concentration on the viscosity of dilute solutions. *Journal of Research of the National Bureau of Standards* **1949**, *42*, 409-418.

65. Antonietti, M.; Briel, A.; Förster, S. Intrinsic viscosity of small spherical polyelectrolytes: Proof for the intermolecular origin of the polyelectrolyte effect. *The Journal of Chemical Physics* **1996**, *105*, 7795-7807.

66. Giannouli, P. Effect of polymeric cosolutes on calcium pectinate gelation. Part 3. Gum arabic and overview. *Carbohydrate Polymers* **2004**, *55*, 367-377.

67. Yang, H.; Zheng, Q.; Cheng, R. New insight into "polyelectrolyte effect". *Colloids and Surfaces A: Physicochemical and Engineering Aspects* **2012**, *407*, 1-8.

68. Cheng, R.; Shao, Y.; Liu, M.; Qian, R. Effect of adsorption on the viscosity of dilute polymer solution. *European Polymer Journal* **1998**, *34*, 1613-1619.

69. Zhong, D.; Huang, X.; Yang, H.; Cheng, R. New insights into viscosity abnormality of sodium alginate aqueous solution. *Carbohydrate Polymers* **2010**, *81*, 948-952.

70. Eckelt, J.; Knopf, A.; Wolf, B.A. Polyelectrolytes: Intrinsic viscosities in the absence and in the presence of salt. *Macromolecules* **2008**, *41*, 912-918.

71. Jamieson, A.M.; Simha, R. Newtonian viscosity of dilute, semidilute, and concentrated polymer solutions. In *Polymer physics*, 2010; pp 17-87.

72. Cohen, J.; Priel, Z. Viscosity of dilute polyelectrolyte solutions: Temperature dependence. *The Journal of Chemical Physics* **1990**, *93*, 9062-9068.

73. Fuoss, R.M.; Strauss, U.P. Electrostatic interaction of polyelectrolytes and simple electrolytes. *Journal of Polymer Science* **1948**, *3*, 602-603.

74. Rubinstein, M.; Colby, R.H.; Dobrynin, A.V. Dynamics of semidilute polyelectrolyte solutions. *Phys Rev Lett* **1994**, *73*, 2776-2779.

75. Amirova, A.I.; Sheremetyeva, N.A.; Filippov, A.P. Temperature dependence of the hydrodynamic and conformational properties of hyperbranched polycarbosilanes. *International Journal of Polymer Analysis and Characterization* **2013**, *18*, 339-345.

76. Maxim, S.; Dumitriu, E.; Ioan, S.; Carpov, A. Dilute solutions of polyelectrolytes i. *European Polymer Journal* **1977**, *13*, 105-108.

77. Bradley, T.D.; Mitchell, J.R. The degradation of the kinetics of polysaccharide thermal degradation using high temperature viscosity measurements. *Carbohydrate Polymers* **1988**, *9*, 257-267.

78. Xu, S.; Xu, X.; Zhang, L. Effect of heating on chain conformation of

branched β-glucan in water. *The Journal of Physical Chemistry B* **2013**, *117*, 8370-8377.

79. Kainthan, R.K.; Brooks, D.E. In vivo biological evaluation of high molecular weight hyperbranched polyglycerols. *Biomaterials* **2007**, *28*, 4779-4787.

80. Gekko, K. Physicochemical studies of oligodextran. Ii. Intrinsic viscosity - molecular weight relationship. *Die Makromolekulare Chemie* **1971**, *148*, 229-238.

81. Fox, T.G.; Flory, P.J. Viscosity—molecular weight and viscosity—temperature relationships for polystyrene and polyisobutylene 1,2. *Journal of the American Chemical Society* **1948**, *70*, 2384-2395.

82. Cui, S.W. *Food carbohidrates: Chemistry, physical properties, and applications*. 1st edition ed.; CRC Press: 2005; p 411.

83. Porter, R.S.; Johnson, J.F. Temperature dependence of polymer viscosity. The influence of shear rate and stress. *Journal of Polymer Science Part C: Polymer Symposia* **1967**, *15*, 365-371.

84. Mezger, T.G. *The rheology handbook: For users of rotational and oscillatory rheometers*. 2nd Edition ed.; Vincentz: Hannover, Germany, 2006.

85. Monkos, K. Concentration and temperature dependence of viscosity in lysozyme aqueous solutions. *Biochimica et Biophysica Acta (BBA) - Protein Structure and Molecular Enzymology* **1997**, *1339*, 304-310.

86. Budtova, T.; Navard, P. Viscosity-temperature dependence and activation energy of cellulose solutions. *Nordic Pulp and Paper research Journal* **2015**, *30 (01)*, 99-104.

87. Varfolomeva, E.P.; Grinberg, V.Y.; Tolstogusov, V.B. On the possibility of estimating weak interactions of macromolecules in solutions from the experimental viscous flow activation energies data. *Polymer Bulletin* **1980**, *2*, 613-618.

88. de Paula, R.C.M.; Santana, S.A.; Rodrigues, J.F. Composition and rheological properties of albizia lebbeck gum exudate. *Carbohydrate Polymers* **2001**, *44*, 133-139.

89. Uppuluri, S.; Keinath, S.E.; Tomalia, D.A.; Dvornic, P.R. Rheology of dendrimers. I. Newtonian flow behavior of medium and highly concentrated solutions of polyamidoamine (pamam) dendrimers in ethylenediamine (eda) solvent. *Macromolecules* **1998**, *31*, 4498-4510.

90. Chalikian, T.V.; Totrov, M.; Abagyan, R.; Breslauer, K.J. The hydration of globular proteins as derived from volume and compressibility measurements: Cross corelating thermodynamic and structural data *Journal Molecular Biology* **1996**, *260*, 588 - 603.

91. Durchschlag, H. Specific volumes of biological macromolecules and some other molecules of biological interest. In *Thermodynamic data for biochemistry and biotechnology*, Hinz, H.-J., Ed. Springer: Berlin, 1986; pp 45 - 128.

92. Kupke, D.W. Density and volume change measurements. In *Physical principles and techniques of protein chemistry, part c*, Leach, S.J., Ed. Academic Press: 1973; pp 3 - 75.

93. Hoiland, H. Partial molar compressibilities of organic solutes in water. In *Thermodynamic data for biochemistry and biotechnology*, Hinz, H.-J., Ed. Springer: Berlin, 1986; pp 129 - 147.

94. Gekko, K.; Noguchi, H. Physicochemical studies of oligodextran. I. Molecular weight dependence of intrinsic viscosity, partial specific compressibility and hydrated water *Biopolymers* **1971**, *10*, 1513 -1524.

95. Gekko, K.; Noguchi, H. Hydration behavior of ionic dextran derivatives. *Macromolecules* **1974**, *7*, 224 - 229.

96. Gekko, K.; Noguchi, H. Compressibility of globular proteins in water at 25 °c. *The Journal of Physical Chemistry* **1979**, *83*, 2706 -2714.

97. Kharakoz, D.P.; Sarvazyan, A., P. Hydrational and intrinsic compressibilities of globular proteins. *Biopolymers* **1993**, *33*, 11 - 26.

98. Kharakoz, D.P. Volumetric properties of proteins and their analogs in diluted water solutions. *Biophysical Chemistry* **1989**, *34*, 115-125.

99. Taulier, N.; Chalikian, T.V. Compressibility of protein transitions. *Biochimica et Biophysica Acta (BBA) - Protein Structure and Molecular Enzymology* **2002**, *1595*, 48-70.

100. Chen, C.R.; Makhatadze, G.I. Protein volume: Calculating molecular van der waals and void volume in proteins. *BMC Bioinformatics* **2015**, *16*, 101-106.

101. Voloshin, V.P.; Medvedev, N.N.; Smolin, N.; Geiger, A.; Winter, R. Exploring volume, compressibility and hydration changes of folded proteins upon compression. *Physical Chemistry Chemical Physics* **2015**, *17*, 8499-8508.

102. Voloshin, V.; Medvedev, N.; Smolin, N.; Geiger, A.; Winter, R. Disentangling volumetric and hydrational properties of proteins. *Journal of Physical Chemistry B* **2015**, *115*, 1881-1890.

103. Shiraga, K.; Ogawa, Y.; Kondo, N.; Irisawa, A.; Imamura, M. Evaluation of the hydration state of saccharides using terahertz time-domain attenuated total reflection spectroscopy. *Food Chemistry* **2013**, *140*, 315-320.

104. Fogarty, A.C.; Laage, D. Water dynamics in protein hydration shells: The molecular origins of the dynamical perturbation. *The Journal of Physical Chemistry B* **2014**, *118*, 7715-7729.

105. Heugen, U.; Schwaab, G.; Bründermann, E.; Heyden, M.; Yu, X.; Leitner, D.M.; Havenith, M. Solute-induced retardation of water dynamics probed directly by terahertz spectroscopy. *PNAS* **2006**, *103*, 12301-12306.

106. Ebbighaus, S.; Kim, S.J.; Heyden, M.; Yu, X.; Heugen, U.; Gruebele, M.; Leitner, D.M.; Havenith, M. An extended dynamical hydration shell around proteins. *PNAS* **2007**, *104*, 20749-20752.

107. Chalikian, T.V.; Filfil, R. How large are the volume changes accompanying protein transitions and binding? *Biophysical Chemistry* **2003**, *104*, 489-499.

108. Chalikian, T.V. Structural thermodynamics of hydration. *The Journal of Physical Chemistry B* **2001**, *105*, 12566-12578.

109. Afrin, T.; Mafy, N.N.; Rahman, M.M.; Mollah, M.Y.A.; Susan, M.A.B.H. Temperature perturbed water structure modification by d(-)-fructose at different concentrations. *RSC Advances* **2014**, *4*, 50906-50913.

110. Banipal, P.K.; Banipal, T.S.; LArk, B.S.; Ahluwalia, J.C. Partial molar heat capacities and volumes of some mono-, di- and tri-saccharides in water at 298.15, 308.15 and 318.15 k. *J. Che.Soc., Faraday Trans* **1997**, *93*, 81 - 87.

111. Chalikian, T.V.; Völker, J.; Anafi, D.; Breslauer, K.J. The native and the heat-induced denatured states of α-chymotrypsinogen a: Thermodynamic and spectroscopic studies 11edited by p. E. Wright. *Journal of Molecular Biology* **1997**, *274*, 237-252.

112. Makhatadze, G.I.; Medvedkin, V.N.; Privalov, P.L. Partial molar volumes of polypeptides and their constituent groups in aqueous solution over a broad temperature range. *Biopolymers* **1990**, *30*, 1001-1010.

113. Häckel, M.; Hinz, H.-J.; Hedwig, G.R. Partial molar volumes of proteins: Amino acid side-chain contributions derived from the partial molar volumes of some tripeptides over the temperature range 10–90°c. *Biophysical Chemistry* **1999**, *82*, 35-50.

114. Bull, H.B.; Breese, K. Temperature dependence of partial volumes of proteins. *Biopolymers* **1973**, *12*, 2351-2358.

115. Gekko, K.; Araga, M.; Kamiyama, T.; Ohmae, E.; Akasaka, K. Pressure dependence of the apparent specific volume of bovine serum albumin: Insight into the difference between isothermal and adiabatic compressibilities. *Biophysical Chemistry* **2009**, *144*, 67-71.

116. Lee, A.; Chalikian, T.V. Volumetric characterization of the hydration properties of heterocyclic bases and nucleosides. *Biophysical Chemistry* **2001**, *92*, 209-227.

117. Chalikian, T.V.; Totrov, M.; Abagyan, R.; Breslauer, K.J. The hydration of globular proteins as derived from volume and compressibility measurements: Cross correlating thermodynamic and structural data. *Academic Press* **1996**, *260*, 588 - 603.

118. Apenten, R.K.O.; Buttner, B.; Mignot, B.; Pascal, D.; Povey, M.J.W. Determination of the adiabatic compressibility of bovine serum albumen in concentrated solution by a new ultrasonic method. *Food Hydrocolloids* **2000**, *14*, 83-91.

119. Gekko, K.; Hasegawa, Y. Compressibility-structure relationship of globular proteins. *Biochemistry* **1986**, *25*, 6563 - 6571.

120. Gekko, K.; Yamagami, K. Flexibility of food proteins as revealed by compressibility. *Journal Agricultural Food Chemisty* **1991**, *39*, 57 - 62.

121. Gekko, K. Hydration-structure-function relationships of polysaccharides and proteins. *Food Hydrocolloids* **1989**, *3*, 289-299.

122. Zhang, Z.; Maya Desdier, L.E.; Scanlon, M.G. Ergometric studies of proteins: New insights into protein functionality in food systems. *Trends in Food Science & Technology* **2015**, *45*, 251 - 263.

123. Chalikian, T.V. On the molecular origins of volumetric data. *J. Phys. Chem. B* **2008**, *112*, 911-917.

124. Blandamer, M.J.; Davis, M.I.; Douheret, G.; Reis, J.C.R. Apparent molar isentropic compressions and expansions of solutions. *Chemical Society Reviews* **2001**, *30*, 8-15.

125. Reis, J.C.R.; Douheret, G.; Davis, M.I.; Fjellanger, I.J.; Hoiland, H. Isentropic expansion and related thermodynamic properties of non-ionic amphiphile-water mixtures. *Physical Chemistry Chemical Physics* **2008**, *10*, 561-573.

126. Gucker, F.T. The apparent molal expansibility of electrolytes and the coefficient of expansibility (thermal expansion) as a function of concentration 1. *Journal of the American Chemical Society* **1934**, *56*, 1017-1021.

127. Kumar, D.; Lomesh, S.K.; Nathan, V. Molecular interaction studies of l-alanine and l-phenylalanine in water and in aqueous citric acid at different temperatures using volumetric, viscosity and ultrasonic methods. *Journal of Molecular Liquids* **2017**, *247*, 75-83.

128. Sharma, S.K.; Singh, G.; Kumar, H.; Kataria, R. Solvation behavior of some amino acids in aqueous solutions of non-steroidal anti-inflammatory drug sodium ibuprofen at different temperatures analysed by volumetric and acoustic methods. *The Journal of Chemical Thermodynamics* **2016**, *98*, 214-230.

129. Hedwig, G.R.; Hastie, J.D.; Hoiland, H. Thermodynamic properties of peptide solutions: 14. Partial molar expansibilities and isothermal compressibilities of some glycyl dipeptides in aqueous solutions. *Journal of Solution Chemistry* **1996**, *25*, 615-633.

130. Nandi, P.; English, N.J.; Futera, Z.; Benedetto, A. Hydrogen-bond dynamics at the bio-water interface in hydrated proteins: A molecular-dynamics study. *Physical Chemistry Chemical Physics* **2017**, *19*, 318-329.

Chapter V: General Conclusions and Perspectives

1. General conclusions

The main objective of this PhD thesis was to study the volumetric properties of Arabinogalactan-proteins (AGPs) from Acacia gums exudates. For this effect, we used the main commercial species of A. gums, A. *senegal* and A. *seyal*, and the macromolecular fractions of the former, HIC-F1, HIC-F2 and HIC-F3 obtained using hydrophobic interaction chromatography (HIC), and IEC-F1 and IEC-F2 obtained using ionic exchange chromatography (IEC). The specific objectives of the study were: (1) to characterize A. gums and AGP fractions in terms of their main volumetric (hydrostatic and hydrodynamic) properties, and (2) to study the effect of changes on the quality of the solvent on these properties, by changing the ionic strength and temperature of the system.

The structural properties, weight-averaged molar mass (M_w), polydispersity (M_w/M_n) and percentage of macromolecules with $M_w<7.5x10^5$ g.mol^{-1} were determined using HPSEC-MALS. Based on their M_w, AGPs from A. gum were arbitrarily classified into three main groups: 'small AGPs' ($M_w<7.5x10^5$ g.mol^{-1}), 'large AGPs' ($M_w>7.5x10^5$ g.mol^{-1}) and 'AGP-based aggregates' ($M_w<2\text{-}3x10^6$ g.mol^{-1}). In this line, A. *senegal* showed a lower M_w ($6.8x10^5$ g.mol^{-1}), but higher polydispersity index (2.0) than A. *seyal* ($7.1x10^5$ g.mol^{-1} and 1.5, respectively). However, both gums are manly formed by 'small AGPs' (86% and 80%, respectively). The HIC-F1 fraction is formed mainly of 'small AGPs' (93%) with mean M_w of $3.5x10^5$ g.mol^{-1} and a polydispersity of 1.4. Meanwhile, the HIC-F2 and HIC-F3 fractions are formed mainly of 'large AGPs' (88% and 67%) with a mean M_w of $1.5x10^6$ and $1.6x10^6$ g.mol^{-1}, respectively, and polydispersity of 1.4 and 1.9 respectively. These results were close to values previously reported in other studies. Regarding the IEC fractions, IEC-F1 was mainly formed of 'AGP based aggregates' (97%) with a mean M_w of $3.1x10^6$ g.mol^{-1} with a polydispersity of 1.2. On the other hand, IEC-F2 was mainly formed of 'small AGPs' (81%) with a mean M_w of $5.3x10^5$ g.mol^{-1} and 1.8 of polydispersity. Moreover, using the amino acid profile and sugar content it was estimated that the IEC-F1 fraction was composed of about 70% of HIC-F3 and 30% of HIC-F2. Therefore, the effect of the presence of AGP based aggregates was studied using this fraction.

The main volumetric (hydrostatic and hydrodynamic) properties, partial specific volume (v_s°), partial specific adiabatic compressibility coefficient (β_s°), partial specific expansibility (E°), intrinsic viscosity ($[\eta]$) and hydrodynamic radius (R_H) were determined using a combined approach of acoustic, viscometric, dynamic light scattering (DLS) and nuclear magnetic resonance spectroscopy (NMR) methods. A summary of the main results obtained is presented in Table V.1, which will be discussed in the aggregate.

1.1. Hyperbranched Acacia gums have an intermediate behavior between that of linear polysaccharides and globular proteins

The main volumetric properties, partial specific volume (v_s°), partial specific adiabatic compressibility coefficient (β_s°) and partial specific expansibility (E°) were obtained by measurements of the density and sound velocity of A. gums dispersions. These properties can be used to assess the hydration and flexibility of the molecule. In this line, a flexible molecule (e. g. globular proteins) is characterized by higher values of v_s° (0.69-0.76 $cm^3.g^{-1}$) and positive values of β_s°. Meanwhile, a hydrated molecule (e.g. polysaccharides and fibrous proteins) is characterized by lower values of v_s° and negative values of β_s°. The sign of β_s° is determined by a competition between the two main contributions of v_s° and β_s°, the molecular and the hydration contributions. The former refers to the intrinsic characteristics of the molecule itself, then, its van der Waals volume (v_{vdW}) and the volume of voids formed in the interior on the molecule (v_{voids}). On the other hand, the hydration of the molecule depends of the quantity of solvent, the hydration number n_h, and the strength of the solute-solvent interactions, which is determined by the difference on the volumetric properties of the water in the hydration shell and bulk.

In a general way, all Acacia gums presented v_s° values in the range of 0.56-0.65 $cm^3.g^{-1}$, which is close to the reported values for neutral polysaccharides (0.60-0.62 $cm^3.g^{-1}$). In addition, negative values β_s° were seen for all gums (Table V.1), which suggest an overcome of the hydration over the molecular contribution, which is given mainly by the volume of voids in the internal structure of the molecule. Furthermore, a linear relationship between v_s° and β_s° ($R^2 = 0.9$) was established (Figure V.1). In this line, A. gums were placed between characteristic values of v_s° and β_s° of linear polysaccharides and globular proteins found in literature.

Table V.1. Partial specific volume ($v_s°$), partial specific adiabatic compressibility coefficient ($\beta_s°$), void volume (%), partial specific expansibility (E°), intrinsic viscosity ([η]), hydrodynamic radius (R_H), gyration radius (R_G), viscosity increment ν, hydration number (n_H) and first transition temperature T1 (°C) of A. gums and AGP fractions

Gum or fraction	$v_s°$ ($cm^3.g^{-1}$)[a]	$\beta_s°$ ($x10^{11}$ Pa^{-1})[a]	Void volume (%)[b]	E° ($x10^4$ $cm^3.g^{-1}.K^{-1}$)[a]	[η] ($mL.g^{-1}$)[c]	R_H (nm)[d]	R_G (nm)[e]	ν[f]	n_H ($gH_2O/gAGP$)[g]	T_1 (°C)[h]
Acacia gums										
A. *senegal*	0.584	-12.2		4.9	16	12 (6)	16	11	*0.8*	69
A. *seyal*	0.577	-13.2		5.3	15	13 (6)	14	10	*0.9*	64
AGP fractions										
HIC-F1	0.562	-18.3	19	4.9	14	9 (4)	14	10	0.85	70
HIC-F2	0.588	-14.4	28	4.6	47	22 (7)	27	37	0.67	65
HIC-F3	0.650	-1.0	40	5.0	50	25 (8)	33	42	0.54	60
IEC-F1	0.610	-9.4			60	33 (10)	43	51	*0.6*	
IEC-F2	0.582	-12.9			13	10 (5)	16	9	*0.8*	

(a) $v_s°$, $\beta_s°$ and E° were calculated from measurements of density and sound velocity, (b) calculated from (1-ρ_M)*100, where ρ_M is the packing density (= V_{vdW}/V_M where V_{dvW} is the van der Waals partial molar volume and V_M is the intrinsic partial molar volume) (c) limiting [η] measured using viscometry and HPSEC-MALS in the 0.1-0.5M ($LiNO_3$) range, then extrapolated to charge neutralization and corrected taking into account gum polydispersity, (d) R_H was calculated from measures of [η] then extrapolated at charge neutralization and corrected according to the polydispersity. Values into parentheses correspond to R_H obtained in 0.1 M $LiNO_3$ using DOSY-NMR, (e) R_G was obtained from HPSEC-MALS measurements using only molecules with R_G higher than 10 nm. (f) Experimental viscosity increment (ν) was obtained from $n_h = (\rho_o)\left(\frac{[\eta]}{\upsilon} - v_s°\right)$ or estimated, (g) Hydration numbers calculated from hydrostatic volumetric properties of HIC-F1, HIC-F2 and HIC-F3 or estimated (italic numbers) from the known molecular composition of fractions. (h) First transition temperature T_1 was obtained using analytical thermogravimetry (TGA).

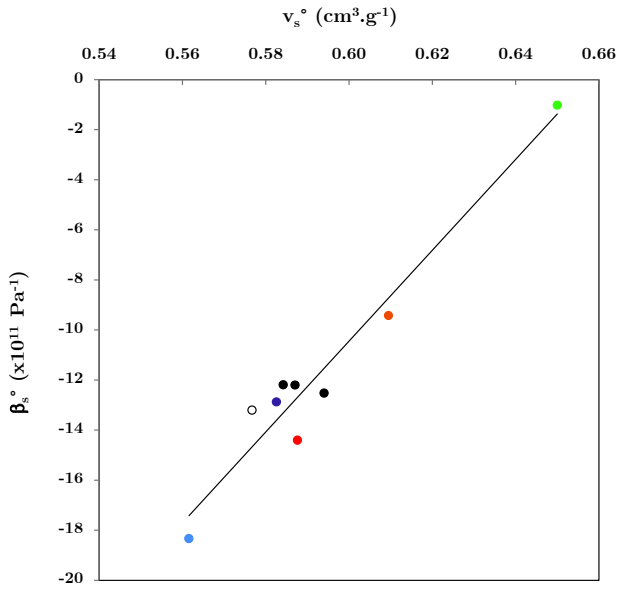

Figure V.1. Relationship between the partial specific volume ($v_s°$, $cm^3.g^{-1}$) and the partial specific adiabatic compressibility coefficient ($\beta_s°$, Pa^{-1}) of all Acacia gums: : A. *senegal* (black), A. *seyal* (white), HIC-F1 (blue), HIC-F2 (red), HIC-F3 (green), IEC-F1 (orange) and IEC-F2 (violet). Measurements were performed at 25 °C in sodium acetate (0.01 M, pH 5), except for A. *senegal* that were performed also in water and $LiNO_3$ (0.1 M, pH 7). Data were fitted to: $\beta_s° = 159.9 * v_s° - 105.7$ $R^2 = 0.9$).

A more in-depth look at Figure V.1 showed that no important differences were seen in dispersions of A. *senegal* prepared in water, sodium acetate (0.01 M, pH 5) and $LiNO_3$ (0.1 M, pH 7), which indicates a negligible effect of the ionic strength in the 0 – 0.01 M range. In addition, since A. *seyal* showed lower values of $v_s°$ and $\beta_s°$ (0.577 $cm^3.g^{-1}$ and -13.2x10^{-11} Pa^{-1}) as compared to A. *senegal* (0.584 $cm^3.g^{-1}$ and -12.2x10^{-11} Pa^{-1}), a slightly more flexible structure, given by its higher protein content, of the latter was inferred. This result might explain the better interfacial properties of A. *senegal* as compared to A. *seyal*.

Among the HIC fractions, HIC-F1 presented a more hydrated and less compressible structure, in relation to its low protein content, suggesting that this fraction is greatly responsible for the good solubility properties of A. gums. On the other hand, HIC-F3 presented a less hydrated and more compressible structure, in relation to its higher protein content. All these characteristics point to the important role played by this fraction on interfacial properties of A. gums. The differences in $v_s°$ and $\beta_s°$ of A. gums and AGP fractions were explained by differences in their overall composition, mainly protein content and neutral to charged sugars, then their polarity. In this line, the flexibility of AGP

fractions increased in the order: HIC-F1<HIC-F2<IEC-F2<IEC-F1<HIC-F3. In addition, using the calculated v_s° and β_s°, other important parameters such as the percentage of voids in the internal structure of the HIC-fractions and the number of water molecules bound to an A. gum molecule (hydration number or n_h) were estimated. The HIC-F1 fraction presented a lower percentage of voids (19%) and a higher n_h (0.85 g H_2O/g AGP) than HIC-F2 (28% and 0.68 g H_2O/g AGP) and HIC-F3 (40% and 0.54 g H_2O/g AGP). These results are in line with the decreasing polarity of HIC-F1>HIC-F2>HIC-F3. The presence of voids is common in the structure of hyperbranched polymers but was not previously suggested in the structure of AGPs. The value found for the HIC-F3 fraction (40%) is coherent with its low polarity but seems high as compared to most globular proteins (around 25%). Either the molecules display a particularly porous structure or this is a consequence of the presence of porous aggregates.

The IEC-F1 fraction presented higher values of v_s° and β_s° (0.610 $cm^3.g^{-1}$ and -9.4x10^{-11} Pa^{-1}) as compared to the IEC-F2 fraction (0.582 $cm^3.g^{-1}$ and -12.9x10^{-11} Pa^{-1}). These results suggest a more flexible structure of the former, which is mainly the consequence of their increased protein content (9.4%) and possibly the presence of AGP aggregates. On the other hand, IEC-F2 presented similar volumetric properties than A. *senegal* which suggests a more hydrated molecule.

Finally, the analysis of the behavior of the partial specific volume allowed the calculation of the partial specific expansibility coefficient (E°). The E° of all A. gums and AGP fractions was in the range of 5x10^{-4} $cm^3.g^{-1}.K^{-1}$ (Table VI.1). This value is in the same range of proteins and other biomolecules, which highlights the importance of their protein moiety.

To conclude this analysis, the results suggested that AGPs of A. gums have a semiflexible structure in which the polysaccharide moiety mainly contributes to the hydrophilic characteristics of A. gums, while the protein moiety greatly contributes to its non-polar characteristics. Furthermore, it was shown that using this relatively simple analysis important information such as the hydration and flexibility, which directly impact the functional properties of A. gums, can be obtained. However, some questions remain in the air, for instance: *What is the effect of changes on the pressure of the system on the flexibility and hydration?* and, *What is the effect the presence of minerals on these properties?* To answer the first question, we can use another volumetric property, the partial specific isotropic

compressibility coefficient (β_T), and for the second question we can use a demineralized gum (arabic acid). These suggestions will be further discussed in the perspectives section.

1.2. Hydrodynamic properties and conformation of A. gums: importance of charges, hyperbranching and amphiphilic characteristics, and presence of AGP based aggregates

The reduced viscosity (η_{red}) of A. gums and AGP fractions in the ionic strength range of 0-0.5 M was obtained using capillary viscometry and HPSEC-MALS. Similarly to other polyelectrolytes, the η_{red} showed an upward bending form at concentrations lower than 10 $g.L^{-1}$, and especially below 5 $g.L^{-1}$. This behavior was more important in salt-free dispersions and as the ionic strength increased the increase of η_{red} was reduced. This behavior was explained as a combined effect of intermolecular electrostatic repulsions (polyelectrolyte effect) due to the presence of negative charges, gum adsorption onto the capillary glass wall due to its amphiphilic nature and presence of AGP based aggregates.

The effect of charges was evidenced by the reduction of the intrinsic viscosity $[\eta]$ with the increase of the ionic strength of the solvent. Furthermore, it was estimated that charge neutralization was achieved at ionic strengths close to 0.5 M. The effect of the adsorption of AGPs on the capillary glass wall was evidenced due to blockage of the steel ball used in some experiments. This phenomenon was especially important in salt-free dispersions and with the more amphiphilic HIC-F2 and HIC-F3 fractions. As the ionic strength of the solvent was increased, the steel ball blockage was significantly reduced or eliminated. Finally, the effect of the presence of aggregates is to increase the intrinsic viscosity $[\eta]$, as can be observed for the IEC-F1 fraction, that is formed mainly by aggregates of HIC-F2 and HIC-F3 fractions (Table VI.1), two fractions prone to self-assembly. As the salt concentration was increased, the $[\eta]$ of these fractions was decreased, in part because of screening of charges and in part due to dissociation of the aggregates. The presence of aggregates in AGPs was confirmed using dynamic light scattering (DLS), since macromolecular populations with R_H>50 nm were identified in salt-free dispersions. As salt concentration was increased, the size of AGP aggregates was reduced. This behavior can be partly explained by the reduction of the solvent polarity, that favors solubilization of less polar objects, and shielding of negative (carried by sugars) and positive (carried by amino acids) charges. This may point out a role

for electrostatic interactions and hydrophobic effects on the formation of these AGP aggregates.

The intrinsic viscosity and hydrodynamic radius of A. gums and AGP fractions were determined at total charge neutralization and corrected to take into account the polydispersity of each gum. In a general way, A. *senegal*, A. *seyal*, HIC-F1 and IEC-F2 presented a low $[\eta]$ (16, 15, 14, 13 $mL.g^{-1}$) and R_H (12, 13, 9, 10 nm) while HIC-F2, HIC-F3 and IEC-F1 presented a higher $[\eta]$ (47, 50, 60 $mL.g^{-1}$) and R_H (22, 25, 33 nm). Upon charge neutralization, hydrodynamic parameters are then mainly determined by the molar mass of AGPs and AGP aggregates and less by the residue composition, highlighting the dominant effect of AGP aggregates on the hydrodynamic properties.

The properties $[\eta]$ and R_G and the weight-averaged molar mass (M_w) of A. gums and AGP fractions were fitted to power law functions to obtain its structural conformation. The main results showed that the conformation did not change with the increase of the ionic strength up to 0.5 M, which was explained by the stabilization of the structure owed to the hyperbranched polysaccharidic moiety of A. gums. Similarly to other studies involving A. gums and HIC fractions, the power law exponent ($\boldsymbol{a}_\eta$) of the $[\eta]$ *vs* M_w relationship (Mark-Houwink-Sakurada analysis) showed the presence of at least two molecular conformations. In a general way, A. *seyal* ($\boldsymbol{a}_\eta = 0.25$) presented a more isotropic spheroidal conformation than A. *senegal* ($\boldsymbol{a}_\eta = 0.4$), which is in good agreement with the more compact structure reported for A. *seyal*. A. *senegal* and its HIC fractions presented three molecular conformations. AGPs with low M_w in the range of 1.5-5.0 $x10^5$ $g.mol^{-1}$ presented a more isotropic configuration ($\boldsymbol{a}_\eta = 0.4$) than AGPs with M_w in the range of 5.0-15.0 $x10^5$ $g.mol^{-1}$, which presented a more elongated configuration ($\boldsymbol{a}_\eta = 0.5 - 0.9$). These more elongated conformations may correspond to the ellipsoidal shapes reported for the HIC-F1, HIC-F2 and HIC-F3 fractions and possibly to hyperbranched random coil conformations. Finally, AGPs with high M_w, in the range of (15-50 $x10^5$ $g.mol^{-1}$), presented a more isotropic conformation ($\boldsymbol{a}_\eta = 0.3 - 0.5$), corresponding probably to AGP aggregates. The conformation analysis using the R_G was also used as an indication of the aggregation of AGPs. Thus, the presence of aggregates was evidenced by an increase of the anisotropy of AGPs in the order HIC-F3<IEC-F1<HIC-F2<A. *senegal*<IEC-F2<HIC-F1. The anisotropy is then directly related to the protein content and self-assembly properties of AGPs.

When the global conformational analysis of A. gums and AGPs was done using sedimentation (S_o) coefficients, a random coil conformation was estimated. However, using the translational diffusion (D_T) results, a more spherical conformation was revealed. This difference was explained by the sensitivity of the DOSY-NMR method used for the determination of D_T, which allowed the discrimination of molecules with R_H lower than 20 nm, thus excluding the aggregates and more elongated AGPs.

To conclude, the study of the hydrodynamic properties of AGPs form A. gums has shed light on the important effect of the presence of AGP based aggregates and charges of the molecule. Furthermore, the presence of macromolecules with a low hydrodynamic radius (R_H) between 4-8 nm was evidenced using a combination of DLS and DOSY-NMR methods. This small population has not been reported before. Therefore, the remaining questions are: *What is the mechanism of formation of AGP aggregates and how they affect the functional properties of A. gums?*, and, *What is the role of the small macromolecule population on the hydrodynamic properties?* Thus, more studies are suggested in order to gain more insight.

1.3. The use of viscosity increment of a sphere leads to overestimation of the hydration number

The viscosity increment (ν) is an anisotropy parameter, then it depends on the shape of the molecule. Several studies tend to use a value of 2.5, which corresponds to molecules with a spherical shape. Previous studies have shown that A. gums are a polydisperse system of macromolecules with ellipsoidal shape. Using ν=2.5, hydration numbers of in the range of 7-24 g H_2O/g AGP were obtained for A. gums. Considering that using acoustic methods, n_h of 0.9, 0.7 and 0.5 g H_2O/g AGP were estimated for HIC-F1, HIC-F2 and HIC-F3, respectively, and that highly hydrophilic polysaccharides (e.g. xantan, hyalunoran and hylan) presented n_h in the range of 2-10 g H_2O/g polymer, then the hydration is clearly overestimated. By combining hydrostatic and hydrodynamic properties, the ELLIPS software and the reported dimensions of HIC-F1, HIC-F2 and HIC-F3, experimental viscosity increment in the range of 10-50 were estimated, for HIC-F1, HIC-F2 and HIC-F3, respectively (Table V.1). These results highlight the high isotropy of AGP molecules. Furthermore, since higher ν values were found in fractions with higher M_w and protein content (HIC-F2, HIC-F2 and IEC-F1), an effect of molar mass and the polarity is suggested.

Finally, a summary of the main results obtained for AGPs taking into account their M_w ('small AGPs', 'large AGPs' and 'AGP based aggregates') is presented in Table V.2. These values can be used to predict hydrodynamic properties, viscosity increment and conformation of AGPs of A. gums, providing their molar mass is known.

Table V. 2. Intrinsic viscosity ([η]), hydrodynamic radius (R_H), viscosity increment (ν) and molecular conformation of 'small AGPs', 'large AGPs' and 'AGP based aggregates'

	[η] (mL.g^{-1})	R_H (nm)	ν	Conformation
Small AGPs	15	< 10	11	Less anisotropic structure
Large AGPs	45	10-40	45	Anisotropic structure
AGP-based aggregates	60	>50		Compact structure

1.4. The increase of temperature had an effect on the hydrostatic properties but not on the hydrodynamic properties

The effect of the increase of the temperature of the system on AGPs from A. gums was first studied in their powdered form using thermogravimetric analysis (TGA). The thermal degradation of all AGPs showed a two-event process. The first event was associated to the loss of bound water (dehydration), which was found in the temperature range of 30-146°C. Meanwhile, the second event corresponds to molecular degradation. However, the HIC-F3 fraction displayed an intermediate event around 171°C, which can be attributed to loss of remaining water or degradation of uronic acids. A. *seyal* showed a lower first transition (T_1) which evidenced a higher sensitivity to dehydration, which is in line with its lower flow activation energy (E_a) compared to A. *senegal* (64°C and 69°C). The HIC fractions, HIC-F1, HIC-F2 and HIC-F3, displayed T_1 values of 70, 65 and 60 °C, respectively, in the order of decreasing AGP polarity, thus, on global affinity for water. These results evidenced once more the important effect of the polarity of A. gums on their functionality.

The effect of temperature on the volumetric (hydrostatic and hydrodynamic) properties in the temperature range of 25-50°C was studied. The main results showed that in this range of temperature, there was little to no effect on the conformation and main hydrodynamic (intrinsic viscosity and hydrodynamic radius) and structural properties (molar mass,

polydispersity and gyration radius) of A. gums and HIC fractions. It is believed that this behavior is the consequence of the hyperbranched and weak polyelectrolyte character of A. gums. Conversely, both v_s° and β_s° increased with the increasing temperature. The behavior of the partial specific volume was due to the increase of the thermal volume (v_T) and interior volume fluctuations (expansion of voids), and weakening of solute-water hydrogen bonds.

The reasons why the hydrodynamic properties are not affected by the temperature, meanwhile, the volumetric properties increase with the rising temperature is not clear. However, it is possible that the hyperbranching characteristic of A. gums might have an effect on stabilization of the structure. In addition, the partial specific expansibility (E°) of A. gums is small ($\sim 5x10^{-4}$ $cm^3.g^{-1}.K^{-1}$), suggesting that volume of the solute is not greatly impacted by the increase of the temperature.

From this study, some questions regarding the effect of the temperature on the dynamics of water were raised. In addition, the effect of presence of aggregates and minerals were not studied, since the study was not performed in all AGP fractions, thus suggesting that more studies are needed.

2. Perspectives

2.1. Pressure perturbation calorimetric (PPC) study

Since in this study we mainly focused on the study on the adiabatic compressibility (K_s) of A. gums and AGP fractions, the first recommendation is to continue the study of the volumetric properties of A. gums by studying the isothermal compressibility (K_T). This volumetric property is defined as the changes on the volume caused by changes of pressure at constant temperature [1-3]:

$$K_T = \beta_T V = -\left(\frac{\partial V}{\partial P}\right)_T \quad (V.1)$$

where β_T (Pa^{-1}) is the isothermal compressibility coefficient. K_T can be obtained by measuring the changes in the heat flow upon a pressure change [4,5], which can be achieved using pressure perturbation calorimetric (PPC) methods. The main advantage of this method is the direct calculation of the thermal expansion coefficient (α) through the relation [4,5]:

$$\frac{\partial Q}{\partial P} = -T\left(\frac{\partial V}{\partial T}\right)_P = -T\,V\,\alpha \quad (V.2)$$

where Q is the heat absorbed or released induced by the changes in pressure (kJ;mol^{-1}), T is the temperature (K) and V the volume (cm^3). Furthermore, using the method we can access an important thermodynamic parameter, the specific heat capacity (C_p, $kJ.g^{-1}K^{-1}$) [1,6]:

$$\beta_s = \beta_T - \alpha^2 T / C_p \quad (V.3)$$

2.2. Study of water dynamics changes

The hydration of A. gums and fractions were studied using their hydrostatic and hydrodynamic properties. It is known that the introduction of a polar molecule in water entrains a change on their dynamics. Then, a study of the extent of the perturbation caused by A. gums is needed to better understand the solute-water interactions and how they impact the structure of A. gums. Changes in water dynamics can be probed using nuclear magnetic resonance (NMR). This technique can provide information regarding water molecule orientation time by measuring the spin relaxation rates of the hydrogen or oxygen atoms present in water [7]. Other interesting technique that can be used are dielectric relaxation and terahertz (THz) spectroscopies. The latter has a high sensitivity which allows to measure dynamic changes in the order of picoseconds [8].

Another interesting method used to obtain information regarding hydration of biomolecules is the infrared absorption spectroscopy (IR). This method has been used to provide information regarding the strength and arrangements of hydrogen bonds, since the O-H stretching mode is sensitive to the neighboring water molecules and hydrogen bond network [9].

2.2 Calorimetric studies of A. gums

The thermal degradation of A. gums was studied using thermogravimetric analysis (TGA). However, one of the main disadvantages seen during the experiments was the impossibility to control the humidity of the initial sample. The thermal properties of biopolymers can be also studied using differential scanning calorimetry (DSC). Moreover, previous studies have already been performed by Phillips et al. (1996) [10] and Hatakeyama et al. (2009) [11]. However, only A. *senegal* was studied. Thus, the study of the ensemble of AGP fractions might provide additional information.

2.3. Effect of salt on volumetric and hydrodynamic properties

In this study, an important effect of the ionic strength of the dispersions on the hydrodynamic properties of A. gums and AGP fractions was evidenced. The results suggested possible interactions of the minerals present with the solvent. However, the effect of the ionic strength on the volumetric (hydrostatic) properties was study only in dispersions with ionic strength of 0.1 M ($LiNO_3$) and involving A. *senegal*. Although no important differences were seen, it is nrcessary to complete this study to have information about the role of the charges of A. gums.

Preliminary studies of the effect of minerals on the main volumetric (hydrostatic) properties were studied using a demineralized fraction of A. *senegal* (Arabic acid). The main results showed v_s° and β_s° of 0.603 $cm^3.g^{-1}$ and -6.7x10^{-11} Pa^{-1}, respectively. Although this fraction contained about 2% (wt) of proteins, it displayed a v_s° and β_s° close to the aggregated IEC-F1 (Table VI.1). This result highlights the important role of the minerals on the flexibility and hydration of A. gums.

2.4 Effect of the aggregates on the volumetric (hydrostatic and hydrodynamic) properties

In this study, we start to study the effect of the presence of AGP based aggregates. It was shown that the presence of these molecules have an effect on the main volumetric (hydrostatic and hydrodynamic) properties of A. gums, since higher values of intrinsic viscosity, hydrodynamic radius, partial specific volume and partial specific adiabatic compressibility were found for HIC-F2, HIC-F2 and the aggregated fraction IEC-F1. However, the mechanism of formation of this aggregates and how they impact functional properties of Acacia gums, as well as to their possible industrial applications is worth of deeper study.

3. References

1. Taulier, N.; Chalikian, T.V. Compressibility of protein transitions. *Biochimica et Biophysica Acta (BBA) - Protein Structure and Molecular Enzymology* **2002**, *1595*, 48-70.
2. Dadarlat, V.M.; Post, C.B. Insights into protein compressibility from molecular dynamics simulations. *The Journal of Physical Chemistry B* **2001**, *105*, 715-724.
3. Chalikian, T.V. Structural thermodynamics of hydration. *The Journal of Physical Chemistry B* **2001**, *105*, 12566-12578.
4. Zhai, Y.; Okoro, L.; Cooper, A.; Winter, R. Applications of pressure perturbation calorimetry in biophysical studies. *Biophysical Chemistry* **2011**, *156*, 13-23.
5. Schweiker, K.L.; Makhatadze, G.I. Chapter 22 use of pressure perturbation calorimetry to characterize the volumetric properties of proteins. In *Methods in enzymology*, Academic Press: 2009; Vol. 466, pp 527-547.
6. Gekko, K. Volume and compressibility of proteins. In *High pressure bioscience: Basic concepts, applications and frontiers*, Akasaka, K.; Matsuki, H., Eds. Springer Netherlands: Dordrecht, 2015; pp 75-108.
7. Laage, D.; Elsaesser, T.; Hynes, J.T. Water dynamics in the hydration shells of biomolecules. *Chemical Reviews* **2017**, *117*, 10694-10725.
8. Arikawa, T.; Nagai, M.; Tanaka, K. Characterizing hydration state in solution using terahertz time-domain attenuated total reflection spectroscopy. *Chemical Physics Letters* **2008**, *457*, 12-17.
9. Grossutti, M.; Dutcher, J.R. Correlation between chain architecture and hydration water structure in polysaccharides. *Biomacromolecules* **2016**, *17*, 1198-1204.
10. Philips, G.O.; Takigami, S.; Takigami, M. Hydration characteristics of the gum exudate from acacia *senegal*. *Food Hydrocolloids* **1996**, *10*, 11-19.
11. Hatakeyama, T.; Uetake, T.; Inui, Y.; Hatakeyama, H. Freezing bound water restrained by gum arabic. In *Gums and stabilisers for the food industry 15*, The Royal Society of Chemistry: 2009; pp 69-76.

Annexes

Résumé en français

1. Introduction

La gomme d'Acacia (E414) est définie comme un exsudat gommeux produit par les arbres d'Acacia *senegal* et Acacia *seyal* [1-3]. Elle est produite comme mécanisme de défense contre un stress environnemental (par exemple des conditions climatiques extrêmes ou des blessures procurées par des animaux)[2,4,5]. Elle est produite principalement dans la région africaine sub-saharienne dans la zone constituée par le Soudan, le Nigéria, le Tchad et le Sénégal [5-7].

Les exsudats de gomme d'Acacia sont composés d'arabinogalactanes protéines (AGPs), faiblement chargés, hyperbranchés avec une forte proportion de sucres neutres (D-arabinose, L-galactose, L-rhamnose) et chargés (acide glucuronique et 4-O-methyl acide glucuronique) [2,4,7-11] d'environ 1-3% de protéines et de minéraux [2]. La partie protéique des AGPs de gomme d'Acacia est principalement composée d'hydroxyproline et de sérine avec également des quantités importantes de proline et d'acide aspartique. La chaîne glucidique principale est composée d'unités de β-D-galactopyranose liées en 1,3. Les chaînes latérales sont composées de deux à cinq unités de β-D-galactopyranose liées en 1,3, jointes à la chaîne principale par des liaisons 1,6. Les chaînes principales et latérales contiennent des unités α-L-arabinofuranose, α-L-rhamnopyranose, β-D-glucuronopyranose et 4-O-methyl-β-D-glucuropyranose, les deux dernières principalement comme unités terminales [2,4,6,12-16]. Les gommes d'Acacia ont une variabilité naturelle qui dépendent de la variété, l'origine, l'âge de l'arbre, des conditions climatiques, de la composition du sol, de l'emplacement de l'arbre et des pratiques post-récolte (par exemple le processus de maturation, du procédé de transformation, etc.) [2,6,7,17-19]. Ces facteurs se reflètent aussi dans la variabilité de la teneur en sucres, la composition en acides aminés et minéraux, la densité de charges, la masse molaire, la conformation, l'anisotropie et la capacité d'assemblage des gommes [4,7,9,12,20-23].

La gomme d'Acacia peut être définie comme un continuum de macromolécules qui différent par leurs propriétés physicochimiques (hydrophobicité et densité de charges notamment) et

leurs propriétés structurales (masse molaire (M_w), rayon de giration ou volume hydrodynamique [4]. Par chromatographie d'interaction hydrophobe (HIC), l'A. *senegal* peut être séparée en trois fractions moléculaires nommées traditionnellement Arabinogalactane (AG), Arabinogalactane-protéine (AGP) et Glycoprotéine (GP) selon leur ordre d'élution et leur teneur en protéines. Ces trois fractions répondent positivement au réactif de Yariv indiquant qu'elles contiennent des chaines de type d'Arabinogalactane. Par conséquent, les molécules composant ces trois fractions HIC peuvent être considérées comme des Arabinogalactane- protéines (AGPs). Dans cette étude et pour éviter des confusions, ces fractions ont donc été nommées HIC-F1 (AG), HIC-F2 (AGP) et HIC-F3 (GP) selon leur ordre d'élution.

Les deux principales variétés de gomme d'Acacia, A. *senegal* et A. *seyal*, se distinguent principalement par leur teneur en sucres, en protéines, par leur composition en acides aminés et leur degré de branchement. A *senegal* a une teneur plus élevée en protéines (3%) et un degré de branchement plus élevé (80%) que A. *seyal* (1% et 60%, respectivement)[7,11]. De plus, A. *seyal* présente une masse molaire moyenne plus élevée (7-10x10^5 g.mol^{-1}) et une structure plus compacte par rapport à l'A. *senegal* (2-7x10x10^5 g.mol^{-1}) [11]. En ce qui concerne les fractions macromoléculaires d'A. *senegal*, la fraction HIC-F1 est la fraction majoritaire (85-90% de la gomme totale), elle a une faible teneur en protéines (~1%), une M_w moyenne de 3x10^5 g.mol^{-1} et un rayon hydrodynamique (R_H) d'environ 9 nm [2,4,9,20,21] [17]. La fraction HIC-F2 correspond à environ 9-15% de la gomme totale avec une teneur en protéines entre 12-15%. Elle a une M_w de 1-3x10^6 g.mol^{-1} et un rayon hydrodynamique (R_H) entre 23-35 nm [2,4,9,14,17,24-29]. La fraction HIC-F3 est la fraction minoritaire de la gomme d'Acacia (1-2% de la gomme totale) avec une teneur élevée de protéines (25-50%). Elle est formée d'au moins trois différentes populations macromoléculaires. Elle a une M_w moyenne entre 2x10^5 et 3x10^6 g.mol^{-1} et un rayon hydrodynamique (R_H) entre 15-30 nm [2,4,9,23].

2. Objectifs de thèse

La gomme d'Acacia est l'une des plus anciennes gommes naturelles dans le monde. Industriellement, elle est utilisée dans les domaines alimentaires et non alimentaires pour ses propriétés fonctionnelles intéressantes telles que ses propriétés interfaciales, sa faible viscosité en comparaison avec les autres gommes alimentaires et sa capacité d'encapsulation. Malgré ses nombreuses applications et son utilisation intensive en industrie, ses propriétés

physicochimiques en solution ne sont pas complètement bien élucidées. Peu d'informations sont notamment disponibles sur ses propriétés volumétriques (hydrostatiques et hydrodynamiques).

Le principal objectif de la thèse était l'étude des propriétés volumétriques (hydrostatiques et hydrodynamiques) des Arabinogalactane-protéines (AGPs) de gomme d'Acacia. Pour cela les deux principales variétés commerciales de gommes d'Acacia, Acacia *senegal* (A. *senegal*) et Acacia *seyal* (A. *seyal*) ont été utilisées, ainsi que des fractions macromoléculaires d'A. *senegal* obtenues par chromatographie d'interaction hydrophobe (3 fractions : HIC-F1, HIC-F2 et HIC-F3) et d'échange ionique (2 fractions : IEC-F1 et IEC-F2). Ces fractions englobent les différents AGPs présents dans la gomme d'Acacia et diffèrent principalement par leur masse molaire, leur affinité pour le solvant et leur capacité d'agrégation.

3. Principaux résultats et conclusions

Dans le premier chapitre intitulé '***Propriétés volumétriques des Arabinogalactane-protéines des exsudats de gomme d'Acacia'***, les AGPs des gommes d'Acacia ont d'abord été caractérisés en déterminant leurs propriétés biochimiques (teneur en minéraux, protéines, sucres neutres et charges et profil d'acides aminés). Un bilan est présenté dans les Tableaux A.1 et A.2.

Tableau A.1. Composition biochimique des gommes d'Acacia et des fractions de gomme d'Acacia *senegal* obtenues par HIC et IEC.

Gommes ou fractions	Ara/Gal	Sucres chargés /sucres neutres	Degré de branchement	Protéines (%)	Minéraux (%)
Gommes d'Acacia					
A. *seyal*	1,4	0,2	0,6	0,8	1,4
A. *senegal*	0,8	0,1	0,8	2,2	3,4
Fractions AGP					
HIC-F1	0,7	0,3	0,8	0,5	3,1
HIC-F2	1,0	0,2	0,8	6,3	1,9
HIC-F3	1,2	0,2	0,8	13,8	4,9
IEC-F1	1,1	0,3	0,8	9,4	2,4
IEC-F2	0,7	0,2	0,8	1,6	4,0

* Données extraits de Mejia Tamayo et al (2018)[30] et les études complémentaires du chapitre III,

Tableau A.2. Composition en acides aminés polaires, non polaires et chargés des gommes Acacia et des fractions de gomme d'Acacia *senegal* obtenues par HIC et IEC.

Gommes ou fractions	Chargés (%)	Polaires (%)	Non polaires (%)	Hyp + Ser (%)	Glu + Asp (%)
Gommes d'Acacia					
A. *seyal*	47,9	27,4	28,5	43,3	10,8
A. *senegal*	49,9	29,7	26,8	40,7	10,0
Fractions AGP					
HIC-F1	52,0	36,4	18,8	51,2	5,7
HIC-F2	48,4	30,8	27,4	41,2	9,6
HIC-F3	45,8	28,6	31,9	29,5	13,5
IEC-F1	47,8	32,4	27,7	34,0	10,7
IEC-F2	48,8	30,1	27,6	39,6	11,1

* Donnés extraits des études complémentaires du chapitre III,

Les propriétés structurales, la masse molaire moyenne en poids (M_w), la polydispersité (M_w/M_n) et le pourcentage de macromolécules avec M_w <7,5x10^5 g.mol^{-1} ont été déterminés par HPSEC-MALS. En prenant en compte leur masse molaire moyenne, les AGPs ont été classés en trois groupes : 'petit AGPs' (M_w<7,5x10^5 g.mol^{-1}), 'larges AGPs' (M_w>7,5x10^5 g.mol^{-1}) et 'agrégats d'AGPs' (M_w<2-3x10^5 g.mol^{-1}). Les gommes d'A. *senegal* et A. *seyal* sont composées principalement de petits AGPs (86% et 80%, respectivement). La gomme d'A. *senegal* est caractérisée par une M_w inférieure (6,8x10^5 g.mol^{-1}) et une polydispersité supérieure (2,0) comparativement à l'A. *seyal* (7,1x10^5 g.mol^{-1} et 1,5, respectivement). Parmi les fractions, HIC-F1 et IEC-F2 sont composées principalement de 'petits AGPs' (93% et 80%) avec une M_w de 3,5x10^5 et 5,3x10^5 g.mol^{-1} et une polydispersité de 1,4 et 1,8, respectivement. Les fractions HIC-F2 et HIC-F3 contiennent principalement de 'large AGPs' (88% et 67%) avec une M_w de 1,5x10^6 et 1,6x10^6 g.mol^{-1} et une polydispersité de 1,4 et 1,9 respectivement. Ces résultats sont proches des valeurs précédemment rapportées dans la littérature. Finalement, la fraction IEC-F1 est principalement constituée par des 'agrégats d'AGPs' (97%) avec une M_w de 3,1x10^6 g.mol^{-1} et une polydispersité de 1,2. De plus, en utilisant les compositions et teneurs en acides aminés des fractions HIC-F2 et HIC-F3, nous

avons estimé que la fraction IEC-F1 est composée d'environ 70% d'AGPs de HIC-F3 et 30% d'AGPs de HIC-F2.

Dans un deuxième temps, les principales propriétés volumétriques, le volume spécifique partiel (v_s^o, $cm^3.g^{-1}$) et le coefficient de compressibilité adiabatique spécifique partiel (β_s^o, Pa^{-1}), des gommes d'Acacia et des fractions HIC ont été déterminés par des mesures de la masse volumique et de vitesse du son. Ces propriétés volumétriques renseignent sur la flexibilité et l'hydratation des molécules en solution qui peuvent être relié aux propriétés interfaciales. Les principaux résultats obtenus sur les gommes d'Acacia *senegal* et *seyal* ont montré que ces AGPs ont un comportement intermédiaire entre des polysaccharides rigides, chargés et fortement hydratés, et des protéines globulaires plus flexibles et moins polaires. Les deux espèces de gommes d'Acacia ont montré des propriétés volumétriques similaires. Les études menées sur les fractions HIC de la gomme d'Acacia *senegal* ont mis en évidence une relation entre les propriétés volumétriques, v_s^o et β_s^o, et la teneur en protéines. La fraction HIC-F1, caractérisée par une faible teneur en protéine, présente une structure plus hydratée et moins flexible. Au contraire, les fractions les plus riches en protéines, HIC-F2 et HIC-F3, présentent des structures plus flexibles et moins hydratées, d'autant plus que la teneur en protéine est importante. Ces résultats suggèrent de meilleures propriétés de solubilisation pour la fraction HIC-F1 en solution aqueuse et des propriétés interfaciales plus importantes pour les fractions HIC-F2 et HIC-F3. En utilisant ces propriétés volumétriques, l'hydratation des gommes d'Acacia et des fractions HIC (nombre d'hydratation ou n_h, g H_2O/g AGP) a été calculée. Les résultats ont montré à nouveau une relation entre la teneur en protéine et l'hydratation, puisque des n_h de 0,85, 0,67 et 0,54 g H_2O/g AGP ont été trouvés pour HIC-F1, HIC-F2 et HIC-F3, respectivement.

Les différences observées entre les propriétés volumétriques des fractions HIC d'Acacia *senegal* sont significativement liées à leur composition, notamment au ratio protéine/sucre ainsi qu'à la nature des acides aminés composant la partie protéique : la fraction polysaccharidique contribuant principalement au caractère hydrophile des AGPs, tandis que la partie protéique contribue principalement au caractère hydrophobe des AGPs.

Dans le deuxième chapitre intitule **'Propriétés Hydrodynamiques des Arabinogalactane-protéines des exsudats des gommes d'Acacia'** les principales propriétés hydrodynamiques (viscosité intrinsèque ($[\eta]$), coefficient de diffusion translationnel

(D_T) et sédimentation (S_o)) ont été déterminées en utilisant des méthodes viscométriques, la diffusion dynamique de la lumière (DLS), la spectroscopie magnétique nucléaire (DOSY-NMR), et l'ultracentrifugation analytique (AUC). A partir de ces propriétés, la masse molaire (M_w), le rayon hydrodynamique (R_H ou $R\eta$), le rayon de giration (R_G), la conformation globale et l'hydratation des gommes A. *senegal*, A. *seyal* et les fractions HIC-F1, HIC-F2, HIC-F3, IEC-F1 et IEC-F2 ont été déterminés.

Les principaux résultats ont montré l'implication de trois phénomènes dans l'augmentation de la viscosité réduite (η_{red}) à des faibles concentrations de gomme: l'effet des charges, l'adsorption de gomme sur la paroi en verre du capillaire et la présence d'assemblages à base d'AGPs (agrégats). Ces facteurs sont d'autant plus importants que les dispersions sont préparées dans de l'eau (faible force ionique). Dans ce type de dispersions, des valeurs plus importantes de viscosité intrinsèques ($[\eta]$) et de rayons hydrodynamiques (R_H) ont été trouvées pour toutes les gommes et fractions. Avec l'augmentation de la force ionique, la viscosité intrinsèque et le rayon hydrodynamique des gommes diminuent en raison d'une réduction de la polarité du solvant, ainsi que de la diminution de la taille (dissociation) des agrégats d'AGPs. La présence des agrégats dans les dispersions de gomme a été confirmée en utilisant la DLS. De plus, en utilisant une analyse combinée de DLS et de DOSY-NMR, la présence d'une population d'AGPs présentant un rayon hydrodynamique compris entre 4 et 9 nm a été mise en évidence. L'analyse de la conformation des AGPs dans les échantillons de gommes d'Acacia et des fractions HIC a montré que trois groupes d'AGPs différents par leur conformation et leur masse molaire (M_w) coexistent dans la gomme d'Acacia *senegal*. Les AGPs de faible M_w entre 1,5-5x10^5 g.mol^{-1} ont une conformation plus isotrope, tandis que les AGPs avec une M_w comprise entre 5-15x10^5 g.mol^{-1} ont une conformation plus allongée et anisotrope. Finalement, les AGPs avec une M_w compris entre 15-100x10^5 g.mol^{-1}, assimilés à des agrégats d'AGPs, ont une conformation plutôt compacte et isotrope.

En utilisant les valeurs de viscosité intrinsèque, le volume spécifique partiel et les dimensions des AGPs reportées dans la littérature, le nombre d'hydratation (n_h) dans la gamme de 0,5-1,0 g H_2O/g AGP a été déterminé pour HIC-F1, HIC-F2 et HIC-F3, respectivement. De plus, il a été montré que l'utilisation des incréments de viscosité (v) correspondant à une forme sphérique dure (2,5) pour analyser des objets anisotropes conduit à des surestimations de l'hydratation. En fait, des valeurs de ν dans la gamme de 10-50 ont été trouvées pour les AGPs des gommes d'Acacia.

Dans le dernier chapitre de la thèse intitulé '**Les effets de la température sur la structure et les propriétés en solutions des Arabinogalactane-protéines de gomme d'Acacia',** les effets de l'augmentation de la température sur le volume spécifique partiel ($v°$), le coefficient de compressibilité adiabatique ($\beta s°$), la viscosité intrinsèque ($[\eta]$) et le rayon hydrodynamique (R_H) ont été étudiés, De plus, l'effet de l'augmentation de la force ionique sur la viscosité intrinsèque a également été étudié ainsi que la dégradation thermique des différents systèmes à l'état de poudre par analyse thermogravimétrique (ATG).

Les principaux résultats ont montré que la dégradation thermique des AGPs est un processus à deux étapes ou évènements. Pour l'A. *senegal*, une première température de transition (T_1) autour de 69°C et correspondant à la perte d'eau liée a été déterminée. L'A. *seyal* a montré une transition de température inférieure (64°C), ce qui suggère une sensibilité plus élevée à la déshydratation. Pour les fractions HIC de l'A. *senegal* HIC-F1 a montré une température de transition plus élevée (70°C) que les fractions HIC-F2 et HIC-F3 (65°C et 60°C, respectivement), ce qui suggère une plus grande sensibilité à la déshydratation des fractions les plus riches en protéines (HIC-F3 et HIC-F2). De plus, une deuxième température de transition autour de 170°C a été observée pour cette fraction, suggérant la perte d'eau restante ou la décomposition de groupes carboxyliques.

L'augmentation de la température de 25 à 45°C a peu d'effet sur les propriétés structurales et hydrodynamiques des AGPs avec des réductions de moins de 10% des paramètres mesurés. A l'inverse des propriétés hydrodynamiques, les propriétés volumétriques sont influencées par la température avec une augmentation du volume spécifique partiel ($v_s°$) et du coefficient de compressibilité adiabatique ($\beta s°$) lors de l'augmentation de la température de 25 à 45°C. Ce résultat a été expliqué comme résultant d'une augmentation du volume thermique, d'un affaiblissement des liaisons hydrogènes et également de pertes d'eau de la couche d'hydratation. Finalement, un coefficient d'expansion thermique partiel ($E°$) d'environ $5x10^{-4}$ $cm^3.g^{-1}.K^{-1}$ a été calculé pour les AGPs de gomme d'Acacia. Cette valeur, également trouvée pour les protéines globulaires et les polysaccharides, suggère un comportement universel de ces propriétés volumétriques avec la température.

Pour conclure, cette thèse a apporté des nouvelles connaissances sur les propriétés volumétriques des AGPs de gomme d'Acacia. De plus, l'utilisation de fractions purifiées (HIC-F1, HIC-F2 et HIC-F3) et d'une nouvelle fraction riche en agrégats (IEC-F1) a permis

de montrer que les différences de comportement observées entre ces fractions peuvent être expliquées par des différences de composition biochimique (la teneur en sucres et en protéines), la polarité des AGPs et la présence d'agrégats d'AGPs.

4. References

1. FAO. Gum arabic. Food and Nutrition Paper 52 1999
2. Sanchez, C.; Nigen, M.; Mejia Tamayo, V.; Doco, T.; Williams, P.; Amine, C.; Renard, D. Acacia gum: History of the future. *Food Hydrocolloids* **2018**.
3. Williams, P.A.; Philips, G.O. Gum arabic. In *Handbook of hydrocolloids*, G. O. Philips, P.A.W., Ed. Boca Raton: CRC Press: 2000; pp 155-168.
4. Renard, D.; Lavenant-Gourgeon, L.; Ralet, M.C.; Sanchez, C. Acacia *senegal* gum: Continuum of molecular species differing by their protein to sugar ratio; molecular weight and charges. *Biomacromolecules* **2006**, 2637-2649.
5. Idris, O.H.M.; Williams, P.A.; Phillips, G.O. Gum arabic's journey from tree to end user. In *Gum arabic*, Kennedy, J.; Williams, P., Eds. RSC Publishing: Cambridge, 2012.
6. Verbeken D.; Dierckx S.; K., D. Exudate gums: Occurence, production, and applications. *Applied Microbiology Biotechnology* **2003**, *63*, 10-21.
7. Islam, A.M.; Phillips, G.O.; Sljivo, A.; Snowden, M.J.; Williams, P.A. A review of recent developments on the regulatory, structural and functional aspects of gum arabic. *Food Hydrocolloids* **1997**, *11*, 493-505.
8. Anderson, D.M.W.; Bridgeman, M.M.E.; Farquhar, J.G.K.; McNab, C.G.A. The chemical characterization of the test article used in toxicological studies of gum arabic (acacia senegal (l.) willd). *International Tree Crops Journal* **1983**, *2*, 245-254.
9. Randall, R.C.; Phillips, G.O.; Williams, P.A. Fractionation and characterization of gum from acacia *senegal*. *Food Hydrocolloids* **1989**, *3*, 65-75.
10. Flindt, C.; Alassaf, S.; Phillips, G.; Williams, P. Studies on acacia exudate gums. Part v. Structural features of acacia *seyal*. *Food Hydrocolloids* **2005**, *19*, 687-701.
11. Lopez-Torrez, L.; Nigen, M.; Williams, P.; Doco, T.; Sanchez, C. Acacia *senegal* vs. Acacia *seyal* gums – part 1: Composition and structure of hyperbranched plant exudates. *Food Hydrocolloids* **2015**, *51*, 41-53.
12. Anderson, D.M.W.; Stoddart, J.F. Studies on uronic acid materials. Part xv. The use of molecular-sieve chromatography on acacia *senegal* gum (gum arabic). *Carbohydrate Research* **1966**, *2*, 104-114.
13. Clarke, A.E.; Anderson, R.L.; Stone, B.A. Form and function of arabinogalactans and arabinogalactan-proteins. *Phytochemistry* **1979**, *18*, 521-540.
14. Williams, P.A.; Philips, G.O.; Randall, R.C. Structure-function relantionships of gum arabic. In *Gums and stabilizers for the industry 5*, IRL Press: 1990; pp 25-36.
15. Ali, B.H.; Ziada, A.; Blunden, G. Biological effects of gum arabic: A review of some recent research. *Food and Chemical Toxicology* **2009**, *47*, 1-8.
16. Anderson, D.M.W. The amino acid composition and quantitative sugar - amino acid relationships in sequential smith - degradation products from acacia polyacantha gum. *Food Additives & Contaminants* **1986**, *3*, 123-132.
17. Idris, O.H.M.; Williams, P.A.; Phillips, G.O. Characterisation of gum from acacia *senegal* trees of different age and location using multidetection gel permation chromatography. *Food Hydrocolloids* **1998**, 379-388.
18. Assaf, S.; Phillips, G.; Williams, P. Studies on acacia exudate gums. Part i: The molecular weight of gum exudate. *Food Hydrocolloids* **2005**, *19*, 647-660.
19. Karamalla, K.A.; Siddig, N.E.; Osman, M.E. Analytical data for acacia senegal var. Senegal gum samples collected between 1993 and 1995

from sudan. *Food Hydrocolloids* **1998**, *12*, 373-378.

20. Mahendran, T.; Williams, P.; Phillips, G.; Al-Assaf, S.; Baldwin, T. New insights into the structural characteristics of the arabinogalactan-protein (agp) fraction of gum arabic. *Journal of Agricultural and Food Chemistry* **2008**, 9269-9276.

21. Sanchez, C.; Schmitt, C.; Kolodziejczyk, E.; Lapp, A.; Gaillard, C.; Renard, D. The acacia gum arabinogalactan fraction is a thin oblate ellipsoid: A new model based on small-angle neutron scattering and ab initio calculation. *Biophysical Journal* **2008**, *94*, 629-639.

22. Renard, D.; Lavenant-Gourgeon, L.; Lapp, A.; Nigen, M.; Sanchez, C. Enzymatic hydrolysis studies of arabinogalactan-protein structure from acacia gum: The self-similarity hypothesis of assembly from a common builiding block. *Carbohydrate Polymers* **2014**, *112*, 648-661.

23. Renard, D.; Lepvrier, E.; Garnier, C.; Roblin, P.; Nigen, M.; Sanchez, C. Structure of glycoproteins from acacia gum: An assembly of ring-like glycoproteins modules. *Carbohydrate Polymers* **2014**, *99*, 736-747.

24. Al-Assaf, S.; Phillips, G.O.; Aoki, H.; Sasaki, Y. Characterization and properties of acacia senegal (l.) willd. Var. Senegal with enhanced properties (acacia (sen) super gum™): Part 1—controlled maturation of acacia senegal var. Senegal to increase viscoelasticity, produce a hydrogel form and convert a poor into a good emulsifier. *Food Hydrocolloids* **2007**, *21*, 319-328.

25. Al-Assaf, S.; Phillips, G.; Williams, P. Studies on acacia exudate gums: Part ii. Molecular weight comparison of the vulgares and gummiferae series of acacia gums. *Food Hydrocolloids* **2005**, *19*, 661-667.

26. Al-Assaf, S.; Sakata, M.; McKenna, C.; Aoki, H.; Phillips, G.O. Molecular associations in acacia gums. *Structural Chemistry* **2009**, *20*, 325-336.

27. Castellani, O.; Al-Assaf, S.; Axelos, M.; Phillips, G.O.; Anton, M. Hydrocolloids with emulsifying capacity. Part 2 – adsorption properties at the n-hexadecane–water interface. *Food Hydrocolloids* **2010**, *24*, 121-130.

28. Elmanan, M.; Al-Assaf, S.; Phillips, G.O.; Williams, P.A. Studies on acacia exudate gums: Part vi. Interfacial rheology of acacia *senegal* and acacia *seyal*. *Food Hydrocolloids* **2008**, *22*, 682-689.

29. Renard, D.; Garnier, C.; Lapp, A.; Schmitt, C.; Sanchez, C. Structure of arabinogalactan-protein from acacia gum: From porous ellipsoids to supramolecular architectures. *Carbohydrate Polymers* **2012**, *90*, 322-332.

30. Mejia Tamayo, V.; Nigen, M.; Apolinar-Valiente, R.; Doco, T.; Williams, P.; Renard, D.; Sanchez, C. Flexibility and hydration of amphiphilic hyperbranched arabinogalactan-protein from plant exudate: A volumetric perspective. *Colloids and Interfaces* **2018**, *2*, 11.

Volumetric Properties of Arabinogalactan-Proteins from Acacia gums

Acacia gum is the oldest and most widely known and used gum, it is a dried gummy exudate from the leaves and branches of the Acacia *senegal* and Acacia *seyal* trees. Acacia gums are weakly charged, amphiphilic hyperbranched arabinogalactan-proteins (AGPs). They are composed of about 90% polysaccharides and from 1-3% of proteins and minerals. In spite of the widely spread of industrial usage of A. gums, their volumetric properties (hydrostatic and hydrodynamic) have not been well studied. These properties have been linked to important properties such as flexibility and hydration of the molecule, which are related to important functional properties of A. gums (e. g. interfacial properties). The main objective of this PhD thesis was to study the volumetric properties of AGPs from Acacia gums exudates. For this effect, the main commercial species, A. *senegal* and A. *seyal*, and the macromolecular fractions of the former, obtained via hydrophobic interaction and ionic exchange chromatographies were studied. The main results showed that AGPs from Acacia gums have a semi-flexible structure. However, differences in their flexibility and hydration were seen among AGP fractions. These differences were explained based on their composition, polarity, molar mass, shape and conformation. Furthermore, an intermediate behavior between proteins and linear polysaccharides was evidenced. In addition, an effect of the presence of AGP based aggregates on the volumetric properties was seen.

Keywords: Acacia gum, Arabinogalactan-proteins, volumetric properties, hydrodynamic properties, flexibility, hydration

Propriétés volumetriques des Arabinogalactanes-protéines d'exsudats des gommes d'Acacia

La gomme d'Acacia est l'une des plus anciennes gommes naturelles dans le monde et la plus connue. Elle est définie comme l'exsudat gommeux produit par les arbres d'Acacia *senegal* et Acacia *seyal*. Les gommes d'Acacia sont composées d'arabinogalactanes protéines (AGPs), faiblement chargés, hyperbranchés avec une forte proportion de sucres (90%) et d'environ 1-3% de protéines et de minéraux. Malgré ses nombreuses applications industrielles, les connaissances sur ses propriétés volumétriques (hydrostatiques et hydrodynamiques) restent à améliorer. Ces propriétés peuvent être liées à la flexibilité et l'hydratation des molécules qui déterminent les propriétés fonctionnelles importantes comme les propriétés interfaciales. L'objectif de cette thèse est l'étude des propriétés volumétriques d'AGPs de la gomme d'Acacia. L'étude a été faite sur les principales variétés des gommes d'Acacia, A. *senegal* et A. *seyal*, ainsi que des fractions macromoléculaires d'A. *senegal*, obtenues par la chromatographie d'interaction hydrophobe et d'échange ionique. Les principaux résultats ont montré que les AGPs de gomme d'Acacia ont une structure semi flexible. De plus, des différences dans la flexibilité et l'hydratation entre les fractions d'AGPs ont été montré. Ces différences ont été expliquées par leurs différences en composition, polarité, masse molaire, forme et conformation. De plus, un comportement intermédiaire entre des protéines et des polysaccharides linéaires ont été montré. Finalement, un effet des agrégats d'AGPs sur les propriétés volumétriques a été mis en avance.

Mots clés: Gomme d'Acacia, protéines d'Arabinogalactane, Propriétés volumétriques, Propriétés hydrodynamiques, Flexibilité, Hydratation.